Supplementary Information (SI) for Physical Chemistry Chemical Physics.
This journal is © the Owner Societies 2026

Supporting Information

Computer-Aided Kinetic Network Modeling of Orthoester Metathesis

Claire Muzyka,[a] *Diana V. Silva-Brenes,*[a,b]

and Jean-Christophe M. Monbaliu[*,a,c]

a. Center for Integrated Technology and Organic Synthesis (CiTOS), MolSys Research Unit, University of Liège, Allée du Six Août 13, B-4000 Liège (Sart Tilman), Belgium

E-mail: jc.monbaliu@uliege.be | www.citos.uliege.be

b. FloW4all Flow Technology Resource Center, University of Liège, B-4000 Liège (Sart-Tilman), Belgium

c. WEL Research Institute, Avenue Pasteur, 6, 1300 Wavre, Belgium.

Table of contents

1 General information 7
2 Reagents and solvents 8
3 Experiments 8
3.1 Kinetic study using 1:1 ratio of 1/2b with *in-line* NMR monitoring 8
3.2 Kinetic study using 1:1 ratio of 1/2b with off-line NMR 9
3.3 Kinetic study using 100:1 ratio of 1/2b with off-line NMR 9
3.4 Kinetic study using 1:1 ratio of 1/2b in neat conditions with off-line NMR 9
3.5 Preparation of compound 3 9
3.6 Kinetic study starting from species 3 and an excess of EtOH with off-line NMR 10
3.7 Preparation of compound 4 10
3.8 Kinetic study starting from species 4 and an excess of EtOH with off-line NMR 10
3.9 Preparation of compound 5 10
3.10 Preparation of compound 6 10
3.11 Preparation of compound 7 11
3.12 Preparation of compound 9 11
3.13 Preparation of compound 14 11
4 Characterization of dynamic covalent exchange products 12
4.1 Structural characterization of a typical crude of DCE using 700 MHz NMR 12
4.1.1 Acyclic orthoesters identified by NMR 12
4.1.2 Cyclic orthoesters identified by NMR 14
4.2 Structural characterization of the typical crude of DCE using GC-MS 16
5 Preliminary experiments of the DCE reaction using in-line NMR and stability assessment of samples over time 17
5.1 Kinetic studies in various conditions of temperature and concentrations 17
5.2 Stability of NMR samples over time 19
6 Python script 1: tensorial decomposition of ^{1}H-NMR raw data treated with a Fourier transform 19
6.1 Selection of non-negative Tucker decomposition 19
6.2 Explanations of the script of non-negative Tucker decomposition 19
7 Python script 2: kinetic modelling of stoichiometric amount of 1 and 2 using 10 mol% FA in dry acetonitrile 22
7.1 Description of Python script 2 22
7.1.1 Evaluation of model accuracy: coefficient of determination (R^2) 23
7.1.2 Evaluation of model accuracy: Root Means Square Error (RMSE) and Mean Average Error (MAE) 23
7.1.3 Bayesian Criterion Information (BIC) and Akaike Information Criterion (AIC) 23
7.1.4 Quantile-quantile plots 23
7.2 Calculation of equilibrium constants (K) 23
7.3 Methodology to refine kinetic models and working hypothesis 24
7.4 Development of model I including species 1, 2b, 3, 5, 6 and EtOH 24
7.4.1 Model I 24
7.4.2 Quantile-quantile plot of model I 25
7.5 Development of model II including species 1, 2b, 3, 4, 5, 6 and EtOH 26
7.5.1 Profile of concentrations and comparison of RMSE and MAE for model II comprising either path (a) or (b) or both (a&b) 26

7.5.2 Quantile-quantile plot for model II including path (a), (b) or (a&b)....27
7.5.3 Final model II of 1 to 6 including path (b)....28
7.6 Development of model III including species 1, 2b, 3, 5, 6, 7 and EtOH....28
7.6.1 Model III including path (a), (b) or (a&b)....28
7.6.2 Quantile-quantile plots for model III including path (a) or (b)....29
7.6.3 Model III including path (a&b) with/without the formation of 4 from 2 molecules of 3....29
7.6.4 of 3 Quantile-quantile plot for model III including path (a&b) including the formation of 4 from 2 molecules 30
7.6.5 Final model of 1 to 7 including path (a&b) including formation of 4 from 2 molecules of 3....30
7.7 Kinetic study using an excess of 100:1 ratio of 1/2b using off-line NMR....30
7.7.1 Model using a 1/100 ratio of 2b/1....31
7.7.2 Quantile-quantile plot....32
7.7.3 System of differential equations describing the kinetic model....32
7.7.4 Model initialization and calculated concentrations and rate constants....33
7.8 Development of model IV including species 1, 2b, 3, 5, 6, 7, 8 and EtOH....34
7.8.1 Comparison of reaction profiles and their corresponding RMSE and MAE for path a.1, a.2 and b and their combinations....34
7.8.2 Quantile-quantile plots....36
7.8.3 Comparison of BIC and AIC for the number of interconnections between species for the various models 38
7.8.4 Final model of 1 to 8 and EtOH including path (b)....38
7.9 Kinetic study of stoichiometric amount of 1 and 2b using 10 mol% of FA in dry acetonitrile to form 3, 4, 5, 6, 7, 8 ,9 and 10....39
7.9.1 Comparison of reaction profiles and their corresponding RMSE and MAE for path a.1, a.2 and b and their combinations....39
7.9.2 Quantile-quantile plots....41
7.9.3 System of differential equations describing the kinetic model....43
7.9.4 Model initialization with calculated concentrations and rate constants....45
7.10 Kinetic study of stoichiometric amount of 1 and 2b using 10 mol% of FA in dry Acetonitrile to form 3, 4, 5, 6, 7, 8 ,9, 10 and 12 (model VIII.2)....46
7.10.1 Kinetic model....46
7.10.2 Quantile-quantile plots....47
7.10.3 System of differential equations describing the kinetic model....48
7.11 Kinetic study in neat conditions....49
7.11.1 to 10 reaction profile and their corresponding RMSE and MAE with addition of interconnection between 4+1 49
7.11.2 Quantile-quantile plots....49
7.11.3 Final model....50
7.11.4 Model initialization with calculated concentrations and rate constants....51
7.12 Kinetic study starting from species 3 and an excess of EtOH....51
7.12.1 Final model....51
7.12.2 Quantile-quantile plot....53
7.12.3 System of differential equations describing the kinetic model....53
7.12.4 Model initialization with calculated concentrations and rate constants....54

7.13 Kinetic study starting from species 4 and an excess of EtOH....55
7.13.1 Final model....55
7.13.2 Quantile-quantile plot....56
7.13.3 System of differential equations describing the kinetic model....56
7.13.4 Model initialization with calculated concentrations and rate constants....57
8 Solvent screening....58
8.1 Kinetic study of stoichiometric amount of 1 and 2b using 10 mol% of FA in dry Dimethyl Sulfoxide58
8.1.1 Final model....58
8.1.2 Quantile-quantile plot....59
8.1.3 Model initialization with calculated concentrations and rate constants....59
8.2 Kinetic study of stoichiometric amount of 1 and 2b using 10 mol% of FA in dry Dimethylformamide60
8.2.1 Final model....60
8.2.2 Quantile-quantile plot....61
8.2.3 Model initialization and calculated concentrations and rate constants....61
8.3 Kinetic study of stoichiometric amount of 1 and 2b using 10 mol% of FA in dry Propylene carbonate62
8.3.1 Final model....62
8.3.2 Quantile-quantile plot....63
8.3.3 Model initialization and calculated concentrations and rate constants....63
9 Reagent screening....64
9.1 Kinetic study of stoichiometric amount of 1 and Trimethyl orthoformate 2a using 10 mol% of FA in dry Acetonitrile 64
9.1.1 Final model....64
9.1.2 Quantile-quantile plot....65
9.1.3 System of differential equations describing the kinetic model....65
9.1.4 Model initialization with calculated concentrations and rate constants....66
9.2 Kinetic study of stoichiometric amount of 1 and Triisopropyl orthoformate (2c) using 10 mol% of FA in dry acetonitrile....67
9.2.1 Final model....67
9.2.2 Quantile-quantile plot....68
9.2.3 System of differential equations describing the kinetic model....69
9.2.4 Model initialization and calculated concentrations and rate constants....70
10 Computations....71
10.1 Computational methods....71
10.2 Cartesian coordinates and energies for representative transition states....71
10.2.1 DCE mechanism for the formation of 3, 4, 5, 6, 7, 10 and 11....71
10.2.2 DCE mechanism for the formation of 8,9 and 12....82
10.2.3 DCE mechanism for the formation of 7, 8, 12 and 9 through the substitution of carbocations....88
10.2.4 Computations for the screening of catalysts....92
10.2.5 Computations for the catalyst screening with 3 molecules of water....102
10.2.6 Computations for the mechanism of hydrolysis....105
10.2.7 Computations for the screening of solvents and reagents....116
10.2.8 Computations for the calculation of the dissociation energies of complex catalysts-solvents....130

11 Mechanistic study of dynamic covalent exchanges toward orthoesters (DCE)....137
11.1 Mechanism of DCE sequence toward the formation of 3, 4, 5, 6, 7, 10 and 11....137
11.2 Mechanism of DCE toward the formation of 8, 9 and 12....138
11.3 DFT computations on the screening of catalysts....139
11.4 DFT computations on the screening of solvents....139
11.5 Mechanism of hydrolysis for species 2b, 3 and cyclic carbocation (from cyclic species)....141
11.6 Mechanistic interpretation of the computational results....143
12 Copies of ^{1}H, ^{13}C NMR spectra and fragmentation of the products observed by GC-MS....146
12.1 Compound 1....146
12.1.1 ^{1}H-NMR spectrum....146
12.1.2 ^{13}C-NMR spectrum....147
12.1.3 Mass spectrum and fragmentation....147
12.2 Compound 2b....148
12.2.1 ^{1}H-NMR spectrum....148
12.2.2 ^{13}C-NMR spectrum....149
12.2.3 Mass spectrum and fragmentation....149
12.3 Compound 3....151
12.3.1 ^{1}H-NMR spectrum....151
12.3.2 ^{13}C-NMR spectrum....151
12.3.3 Mass spectrum and fragmentation....152
12.4 Compound 4....154
12.4.1 ^{1}H-NMR spectrum....154
12.4.2 ^{13}C-NMR spectrum....154
12.4.3 Mass spectrum and fragmentation....155
12.5 Compound 5....157
12.5.1 ^{1}H-NMR spectrum....157
12.5.2 ^{13}C-NMR spectrum....157
12.5.3 Mass spectrum and fragmentation....158
12.6 Compound 6....159
12.6.1 ^{1}H-NMR spectrum....159
12.6.2 ^{13}C-NMR spectrum....159
12.6.3 Mass spectrum and fragmentation....160
12.7 Compound 7....161
12.7.1 ^{1}H-NMR spectrum....161
12.7.2 ^{13}C-NMR spectrum....161
12.7.3 Mass spectrum and fragmentation....162
12.8 Compound 8....163
12.8.1 2 2D-HSQC and HMBC NMR spectra....163
12.8.2 Mass spectrum and fragmentation....164
12.9 Compound 9....165
12.9.1 ^{1}H-NMR spectrum....165
12.9.2 ^{13}C-NMR spectrum....165

12.9.3 Mass spectrum and fragmentation....166
12.10 Compound 10....167
12.11 Compound 11....168
12.11.1 ^{1}H-NMR spectrum....168
12.11.2 2D-HSQC and HMBC NMR spectra....168
12.12 Compound 13 (commercial reference)....169
12.12.1 ^{1}H-NMR spectrum....169
12.12.2 ^{13}C-NMR spectrum....169
12.13 Compound 14....170
12.13.1 ^{1}H-NMR spectrum....170
12.13.2 ^{13}C-NMR spectrum....170
13 References....171

1 General information

Conversions and yields for the dynamic covalent exchanges reactions toward orthoesters (DCE) were determined by Gas Chromatography (GC) coupled to mass spectrometer (Shimadzu GC-MS-QP2020 NX). The GC-MS is equipped with a 14% cyanopropylphenyl / 86% dimethyl polysiloxane (0.25 mm ID x 0.25 µm x 30 m) column while the program of temperature consisted in a plateau at 30 °C hold 5 min, a 5 °C min^{-1} ramp to 50 °C hold 8 min, a 30 °C min^{-1} ramp to 120 °C hold 6 min, a 10 °C min^{-1} ramp to 175 °C and a 30°C min^{-1} ramp to 250 °C hold 2 min. A split ratio of 5 was used.

Yields for the dynamic covalent exchange reactions toward orthoesters were determined by ^{1}H NMR spectroscopy conducted on a high field Bruker Avance III HD 700 MHz spectrometer equipped with a 5 mm cooled probe(CryoProbe^{tm}) triple nuclei HCN (TCL) in CD_3CN. The chemical shifts were reported in ppm relative to the solvent residual peak. Octamethylcyclotetrasiloxane was used as internal standard. Preparation of the samples consisted in the prior weighing of the internal standard (6-8 mg), its further solvation in 580 CD_3CN and the final addition of 20 µl of reactional crude. Commercial references of ethylene glycol (**1**), triethylorthoformate (**2b**) and ethyl formate (**13**) were used to perform peaks assignment on a ^{1}H NMR spectrum obtained from a typical reactional crude. Other compounds were identified based on reference spectra obtained from their isolation (**3** to **7** and **9**) or through careful structural analysis (**10** and **11**) reported in Section S12. Given that all signals arising from the ^{1}H spectrum were identified and assigned, a mass balance could be calculated for the determination of both the conversion as well and yields of all products.

A Spinsolve™ Ultra NMR (43 MHz) spectrometer from Magritek® equipped with a flow-through cell was used for the real-time monitoring of dynamic covalent exchanges (DCE) reaction. This experiment used a loop system, allowing the crude mixture to be pumped through a peristaltic pump (Magritek® - controlled by Spinsolve software) for analysis before being returned to the batch reactor. A ^{1}H-NMR spectrum (1D Extended) was recorded after each loop, consisting of 2 scans (50 s of repetition time, 90° of pulse angle).

2 Reagents and solvents

The reagents and solvents are purchased from commercial sources; these compounds are used without purification (Table S1). All reagents were used as received, unless otherwise stated. Solvents were dried over 4 Å molecular sieve.

Table S1 Chemicals and suppliers.

Solvents	Purity (%)	CAS number	Supplier
Acetonitrile	>99%	64-17-5	VWR
Propylene carbonate	>99.8%	108-32-7	Sigma Aldrich
Dimethylformamide	>99.5%	68-12-2	VWR
Dimethyl sulfoxide	>99%	67-68-5	VWR
Ethyl acetate	>99.5%	141-78-6	VWR
D3-acetonitrile	>99.8%	2206-26-0	Eurisotop
Dichloromethane	>98%	75-09-2	VWR
Methanol	>98%	67-56-1	VWR
Chemicals	Purity (%)	CAS number	Supplier
Ethylene glycol (**1**)	99.8	107-21-1	VWR
Triethyl orthoformate (**2b**)	>98%	122-51-0	Sigma Aldrich
Trimethyl orthoformate (**2a**)	>98%	149-73-5	Sigma Aldrich
Triisopropyl orthoformate (**2c**)	>98%	4447-60-3	Sigma-Aldrich
Formic acid (FA)	>96%	64-18-6	VWR International
Acetic acid (AA)	>99%	64-19-7	VWR International
Pimelic acid (PA)	>98%	111-16-0	Acros
Benzoic acid (Bz)	>99%	65-85-0	UCB
Succinic acid (SA)	>99%	110-15-6	Merck-Darmstadt
Oxalic acid (OA)	>98%	144-62-7	Sigma Aldrich
Trichloroacetic acid (TCA)	>98%	76-03-9	Baker
Trifluoroacetic acid (TFA)	>99%	76-05-1	Acros
Octamethylcyclotetrasiloxane	>98%	556-67-2	Sigma Aldrich

3 Experiments

3.1 Kinetic study using 1:1 ratio of 1/2b with *in-line* NMR monitoring

A 0.73 M solution of ethylene glycol (**1**) and triethyl orthoformate (**2b**) was prepared by dissolving **1** (1.10 g, 17 mmol, 1 equiv.) and **2b** (2.60 g, 17 mmol, 1 equiv.) in 20 mL of dry acetonitrile. The medium was preheated to 60 °C for 15 min and magnetically stirred at 500 rpm prior to the addition of the catalyst. Then, l0 mol% of FA (0.078 g, 1.7 mmol, 0.1 equiv.) was added to the heated medium to trigger the reaction. The reaction was carried out over 1 h and monitored by in-line NMR as described in Section 3.2.

3.2 Kinetic study using 1:1 ratio of 1/2b with off-line NMR

A 0.73 M solution of ethylene glycol (**1**) and triethyl orthoformate (**2b**) was prepared by dissolving **1** (0.272 g, 4.38 mmol, 1 equiv.), **2b** (0.650 g, 4.38 mmol, 1 equiv.) and internal standard octamethylcyclotetrasiloxane (0.050 g, 0.16 mmol) in 5 mL of dry acetonitrile. This solution was weighed and mixed in a round bottom flask, which had been preliminary dried under vacuum and then purged with Argon. The reaction medium was preheated to 60 °C for 15 min and magnetically stirred at 500 rpm prior to the addition of the catalyst. A sample was collected before the addition of FA to ensure the reaction had not yet started. Then, l0 mol% of FA (0.020 g, 0.43 mmol, 0.1 equiv.) was added to the heated medium to trigger the reaction. The reaction was carried out over 3 h with regular aliquots of 30µL collected in Eppendorf tubes. Finaly, 20 µl of the crude was pipetted out and diluted with 580 µL of d_3-MeCN and transferred into NMR tubes for analysis. The same procedure was followed for the screening of catalysts using 5 or 10 mol% of catalyst according to the experiment and undried acetonitrile.

3.3 Kinetic study using 100:1 ratio of 1/2b with off-line NMR

The same procedure as described in section S3.1 was performed. A solution of ethylene glycol (**1**, 14.80 M) and of triethyl orthoformate (0.1480 M) was prepared by dissolving **1** (6.218 g, 0.1 mol, 100 equiv.), **2b** (0.148 g, 1 mmol, 1 equiv.) and the internal standard octamethylcyclotetrasiloxane (0.013 g, 0.04 mmol) in 1 mL of dry acetonitrile. Then, l0 mol% of FA (0.005 g, 0.11 mmol, 0.1 equiv.) was added to the heated medium to trigger the reaction.

3.4 Kinetic study using 1:1 ratio of 1/2b in neat conditions with off-line NMR

The same procedure as described in section S3.1was performed. A solution of ethylene glycol (**1**, 4.5 M) and triethyl orthoformate (**2b**, 4.5 M) was prepared by dissolving **1** (1.89 g, 4.5 mmol, 1 equiv.), **2b** (4.52 g, 4.5 mmol, 1 equiv.) and the internal standard octamethylcyclotetrasiloxane (0.137 g, 0.46 mmol). Then, l0 mol% of FA (0.15 g, 0.45 mmol, 0.1 equiv.) was added to the heated medium to trigger the reaction.

3.5 Preparation of compound 3

In a 500 mL round-bottom flask, a solution of **1** and **2b** was prepared dissolving **1** (3.12 g, 50 mmol, 1 equiv.) and **2b** (39.30 g, 265 mmol, 5.3 equiv.) in 250 mL of acetonitrile. Then, 0.5 equivalent of formic acid (1.16 g, 25 mmol, 0.5 equiv.) was added to the solution to trigger the reaction. The medium was magnetically stirred and cooled down in an ice batch for 2 min to enable the complete consumption of **1**. The reaction medium was rapidly quenched with Na_2CO_3 and subsequently filtered to recover the neutralized solution The reaction effluent was then purified by a vacuum distillation to remove the unreacted **2b**. ^{1}H NMR (400 MHz, CD_3CN) δ 5.16 (s, 1H), 3.67 – 3.54 (m, 4H), 3.51 (s, 1H), 1.17 (d, J = 7.1 Hz, 5H). ^{13}C NMR (101 MHz, CD_3CN) δ 118.26, 66.29, 61.93, 60.44.

3.6 Kinetic study starting from species 3 and an excess of EtOH with off-line NMR

The same procedure as described in section S3.1 was performed. A solution 0.27 M of compound **3** was prepared by dissolving **3** (0.2190 g, 1.33 mmol, 1 equiv.) with EtOH (0.1983 g, 4.30 mmol, 3.2 equiv.) and internal standard octamethylcyclotetrasiloxane (0.0273 g, 0.09 mmol) in 4.3 mL of dry acetonitrile. Then, 52 mol% of FA (0.0326 g, 0.7 mmol, 0.52 equiv.) was added to the heated medium to trigger the reaction.

3.7 Preparation of compound 4

In a 500 mL round-bottom flask, a solution of **1** and **2b** was prepared dissolving **1** (1.60 g, 25.7 mmol, 1 equiv.) and **2b** (38.50 g, 260 mmol, 10 equiv.) in 250 mL of acetonitrile. Then, 0.1 equivalent of formic acid (0.1183 g, 2.57 mmol, 0.1 equiv.) was added to the solution to trigger the reaction. The medium was magnetically stirred and heated at 60 °C over 2 hours. The reaction medium was rapidly quenched with Na_2CO_3 and subsequently filtered to recover the neutralized solution. The reaction effluent was then purified by a vacuum distillation to remove the remaining unreacted **2b**. ^{1}H NMR (400 MHz, CD_3CN) δ 5.18 (s, 1H), 3.65 (s, 2H), 3.58 (q, J = 7.1 Hz, 4H), 1.18 (t, J = 7.1 Hz, 6H). ^{13}C NMR (101 MHz, CD_3CN) δ 117.31, 62.69, 59.50, 14.34.

3.8 Kinetic study starting from species 4 and an excess of EtOH with off-line NMR

The same procedure as described in section S3.1 was performed. A solution 0.192 M of compound **4** by dissolving (0.4681 g, 1.75 mmol, 1 equiv.), EtOH (0.4784 g, 10.38 mmol, 5.9 equiv.) and the internal standard octamethylcyclotetrasiloxane (0.0369 g, 0.12 mmol) in 8 mL of dry acetonitrile. Then, 48 mol% of FA (0.0385 g, 0.83 mmol, 0.48 equiv.) was added to the heated medium to trigger the reaction.

3.9 Preparation of compound 5

In a 50 mL round-bottom flask, a solution of **1** and **2b** was prepared dissolving **1** (10.0 g, 161 mmol, 1 equiv.) and **2b** (9.56 g, 64.5 mmol, 0.4 equiv.) in dry acetonitrile. Then, 0.004 equivalent of FA (0.03 g, 0.6 mmol, 0.004 equiv.) was added to the solution to trigger the reaction. The medium was magnetically stirred and cooled at 0 °C in an ice bath over 5 min. The reaction medium was rapidly quenched with Na_2CO_3 and subsequently filtered to recover the neutralized solution The reaction effluent was then purified by a silica column separation using a mixture of 7:3 acetonitrile/ethyl acetate as eluent. Finally, the column was flushed with a 9:1 dichloromethane/methanol effluent to recover a fraction mainly containing **5** (Section S12). ^{1}H NMR (400 MHz, CD_3CN) δ 5.21 (s, 1H), 3.70 – 3.53 (m, 7H), 1.17 (t, J = 7.2 Hz, 3H). ^{13}C NMR (101 MHz, CD_3CN) δ 112.81, 65.36, 60.99, 59.53, 14.34.

3.10 Preparation of compound 6

In a 500 mL round-bottom flask, a solution of **1** and **2b** was prepared dissolving **1** (15.52 g, 250 mmol, 1 equiv.) and **2b** (37.09 g, 250 mmol, 1 equiv.) in 250 mL of acetonitrile. Then, 0.1 equivalent of formic acid (1.14 g, 24.7 mmol, 0.1 equiv.) was added to the solution to trigger the reaction. The medium was magnetically stirred and heated at 60 °C over 3 hours. The medium was then rapidly quenched with Na_2CO_3 and then, filtered to recover the neutralized solution. The reaction effluent was then purified by a vacuum distillation. ^{1}H NMR (400 MHz, CD_3CN) δ 5.79 (s, 1H), 4.07 – 3.85 (m, 4H), 3.55 (q, J = 7.1 Hz, 2H), 1.17 (t, J = 7.1 Hz, 3H). ^{13}C NMR (101 MHz, CD_3CN) δ 114.96, 63.68, 14.45. CAS 4544-20-1.

3.11 Preparation of compound 7

In a 50 mL round-bottom flask, a solution of **1** and **2b** was prepared dissolving **1** (7.76 g, 125 mmol, 1 equiv.) and **2b** (3.70 g, 25 mmol, 0.2 equiv.) in 25 mL of dry acetonitrile. Then, 0.02 equivalent of formic acid (0.115 g, 2.5 mmol, 0.02 equiv.) was added to the solution to trigger the reaction. The medium was magnetically stirred and heated at 70 °C overnight. The reaction medium was rapidly quenched with Na_2CO_3 and subsequently filtered to recover the neutralized solution The reaction effluent was then purified by a silica column separation using a mixture of 5:5 acetonitrile/ethyl acetate as eluent. ^{1}H NMR (400 MHz, CD_3CN) δ 5.81 (s, 1H), 4.09 – 3.84 (m, 4H), 3.63 – 3.48 (m, 3H). ^{13}C NMR (101 MHz, CD_3CN) δ 115.17, 65.60, 63.76, 60.94. CAS 30928-72-4.

3.12 Preparation of compound 9

In a 50 mL round-bottom flask, a solution of **1** and **6** was prepared dissolving **1** (0.5 g, 8 mmol, 1 equiv.) and **6** (4.14 g, 35 mmol, 4.4 equiv.) in 25 mL of acetonitrile. Then, 0.2 equivalent of formic acid (0.08 g, 1.7 mmol, 0.2 equiv.) was added to the solution to trigger the reaction. The medium was magnetically stirred and heated at 70 °C overnight. The reaction medium was rapidly quenched with Na_2CO_3 and subsequently filtered to recover the neutralized solution The reaction effluent was then purified by a vacuum distillation to remove the excess of **6**. ^{1}H NMR (400 MHz, CD_3CN) δ 5.80 (s, 1H), 4.06 – 3.83 (m, 4H), 3.60 (s, 2H). ^{13}C NMR (101 MHz, CD_3CN) δ 115.03, 63.77, 62.94. CAS 4544-19-8.

3.13 Preparation of compound 14

The same procedure as described in section S3.11 was performed. ^{1}H NMR (400 MHz, CD_3CN) δ 8.10 (t, J = 0.8 Hz, 1H), 4.20 – 4.13 (m, 1H), 3.73 – 3.64 (m, 2H). ^{13}C NMR (101 MHz, CD_3CN) δ 163.11, 65.30, 59.65.

4 Characterization of dynamic covalent exchange products

4.1 Structural characterization of a typical crude of DCE using 700 MHz NMR

4.1.1 Acyclic orthoesters identified by NMR

Based on NMR analysis, we identified two separate regions within 5-6 ppm range, which allowed to characterize the product distribution. Specifically, compounds in the spectral window of 5 - 5.30 ppm were attributed to acyclic orthoesters while their cyclic counterparts were found between 5.70 and 6 ppm (Figure S1- acidic proton in blue).

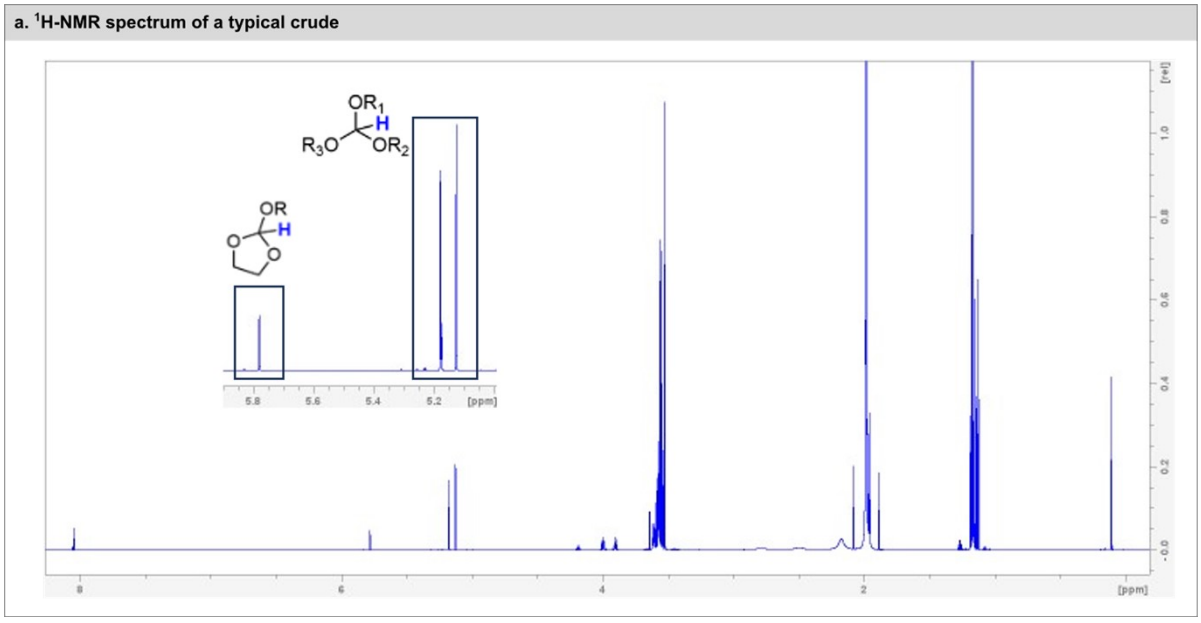


Figure S1 ^{1}H NMR of a typical crude of DCE (700 MHz – CD_3CN).

Focusing on the acyclic orthoester area, which includes **2b** and various intermediates, 2D-HSQC and HMBC experiments were combined to assign their signals (Figure S1) and determine their structures. The scaffold of the first acyclic product, species **3**, was elucidated by analyzing the correlations between the CH and CH_2 groups. Notably, the orthoformate proton at 5.18 ppm (Figure S2a – blue proton) exhibited correlations with two distinct types of CH_2 groups in the 2D-HMBC spectrum (2D-HMBC correlations highlighted in the green box). Examining the spectra of species **3** (Figure S2b), the first correlation appears to be similar to that of **2b**, specifically with a methylene from an ethoxy moiety (Figure S2b1). The second corresponds to that with a hydroxy ethoxy group (-O-CH_2-CH_2-OH) (Figure S2b2).

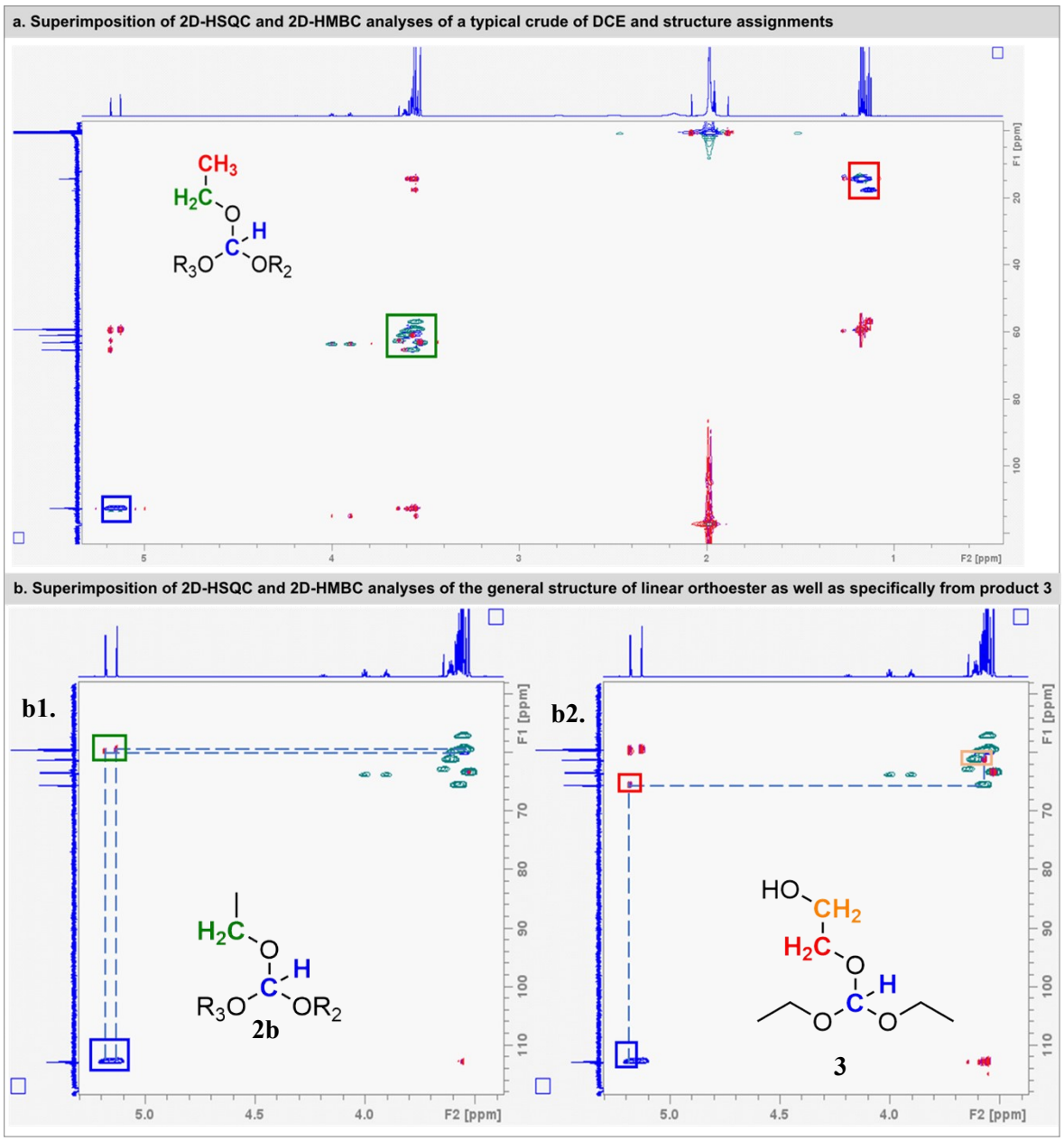


Figure S2 (a) Superimposition of the 2D-HSQC (blue-green signals) and HMBC (red) spectra obtained from a typical crude of DCE and corresponding assignments of the structural scaffold of acyclic orthoesters.; (b1) Superimposition of 2D-HSQC/HMBC correlations of **2b** and (b2), the acyclic product **3**.

A similar pattern of CH/CH_2 correlations is observed for the proton at 5.234 ppm, which corresponds to the second acyclic molecule **5** (Figure S3a). Conversely, the intensity of the correlation between the orthoformate proton and the hydroxy ethoxy group is greater than with the ethoxy group. This suggests that **5** results from the exchange of two molecules of **1** with **2b**. Additionally, a third compound **4** was identified. Unlike **3** and **5**, **4** does not show any correlation to an $O\text{-}CH_2\text{-}CH_2\text{-}OH$ group (Figure S3b). Instead, its orthoformate proton (5.175 ppm) is correlated to a CH_2 whose proton signal appears as a singlet, with a constant CH to CH_2 proton integration ratio of 1:2. Furthermore, the correlation to the ethoxy group is more intense.

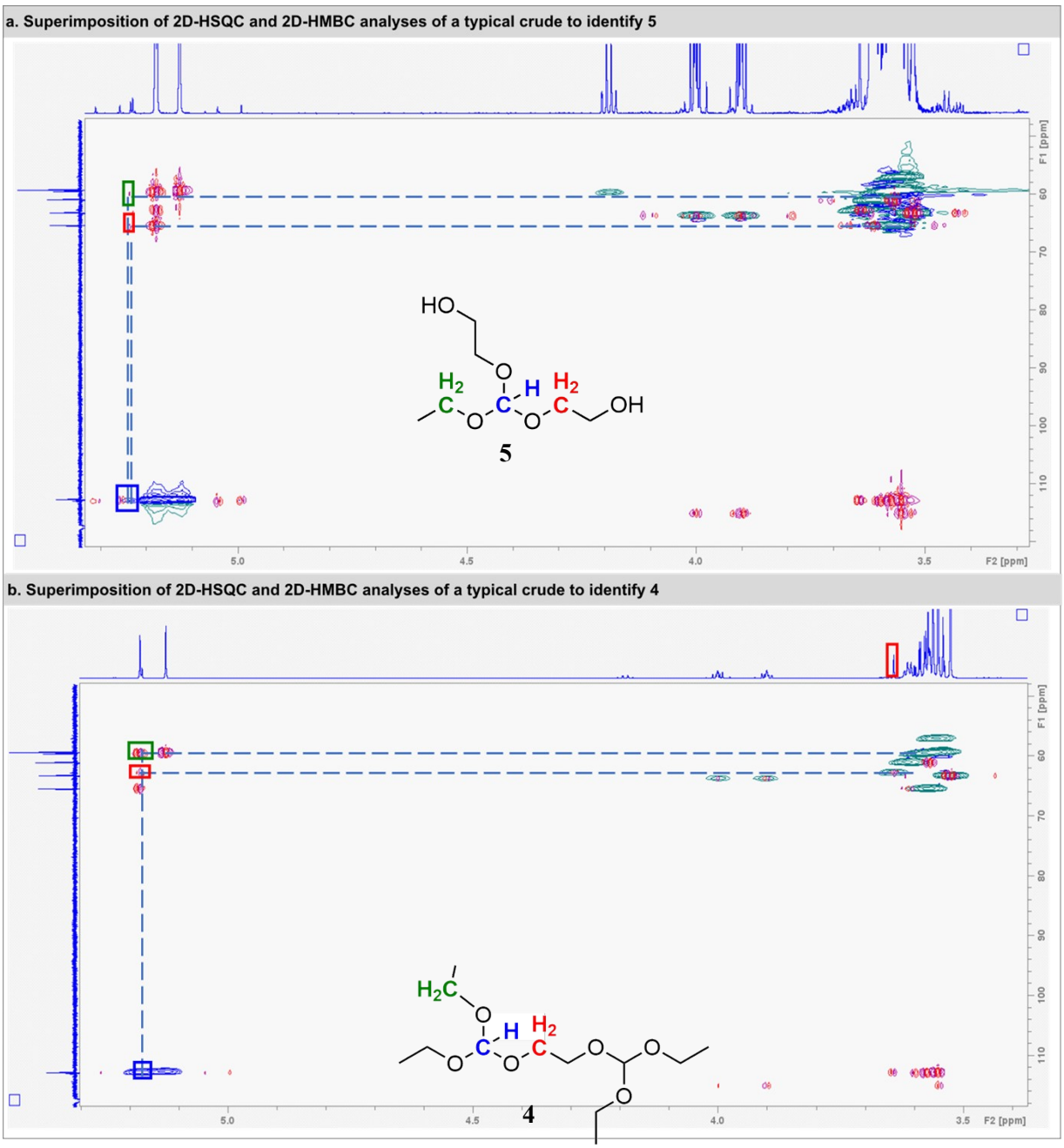


Figure S3 (a) Superimposition of the 2D-HSQC (blue-green signals) and HMBC (red) spectra obtained from a typical crude of DCE and corresponding assignments of the structural scaffold of acyclic orthoester **5;** and (b) **4**.

4.1.2 Cyclic orthoesters identified by NMR

Using the same approach for cyclic orthoesters, the structure of two products, **6** and **7**, was determined by NMR. Both compounds exhibited correlations with cyclic CH_2 groups (Figure S4a&b), with this correlation being the most intense for both. By increasing the intensity of the 2D-HMBC spectrum, an additional correlation to an ethoxy CH_2 then appears for **6** (Figure S4a), while **7** is correlated to an O-CH_2-CH_2-OH group (Figure S4b). Based on these findings, **6** and **7** are identified as dioxolanes substituted respectively by an ethoxy and an O-CH_2-CH_2-OH group.

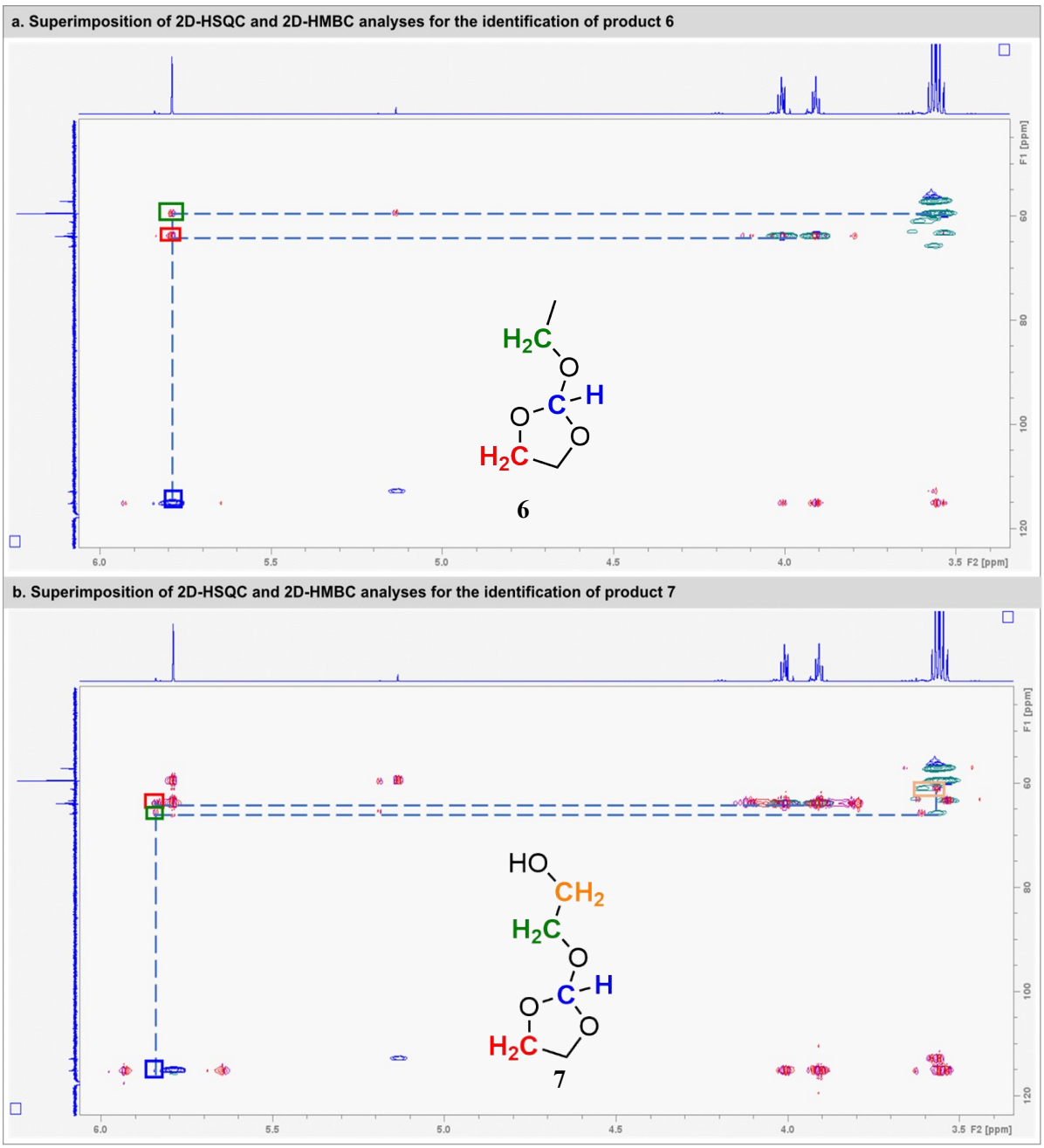


Figure S4 (a) Superimposition of the 2D-HSQC (blue-green signals) and HMBC (red) spectra and corresponding assignments of the structural scaffold of cyclic orthoester **6**; and (b) **7**.

Additionally, two formates were identified as hydrolysis products of **2b** and **3**: ethyl formate **13**, with a formate proton signal at 8.06 ppm, and 2-hydroxyethyl formate **14**, with a formate proton signal at 8.12 ppm (Figure S5). These assignments were based on the reference spectra of ethyl formate **13** obtained commercially (Section S12).

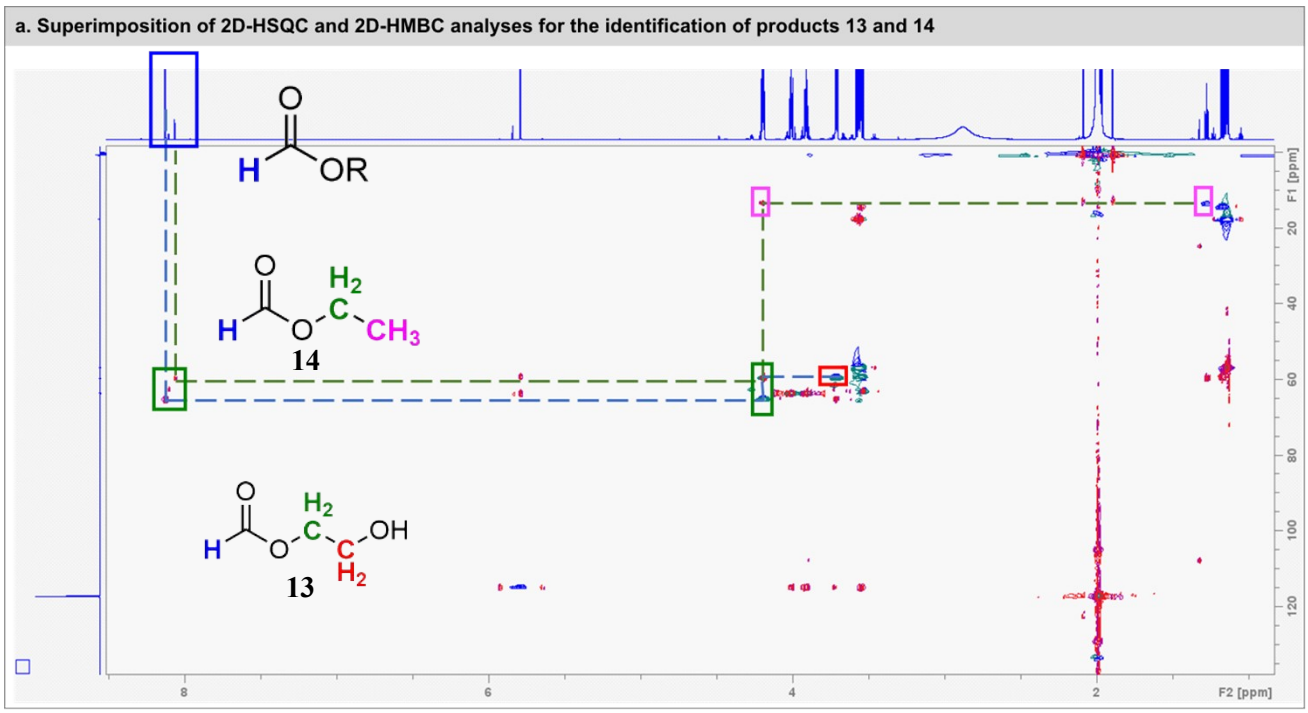


Figure S5 Superimposition of the 2D-HSQC (blue-green signals) and HMBC (red) spectra and corresponding assignments of the structural scaffold of side products **13** and **14**.

4.2 Structural characterization of the typical crude of DCE using GC-MS

Following NMR characterization, GC-MS provided another layer of useful information to the understanding of the reaction. First, as it allowed to confirm the structures previously determined by NMR. Then, as it allowed to characterize the reaction crude more deeply based on fragmentation patterns. Indeed, from the total ion chromatogram (TIC) (Figure S6a), it can be seen that many more products are formed throughout the reaction, underlining its complexity. While some of these minor products could be identified first by GC-MS and then by NMR, others could solely be identified by GC-MS.

Mass spectra and fragmentation patterns are reported in Section 12. Generally, all the fragmentation patterns observed for the acyclic and cyclic orthoesters include the systematic loss of the orthoformate proton from the molecular ion, leading to an m/z loss of 1 per orthoester, i.e. molecular ion was not detected. Besides, the isomerization of alcohol functions of **3**, **5**, **7** into aldehydes was observed, leading to an additional m/z loss of 2 per alcohol function (Figure S6b). Noteworthy, compounds **10** and **11** could only be observed by NMR.

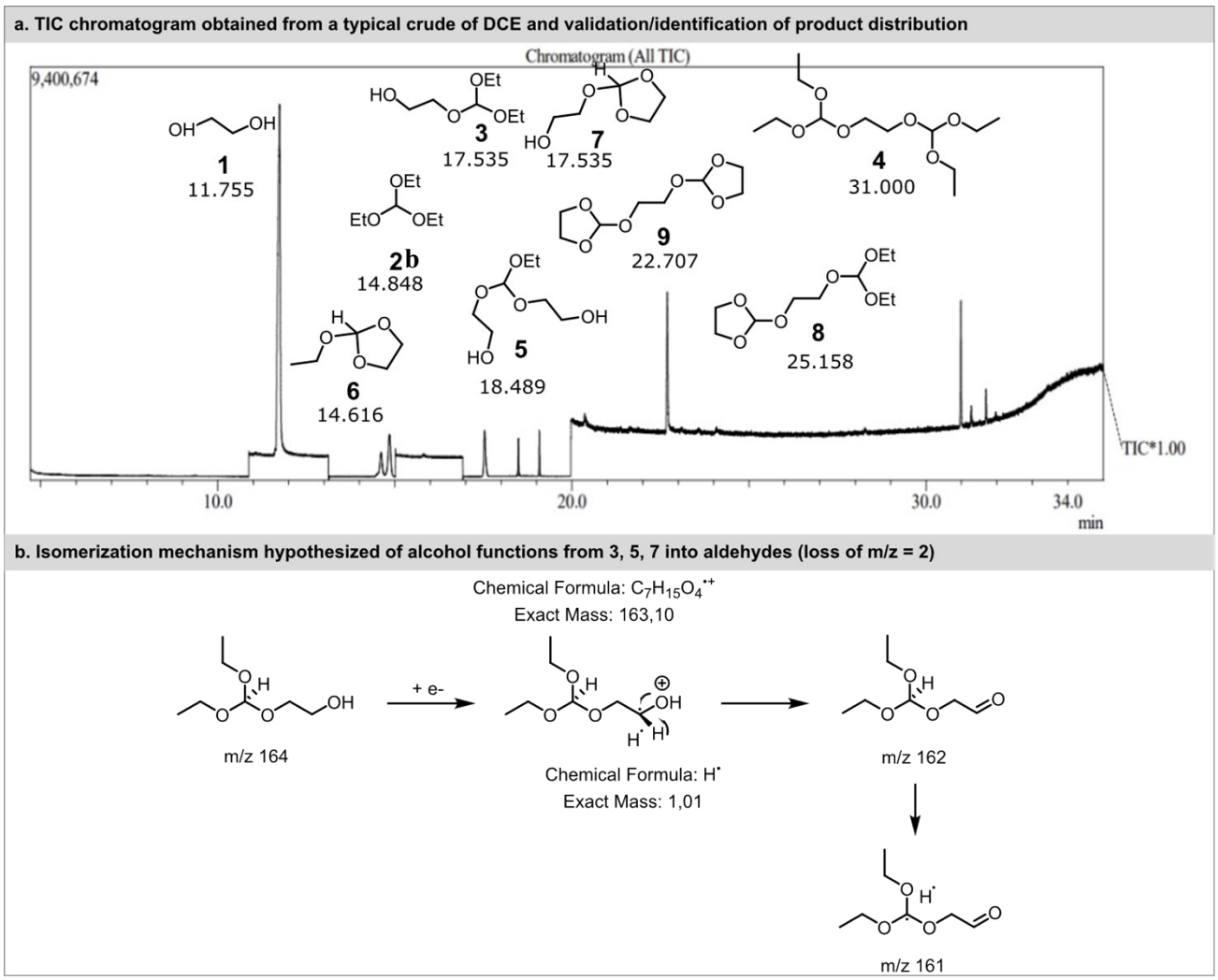


Figure S6 (a) TIC chromatogram obtained from a typical crude of DCE experiment and validation/identification of product distribution; (b) Hypothesized mechanism of alcohol isomerization into aldehydes.

5 Preliminary experiments of the DCE reaction using in-line NMR and stability assessment of samples over time

5.1 Kinetic studies in various conditions of temperature and concentrations

Preliminary experiments using stoichiometric amount of **1** and **2b** (described in section S5.1) were carried out at 0.58 and 0.72 M at 50°C as well as 0.72 M at 60 °C (Figure S7a&b). Higher temperatures were not considered due to the boiling point of acetonitrile, which is approximatively at 82 °C. Species quantification was based on the integration of **2b** signal before the addition of the acidic catalyst. The results showed that increasing the temperature from 50 to 60 °C at 0.58 M enhanced the reaction kinetic. However, the formation of products such as **7** remains very low, preventing any accurate quantification with the 43 MHz NMR, and we decided to further increase the concentration of **1** and **2b** to 0.72 M. These results are coherent and comparable to those obtained in the same conditions with an off-line high field NMR (700 MHz).

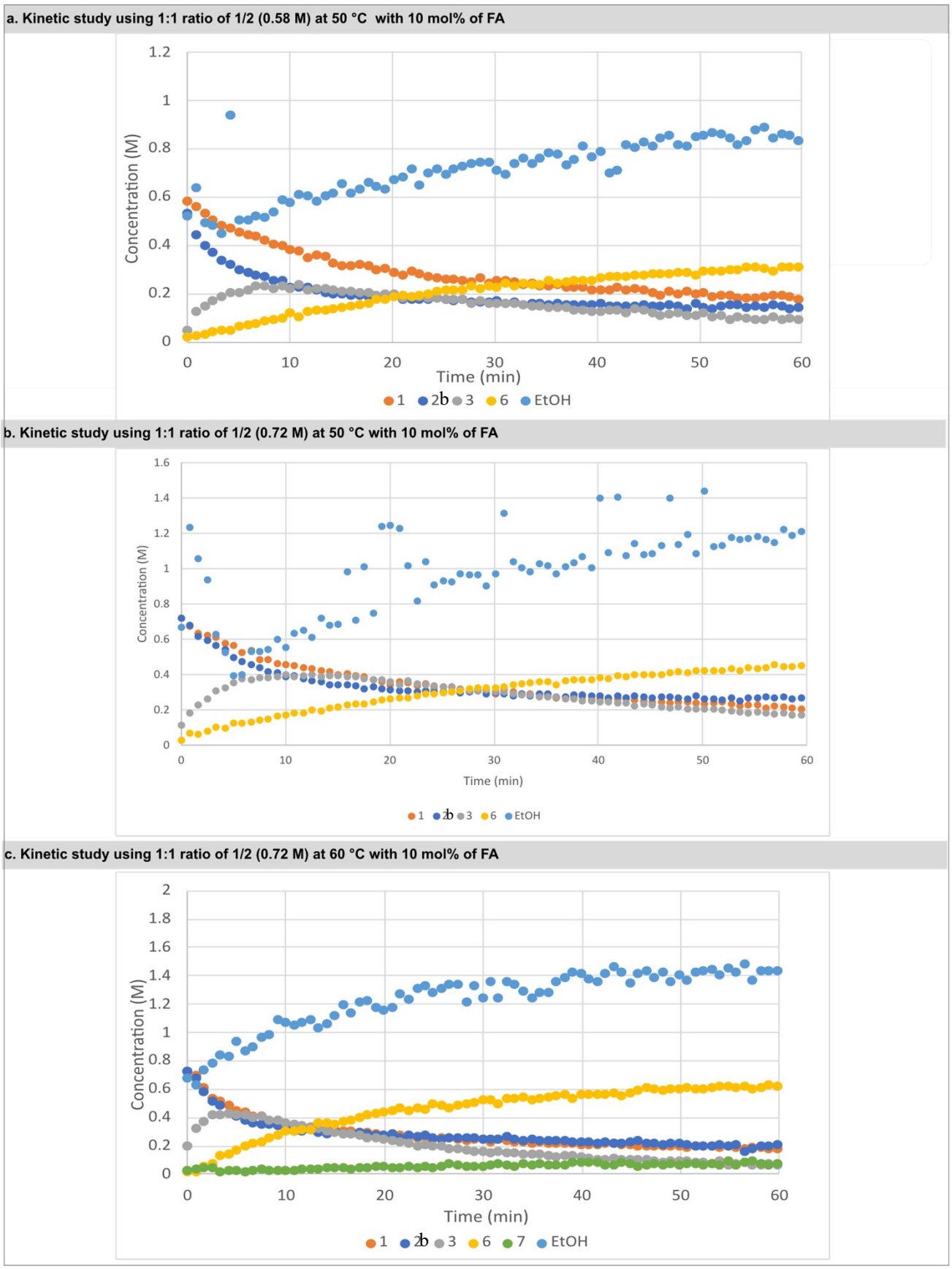


Figure S7 Kinetic studies using 1:1 ratio of **1**/**2b** at 0.58 M at 50 °C (a), 0.72 M at 50 °C (b) and 0.72 M at 60 °C (c) monitored by 43 MHz ™Spinsolve NMR (^{1}H NMR).

5.2 Stability of NMR samples over time

The ^{1}H-NMR analysis of the same crude sample was performed seven times at 15 min intervals to evaluate the stability of the collected samples throughout the kinetic study. The spectral windows corresponding to acyclic and cyclic orthoesters were integrated, and the calculated ratios between the two regions were compared. The integration of cyclic orthoesters was systematically calibrated to 1. Variations ranging from 0.2567 to 0.2624 were observed across repetitions, except for the last one, which showed a ratio of 0.2533. This suggests that NMR samples prepared as described in Section S1 can be reliably analyzed within 1 hour and 30 min after collection before slow degradation begins.

6 Python script 1: tensorial decomposition of ^{1}H-NMR raw data treated with a Fourier transform

6.1 Selection of non-negative Tucker decomposition

Our data posed two main constraints: the necessity for strictly positive factorized results to ensure realistic interpretation of NMR signal, and the three-dimensional nature of our data, which includes chemical shifts, intensity (from spectra) and, time (from kinetics). We considered a wide array of factorization methods to identify the most suitable algorithm. Classical methods like Principal Component Analysis (PCA) or Singular Value Decomposition (SVD) were quickly ruled out because their eigenvectors often contain negative values, creating artifacts like inverted signals in reconstructed ^{1}H spectra (physically impossible in 1H NMR data). Furthermore, these methods are inherently designed for 2D data structures and cannot efficiently capture the temporal dimension inherent in our dataset. Other methods, such as independent Component analysis (ICA), were also excluded because they assume statistical independence of components, which is unrealistic for NMR data. Non-Negative Matrix Factorization (NMF) was briefly considered but found inadequate for the handling of higher-dimensional data. Multivariate curve resolution (MCR) was also reviewed but require prior knowledge of either species concentration profiles or pure compound spectra present in the crude sample. Ultimately, we opted for tensor decomposition due to its ability to meet the requirement of non-negative factorization and handle higher-dimensional data. We considered two candidates: PARAFAC and Tucker decomposition. The latter was chosen for its ability to handle complex patterns involving combinations of temporal, chemical shifts and intensity dimensions, which is crucial for capturing the dynamic nature of chemical reactions.

6.2 Explanations of the script of non-negative Tucker decomposition

The Python script allows to perform a tensorial factorization of raw ^{1}H-NMR data using a non-negative tucker decomposition. This code was constructed as followed: (a) loading of data, (b) signal treatment, (c) transformation of data into tensors, (d) non-negative tucker analysis on the treated data and graphical output, (e) cross validation and graphical output, (f) operator decision according to the number of compounds (based rank) based on the graphical output,(g) and sensitivity analysis on the best rank as well as the precedent (best rank -1) and following rank (best rank +1). The script can be simply run by replying to the three dialog boxes generated during the whole code execution.

(a) Loading of data: a excel sheet must be provided following the required architecture: the first line contains the scale of time whereas the first column contains the chemical shifts. The first cell of the excel sheet must stay empty. Starting from that, every spectrum for a given time consists in a column. The loading of data is controlled by a dialog box that will open directly to the user explorer, allowing the user to select the proper excel file.

(b) Signal treatment: once the data are loaded, an automated treatment of data is performed, including a 2D medfilter and a Savitsky-Golay filter. Combination of both enables to improve the signal to noise ratio while maintaining the crucial spectral information such as signal width, height, proton coupling to name a few. This section eventually leads to the visualization of the treated data via a graphical output.

(c) Transformation of 2D matrix (NMR data) into a 3D tensor. This is performed by sequentially sampling the chemicals shifts in five matrices of same size, which allows to introduce a third dimension and use tensorial decomposition. As an illustration, chemical shifts at 1, 1.01, 1.02, 1.03 and 1.04 ppm are each going to be separated in a different matrix.

(d) Non-negative tucker analysis on the treated data and graphical output: a non-negative decomposition was selected to ensure the positive nature of NMR data but can also work for other spectral methods such as Raman or Infra-red spectroscopy. Data are then factorized according to 1 to 12 ranks, which corresponds in 1 to 12 species potentially present within the NMR kinetic data. Upstream to this decomposition, a non-negative matrix factorization (NMF) is implemented on the data. This 2D factorization is initialized by a NNDSVDAR (non-negative double singular value decomposition with alternating random initialization), using a coordinate descent (CD) solver, regularization strengths for αH and αW set at 0.1, a L1 ratio of 0.01 and Frobenius Norm as a cost function. This factorization gave the matrices of component and coefficient W and H respectively, which are subsequently used to initialize the two first factors (two first dimensions) of the non-negative tucker decomposition, fastening the computation time. The third factor is randomly generated due to NMF limitation to 2D matrixes. The tensor core is also randomly generated. Upon tensorial decomposition, a reconstructed tensor is calculated for every rank. Quantitative metrics are then calculated to evaluate the accuracy of the reconstructed tensor, comprising the relative error of reconstruction (rel_error) of a tensor X (dimensions IxJxK) and the explained variance relying on Frobenius norm $(\|\|_F)$:

$$\| X \|_F = \sqrt{\sum_{i=1}^{m}\sum_{j=1}^{n} |a_{i,j}|^2}$$

$$rel_error = \frac{\| X - X_{approx} \|_F}{\| X \|_F}$$

$$explained_variance = 1 - rel_error$$

Where X corresponds to the original matrix and X_{approx} to the reconstructed matrix obtained from the non-negative Tucker algorithm

(e) Cross validation: a temporal cross validation is performed on the unfolded tensors at each rank. Tensor unfolding consists of converting a 3D tensor into a 2D matrix, generating the same dimension and shape of data initially introduced in point (a). The unfolded matrixes of each rank are then evaluated along the time dimension. Training starts with the first 5 times of the original data, and the models developed in point (d) are tested on the next point (the 6th). At each iteration, the Bayesian information criterion (BIC) and the Akaike information criterion (AIC) are calculated. The process is repeated for subsequent time points, from the 6th up to the last one. Finally, the mean BIC and AIC values are calculated for each rank. These statistical criteria help determine the best trade-off between model accuracy and complexity.

$$BIC = n * \ln\left(\frac{RSS}{n}\right) + k * \ln(n)$$

$$AIC = n * \ln\left(\frac{RSS}{n}\right) + 2 * k$$

RSS corresponds to residual sum of squares, n to the number of observations from the dataset and, k to the total number of parameters in the model.

(f) Operator decision: all these parameters are presented in a graphical output along the derivative of both the reconstruction error, the explained variance, the learning curves, the error derivative and training error evolution obtained for each rank (Figure S7). Based on these results, the user is asked to provide the best rank according to the quantitative metrics.

(g) Sensitivity analysis on the best rank and best rank±1: Once the best rank is determined, 10 repetitions of the non-negative Tucker decomposition are performed with 10 distinct NMF initializations. The relative error and explained variance are calculated for each tensor in every iteration. A second graphical output is then generated, displaying the variability of these two quantitative metrics for the best rank and best rank ±1. This provides insight into the variability of the results across different initializations and an assessment of the decomposition's robustness. Additionally, a hypothesis regarding the concentration profile is presented for each rank.

This tool provides preliminary statistical indicators to assist in the analysis of complex NMR kinetic data. It is designed to estimate a minimal number of compounds present in the mixture and guide targeted sampling for more advanced analyses. However, this tool does not replace a complete structural characterization. Its output should be considered as a working hypothesis to be validated, a guide to assist in optimizing subsequent reactions and a filter to narrow the search space. Efficiency of the tool is drastically demised for the identification of trace species as well as for compounds with multiple overlaps.

7 Python script 2: kinetic modelling of stoichiometric amount of 1 and 2 using 10 mol% FA in dry acetonitrile

7.1 Description of Python script 2

This script was inspired by the available '*Chemical Kinetics*' package, which utilizes the lmfit package to solve systems of differential equations.[1,2] It has been enhanced by incorporating quantitative metrics and quantile-quantile plots, enabling a more thorough evaluation of model accuracy, along with a user-friendly data loading process as presented in section S6. All figures generated by the script are saved in a folder selected by the user. This script can be easily utilized by following these steps: (a) loading the data, (b) formulating the differential equations, and (c) providing an initial approximation of the rate constants and concentrations.

(a) Loading of data: a CSV file must be provided following the required format: the first row contains the compound names, while the columns contain their respective concentrations. The first cell of the sheet must be labeled "t", and its column should contain the time data. Data loading is managed through a dialog box that automatically opens the user's file explorer, allowing them to select the appropriate Excel file. Immediately after, a second dialog box appears, prompting the user to choose a folder for saving the generated figures.

(b) Formulating the differential equations: this part is illustrated in the code provided with the supporting information (Figure S8).

```
def derivatives(y, t, p):

    """Calculates the derivatives of the concentrations at t.

    Used scipy.integrate.odeint to numerically solve the differential
    equations in a given time range.

    Lists ("y" and "dy") used by scipy.integrate.odeint are converted
    to dictionaries ("c" and "dc") in order to make the differentials
    easier to write and read for humans.

    Parameters:
        y (list): concentration values at t
        t (float): time value where the derivatives are calculated
        p (dict): dictionary containing the parameters used to
        calculate the derivatives e.g. time constants
    """

    # list ("y") to dict ("c") conversion
    c = { "I3" : y[0],"I1" : y[1], "TEOF" : y[2],"EG" : y[3], "P1" : y[4], "EtOH" : y[5], "I2" : y[6]}

    # calculate the differentials
    dc = dict()
    dc["I3"] = p["k_1"]*c["TEOF"]*c["I1"] + p["k_12"]*c["I1"]*c["I1"] - p["k_6"]*c["I3"]*c["EG"] - p["k_2"]*c["EtOH"]*c["I3"]

    dc["I1"] =  p["k_2"]*c["EtOH"]*c["I3"] + p["k_8"]*c["EtOH"]*c["I2"] - p["k_3"]*c["EtOH"]*c["I1"] - p["k_12"]*c["I1"]*c["I1"]

    dc["TEOF"] = p["k_2"]*c["EtOH"]*c["I3"] - p["k_1"]*c["TEOF"]*c["I1"] + p["k_3"]*c["EtOH"]*c["I1"] - p["k_4"]*c["EG"]*c["TEOF"]

    dc["EG"] =   + p["k_8"]*c["EtOH"]*c["I2"] + p["k_3"]*c["EtOH"]*c["I1"] - p["k_4"]*c["EG"]*c["TEOF"] - p["k_7"]*c["EG"]*c["I1

    dc["P1"] = + p["k_5"]*c["I1"] - p["k_11"]*c["P1"]*c["EtOH"] - p["k_41"]*c["P1"]*c["EG"]

    dc["EtOH"] = - p["k_2"]*c["EtOH"]*c["I3"] - p["k_8"]*c["EtOH"]*c["I2"] + p["k_4"]*c["EG"]*c["TEOF"] + p["k_5"]*c["I1"]

    dc["I2"] =  + p["k_7"]*c["EG"]*c["I1"] + p["k_41"]*c["P1"]*c["EG"] - p["k_8"]*c["EtOH"]*c["I2"]









    # dict ("dc") to list ("dy") conversion
    dy = [dc["I3"],dc["I1"], dc["TEOF"], dc["EG"], dc["P1"], dc["EtOH"], dc["I2"]]

    return dy
```

Figure S8 Formulation of the differential equations in the Python script.

(c) Initialization of the rate constants and concentrations has to be done in the Python script (two distinct dictionaries): this part is illustrated in the script provided with the supporting information.

7.1.1 Evaluation of model accuracy: coefficient of determination (R^2)

The calculation of R^2 is performed as the difference between 1 and the ratio of the sum of squared differences between the observed values (y_i) and the predicted values ($y_{i\ approx}$) to the sum of squared differences between the observed values and their mean (y_{mean}).

$$R^2 = 1 - \frac{\sum_{i=1}^{n}(y_i - y_{i_{approx}})^2}{\sum_{i=1}^{n}(y_i - y_{mean})^2}$$

The calculation of R^2 includes an interpolation function to match the number of experimental points with those of the theoretical fit (150 time points).

7.1.2 Evaluation of model accuracy: Root Means Square Error (RMSE) and Mean Average Error (MAE)

Calculation of RMSE and MAE are performed as follows:

$$RMSE = \sqrt{\frac{1}{n} * \sum_{i=1}^{n}(y_i - y_{i_{approx}})^2}$$

$$MAE = \frac{1}{n} * \sum_{i=1}^{n}|y_i - y_{mean}|$$

7.1.3 Bayesian Criterion Information (BIC) and Akaike Information Criterion (AIC)

The calculation of BIC and AIC follows the approach outlined in Section 6d. Here, k represents the number of constants used in the system of differential equations, while n corresponds to the total number of experimental data points.

7.1.4 Quantile-quantile plots

Details about the calculations are described into the script provided with the supporting information.

7.2 Calculation of equilibrium constants (*K*)

The equilibrium constants (*K*) have been calculated from the rate constants of reversible reactions. These reactions may exhibit different order dependencies in the forward and reverse directions. For instance, reversible reaction can display a two-order dependency towards a product and a one order dependency back to the reagents. In these cases, the calculated *K*' value possesses units reflecting the difference in reaction order between forward and reverse reactions. In this work, only rate constants and *K* of same unit or unitless are compared in order to facilitate the discussion. When *K*>> is indicated in a figure, it means that the reaction is considered irreversible under this set of experimental conditions.

All references to compounds **2**, **2.1** and **2.2** in the figures and tables correspond specifically to compounds **2b**, **2a** and **2c** respectively.

7.3 Methodology to refine kinetic models and working hypothesis

As working hypothesis, the system of differential equations formulated for each product always includes the reversibility of each step. Once the model is obtained, neglectable contributions from either the reversible reaction or non-occurring reaction between species are removed.

7.4 Development of model I including species 1, 2b, 3, 5, 6 and EtOH

First modeling of the dynamic covalent exchanges toward orthoesters comprised reagents **1** and **2b** as well as the first product of their reaction, intermediate **3**, as well as **5** and **6**.

7.4.1 Model I

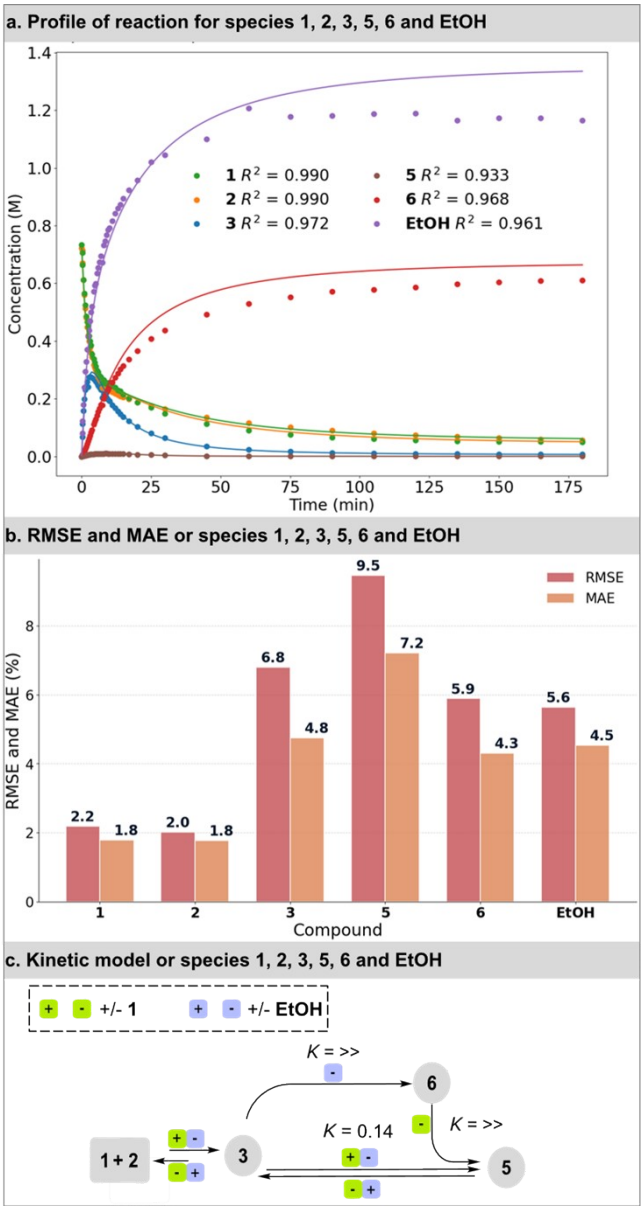


Figure S9 (a) Profile of concentrations of the various species **1**, **2b**, **3**, **5**, **6** and **EtOH** over time; (b) RMSE and MAE obtained from **model I**; and (c) the system obtained from kinetic modelling of NMR data with the theoretical **model I**.

7.4.2 Quantile-quantile plot of model I

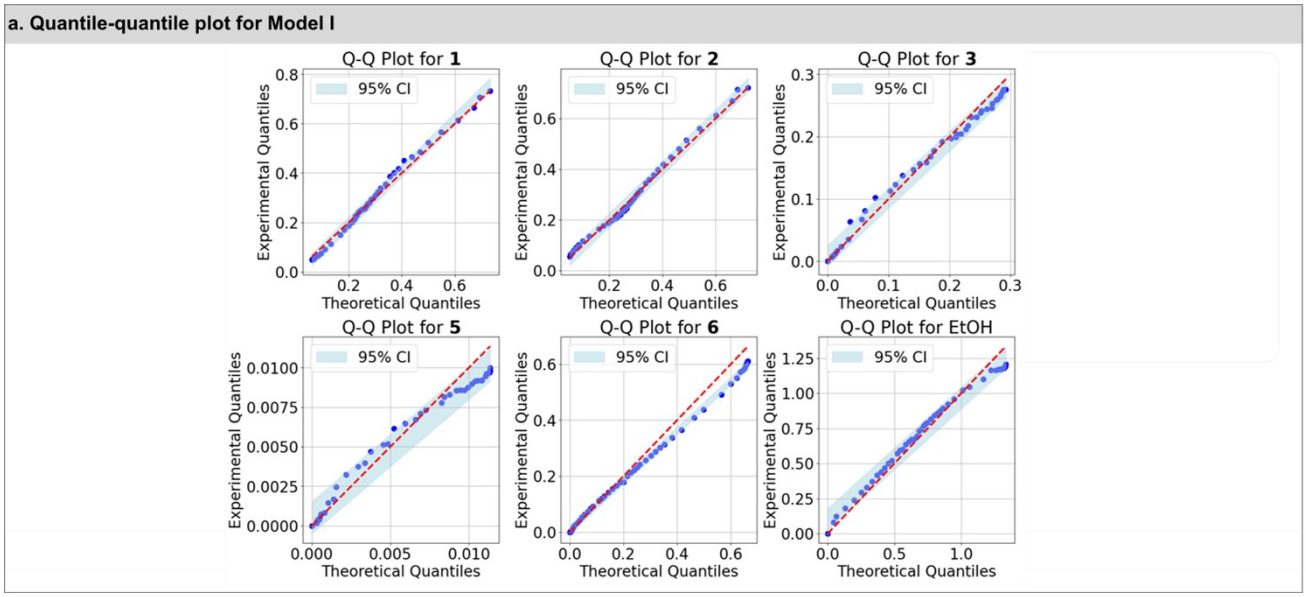


Figure S10 Quantile-quantile plot obtained from the species **1**, **2b**, **3**, **5**, **6** and **EtOH** with **model I**.

7.5 Development of model II including species 1, 2b, 3, 4, 5, 6 and EtOH

7.5.1 Profile of concentrations and comparison of RMSE and MAE for model II comprising either path (a) or (b) or both (a&b)

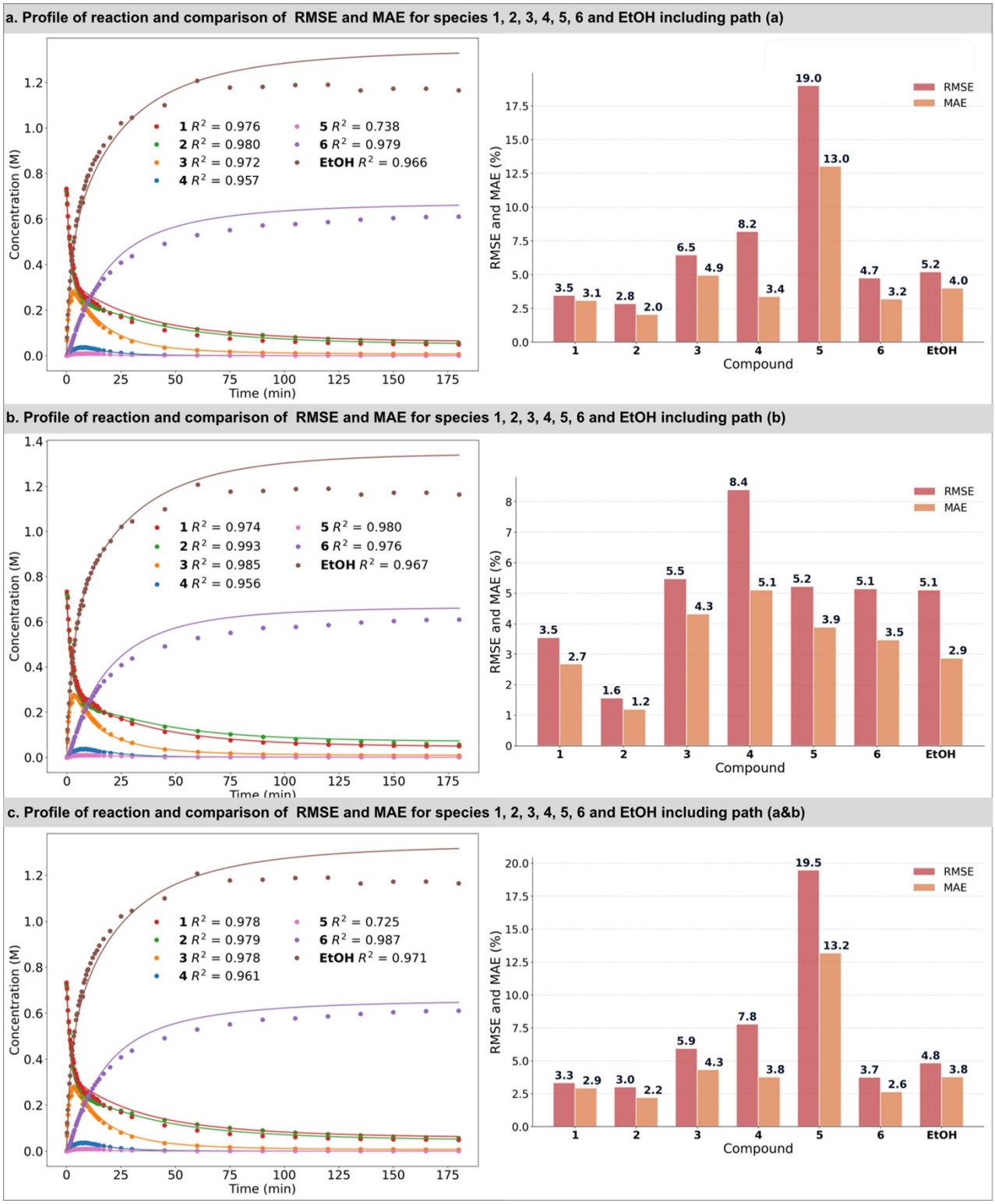


Figure S11 Profile of concentrations of the various species **1**, **2b**, **3**, **5**, **6** and **EtOH** over time and RMSE and MAE obtained from **model II** including path (a), (b) or (a&b).

7.5.2 Quantile-quantile plot for model II including path (a), (b) or (a&b)

Despite the accurate description obtained thus far for each species, the Q-Q plot generated for each species including a 95% confidence intervale clearly indicates that **model II** is incomplete, with residuals of **1**, **2b** and **5** that do not follow a normal distribution.

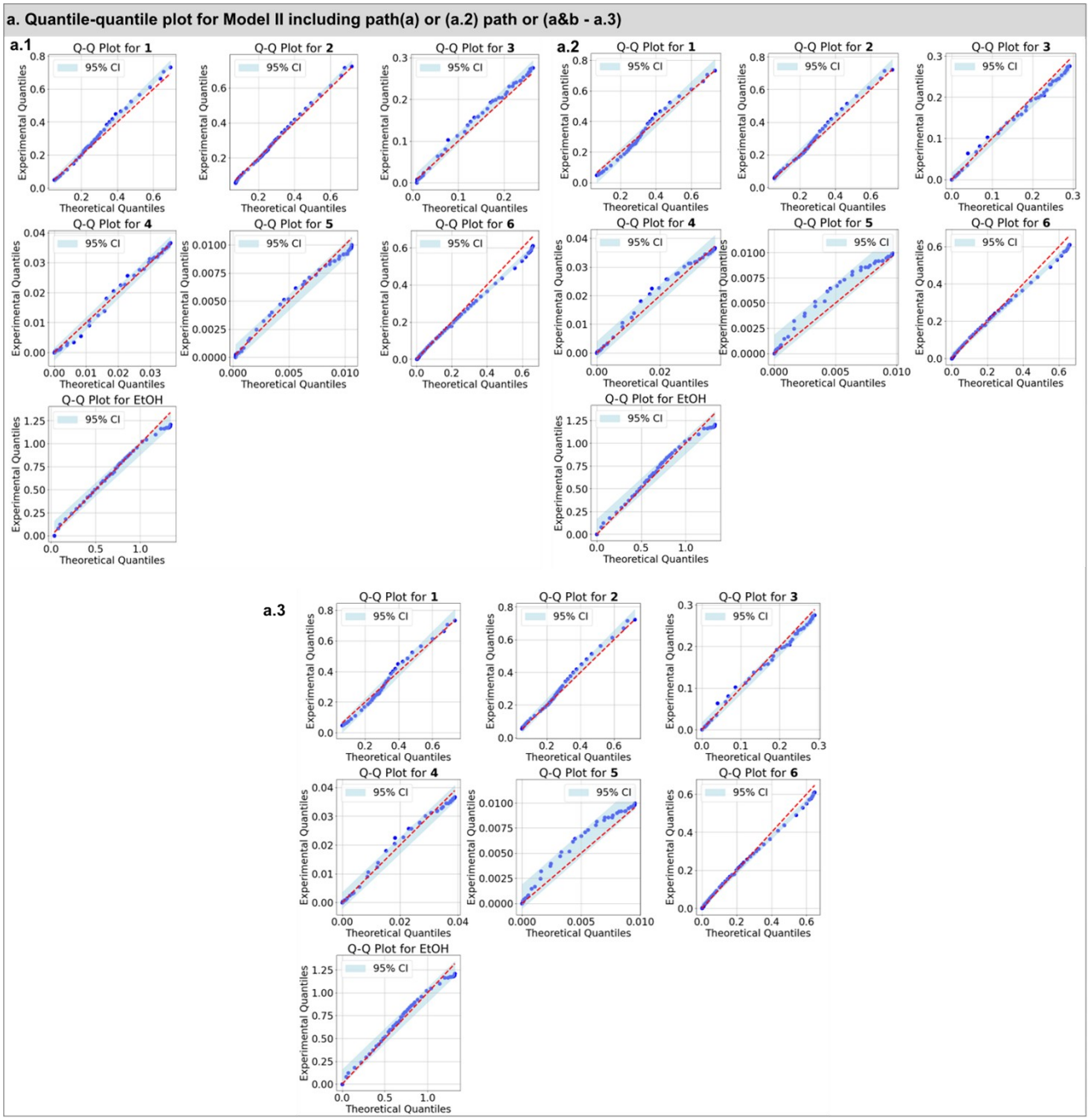


Figure S12 Quantile-quantile plots obtained from the species **1**, **2b**, **3**, **4**, **5**, **6** and **EtOH** using **model II** including path (a – a.1), (b – a.2) or (a&b – a.3).

7.5.3 Final model II of 1 to 6 including path (b)

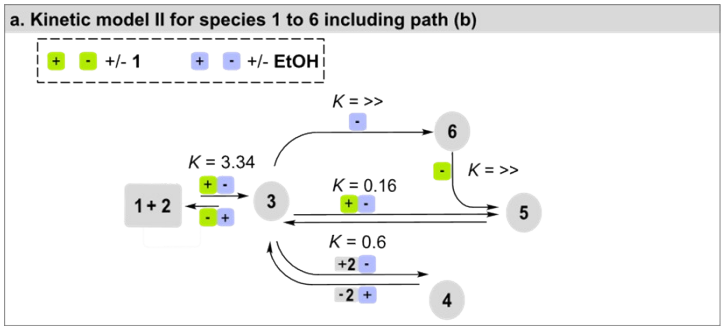


Figure S13 Reaction system obtained from kinetic modelling of NMR data with the theoretical **model II**.

7.6 Development of model III including species 1, 2b, 3, 5, 6, 7 and EtOH

7.6.1 Model III including path (a), (b) or (a&b)

Figure S14 displays the kinetics for model III including either the intramolecular cyclization of **5** into **7** (path a) or the substitution of **6** with **1** (path b). **Model III** is derived only from path a, providing a poor accuracy over the experimental data. By contrast, adjustment of **model III** with path b leads to a high improvement in model accuracy, especially for **5** and **7**, with RMSE values reduced from 34% and 24% to 5% and 3%, respectively.

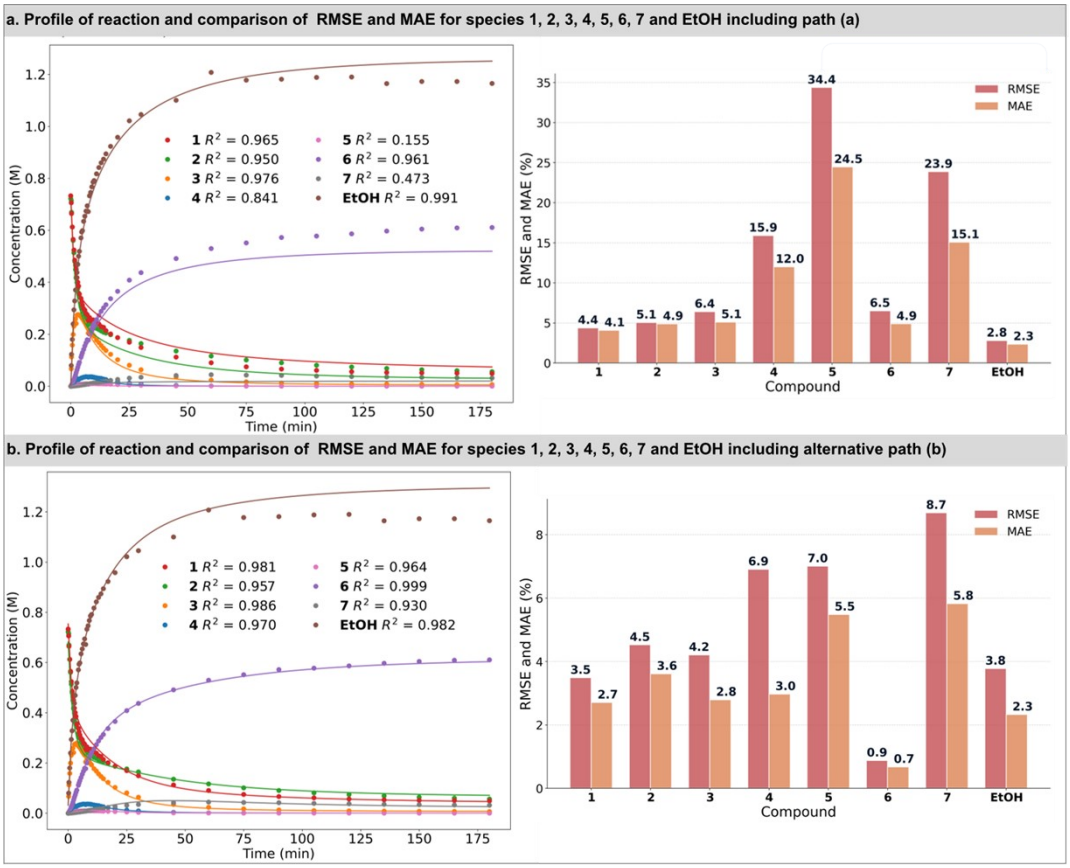


Figure S14 Profile of concentrations of the various species **1**, **2b**, **3**, **5**, **6**, **7** and **EtOH** over time and RMSE nd MAE obtained from **model III** including path (a), (b) or (a&b)

7.6.2 Quantile-quantile plots for model III including path (a) or (b)

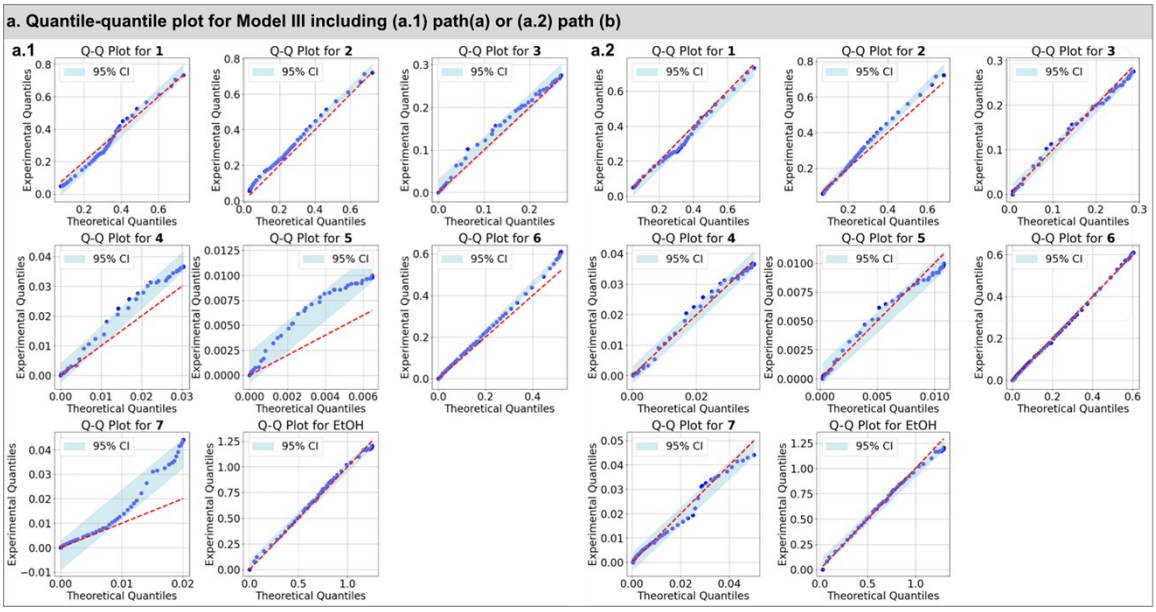


Figure S15 Quantile-quantile plots for model III including path (a) or (b).

7.6.3 Model III including path (a&b) with/without the formation of 4 from 2 molecules of 3

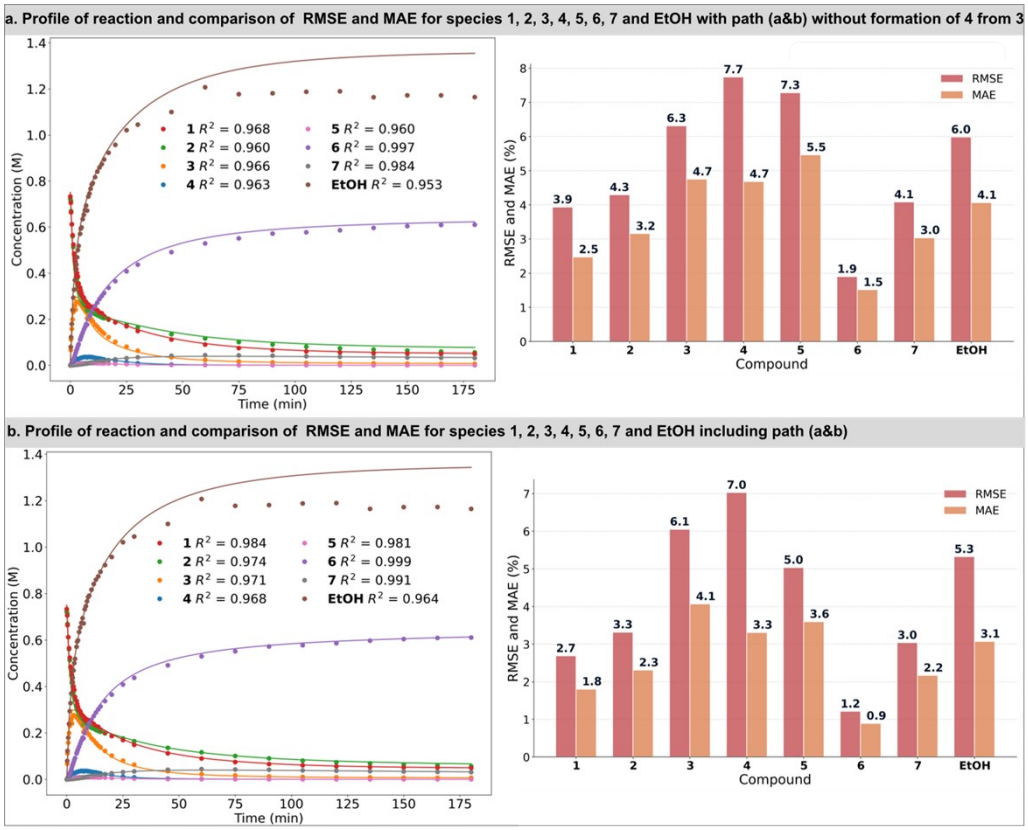


Figure S16 Profile of concentrations of the various species **1**, **2b**, **3**, **5**, **6**, **7** and **EtOH** over time and RMSE and MAE obtained from **model III** including path (a&b) with/without formation of **4** from 2 molecules of **3**.

7.6.4 Quantile-quantile plot for model III including path (a&b) including the formation of 4 from 2 molecules of 3

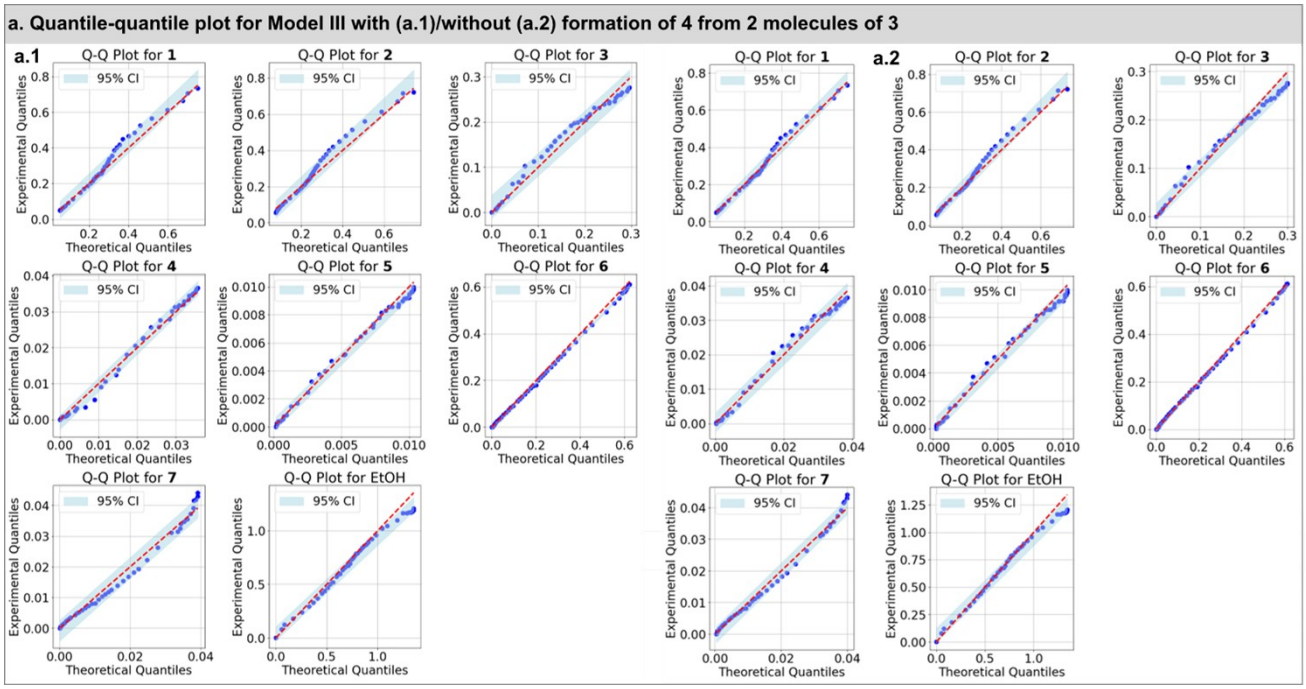


Figure S17 Quantile-quantile plots for **model III** including path (a) or (b).

7.6.5 Final model of 1 to 7 including path (a&b) including formation of 4 from 2 molecules of 3

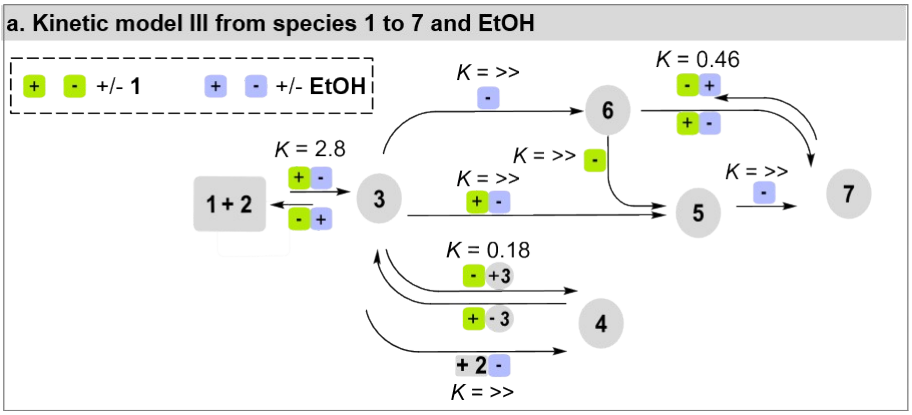


Figure S18 Reaction system obtained from kinetic modelling of NMR data with the theoretical **model III**.

7.7 Kinetic study using an excess of 100:1 ratio of 1/2b using off-line NMR

This kinetic study was performed to validate the occurrence of path b (Section S7.6). Using a large excess of **1** allowed to both shift the equilibrium toward the cyclic species **6** and **7**, and to ease kinetic modeling by considering pseudo first order conditions. The resulting kinetic model validated the hypothesis and competitive mechanisms toward **7**. Contrasting with **model III** in stoichiometric amount, the rate constant toward the formation of **3** is very high, at 3.15 L $mol^{-1}s^{-1}$, logically attributed to the excess of **1**. However, reversible reactions driven by **EtOH** still occur, hampering the formation of thermodynamic products **7** and its tri-hydroxylated species **11** (characterization in Section 12).

7.7.1 Model using a 1/100 ratio of 2b/1

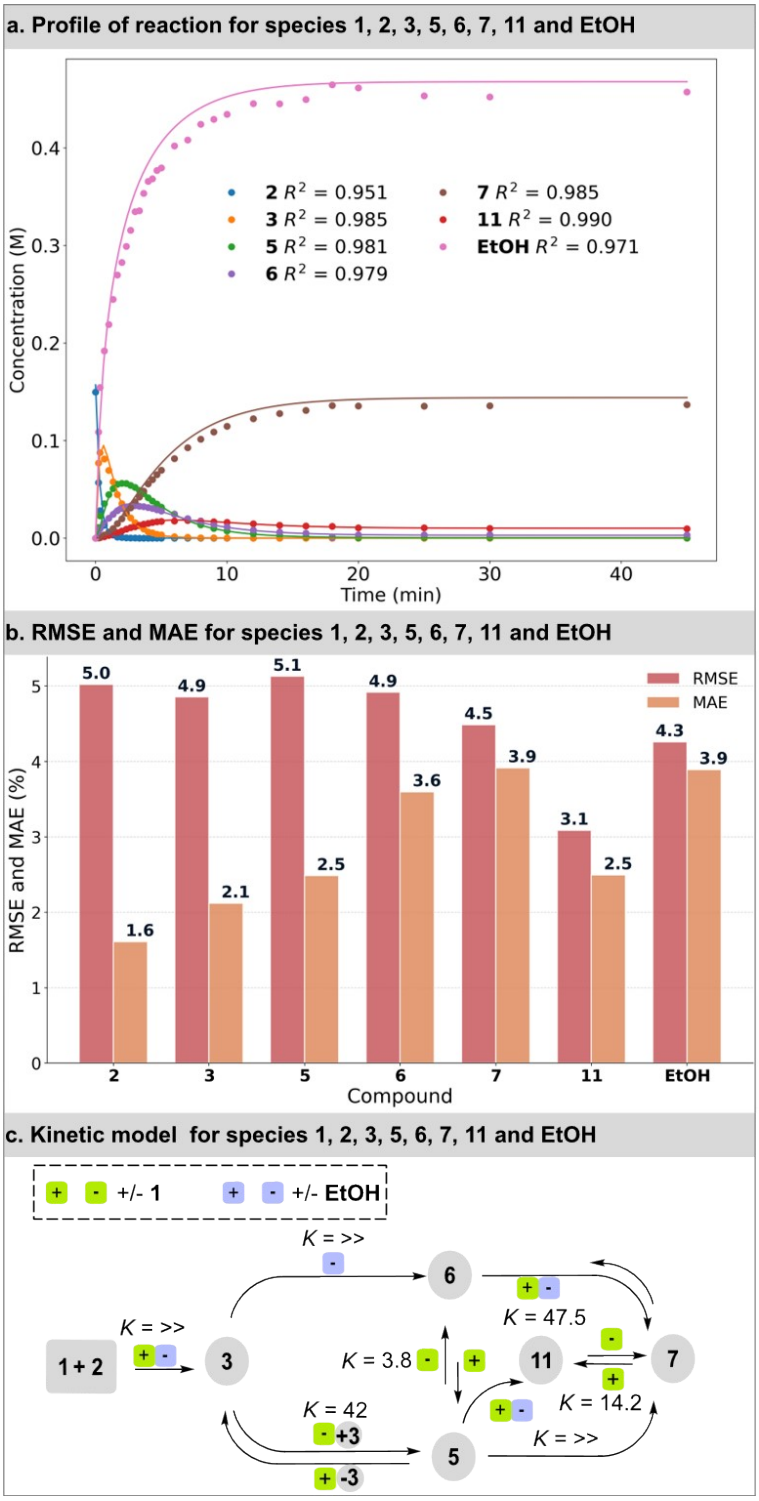


Figure S19 (a) Profile of concentrations of the various species **1**, **2b**, **3**, **5**, **6**, **7** and **EtOH** over time; (b) RMSE and MAE obtained; and (c) the system obtained from kinetic modelling of NMR data with the theoretical model.

7.7.2 Quantile-quantile plot

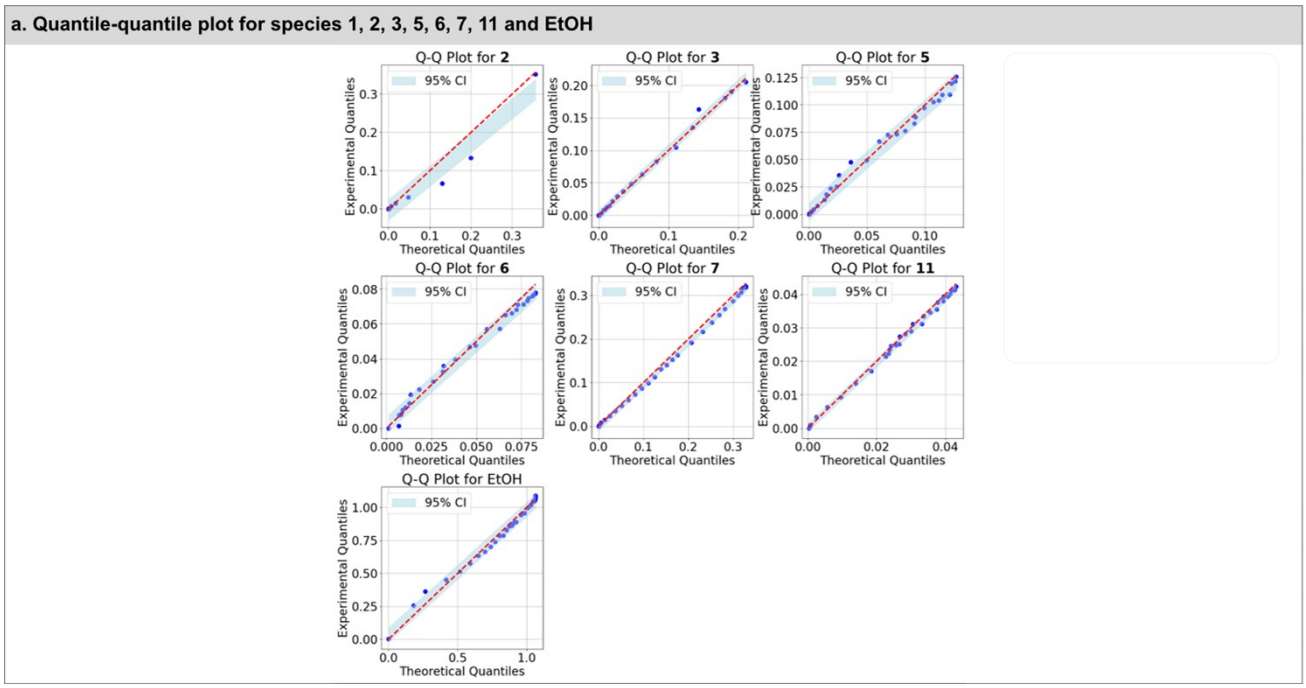


Figure S20 Quantile-quantile plots for model with 100:1 ratio of **1**/**2b**.

7.7.3 System of differential equations describing the kinetic model

This kinetic study was conducted with a large excess of **1**, allowing it to be considered constant throughout the reaction, achieving a pseudo-first-order reaction with respect to **1**.

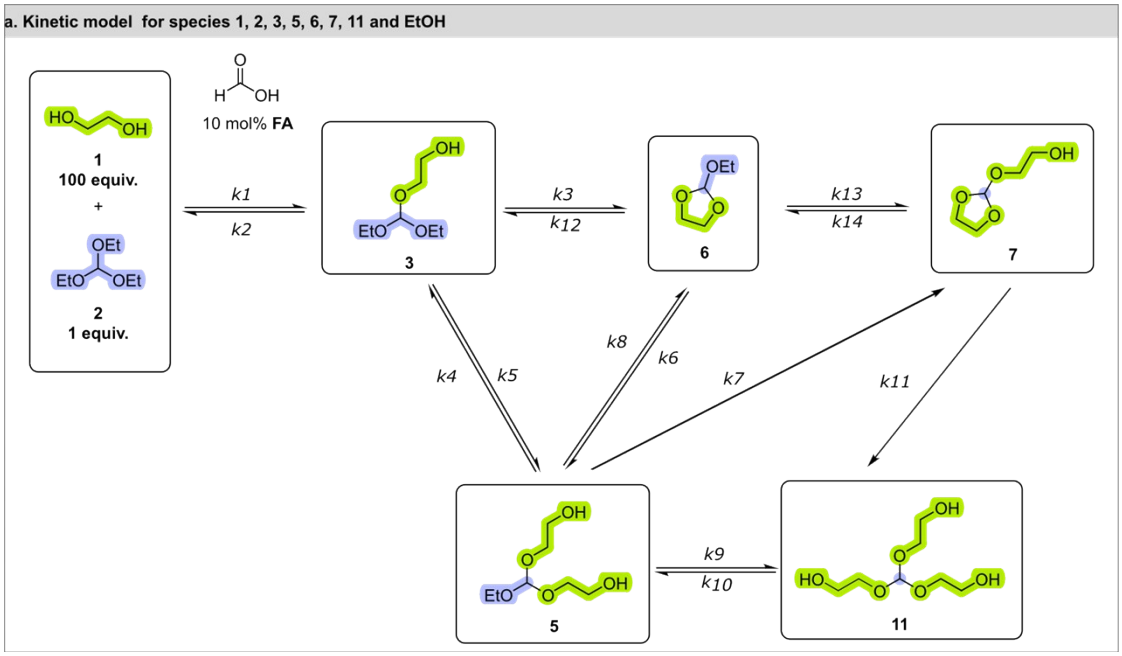


Figure S21 Representation of kinetic model including the rate constants.

$$\frac{dC[2]}{dt} = -\ k1 * [2] + k2 * [3] * [EtOH]$$

$$\frac{dC[3]}{dt} = \ k1 * [2] - k2 * [3] * [EtOH] - k3 * [3] - k4 * [3] + k5 * [3] - k4 * [5] * [EtOH]$$

$$\frac{dC[5]}{dt} = \ k5 * [3] - k4 * [5] * [EtOH] + k6 * [6] - k7 * [5] - k8 * [5] + k10 * [11] * [EtOH] - k9 * [5$$

$$\frac{dC[11]}{dt} = \ -k10 * [11] * [EtOH] + k9 * [5] + k11 * [7]$$

$$\frac{dC[6]}{dt} = \ -k12 * [6] * [EtOH] - k6 * [6] + k8 * [5] - k13 * [6] + k3 * [3] - k14 * [7] * [EtOH]$$

$$\frac{dC[7]}{dt} = k7 * [5] + k13 * [6] - k14 * [7] * [EtOH] - k11 * [7]$$

$$\frac{dC[EtOH]}{dt} = k1 * [2] - k2 * [3] * [EtOH] + k3 * [3] + k5 * [3] - k4 * [5] * [EtOH] + k7 * [5] - k12 * [6] * [EtOH] - k14 * [7] * [EtOH] + k13 * [6] + k9 * [5]$$

7.7.4 Model initialization and calculated concentrations and rate constants

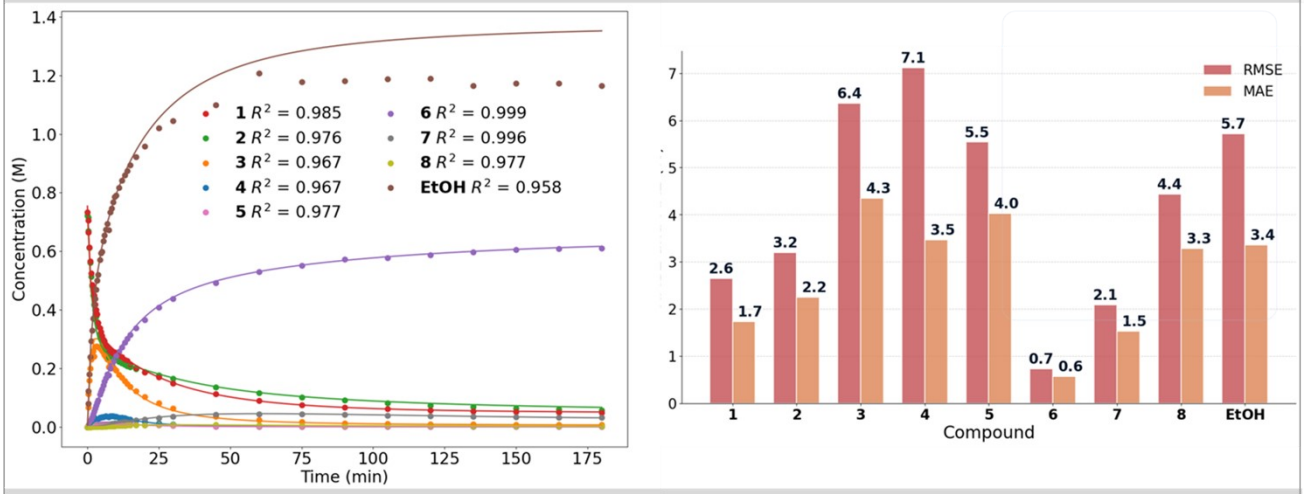
Table S2 Model initialization with calculated concentrations and rate constants for kinetic study using a 1:100 ratio of **2b**/**1**.

Calculated rate constants		Model initialization		Optimized values of initialization		R^2	RMSE	MAE
k_2	0.0458	c0_2	0.15	c0_2	0.156	0.95	0.00751	0.00239
k_1	3.23	c0_3	0	c0_3	0	0.985	0.00429	0.00185
k_3	0.292	c0_5	0	c0_5	6.92e-05	0.98	0.00294	0.00141
k_12	9.93e-06	c0_11	0	c0_11	0.000159	0.992	0.000493	0.000402
k_5	0.619	c0_6	0	c0_6	7.69e-05	0.979	0.00164	0.0012
k_4	0.0287	c0_7	0	c0_7	0.000262	0.988	0.00539	0.00467
k_7	0.137	c0_EtOH	0	c0_EtOH	9.99e-07	0.978	0.0175	0.0156
k_13	0.281							
k_8	0.0972							
k_6	0.0383							
k_14	0.0135							
k_9	0.122							
k_10	0.229							
k_11	0.0158							

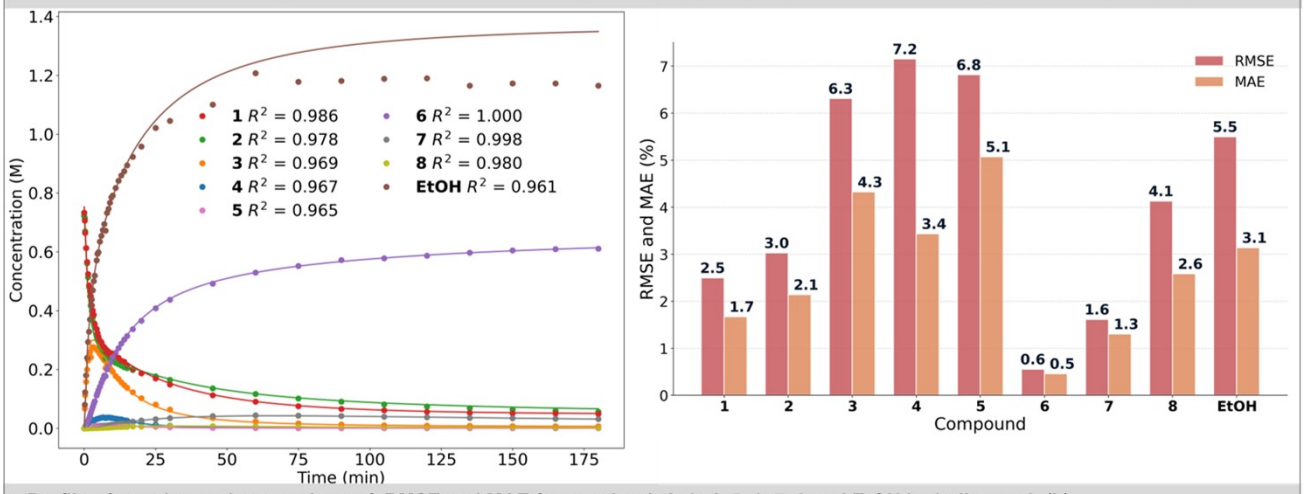
7.8 Development of model IV including species 1, 2b, 3, 5, 6, 7, 8 and EtOH

7.8.1 Comparison of reaction profiles and their corresponding RMSE and MAE for path a.1, a.2 and b and their combinations

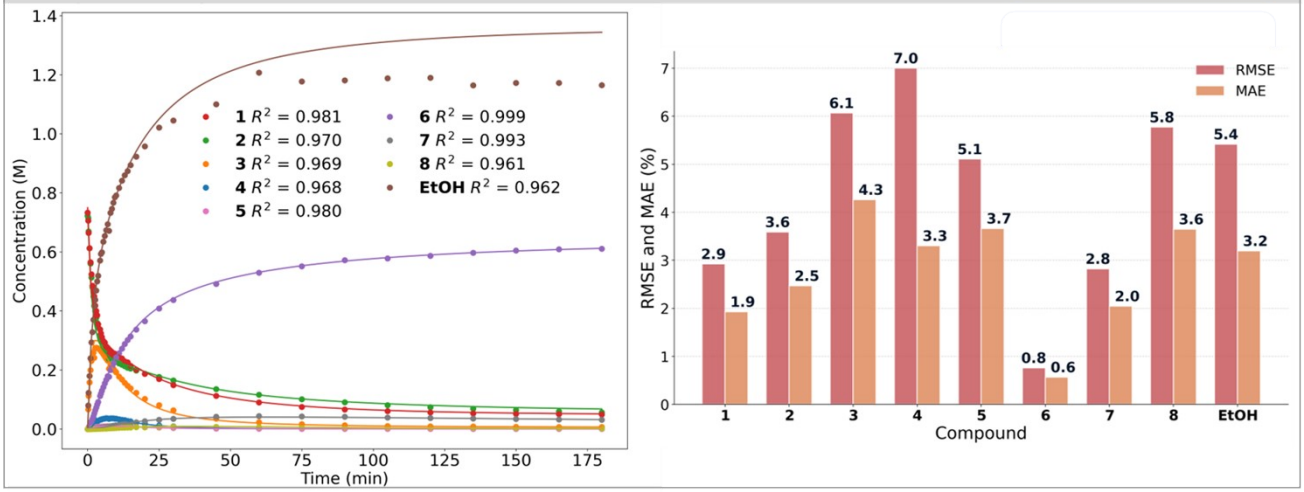
a. Profile of reaction and comparison of RMSE and MAE for species 1, 2, 3, 4, 5, 6, 7 ,8 and EtOH including path (a.1)



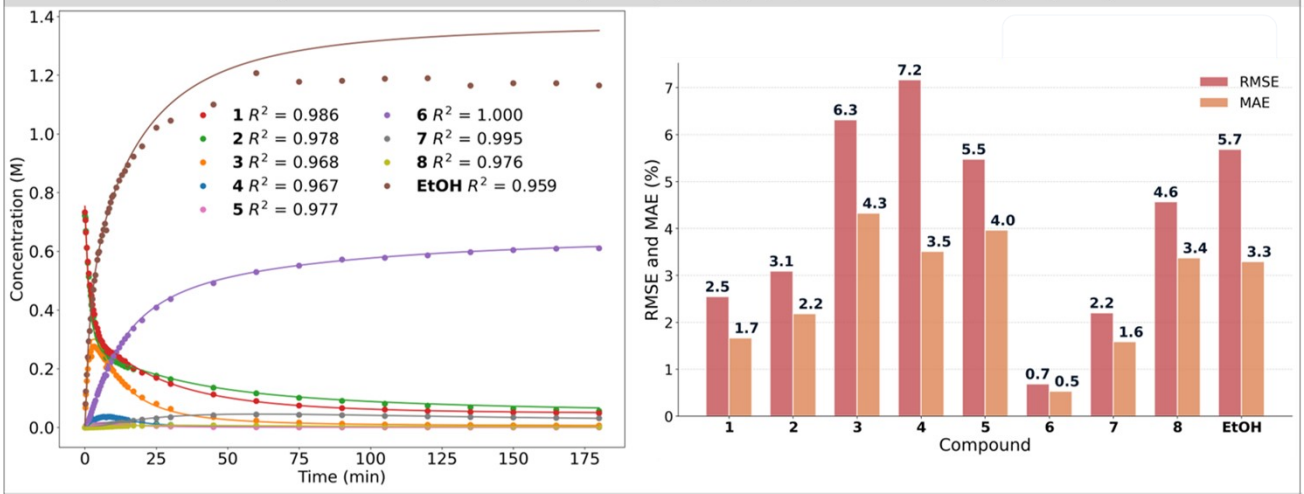
b. Profile of reaction and comparison of RMSE and MAE for species 1, 2, 3, 4, 5, 6, 7, 8 and EtOH including alternative path (a.2)



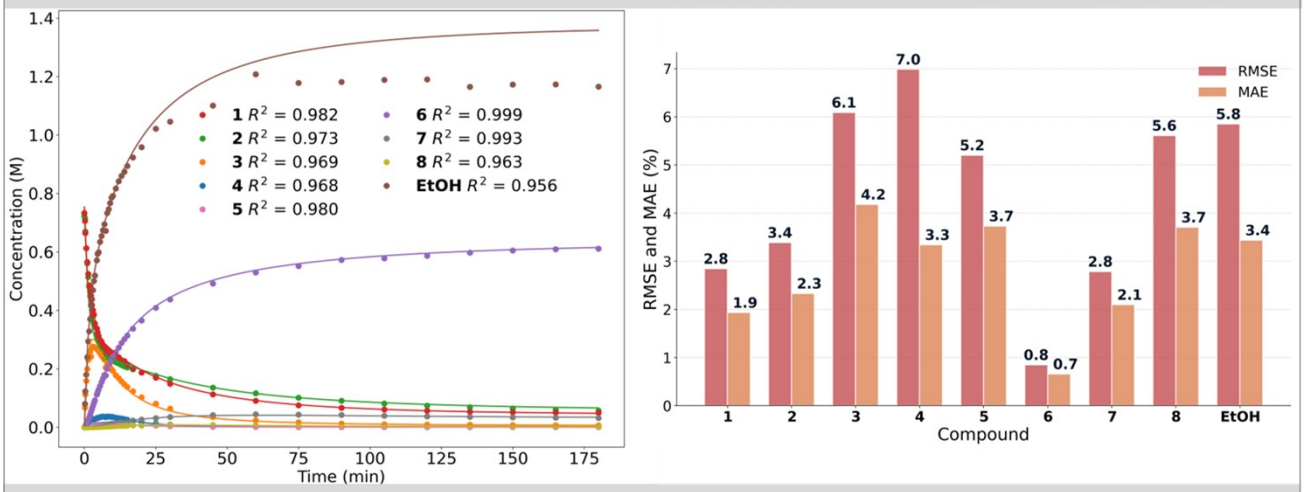
c. Profile of reaction and comparison of RMSE and MAE for species 1, 2, 3, 4, 5, 6, 7, 8 and EtOH including path (b)



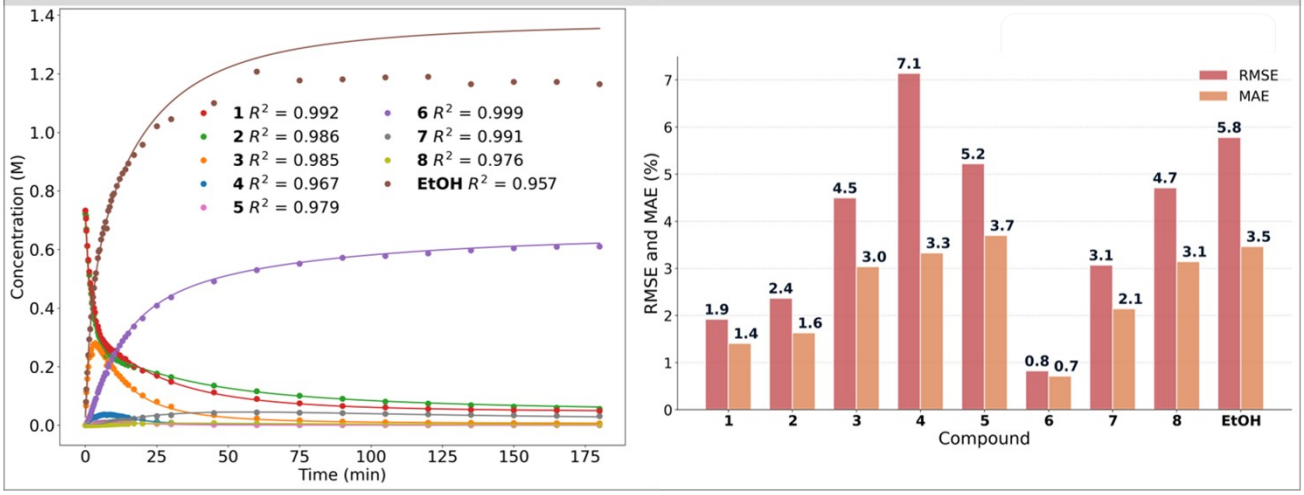
d. Profile of reaction and comparison of RMSE and MAE for species 1, 2, 3, 4, 5, 6, 7 ,8 and EtOH including path (a.1&b)



e. Profile of reaction and comparison of RMSE and MAE for species 1, 2, 3, 4, 5, 6, 7, 8 and EtOH including alternative path (a.2&b)



f. Profile of reaction and comparison of RMSE and MAE for species 1, 2, 3, 4, 5, 6, 7, 8 and EtOH including path (a.1&a.2)



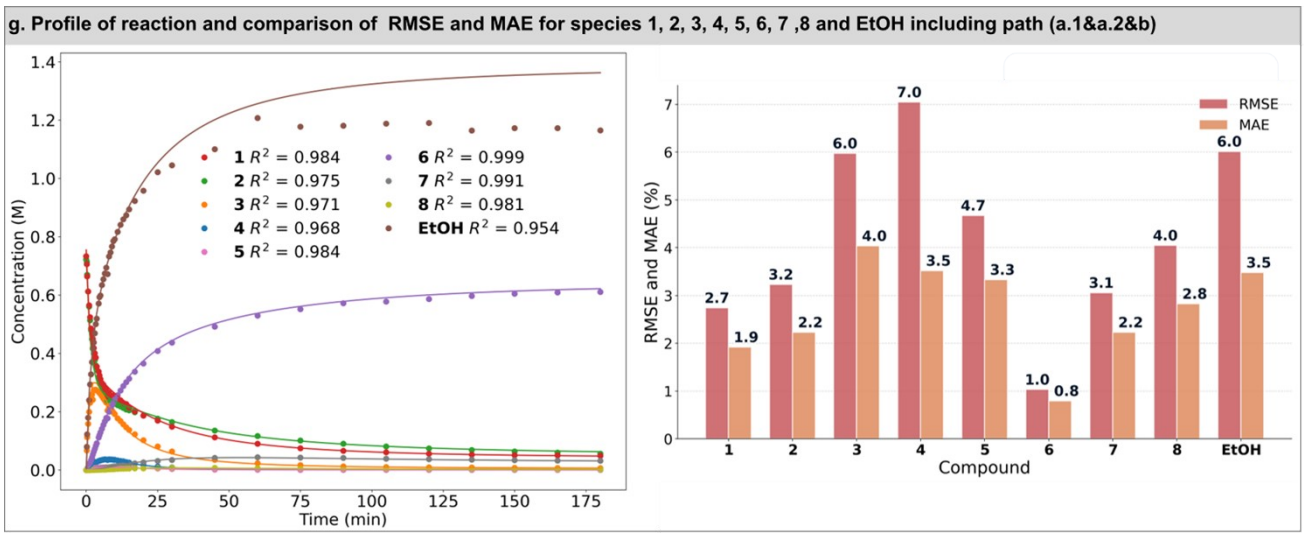
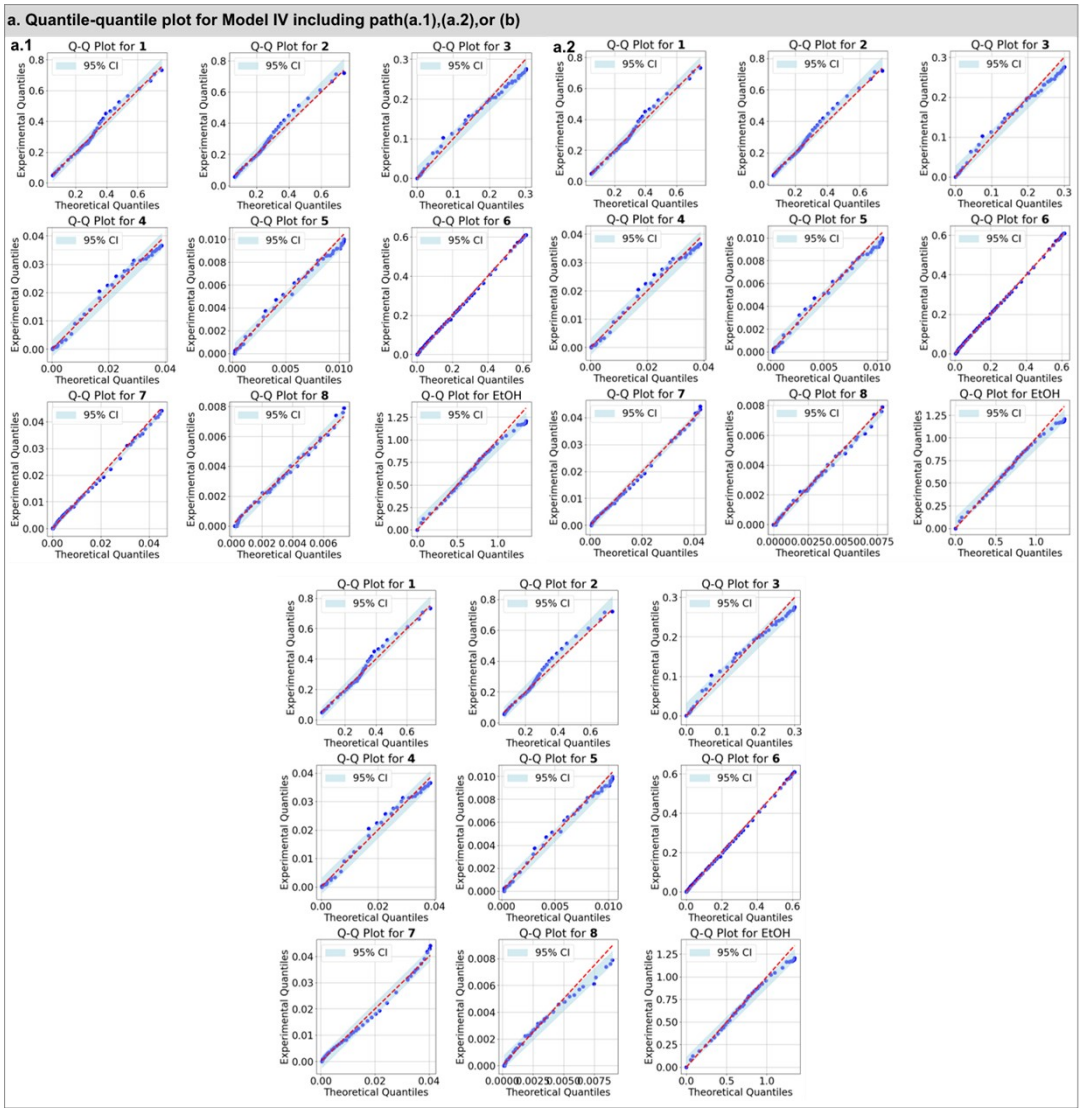


Figure S22 Profile of concentrations of the various species **1** to **8** and **EtOH** over time and RMSE and MAE obtained for paths (a.1), (a.2), (b), combination of (a.1&a.2), (a.1&b), (a.2&b), (a.1&a.2&b).

7.8.2 Quantile-quantile plots



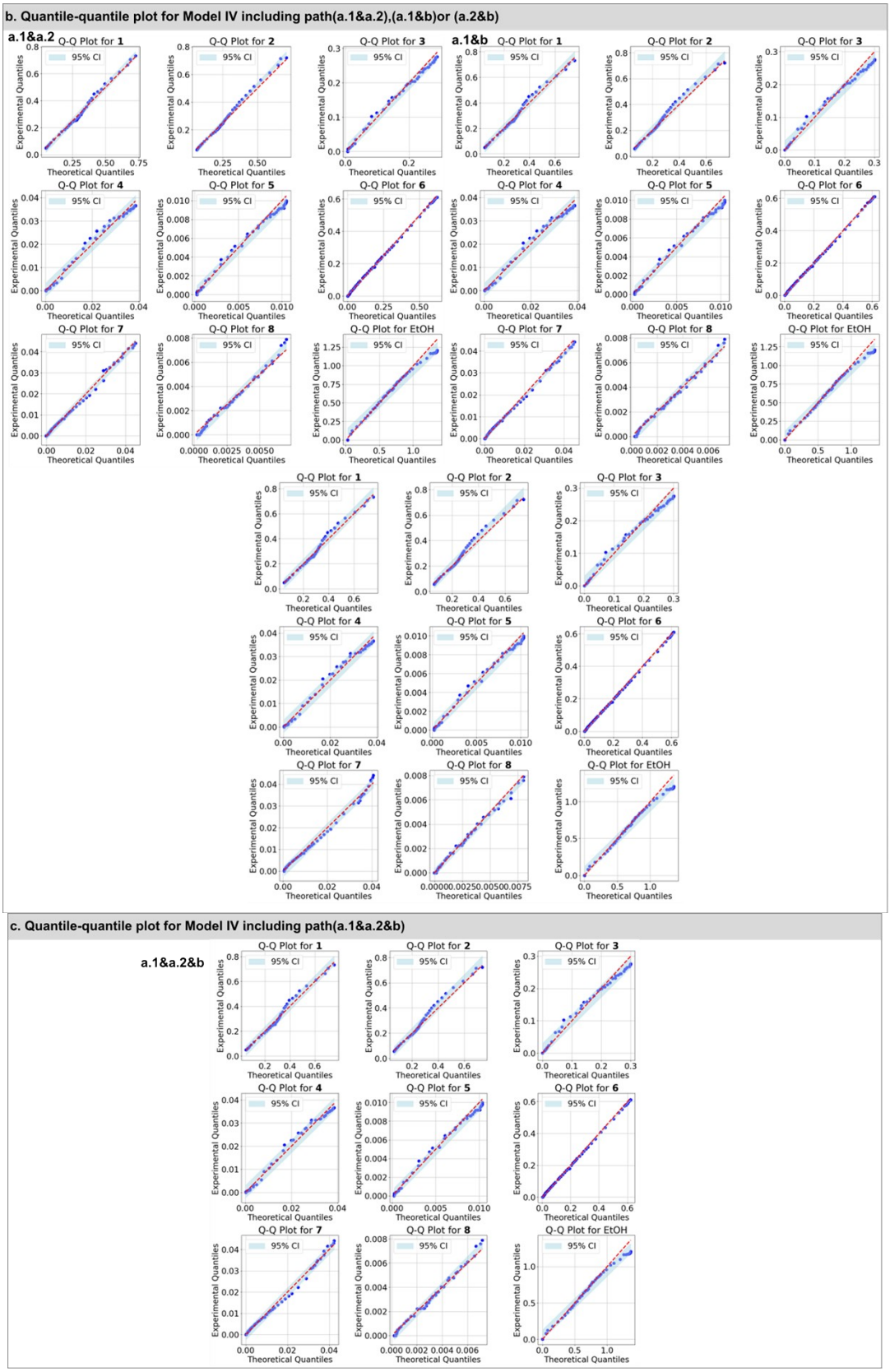


Figure S23 Quantile-quantile plots for paths (a.1), (a.2), (b), combination of (a.1&a.2), (a.1&b), (a.2&b), (a.1&a.2&b).

7.8.3 Comparison of BIC and AIC for the number of interconnections between species for the various models

Path (a1&a2) was found to offer the best trade-off balance between model complexity and accuracy, as evidenced by the most negative value of BIC (Figure S24). AIC values give the same results, therefore supporting the occurrence of only path b. Further complexification of the model gave lower values of BIC and AIC compared to path b. These results suggest that **model IV** may not fully capture all reaction pathways, especially those involving compound **8**. The difficulty in incorporating compound **8** clearly highlights the challenge of modeling low-concentration species with minimal impact on the DCE system.

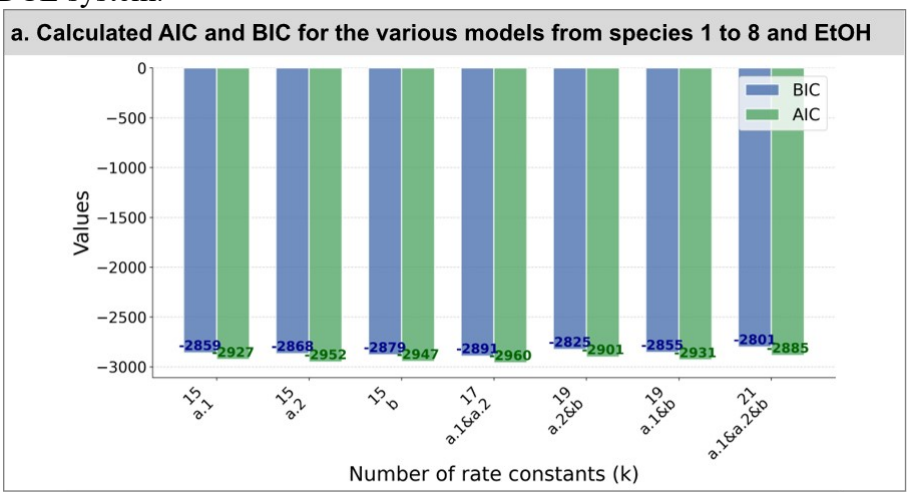


Figure S24 Calculated BIC and AIC values for paths (a.1), (a.2), (b), combination of (a.1&a.2), (a.1&b), (a.2&b), (a.1&a.2&b) including the number of rate constants as metric of model complexification.

7.8.4 Final model of 1 to 8 and EtOH including path (b)

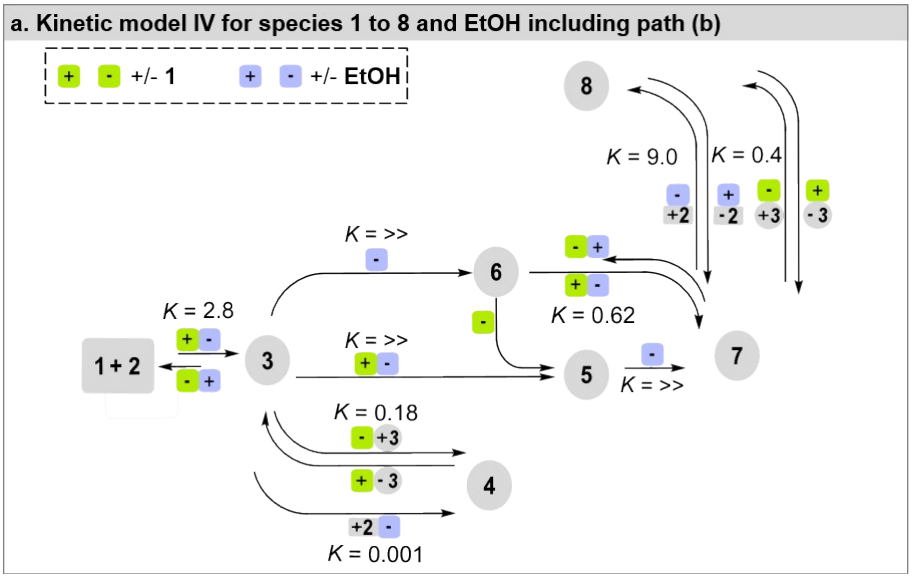
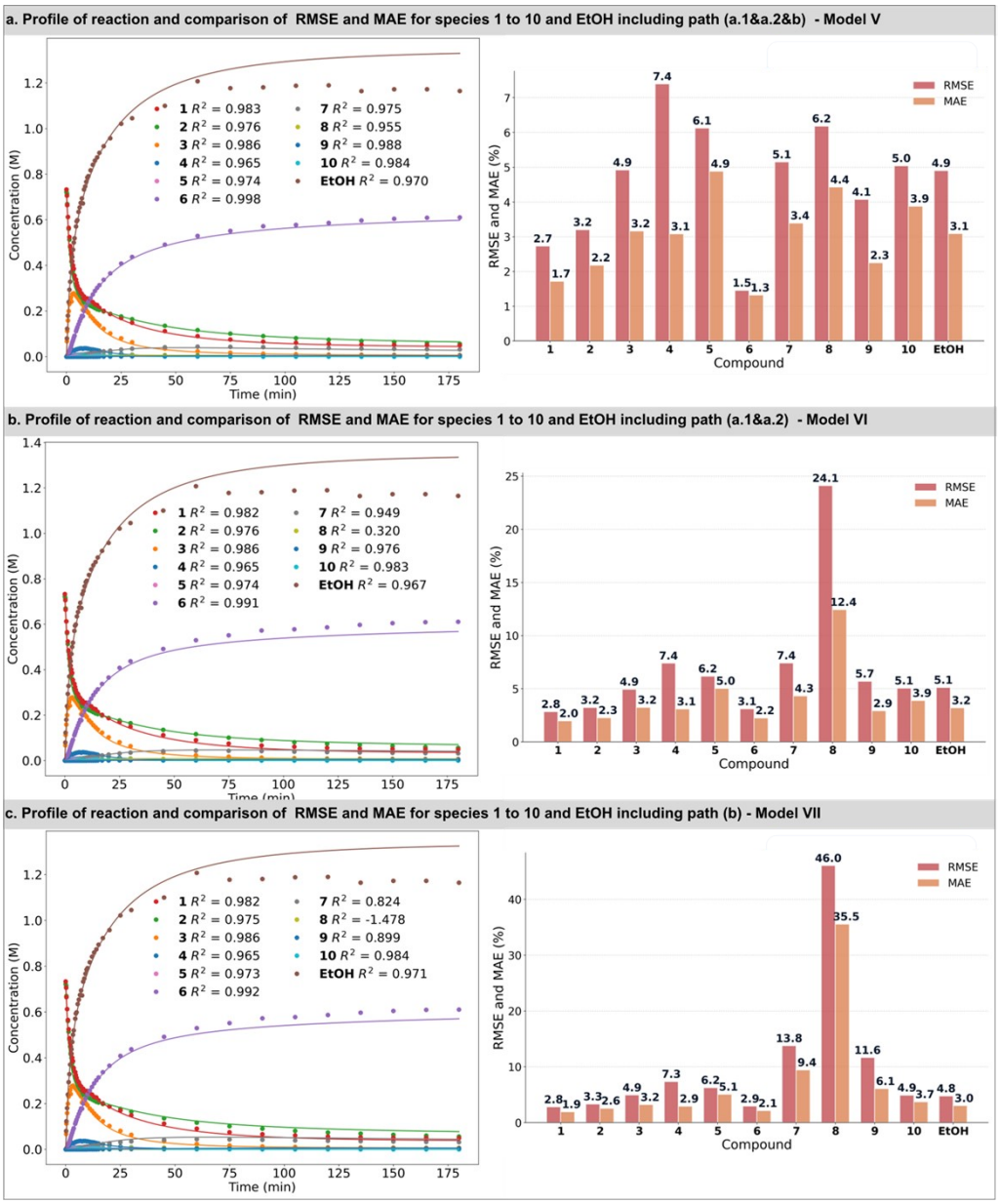


Figure S25 Representation of **model IV**.

7.9 Kinetic study of stoichiometric amount of 1 and 2b using 10 mol% of FA in dry acetonitrile to form 3, 4, 5, 6, 7, 8 ,9 and 10

7.9.1 Comparison of reaction profiles and their corresponding RMSE and MAE for path a.1, a.2 and b and their combinations

Formation of **9** is hypothesized to occur via the nucleophilic substitution of **6** with **7** or with two molecules of **7**, whereas generation of **10** comes from the reaction of **5** with **2b** or **3**. Due to the unconclusive results obtained for the formation of **8** in model **IV**, paths (a.1), (a.2) and (b) are all considered in **model V** (k = 21). Notably, the model featuring solely paths (a.1&a.2 – **model VI**, k = 22) exhibits a low accuracy for **8** with R^2 and MAE values of 0.33 and 24%. Interestingly, while path (b) provided the best fit for the 8-compound model (**model IV**), this is not the case for **model VIII**. Indeed, the addition of two more molecules to the system creates an even more interconnected network and reveals that contributions previously insignificant can become relevant in a more complex system.



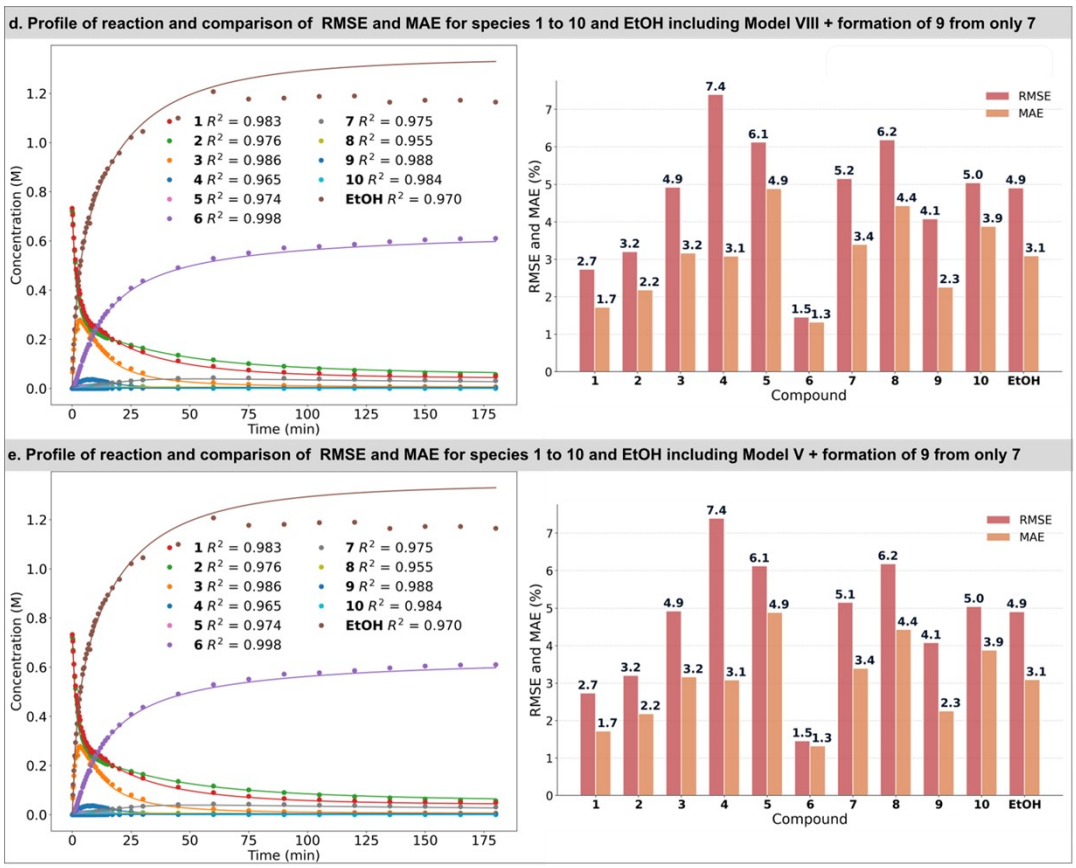


Figure S26 Profile of concentrations of the various species **1** to **10** and **EtOH** over time and RMSE and MAE obtained for **models V** to **X**.

Removal of unsignificant contribution from the **model IX** led to **model X**, therefore yielding exactly the same metrics of accuracy.

7.9.2 Quantile-quantile plots



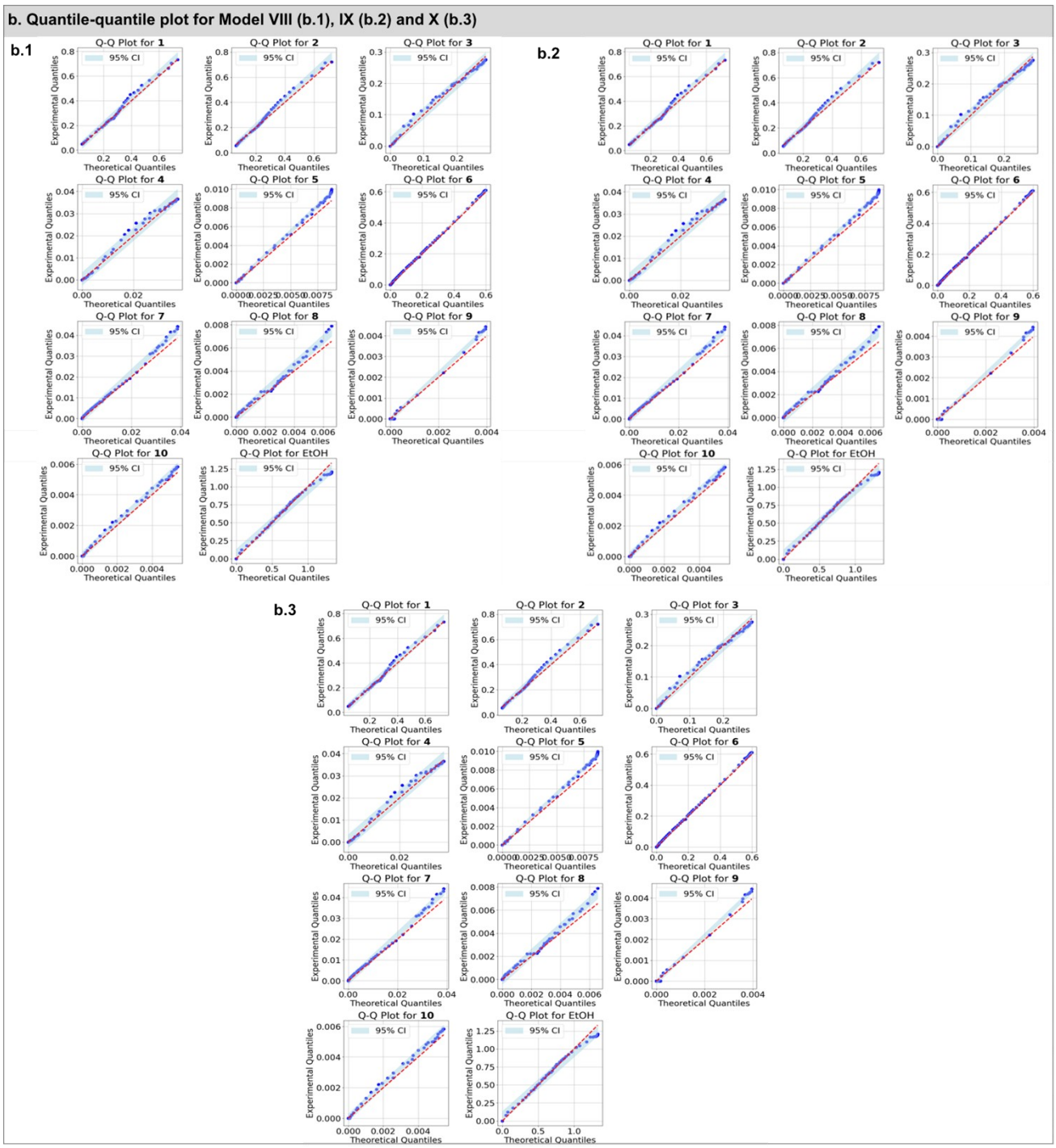


Figure S27 Quantile-quantile plots for models **V** to **X**.

7.9.3 System of differential equations describing the kinetic model

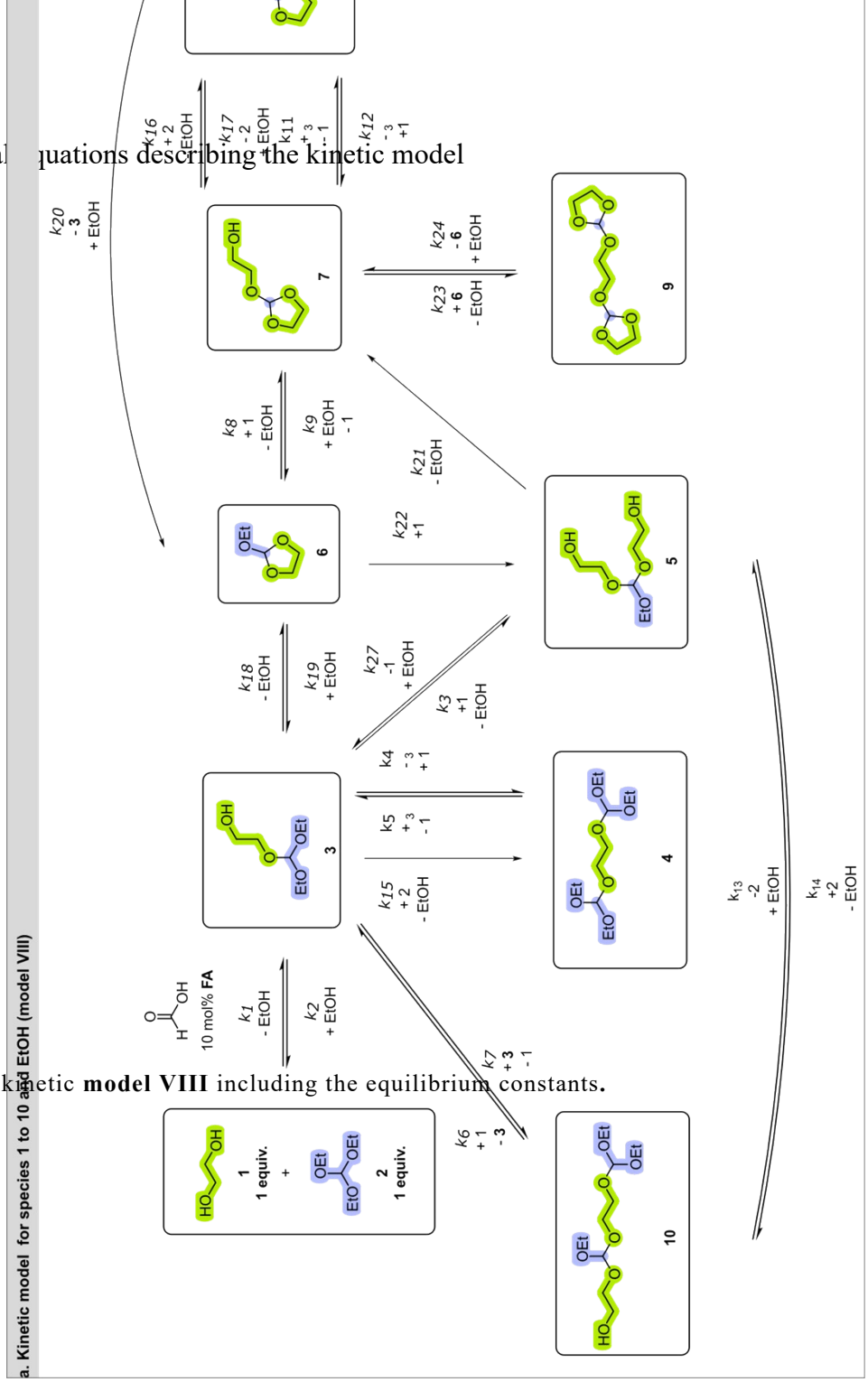


Figure S28 Representation of kinetic **model VIII** including the equilibrium constants.

$$\frac{d[C1]}{dt} = -k1*[1]*[2] + k2*[3]*[EtOH] - k3*[3]*[1] + k4*[3]*[3] - k5*[4]*[1] - *[3] - k8*[6]*[1] + k9*[7]*[EtOH] + k11*[7]*[3] - k12*[8]*[1] + k27*[5] + k25*[4]*[EtOH]$$

$$\frac{d[C2]}{dt} = -k1*[1]*[2] + k2*[3]*[EtOH] + k13*[10]*[EtOH] - k14*[5]*[2] + k15* + k17*[8]*[EtOH] + k25*[4]*[EtOH]$$

$$\frac{d[C3]}{dt} = k1*[1]*[2] - k2*[3]*[EtOH] - k5*[3]*[3] + k4*[4]*[1] - k15*[3]*[2] + *[3] - k3*[3]*[1] - k11*[7]*[3] + k12*[8]*[1] - k18*[3] + k19*[6]*[EtO *[EtOH] + k27*[5]*[EtOH]$$

$$\frac{d[C4]}{dt} = k4*[3]*[3] - k5*[4]*[1] + k15*[3]*[2] - k25*[4]*[EtOH]$$

$$\frac{d[C5]}{dt} = -k3*[3]*[1] + k13*[10]*[EtOH] - k14*[5]*[2] + k6*[10]*[1] - k7*[5]* [6]*[1]$$

$$\frac{d[C6]}{dt} = k18*[3] - k19*[6]*[EtOH] - k22*[6]*[1] - k8*[6]*[1] + k9*[7]*[EtOH] k23*[6]*[7] - k24*[9]*[EtOH]$$

$$\frac{d[C7]}{dt} = -k23*[6]*[7] + k24*[9]*[EtOH] + k8*[6]*[1] - k9*[7]*[EtOH] - k11* - k16*[2]*[7] + k17*[8]*[EtOH] + k21*[5]$$

$$\frac{d[C8]}{dt} = k11*[7]*[3] - k12*[8]*[1] + k16*[2]*[7] - k17*[8]*[EtOH] - k20*[8]*$$

$$\frac{d[C9]}{dt} = k23*[6]*[7] - k24*[9]*[EtOH]$$

$$\frac{d[C10]}{dt} = -k13*[10]*[EtOH] + k14*[5]*[2] - k6*[10]*[1] + k7*[5]*[3] + k16*[2]$$

$$\frac{d[CEtOH]}{dt} = k23*[6]*[7] - k24*[9]*[EtOH] - k20*[8]*[EtOH] - k13*[10]*[EtOH] + [1]*[2] - k2*[3]*[EtOH] + k8*[6]*[1] - k9*[7]*[EtOH] + k18*[3] - k19*[+ k21*[5] + k16*[2]*[7] - k17*[8]*[EtOH] + k15*[2]*[3] + k3*[3]*[1] - *[EtOH] - k25*[4]*[EtOH]$$

7.9.4 Model initialization with calculated concentrations and rate constants

Table S3 Model initialization with calculated concentrations and rate constants for kinetic study using a 1:1 ratio of **2b**/**1**.

Calculated rate constants		Model initialization		Optimized values of initialization		R^2	RMSE	MAE
k_15	0.00947	c0_4	0	c0_4	0	0.965	0.002	0.001
k_2	0.213	c0_3	0	c0_3	0	0.986	0.013	0.008
k_1	0.609	c0_2	0.722	c0_2	0.722	0.976	0.023	0.015
k_18	0.101	c0_1	0.733	c0_1	0.733	0.983	0.02	0.012
k_6	0.974	c0_6	0	c0_6	0	0.998	0.008	0.008
k_3	0.0347	c0_EtOH	0	c0_EtOH	0	0.97	0.059	0.037
k_21	0.2	c0_5	0	c0_5	0	0.974	0.000	0.00048
k_19	0.00062	c0_7	0	c0_7	0	0.975	0.002	7
k_4	8	c0_8	0	c0_8	0	0.955	0.000	0.001
k_8	0.182	c0_10	0	c0_10	0	0.984	0.001	0.000
k_7	0.00667	c0_9	0	c0_9	0	0.988	0.001	0.000
k_6	0.524							0.001
k_11	0.227							
k_12	0.835							
k_22	2							
k_16	0.0011							
k_17	0.121							
k_13	0.00524							
k_14	0.157							
k_23	0.12							
k_9	0.00731							
k_24	0.00459							
k_20	0.0271							
K_27	0.0401							
	0.00001							

7.10 Kinetic study of stoichiometric amount of 1 and 2b using 10 mol% of FA in dry Acetonitrile to form 3, 4, 5, 6, 7, 8 ,9, 10 and 12 (model VIII.2)

To confirm that **model VIII** represented an optimal balance between data fit and model parsimony, **model VIII.2** was developed by integrating compound **12**. Although the improvement of ΔAIC/BIC was higher to 10, the change in the slope at **model VIII** indicates an inflexion point where additional complexity yields proportionally smaller improvements in accuracy, of approximatively 20 % less, compared to previous complexification (**model I** to **VIII**).

7.10.1 Kinetic model

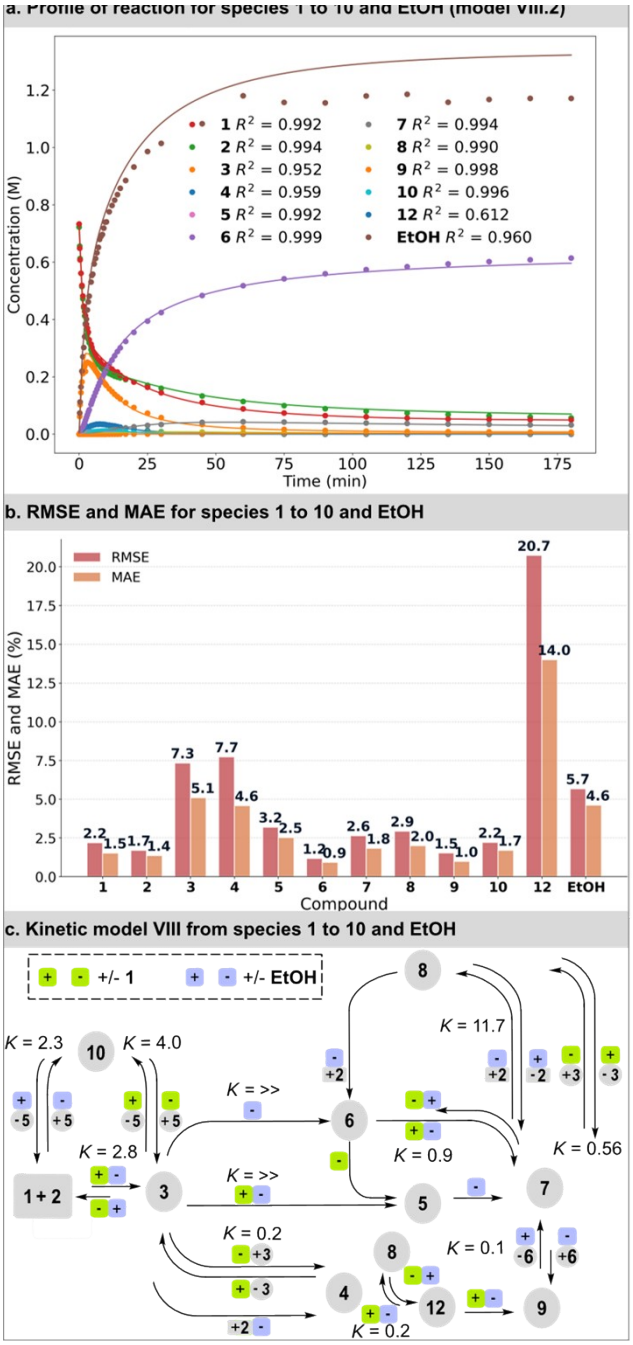


Figure S29 Representation of kinetic **model VIII.2** including the equilibrium constants.

Errors observant for product **12** due to the absence of signal assignment within the NMR kinetic.

7.10.2 Quantile-quantile plots

a. Quantile-quantile plot for species 1, 2, 3, 5, 6, 7, 8, 9, 10, 12 and EtOH

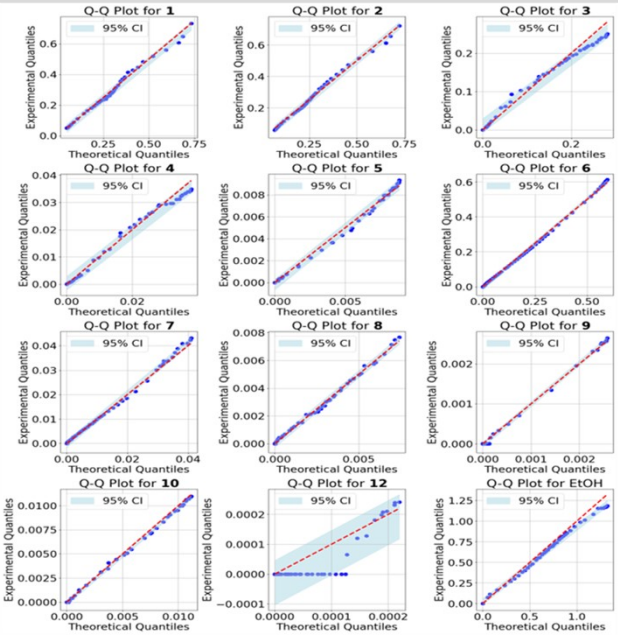


Figure S30 Quantile-quantile plots for model **VIII.2**.

7.10.3 System of differential equations describing the kinetic model

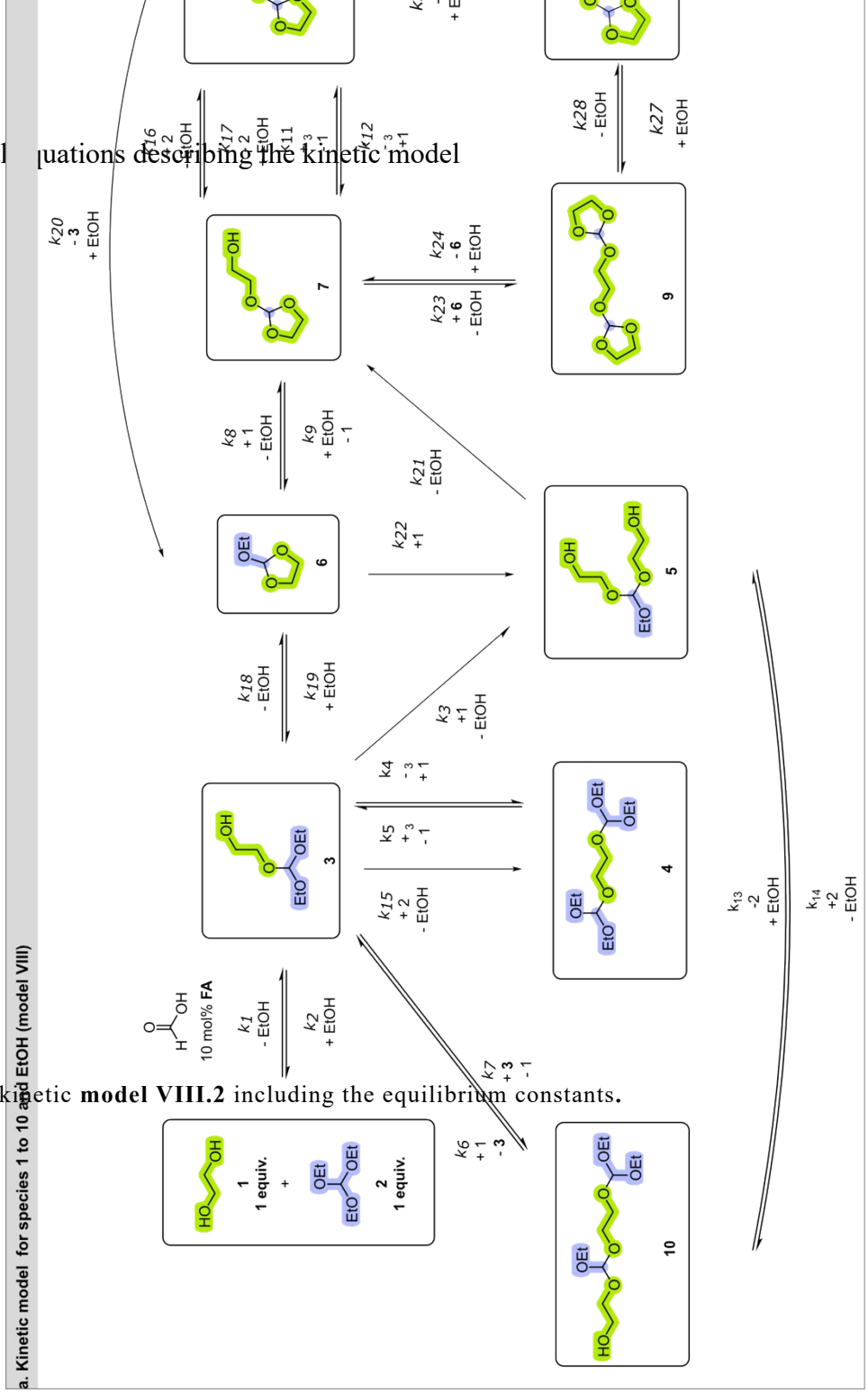


Figure S31 Representation of kinetic **model VIII.2** including the equilibrium constants.

7.11 Kinetic study in neat conditions

7.11.1 reaction profile and their corresponding RMSE and MAE with addition of interconnection between 4+1 to 10

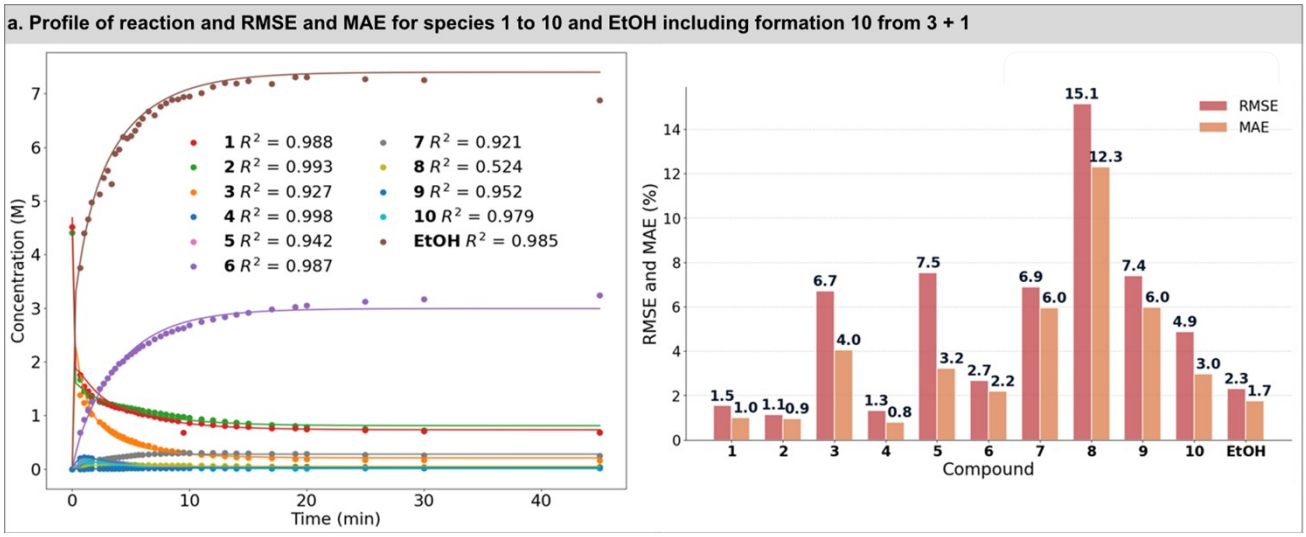


Figure S32 Alternative profile of concentration of species **1** to **10** and **EtOH** over time and RMSE and MAE under neat conditions.

7.11.2 Quantile-quantile plots

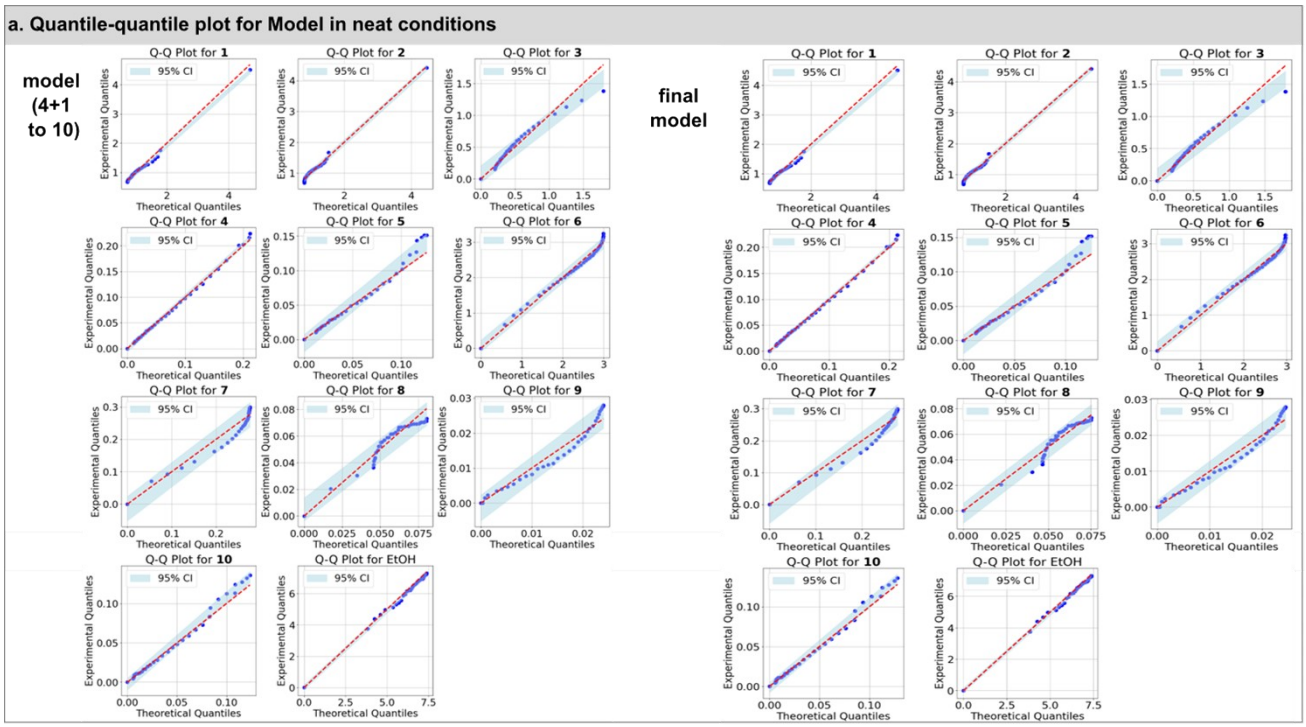


Figure S33. Quantile-quantile plots for **model** using neat conditions.

7.11.3 Final model

This model is obtained from the treatment of the kinetic data with **model VIII**.

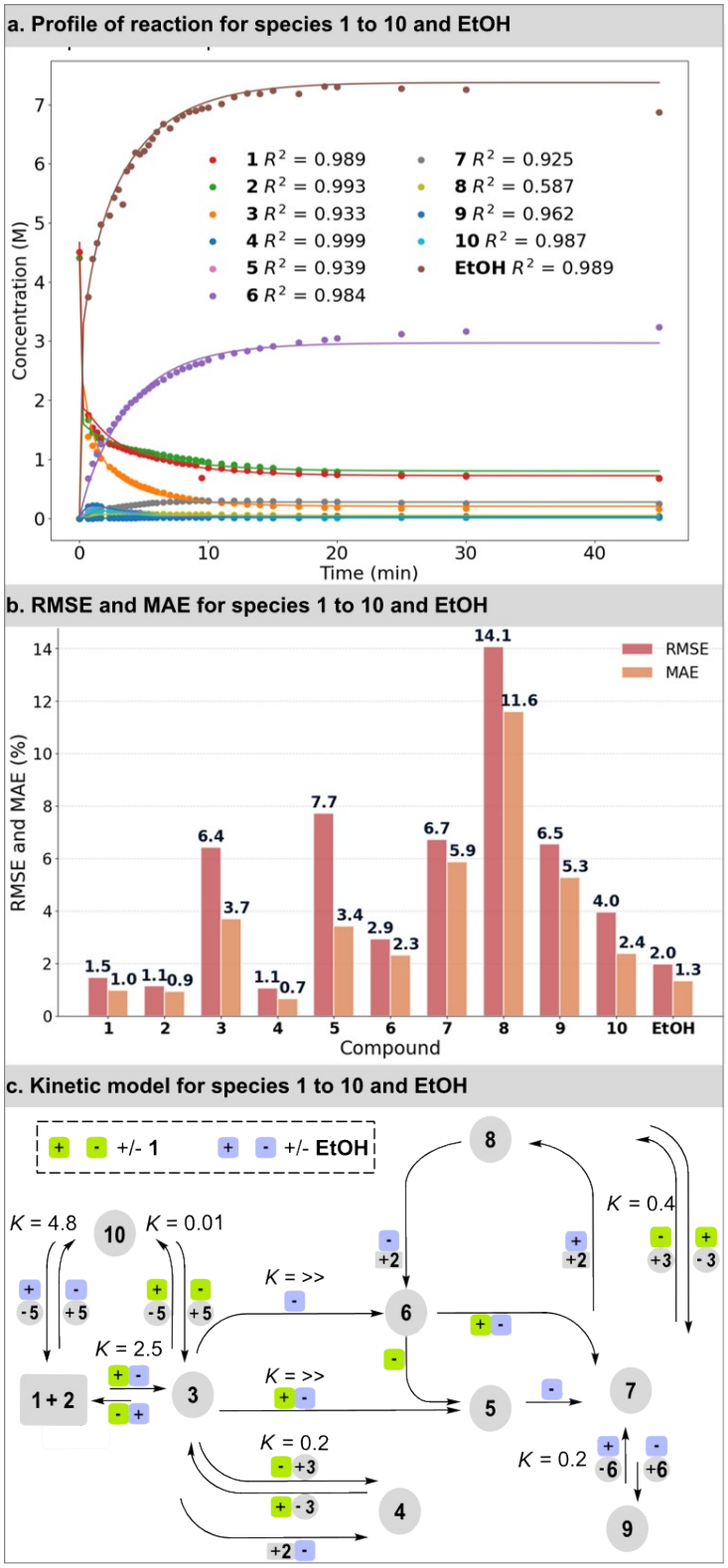


Figure S34 (a) Profile of concentrations of the various species **1** to **10** and **EtOH** over time; (b) RMSE and MAE obtained; and (c) the system obtained from kinetic modelling of NMR data with the theoretical model.

7.11.4 Model initialization with calculated concentrations and rate constants

Table S4 Model initialization and calculated concentrations and rate constants for kinetic study using a 1:1 ratio of **2b**/**1**.

Calculated rate constants		Model initialization		Optimized values of initialization		R^2	RMSE	MAE
k_15	0.00161	c0_4	0	c0_4	0	0.999	0.002	0.001
k_2	6.99	c0_3	0	c0_3	0	0.933	0.088	0.051
k_1	17.5	c0_2	4.51	c0_2	4.45	0.993	0.05	0.041
k_18	0.409	c0_1	4.51	c0_1	4.64	0.989	0.066	0.044
k_6	2.15	c0_6	0	c0_6	0	0.984	0.095	0.074
k_3	0.0886	c0_EtOH	0	c0_EtOH	0	0.989	0.144	0.098
k_21	1.16	c0_5	0	c0_5	0	0.939	0.011	0.005
k_19	0.00438	c0_7	0	c0_7	0	0.925	0.020	0.017
k_4	0.0806	c0_8	0	c0_8	0	0.587	0.010	0.008
k_8	0.134	c0_10	0	c0_10	0	0.987	0.005	0.003
k_7	0.444	c0_9	0	c0_9	0	0.962	0.001	0.001
k_11	0.00256							
	20.0058							
k_12	5							
k_22	0.0005							
k_16	1.37							
	0.00000							
k_17	1							
k_13	0.00589							
k_14	0.506							
k_23	0.0147							
k_9	0.00001							
k_24	0.0271							
k_20	0.0669							
K_20	0.884							
K_27	0.00001							

7.12 Kinetic study starting from species 3 and an excess of EtOH

7.12.1 Final model

Due to the low concentration of species **7**, **8**, **9** and **10**, it was not possible to determine an accurate model of the system. Furthermore, some minor overlapping signals were observed with the triplet of EtOH, resulting in biased integration. As a result, the **model** only describes the DCE system up to compound **6**. However, the remaining products were accurately described (R^2 = 0.91 – 0.99), highlighting the robustness of **model VIII** when applied to different systems starting with distinct reagents.

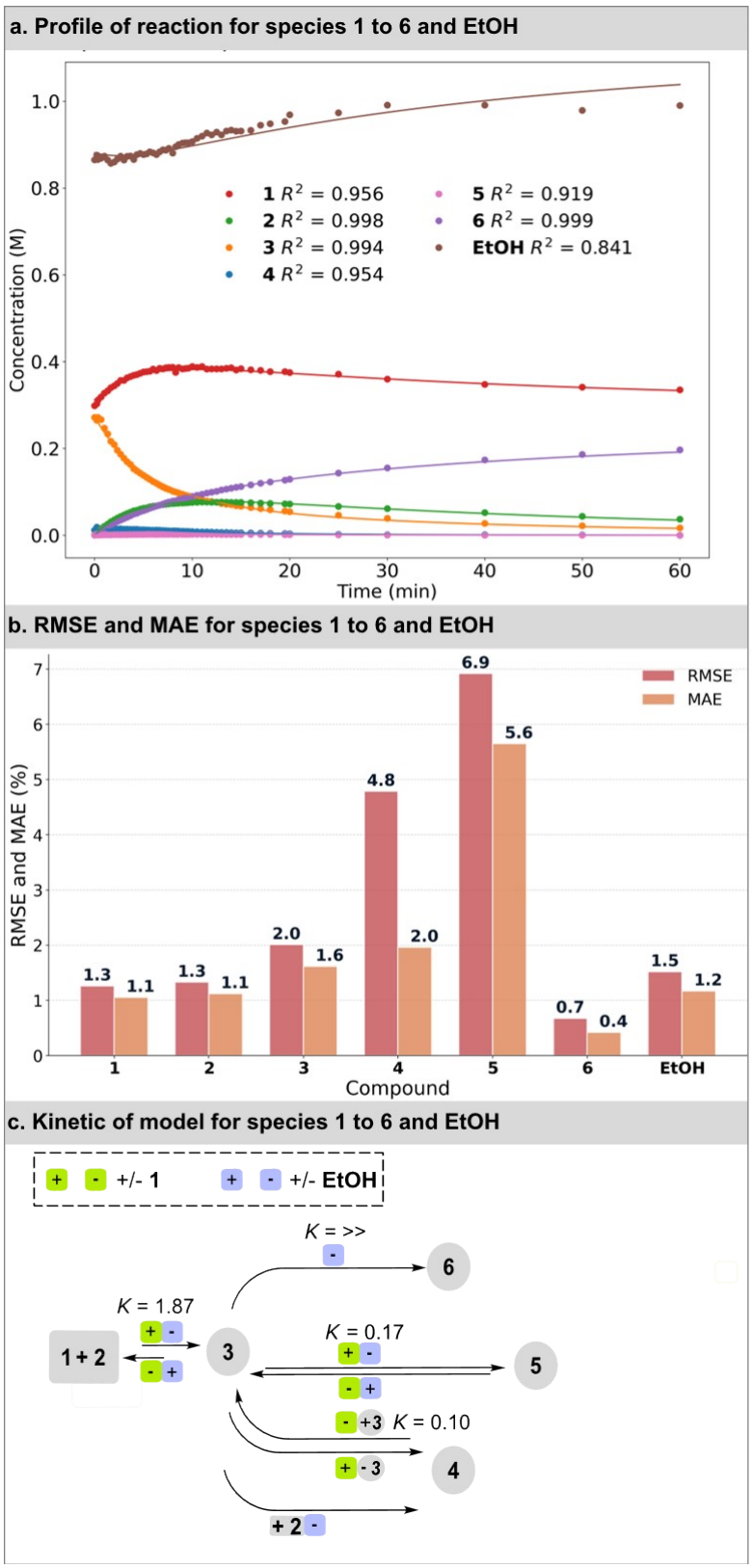


Figure S35 (a) Profile of concentrations of the various species **1** to **7** and **EtOH** over time; (b) RMSE and MAE obtained; and (c) the system obtained from kinetic modelling of NMR data with the theoretical model.

7.12.2 Quantile-quantile plot

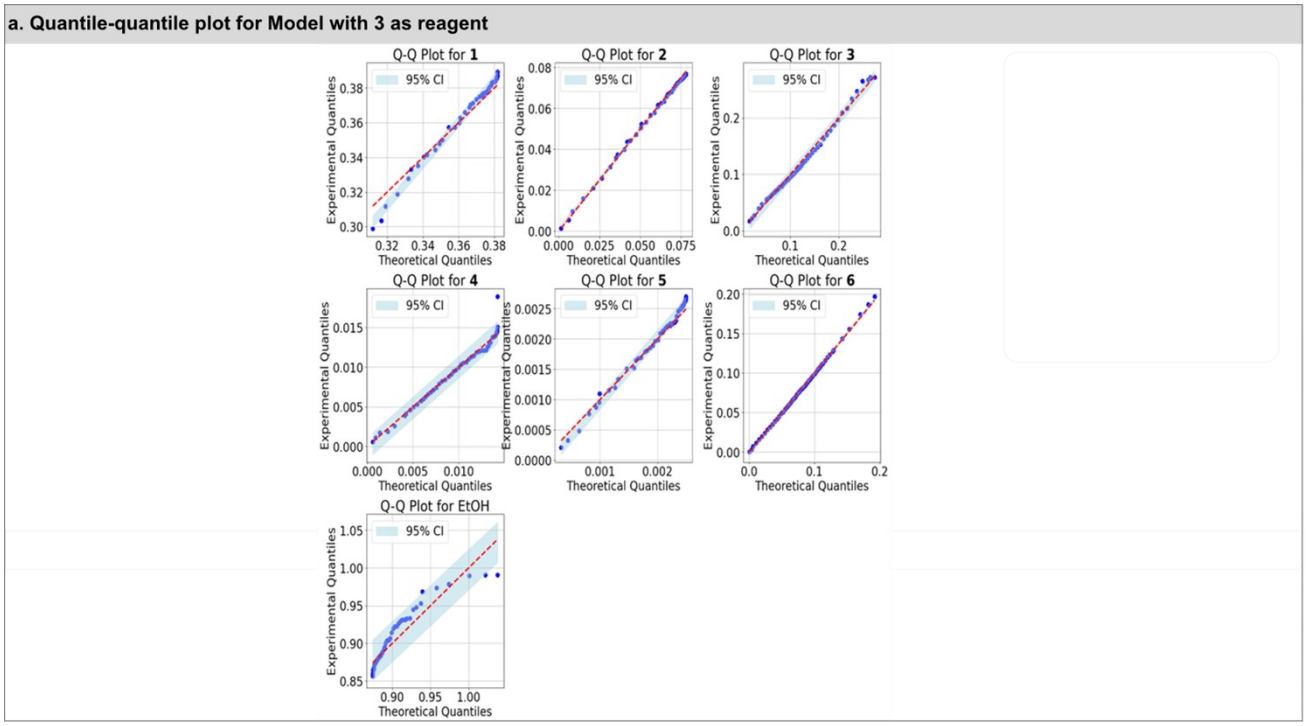


Figure S36 Quantile-quantile plots for **model** using **3** as reagent.

7.12.3 System of differential equations describing the kinetic model

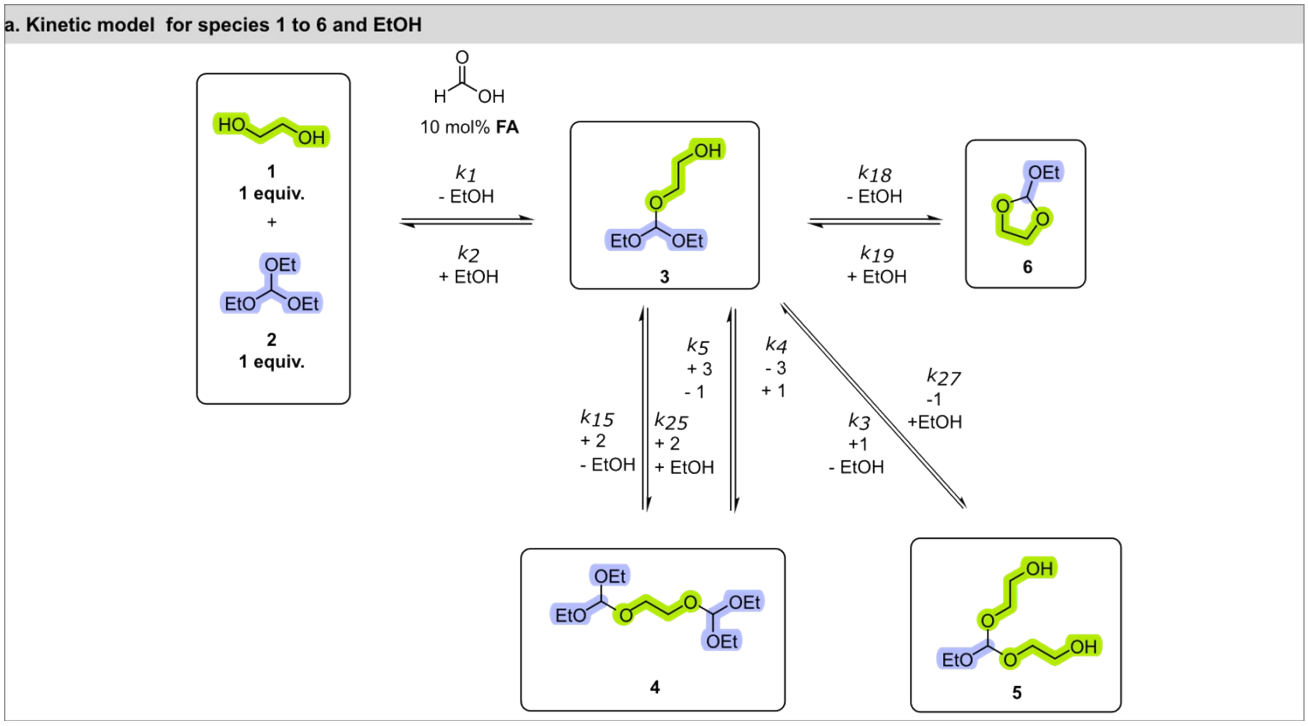


Figure S37 Representation of kinetic model starting from intermediate **3** including the rate constants.

$$\frac{d[C1]}{dt} = -\ k5 * [4] * [1] - k1 * [1] * [2] + \ k4 * [3] * [3] + k3 * [5] * [EtOH] - k27 - [3] * [1]$$

$$\frac{d[C2]}{dt} = -\ k1 * [1] * [2] + \ k15 * [4] * [EtOH] - \ k25 * [3] * [2]$$

$$\frac{d[C3]}{dt} = k1 * [1] * [2] - k2 * [3] * [EtOH] - k25 * [3] * [2] \ - k27 * [3] * [1] + k3 * [5] * [Et$$
$$[6] * [EtOH] + \ k15 * [4] * [EtOH] + \ k5 * [4] * [1] - k4 * [3] * [3]$$

$$\frac{d[C4]}{dt} = + k25 * [3] * [2] - \ k15 * [4] * [EtOH] + \ k5 * [3] * [3] - \ k4 * [4] * [1]$$

$$\frac{d[C5]}{dt} = -\ k27 * [3] * [1] - k3 * [5] * [EtOH]$$

$$\frac{d[C6]}{dt} = k18 * [3] - k19 * [6] * [EtOH]$$

$$\frac{d[CEtOH]}{dt} = \ k25 * [3] * [2] - \ k15 * [4] * [EtOH] + k1 * [1] * [2] + k18 * [3] - k19 * [6] * [EtO$$
$$+ k27 * [3] * [1]$$

7.12.4 Model initialization with calculated concentrations and rate constants

Table S5 Model initialization and calculated concentrations and rate constants for kinetic study using a compound **3**.

Calculated rate constants		Model initialization		Optimized values of initialization		R^2	RMSE	MAE
k_25	0.238	c0_4	0.0131	c0_4	0	0.954	0.0009	0.00037
k_2	0.0941	c0_3	0.273	c0_3	0.272	0.994	0.00546	0.0044
k_1	0.174	c0_2	0.00147	c0_2	0	0.998	0.00102	0.00086
k_18	0.0576	c0_1	0.312	c0_1	0.299	0.956	0.0049	0.0041
k_5	0.867	c0_6	0.00066	c0_6	0	0.999	0.00133	0.00083
k_3	0.00793	c0_EtOH	0.881	c0_EtOH	0.865	0.841	0.0145	0.116
k_27	0.152					0.919	0.00019	0.00015
k_19	0.000351	c0_5	0.00078	c0_5	0			
k_4	0.0604							

7.13 Kinetic study starting from species 4 and an excess of EtOH

7.13.1 Final model

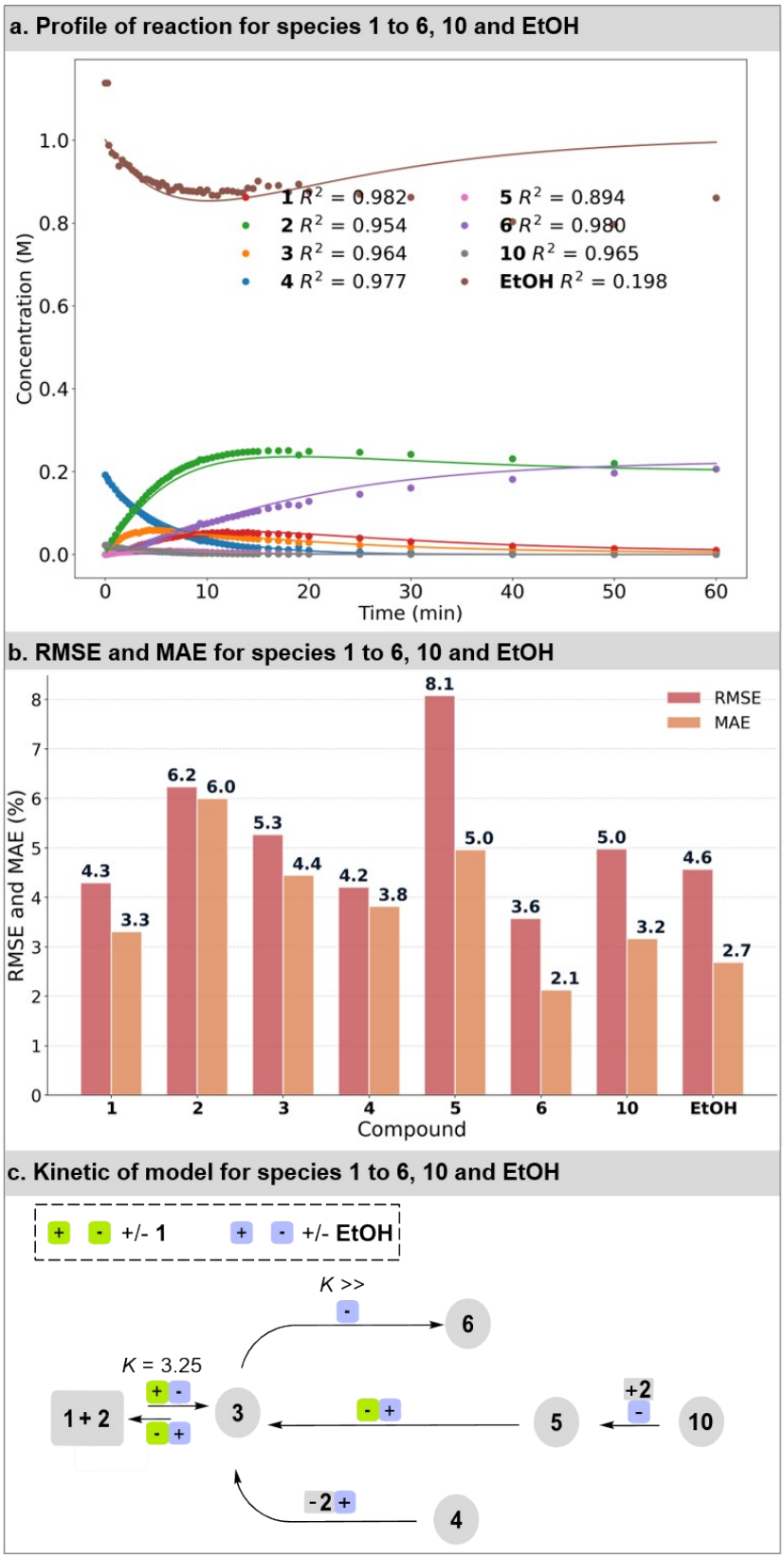


Figure S38 (a) Profile of concentrations of the various species **1** to **6**, **10** and **EtOH** over time; (b) RMSE and MAE obtained; and (c) the system obtained from kinetic modelling of NMR data with the theoretical model.

7.13.2 Quantile-quantile plot

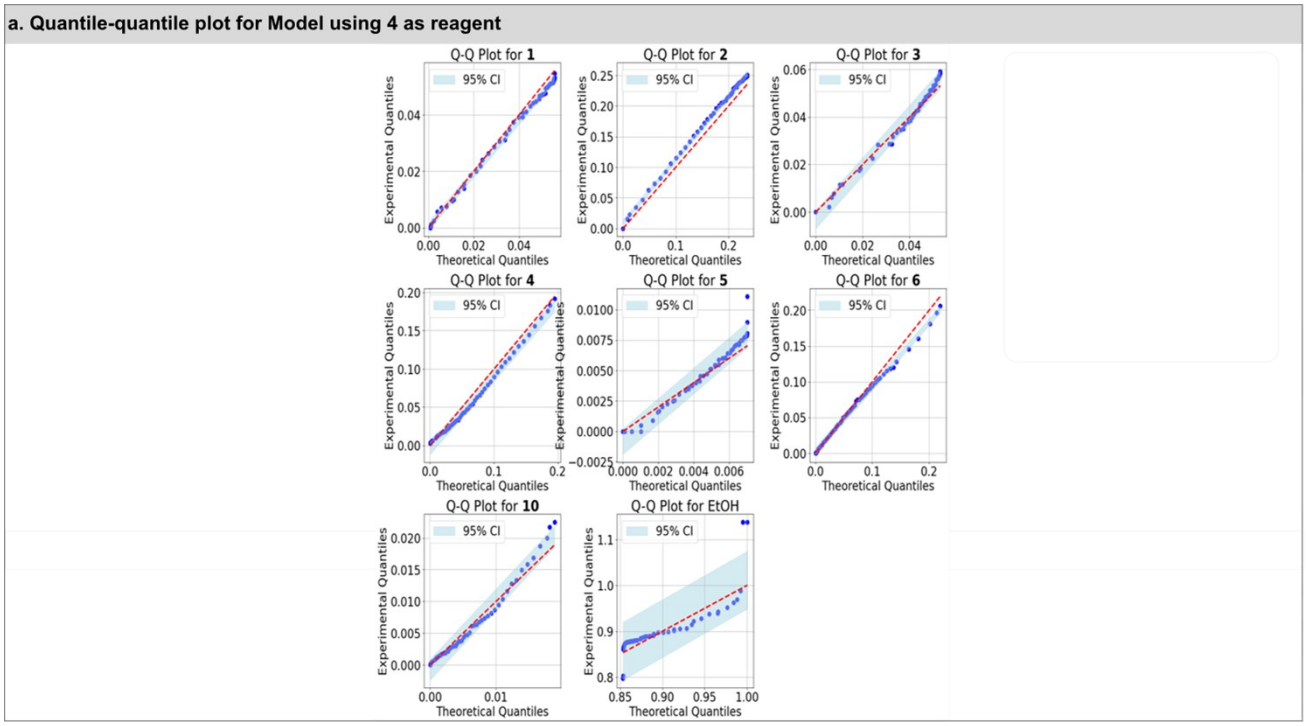


Figure S39 Quantile-quantile plots for **model** using 4 as a reagent.

7.13.3 System of differential equations describing the kinetic model

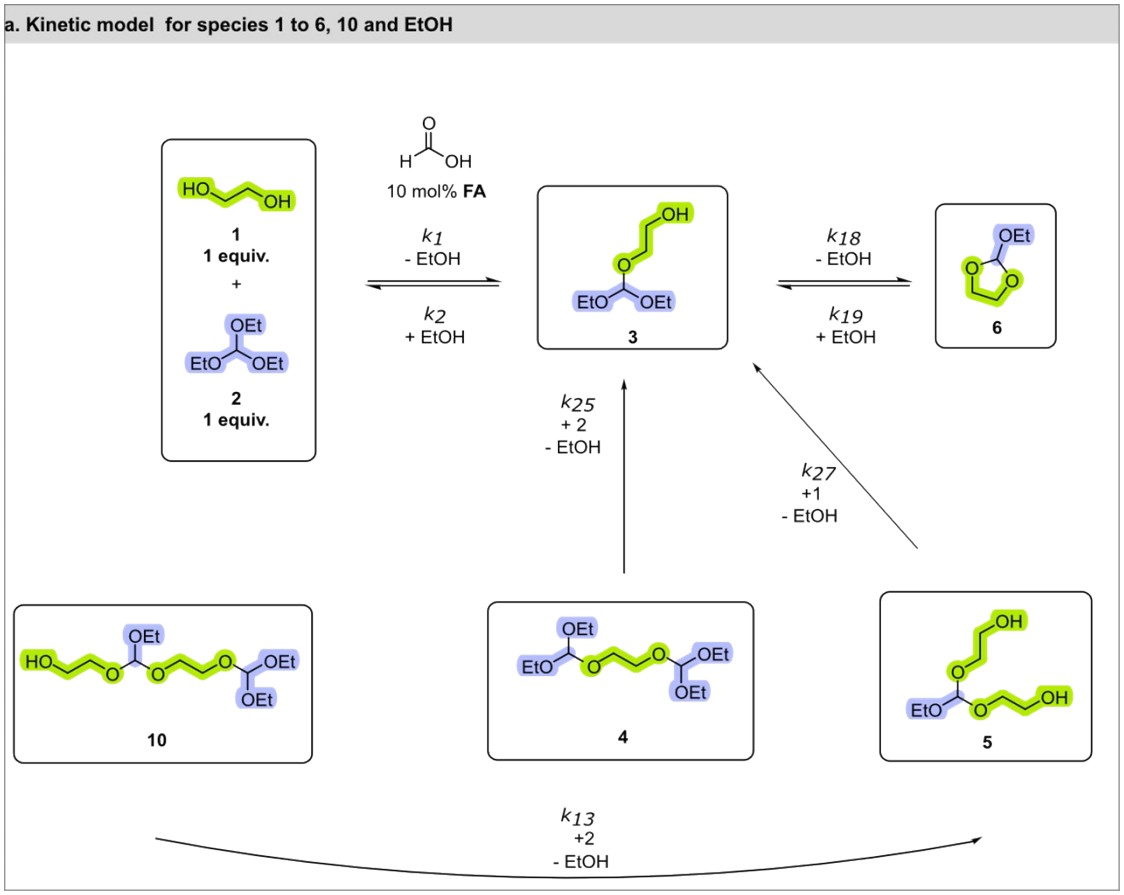


Figure S40 Representation of kinetic **model** using **4** as reagent including the rate constants.

$$\frac{d[C1]}{dt} - k1 * [1] * [2] + k2 * [3] * [EtOH] + k13 * [10] * [EtOH] + k27 * [5] * [EtOH]$$

$$\frac{d[C2]}{dt} = -k1 * [1] * [2] + k2 * [3] * [EtOH] + k25 * [4] * [EtOH] + k13\$[10] * [EtOH]$$

$$\frac{d[C3]}{dt} = k1 * [1] * [2] - k2 * [3] * [EtOH] + k27 * [5] * [EtOH] - k18 * [3] + k19 * [6] * [E$$

$$\frac{d[C4]}{dt} = -k25 * [4] * [EtOH]$$

$$\frac{d[C5]}{dt} - k27 * [5] * [EtOH]$$

$$\frac{d[C6]}{dt} = k18 * [3] - k19 * [6] * [EtOH]$$

$$\frac{d[CEtOH]}{dt} = -k25 * [4] * [EtOH] + k1 * [1] * [2] - k2 * [3] * [EtOH] + k18 * [3] - k19 * [6] * [* [EtOH] - k27 * [5] * [EtOH]$$

7.13.4 Model initialization with calculated concentrations and rate constants

Table S6 Model initialization and calculated concentrations and rate constants for kinetic study using a compound **4**.

Calculated rate constants		Model initialization		Optimized values of initialization		R^2	RMSE	MAE
k_25	0.177	c0_4	0.195	c0_4	0.195	0.977	0.00808	0.00733
k_2	0.181	c0_3	0	c0_3	0	0.964	0.00312	0.00263
k_1	0.59		0.00076		0.00076	0.954	0.0156	0.0151
k_18	0.17	c0_2	7	c0_2	7	0.982	0.00235	0.00181
k_27	0.206	c0_1	1.03e-05	c0_1	1.03e-05	0.98	0.00736	0.00438
k_19	0.00215	c0_6	0.00072	c0_6	0.00072	0.198	0.052	0.0306
k_13	0.19	c0_ EtOH	1.15	c0_ EtOH	1.15	0.894	0.00089	0.00055
			0.00035		0.00035			0.00071
		c0_5	3	c0_5	3			
		c0_10	0.0197	c0_10	0.0197			

8 Solvent screening

8.1 Kinetic study of stoichiometric amount of 1 and 2b using 10 mol% of FA in dry Dimethyl Sulfoxide

8.1.1 Final model

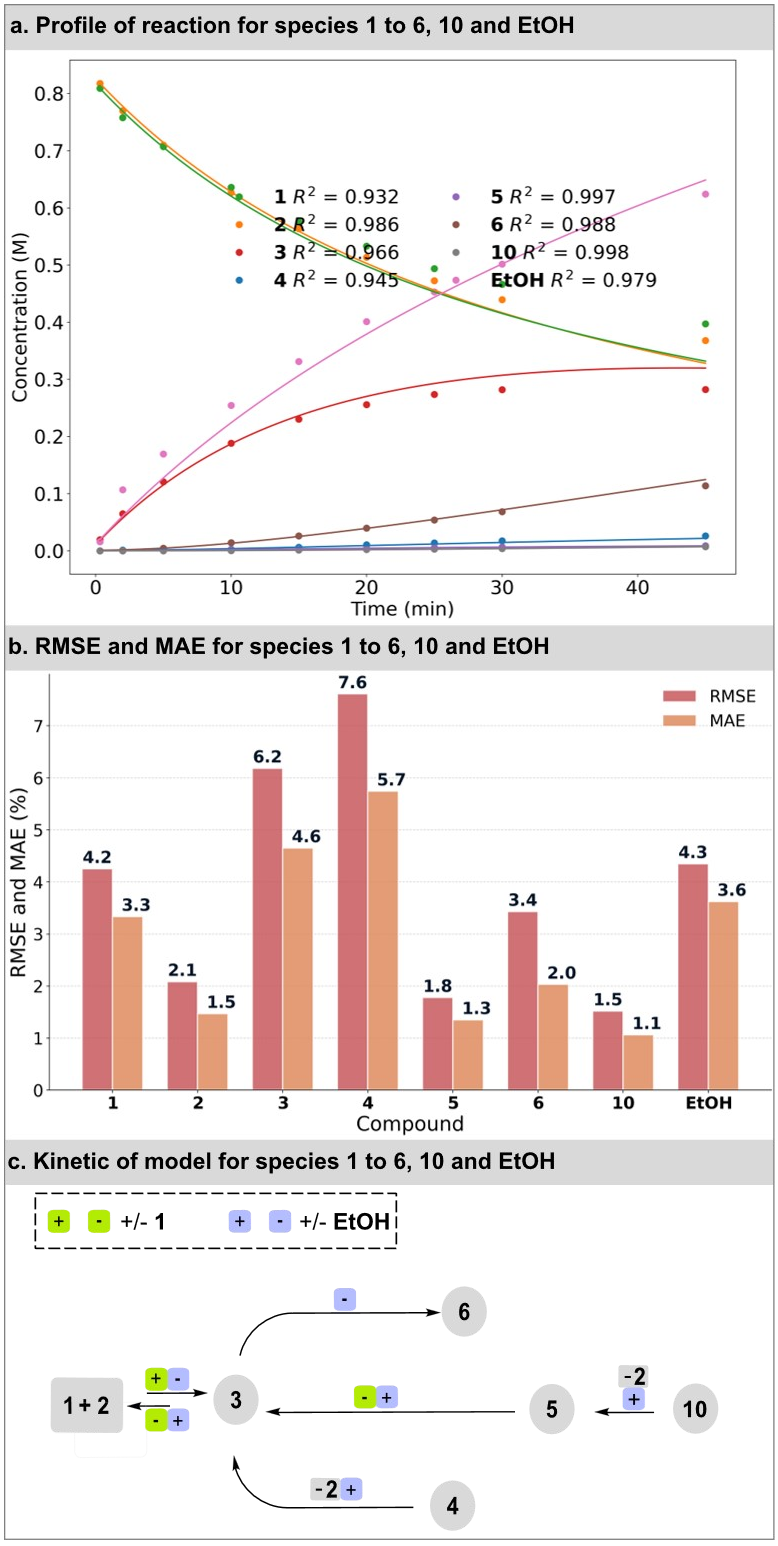


Figure S41 (a) Profile of concentrations of the various species **1** to **6**, **10** and **EtOH** over time using dimethyl sulfoxide (DMSO) as a solvent; (b) RMSE and MAE obtained; and (c) the system obtained from kinetic modelling of NMR data with the theoretical model.

8.1.2 Quantile-quantile plot

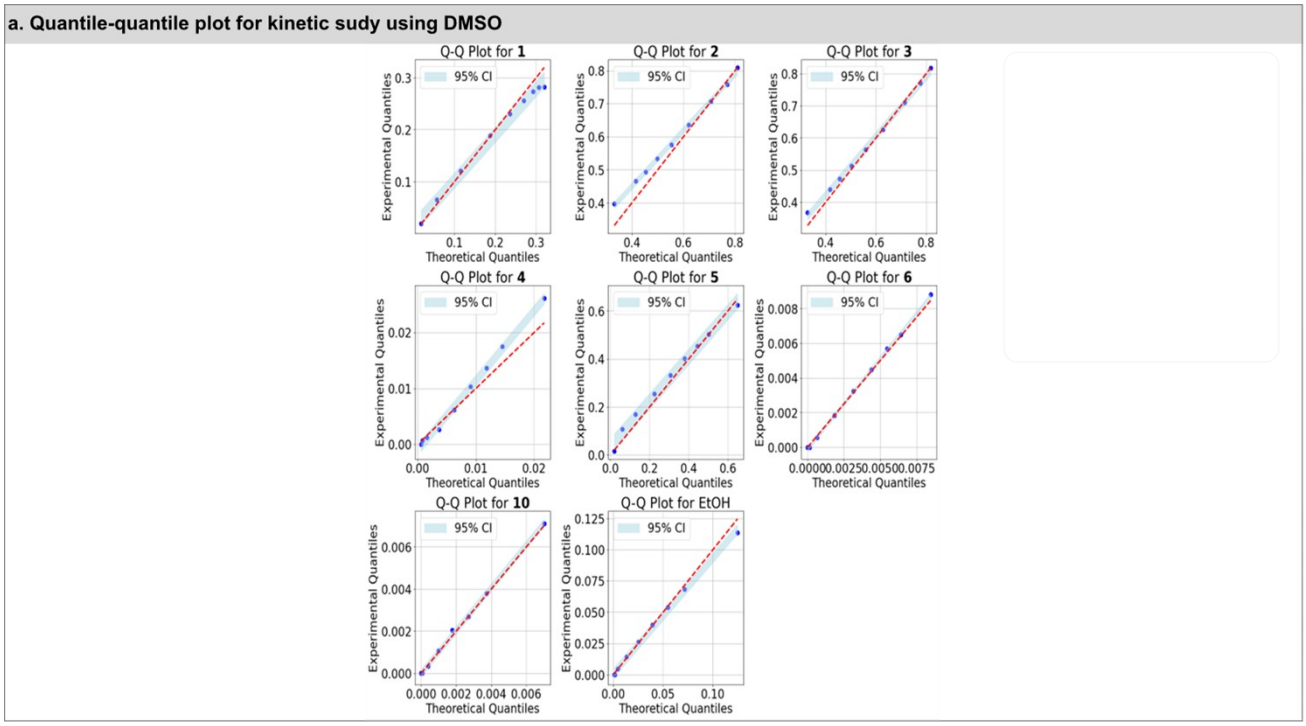


Figure S42 Quantile-quantile plots for kinetic study using dimethyl sulfoxide (DMSO) as a solvent.

8.1.3 Model initialization with calculated concentrations and rate constants

Table S7 Model initialization and calculated concentrations and rate constants for kinetic study using dimethyl sulfoxide as a solvent.

Calculated rate constants		Model initialization		Optimized values of initialization		R^2	RMSE	MAE
k_15	0.00411	c0_4	0.000601		0.00060	0.945	0.00199	0.0015
k_1	0.0379	c0_2	0.818	c0_4	1	0.986	0.017	0.012
k_18	0.0111	c0_1	0.809	c0_2	0.818	0.932	0.0344	0.027
k_3	0.00303	c0_3	0.0183	c0_1	0.809	0.966	0.0174	0.0131
k_13	0.0791	c0_5	0	c0_3	0.0183	0.997	0.00015	0.00011
		c0_6	0.000989	c0_5	0	0.988	0.0039	0.00231
		c0_ EtOH	0.0198		0.00098	0.979	0.0271	0.0226
		c0_10	0	c0_ 6	9		0.000108	7.54e-05
				c0_EtO H	0.0198			
				c0_10	0			

8.2 Kinetic study of stoichiometric amount of 1 and 2b using 10 mol% of FA in dry Dimethylformamide

8.2.1 Final model

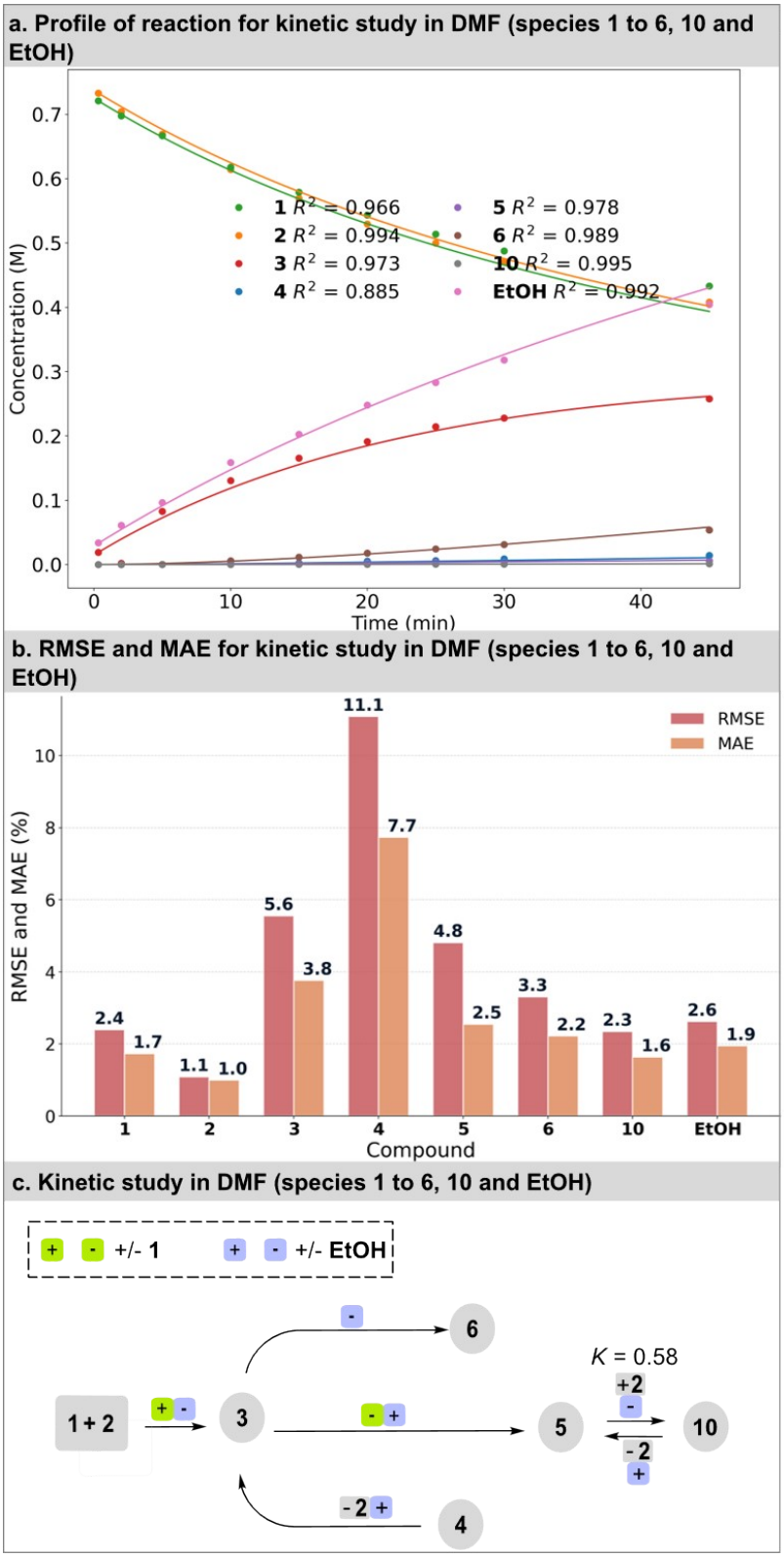


Figure S43 (a) Profile of concentrations of the various species **1** to **6**, **10** and **EtOH** over time using dimethylformamide (DMF) as a solvent; (b) RMSE and MAE obtained; and (c) the system obtained from kinetic modelling of NMR data with the theoretical model.

8.2.2 Quantile-quantile plot

a. Quantile-quantile plot for kinetic study in DMF

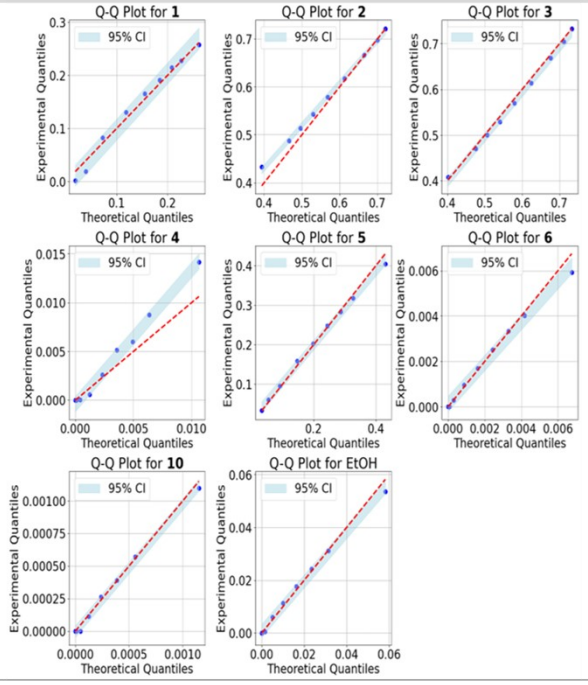


Figure S44 Quantile-quantile plots for kinetic study using dimethylformamide (DMF) as a solvent.

8.2.3 Model initialization and calculated concentrations and rate constants

Table S8 Model initialization with calculated concentrations and rate constants for kinetic study using dimethylformamide as a solvent.

Calculated rate constants		Model initialization		Optimized values of initialization		R^2	RMSE	MAE
k_15	0.00265	c0_4	0	c0_4	0	0.885	0.00157	0.00109
k_1	0.0246	c0_2	0.733	c0_2	0.733	0.994	0.00796	0.00728
k_18	0.00727	c0_1	0.721	c0_1	0.721	0.966	0.0172	0.0125
k_3	0.00201	c0_3	0.0189	c0_3	0.0189	0.973	0.0143	0.00969
k_14	0.0372	c0_5	0	c0_5	0	0.978	0.00028	0.00015
k_13	0.0217	c0_6	0	c0_ 6	0	0.989	0.00177	0.00119
		c0_ EtOH	0.033	c0_EtOH	0.033	0.992	0.0106	0.00786
		c0_10	0	c0_10	0		2.57e-05	1.79e-05

8.3 Kinetic study of stoichiometric amount of 1 and 2b using 10 mol% of FA in dry Propylene carbonate

8.3.1 Final model

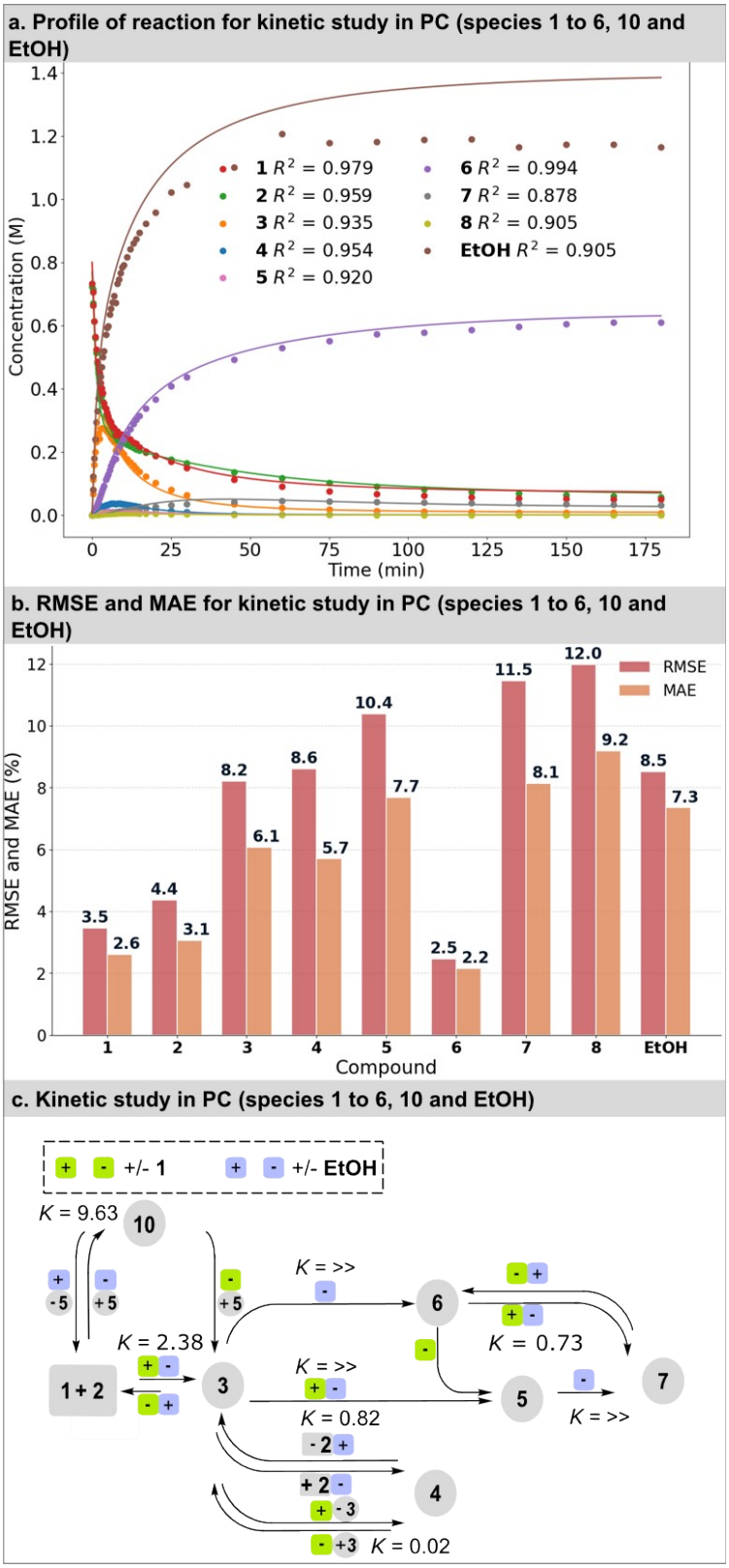


Figure S45 (a) Profile of concentrations of the various species **1** to **6**, **10** and **EtOH** over time using propylene carbonate (PC) as a solvent; (b) RMSE and MAE obtained; and (c) the system obtained from kinetic modelling of NMR data with the theoretical model.

8.3.2 Quantile-quantile plot

a. Quantile-quantile plot for kinetic study in PC

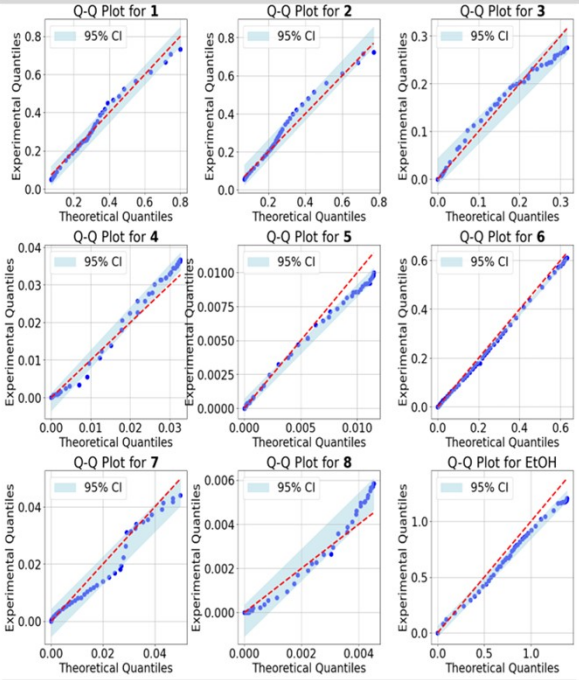


Figure S46 Quantile-quantile plots for kinetic study using propylene carbonate (PC) as a solvent.

8.3.3 Model initialization and calculated concentrations and rate constants

Table S9 Model initialization with calculated concentrations and rate constants for kinetic study using propylene carbonate as a solvent.

Calculated rate constants		Model initialization		Optimized values of initialization		R^2	RMSE	MAE
k_15	0.0818	c0_4	0	c0_4	0	0.954	0.00315	0.00209
k_25	0.0996	c0_3	0	c0_3	0	0.935	0.0226	0.0167
k_2	0.291	c0_2	0.77	c0_2	0.77	0.959	0.0315	0.022
k_1	0.695	c0_1	0.80	c0_1	0.80	0.979	0.0254	0.0191
k_18	0.107	c0_6	0	c0_6	0	0.994	0.015	0.0132
k_5	0.211	c0_		c0_			0.103	0.0887
k_3	0.0337	EtOH	0	EtOH	0	0.905	0.00104	0.00076
k_21	0.153	c0_5	0	c0_5	0	0.92	0.005	0.0035
k_19	0.00092	c0_7	0	c0_7	0	0.878	0.007	0.0005
k_4	0.00506	c0_10	0	c0_10	0	0.905		
k_8	0.015							
k_13	4.26							
k_14	0.442							
k_6	8.01							
k_7	0.037							
k_9	0.0204							

9 Reagent screening

9.1 Kinetic study of stoichiometric amount of 1 and Trimethyl orthoformate 2a using 10 mol% of FA in dry Acetonitrile

9.1.1 Final model

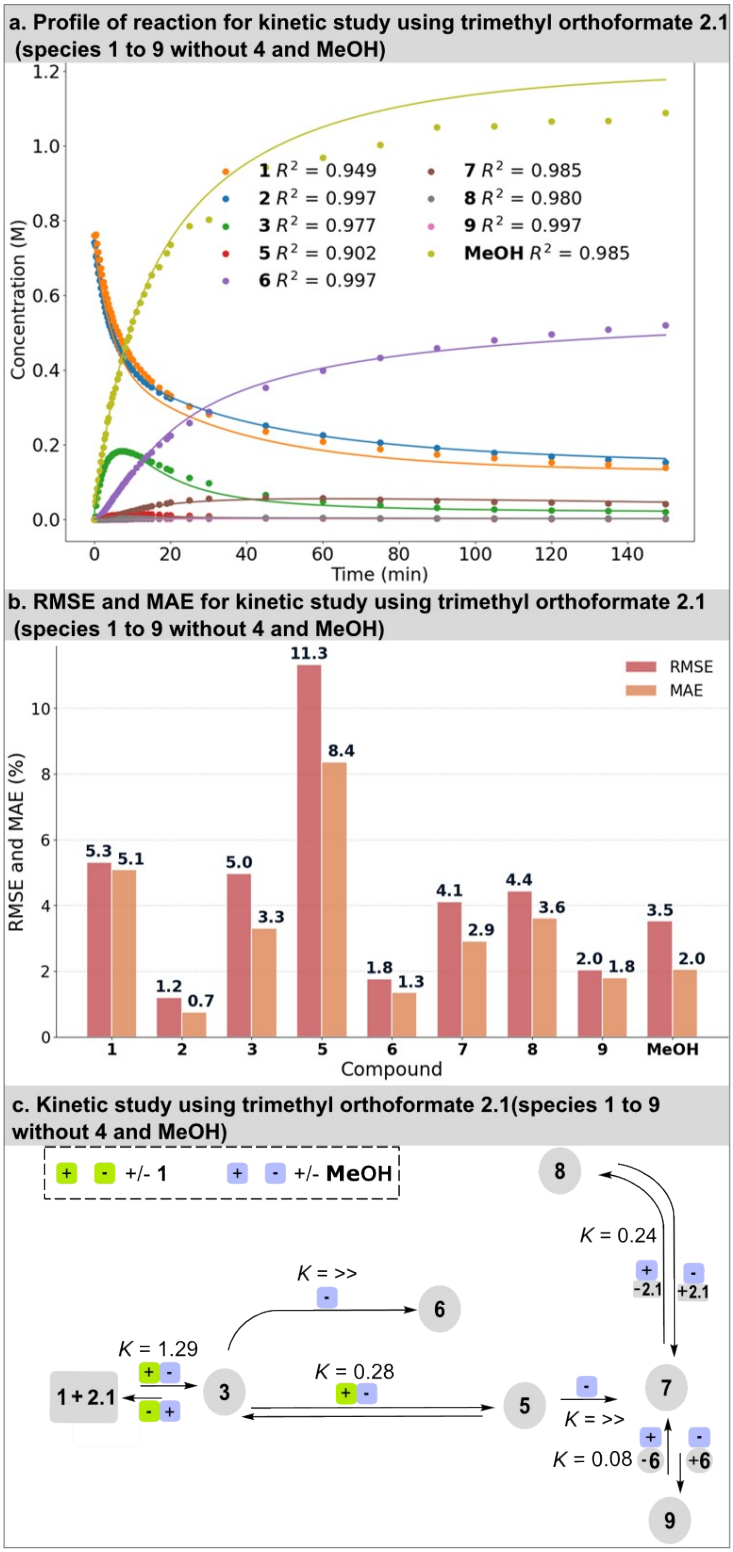


Figure S47 (a) Profile of concentrations of the various species **1**, **2a**, **3**, **5**, **6,** 7, **8**, **9** and **MeOH** over time using trimethyl orthoformate (**2a**) as a solvent; (b) RMSE and MAE obtained; and (c) the system obtained from kinetic modelling of NMR data with the theoretical model.

9.1.2 Quantile-quantile plot

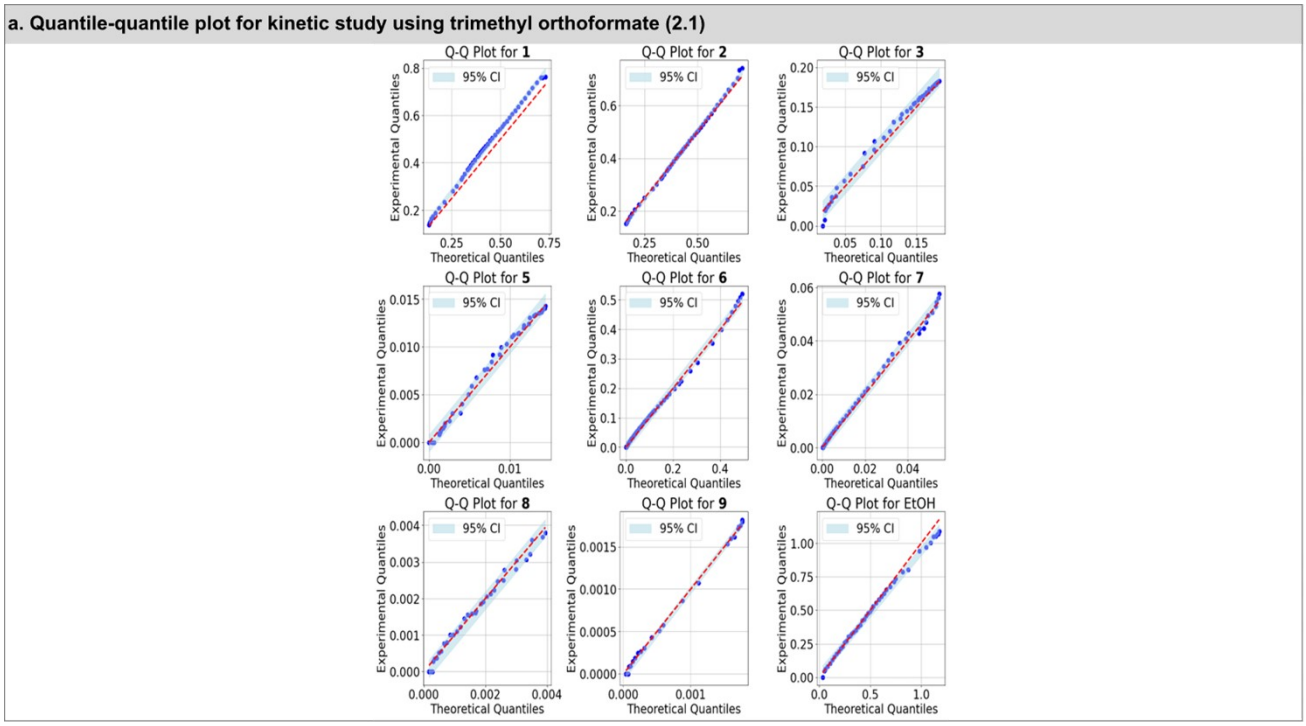


Figure S48 Quantile-quantile plots for kinetic study using trimethyl orthoformate (**2a**) as a reagent.

9.1.3 System of differential equations describing the kinetic model

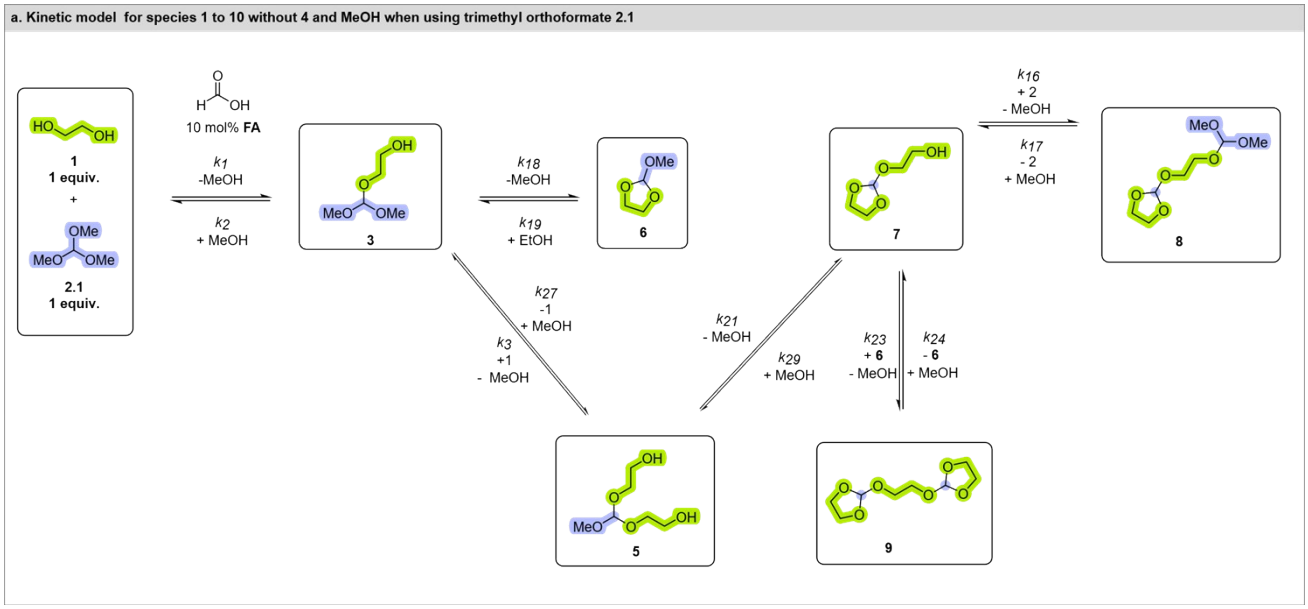


Figure S49 Representation of kinetic of reaction between **1** and trimethyl orthoformate (**2a**), including the rate constants.

$$\frac{d[C1]}{dt} - k1 * [1] * [2] + k2 * [3] * [MeOH] + k3 * [3] * [1] + k27 * [5] * [MeOH]$$

$$\frac{d[C2]}{dt} = - k1 * [1] * [2] + k2 * [3] * [MeOH] + k16 * [2] * [7] - k17 * [8] * [MeOH]$$

$$\frac{d[C3]}{dt} = k1 * [1] * [2] - k2 * [3] * [MeOH] + k27 * [5] * [MeOH] - k3 * [3] * [1] - k18 * [3$$

$$\frac{d[C5]}{dt} = + k3 * [3] * [1] - k27 * [5] * [EtOH] - k21 * [5] + k29 * [7] * [MeOH]$$

$$\frac{d[C6]}{dt} = k18 * [3] - k19 * [6] * [MeOH]$$

$$\frac{d[C7]}{dt} = - k21 * [5] - k29 * [7] * [MeOH] - k16 * [2] * [7] + k17 * [8] * [MeOH] - k23 * [6$$

$$\frac{d[C8]}{dt} = k16 * [2] * [7] - k17 * [8] * [MeOH]$$

$$\frac{d[C9]}{dt} = k23 * [6] * [7] - k24 * [9] * [MeOH]$$

$$\frac{d[CMeOH]}{dt} = k1 * [1] * [2] - k2 * [3] * [MeOH] + k18 * [3] - k19 * [6] * [MeOH] + k3 * [3] * [1 + k21 * [5] - k29 * [7] * [MeOH] + k16 * [2] * [7] - k17 * [8] * [MeOH] + k23 * [6] * [9] * [MeOH]$$

9.1.4 Model initialization with calculated concentrations and rate constants

Table S10 Model initialization with calculated concentrations and rate constants for kinetic study using trimethyl orthoformate (**2a.**).

Calculated rate constants		Model initialization		Optimized values of initialization		R^2	RMSE	MAE
k_2	0.107	c0_2	0.711	c0_2	0	0.997	0.00891	0.00553
k_1	0.138	c0_1	0.73	c0_1	0	0.949	0.0405	0.0387
k_18	0.0814	c0_3	0.0187	c0_3	0.77	0.977	0.00905	0.00604
k_19	0.0022	c0_5	0	c0_5	0.80	0.902	0.00162	0.0012
k_3	0.0613	c0_6	0	c0_6	0	0.997	0.00913	0.00698
k_27	0.216	c0_7	0.0002	c0_7	0	0.985	0.00237	0.00168
k_21	0.224		4.11e-05	c0_9	0	0.997	3.69e-05	3.26e-05
k_29	0.00792	c0_9		c0_8				
k_16	0.046	c0_8	0.0001	0				
k_17	0.188	c0_MeOH	0.0343	c0_MeOH				
k_23	0.0143							
k_24	0.173							

9.2 Kinetic study of stoichiometric amount of 1 and Triisopropyl orthoformate (2c) using 10 mol% of FA in dry acetonitrile

9.2.1 Final model

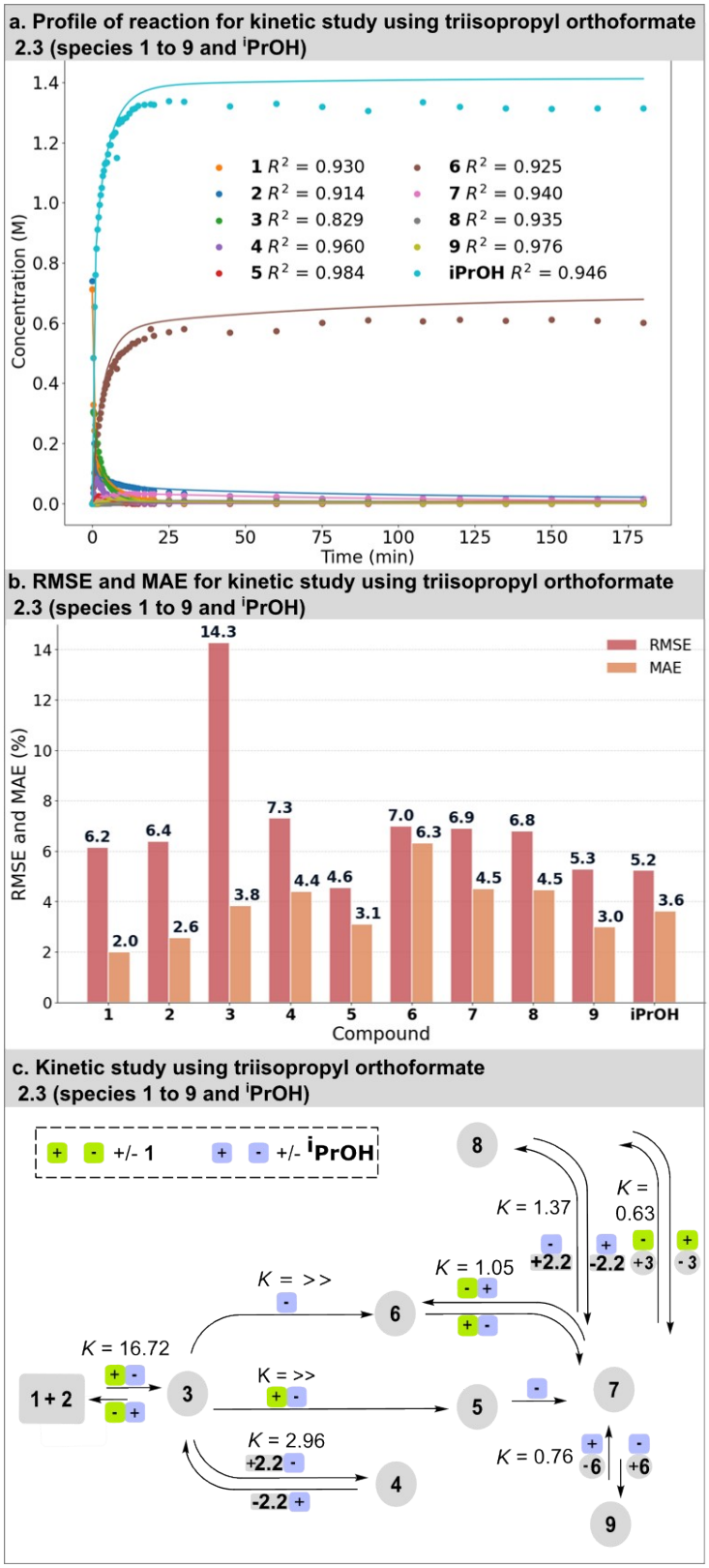


Figure S50 (a) Profile of concentrations of the various species **1**, **2c**, **3**, **5**, **6**, **7**, **8**, **9** and **^{i}POH** over time using trimethyl orthoformate (**2c**) as a solvent; (b) RMSE and MAE obtained; and (c) the system obtained from kinetic modelling of NMR data with the theoretical model.

9.2.2 Quantile-quantile plot

a. Quantile-quantile plot for kinetic study using triisopropyl orthoformate (2.2)

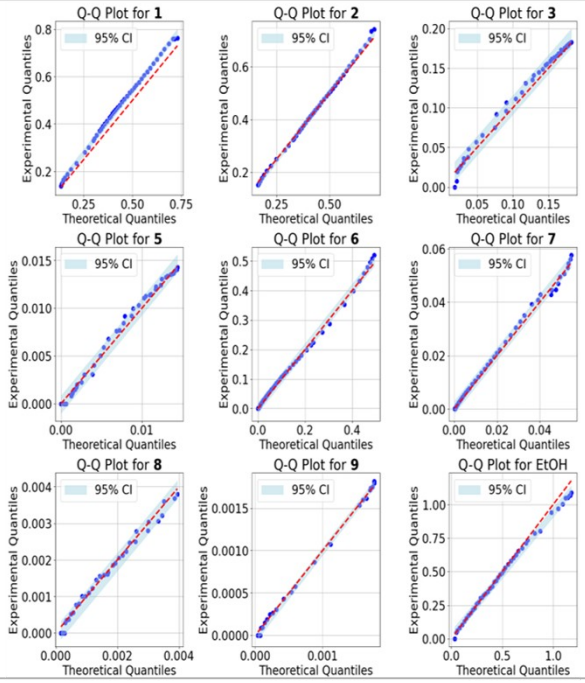


Figure S51 Quantile-quantile plots for kinetic study using triispropyl orthoformate (**2c**) as a reagent

9.2.3 System of differential equatic describing the kinetic model

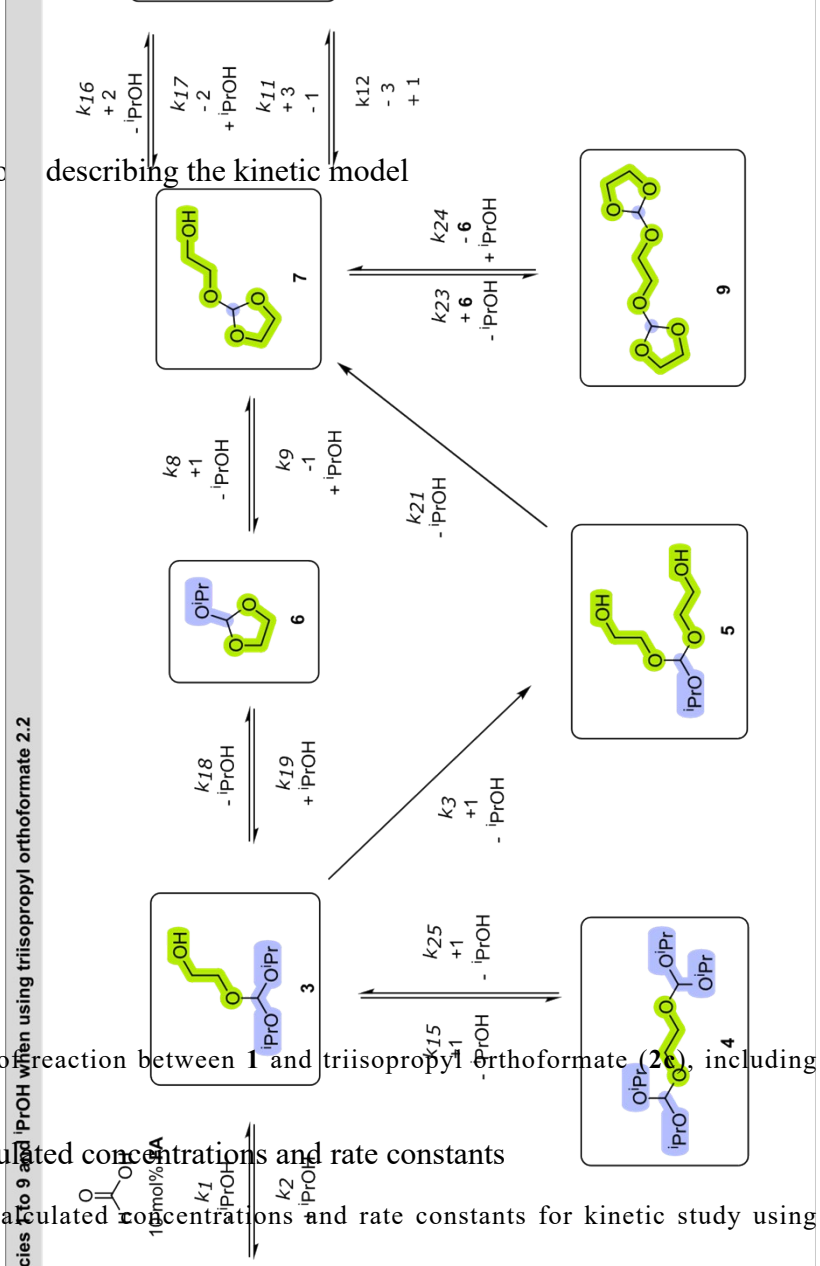


Figure S52 Representation of kinetic of reaction between **1** and triisopropyl orthoformate (**2c**), including the rate constants.

9.2.4 Model initialization and calculated concentrations and rate constants

Table S11 Model initialization with calculated concentrations and rate constants for kinetic study using triisopropyl orthoformate (**2c.**)

Calculated rate constants		Model initialization		Optimized values of initialization		R^2	RMSE	MAE
k_15	1.34	c0_2	0.72	c0_2	0.72	0.914	0.0472	0.0189
k_25	0.452	c0_1	0.72	c0_1	0.72	0.93	0.0438	0.0143
k_2	0.486	c0_3	0	c0_3	0	0.829	0.0433	0.0117
k_1	8.13	c0_5	0	c0_5	0	0.984	0.0011	0.000754
k_18	0.546	c0_4	0	c0_4	0	0.96	0.00642	0.00387
k_3	0.326	c0_6	0			0.925	0.0427	0.0386
k_21	0.409	c0_7	0	c0_6	0	0.94	0.00224	0.00146
k_19	0.0009	c0_9	0	c0_7	0			
k_8	0.0114	c0_8	0	c0_9	0			
k_11	8.07	c0_iPOH	0	c0_8	0			
k_12	12.7			c0_iPOH	0			
k_16	0.0989							
k_17	0.0719							
k_23	0.0715							
K_9	0.0109							
K_24	0.0938							

10 Computations

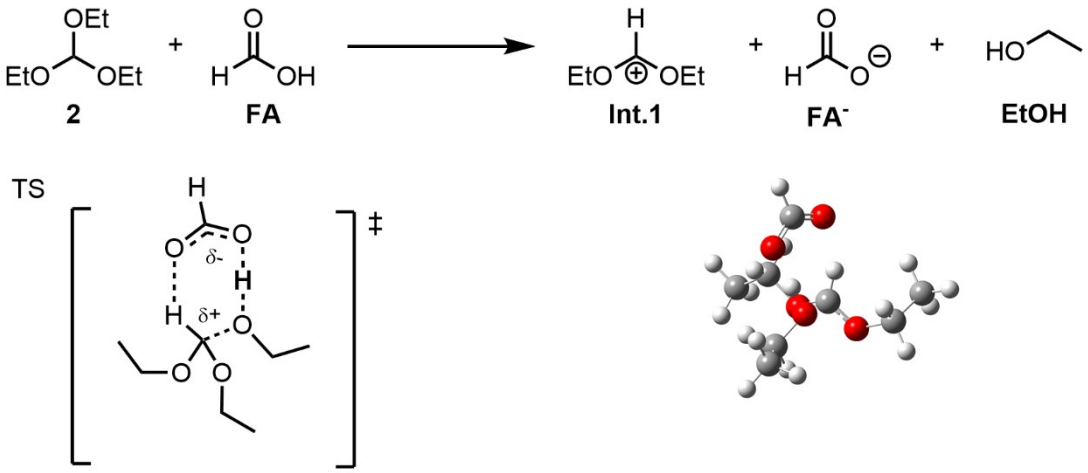
10.1 Computational methods

DFT computations were performed using the Gaussian 16 (Revision C.01)[3] software package. All stationary points were optimized and localized at the B3LYP-GD3BJ/6-31+G*(d) level of theory. The SMD method was used to model solvent effects using the built-in parameters for acetonitrile (MeCN, ε = 38.8). Stationary points were characterized by frequency calculations (local minima with only real frequencies and transition states with one imaginary frequency) and a systematic attempt to locate the lowest-energy conformers. Low-energy stationary structures were identified through a systematic exploration of chemically reasonable starting geometries, followed by geometry optimization and frequency analysis at the chosen level of theory. Transition states were further validated by intrinsic reaction coordinate (IRC) calculations.

10.2 Cartesian coordinates and energies for representative transition states

10.2.1 DCE mechanism for the formation of 3, 4, 5, 6, 7, 10 and 11

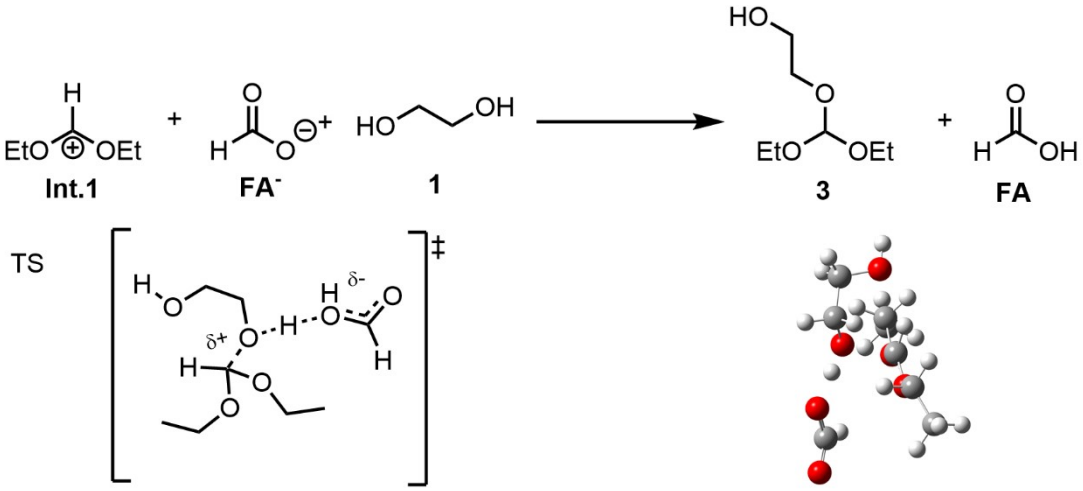
Table S12 Transition state: activation of **2** in carbocation int.**1**



Coordinates of the TS (atom, X, Y, Z)	Energies
0 1 C -0.73600800 -0.49526400 -0.37547200 H -0.74122900 -0.56797700 0.71553800 O -1.79142200 -0.09024900 -1.02965900 O 0.01754200 -1.30046500 -1.07728100 O 0.28237700 1.14710500 -0.22163600 C -2.78948500 0.65377600 -0.24436200 H -3.30915000 1.25401200 -0.99178600 H -2.25370900 1.31627600 0.43889400 C -3.72106700 -0.29921000 0.47391700 H -3.18114000 -0.90959900 1.20668500 H -4.47947000 0.28452700 1.00911200 H -4.23024200 -0.96073900 -0.23539400 C 1.12679700 -1.95006300 -0.36038500 H 1.75867600 -1.16551800 0.06136800 H 0.69249900 -2.54366000 0.44786000 C 1.87050300 -2.80216300 -1.36059500 H 2.28236400 -2.19001700 -2.17019500 H 2.70104100 -3.30156700 -0.84881800	H = -691.58975 Hartree G = -691.65602 Hartree

H 1.21733300 -3.57001600 -1.78933400 C 1.07294500 1.45279000 -1.38673000 H 1.95990700 0.80823400 -1.40611500 H 0.45223100 1.21010300 -2.25449400 C 1.46225600 2.92200800 -1.39631600 H 2.03944400 3.14347500 -2.30283200 H 0.57083300 3.55972100 -1.38818300 H 2.08114400 3.17343700 -0.52723400 C 1.20382600 0.13353900 2.72423900 H 1.79849800 -0.02996000 3.64905300 O 0.08269800 -0.41590400 2.64489600 O 1.76087100 0.87656000 1.84863700 H 0.88584400 1.06039700 0.62044200	

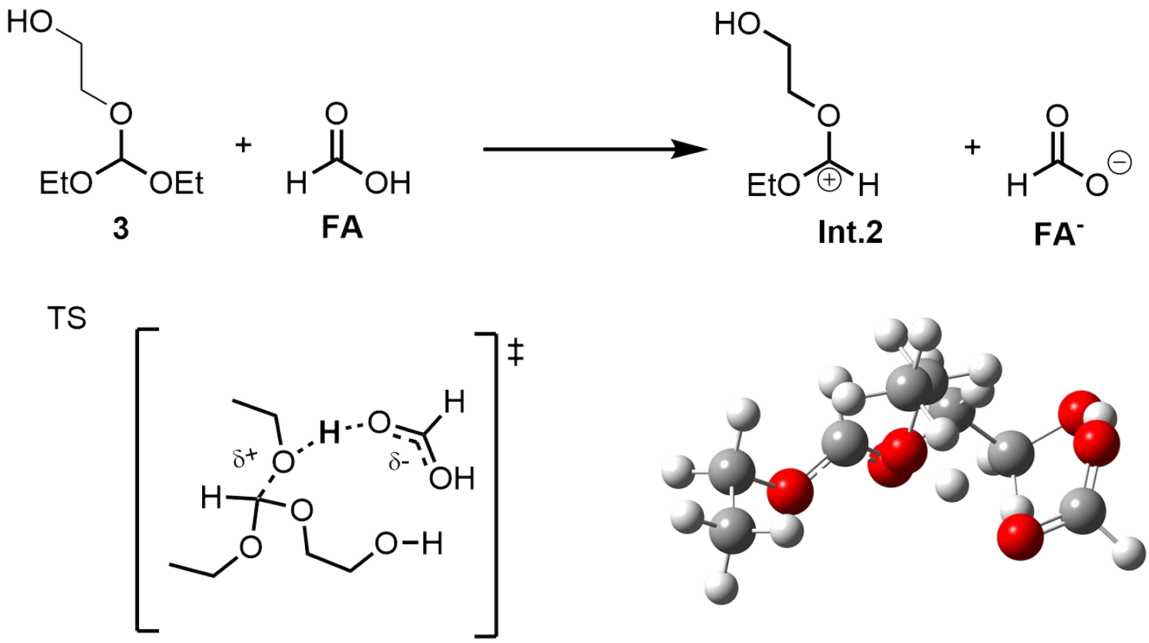
Table S13 Transition state: substitution of carbocation int.**1** by **1**



Coordinates of the TS (atom, X, Y, Z)	Energies
0 1 C -0.48691100 0.42200100 0.76777300 H -1.14502500 -0.32406700 1.21298800 O -0.98759600 1.53003300 0.29651200 O -0.32582500 -0.64502700 -0.85354300 O 0.73813100 0.56631000 1.19358800 C -2.40701200 1.51097700 -0.08390800 H -2.97536500 1.11845600 0.76316800 H -2.50150500 0.83571500 -0.93631000 C -2.79928800 2.92793800 -0.42949200 H -2.20294000 3.30850300 -1.26588800 H -3.85441500 2.93838500 -0.72590700 H -2.67529900 3.59478500 0.43070300 C -0.66112200 -2.04464100 -0.78514800 H -0.27682200 -2.52342100 -1.69298000 H -0.17789000 -2.50940700 0.08364500 C -2.15571500 -2.24380400 -0.71866800 H -2.64773700 -1.67935900 -1.52131700 H -2.37127800 -3.31225400 -0.85559700 C 1.37619700 -0.59518600 1.82720000 H 0.63778600 -1.07778900 2.47422900 H 1.66747200 -1.27444100 1.02399400 C 2.57500200 -0.08811000 2.59310800 H 3.08315400 -0.94116400 3.05697000	H = -766.79962Hartree G = -766.86864Hartree

H 3.28250200 0.41088100 1.92198800 H 2.27593500 0.60938500 3.38299300 O -2.62043000 -1.80193200 0.56695400 H -3.59222200 -1.83404200 0.57480900 H 0.68759600 -0.56323500 -1.15686300 C 2.66577800 0.57121200 -1.47323300 H 1.99866000 1.43663800 -1.26229000 O 3.87907900 0.79787700 -1.62986700 O 2.08486900 -0.56924800 -1.53541000	

Table S14 Transition state: activation of **3** in carbocation int.**2** (first structure identified)



Coordinates of the TS (atom, X, Y, Z)	Energies
0 1 C -1.20429400 0.84285000 -0.50559600 H -1.30718500 1.24424500 -1.51251600 O -1.62426700 -0.36550200 -0.25702700 O -1.29819000 1.74107900 0.43468100 O 0.70285700 0.65763200 -0.69542000 C -1.67950300 -1.30698500 -1.38535900 H -0.66058400 -1.66491500 -1.54572000 H -2.02737400 -0.75847200 -2.26582200 C -2.61823300 -2.42479000 -0.99773900 H -3.63112600 -2.04853500 -0.81783600 H -2.65809200 -3.15020400 -1.81844000 H -2.26228400 -2.94082400 -0.09955300 C -1.40289200 1.36841500 1.85366500 H -1.72285000 2.30487300 2.31244500 H -2.18681400 0.61574300 1.96201200 C -0.09500800 0.89915300 2.47127600 H 0.73815500 1.48780200 2.06873800 H -0.17350800 1.12427700 3.54595100 C 1.23878600 1.30551600 -1.87117900 H 2.23094700 0.87793400 -2.04876500 H 0.60597200 1.06525100 -2.73652100	H = -766.80181 Hartree G =-766.86834 Hartree

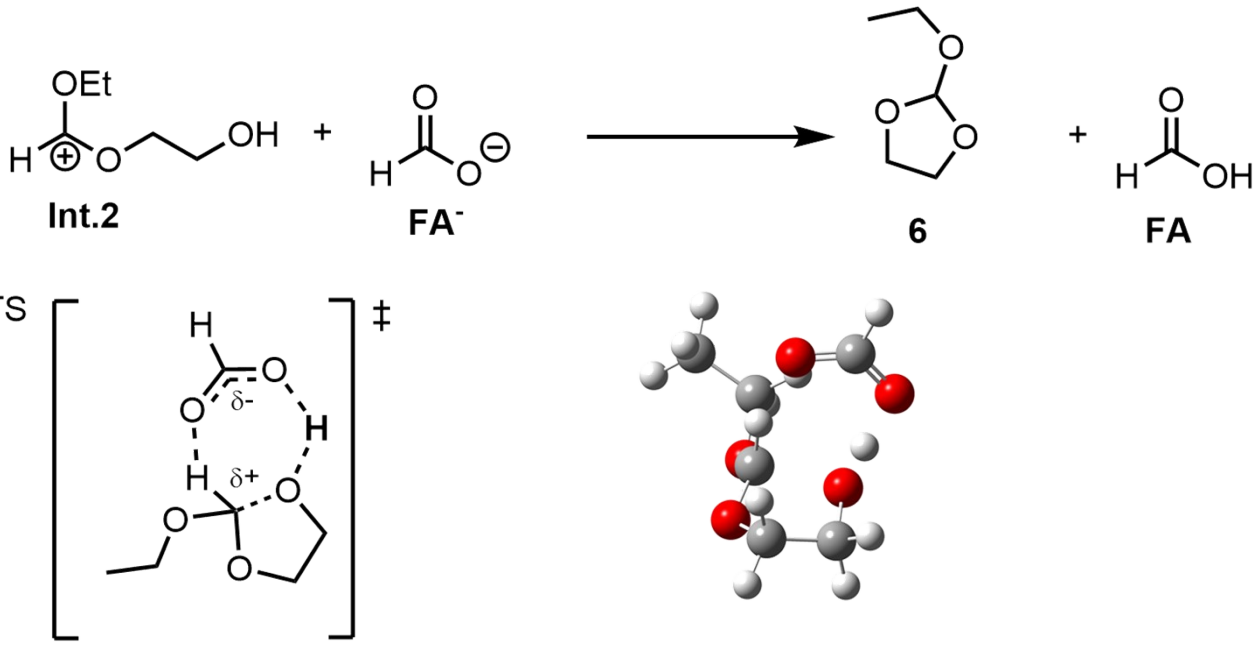
C 1.32257700 2.80375600 -1.64998600 H 1.76681000 3.27920200 -2.53279200 H 0.33251700 3.24457700 -1.48998800 H 1.94909000 3.03170300 -0.78007900 O 0.11170100 -0.49229400 2.30450700 H 0.97563000 -0.68219200 1.86388100 H 1.02223200 -0.32633200 -0.68264000 C 2.40617100 -2.00629100 0.17249400 H 3.07318200 -2.88043500 0.02151200 O 2.47110100 -1.41457800 1.27725200 O 1.65300500 -1.71551600 -0.81015800	

Table S15 Transition state: activation of **3** in carbocation int.**2** (second geometry identified)

Coordinates of the TS (atom, X, Y, Z)	Energies
0 1 C -0.91574900 -1.21624800 -0.36319800 H -1.07702700 -1.05955100 -1.43088400 O -1.91009400 -1.56903300 0.39681900 O -0.81924100 0.68671600 -0.08410700 O 0.23257100 -1.68064200 0.05227100 C -3.26595800 -1.17665800 -0.02202600 H -3.80983600 -2.11770400 -0.12739700 H -3.20159500 -0.68508800 -0.99538700 C -3.87283400 -0.28240500 1.03532000 H -3.30064400 0.64339300 1.14227800 H -4.89720300 -0.03110200 0.73530800 H -3.91469100 -0.79369700 2.00325300 C -0.74673100 1.54060900 -1.24770200 H 0.28393200 1.89674400 -1.35234300 H -0.98350200 0.92348400 -2.12164400 C -1.72959500 2.69179500 -1.12349300 H -1.49894200 3.31042100 -0.24847800 H -1.67176100 3.32539600 -2.01765700 H -2.75615000 2.31976800 -1.02879300 C 1.39205600 -1.37966100 -0.78941900 H 1.34007300 -2.00996900 -1.68104100	H = -766.80102 Hartree G -766.86789 Hartree

H 1.34902400 -0.32501400 -1.06412800 C 2.64204700 -1.63969900 0.04590800 H 2.46292400 -1.30027700 1.07503200 H 2.88360800 -2.70596000 0.07335500 C 2.15030300 1.58545800 1.24180600 H 2.85734700 1.83943200 2.05923600 O 2.61245200 1.49534900 0.07767600 O 0.94348100 1.41848800 1.60477000 H -0.06927700 0.95421100 0.58864100 O 3.75374100 -0.96552900 -0.53200500 H 3.57920200 -0.00642300 -0.39592200	

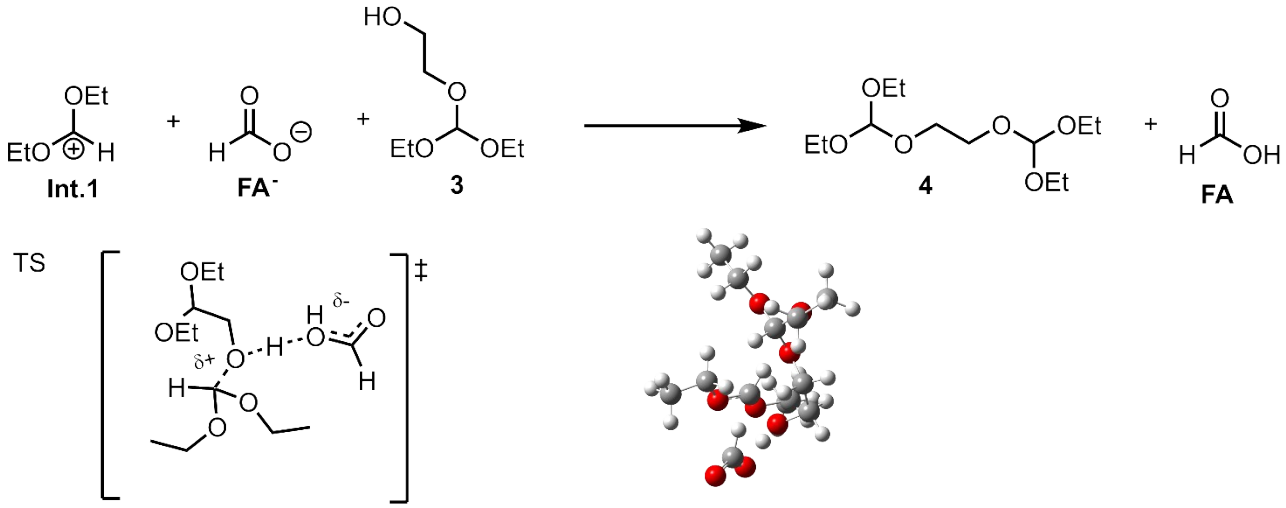
Table S16 Transition state: intramolecular cyclization of int.**2** in **6**



Coordinates of the TS (atom, X, Y, Z)	Energies
0 1 C -0.52938200 -0.76669500 0.20479700 H -0.30122800 0.19346900 0.67899100 O -0.06079800 -1.88406900 0.73881300 O -1.64232700 -0.92533700 -0.44882400 C -2.38446000 0.30866300 -0.77116500 H -1.65803000 1.07257000 -1.06035900 H -2.97757000 0.02896200 -1.64202300 C 1.38188000 -1.80432700 0.89044400 H 1.71288100 -2.77577200 1.25495000 H 1.62692300 -1.01763300 1.60955200 C -3.24428500 0.73504900 0.39832100 H -3.81636600 1.62453500 0.10888400 H -3.94984700 -0.05574800 0.67530600 H -2.63318400 0.99102400 1.27109300 C 1.87004000 -1.46674800 -0.52072100 H 2.86549600 -1.01406400 -0.49728900 H 1.87927900 -2.35548400 -1.15631600 O 0.90914400 -0.54561400 -1.05026900 H 1.25607300 0.46766700 -0.93802200 C 1.40105800 2.39567800 0.24604000	H = -611.81983 Hartree G= -611.87285 Hartree

H 1.77703300 3.43613500 0.33035600 O 1.72554100 1.79884800 -0.84030400 O 0.72461800 1.93049900 1.18540700	

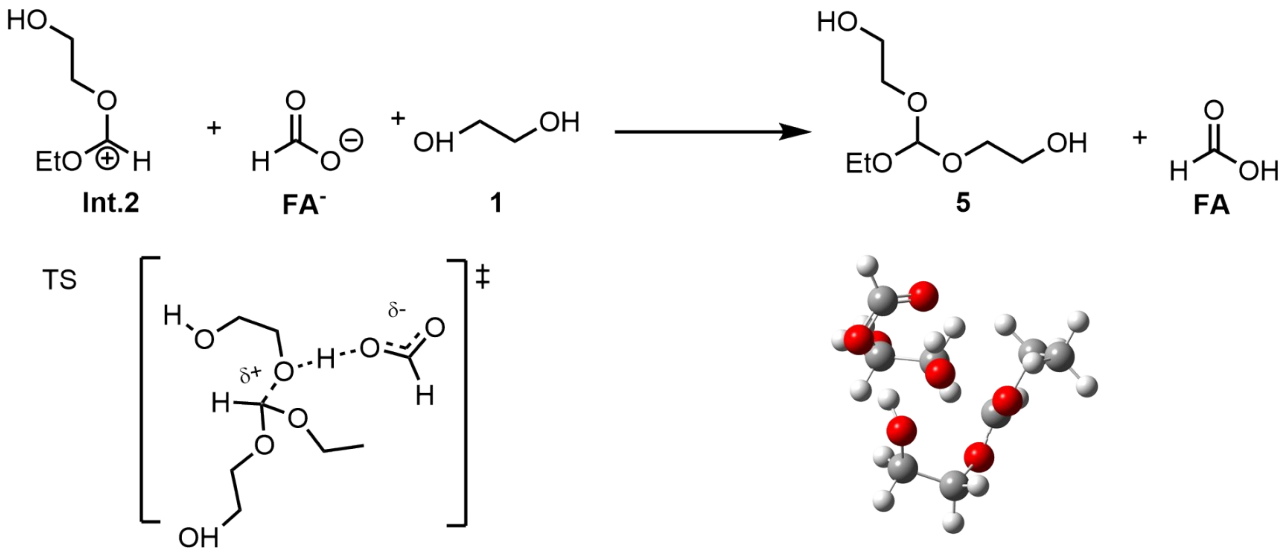
Table S17 Transition state: addition of **3** on int.**1** to **4**



Coordinates of the TS (atom, X, Y, Z)	Energies
0 1 C -1.94457100 -0.92614700 -0.23186100 H -0.97524700 -1.30345700 0.09082400 O -2.04186000 -0.29357700 -1.37222700 O -3.03490300 -1.57668500 0.07831600 C -0.79519700 0.25429500 -1.92483200 H -0.13172800 -0.58715100 -2.13886400 H -0.34347500 0.88950500 -1.16253200 C -1.15343100 1.03734100 -3.16435600 H -1.82616800 1.86729800 -2.92388000 H -0.23506400 1.45142700 -3.59615000 H -1.62889100 0.39600400 -3.91445200 C -2.99849200 -2.36770500 1.31264700 H -1.99425300 -2.78934800 1.41875000 H -3.19306100 -1.67648500 2.13579900 C -4.05786200 -3.43986500 1.20680900 H -4.06290400 -4.02382300 2.13429700 H -5.05176200 -2.99905500 1.07293200 H -3.85188200 -4.11788000 0.37145600 H -2.09027300 1.46039800 0.66053000 C -1.51720700 3.46224800 -0.32100000 H -0.50369100 3.00434300 -0.33322000 O -1.64633400 4.59807400 -0.80858000 O -2.43988100 2.74870300 0.21241400 C 2.02829500 -0.32847800 0.17262900 H 1.96301100 0.57379300 -0.45750900 O 2.09069600 -1.47884300 -0.60314400 O 0.85881200 -0.49159700 0.92005600 O 3.14962200 -0.22867800 1.01463400 C 3.10755100 -1.43143900 -1.61848800 H 4.09404100 -1.35889400 -1.14429300 H 2.95498600 -0.53431300 -2.23601800 C 2.99942200 -2.69075700 -2.45466600 H 2.01608600 -2.76083100 -2.93398300 H 3.76586300 -2.67933700 -3.23857600	H = -1113.6819 Hartree G = -1113.7724 Hartree

H 3.15219900 -3.58367500 -1.83729800 C 0.47652800 0.66479600 1.67432100 H 1.12070200 0.77236000 2.55642700 H 0.57817500 1.56577300 1.05501500 C -0.95678900 0.48079000 2.12661000 H -1.06302500 -0.46492100 2.66648000 H -1.22336700 1.29701600 2.80823600 C 3.88427200 1.00859100 0.92949300 H 4.22552200 1.16005800 -0.10317700 H 3.22843300 1.84647100 1.19999700 C 5.06201600 0.92065900 1.87839500 H 5.64223900 1.84997700 1.83413400 H 4.72203900 0.77501200 2.91042000 H 5.72140900 0.08809600 1.60658200 O -1.91329000 0.47456200 1.05651700	

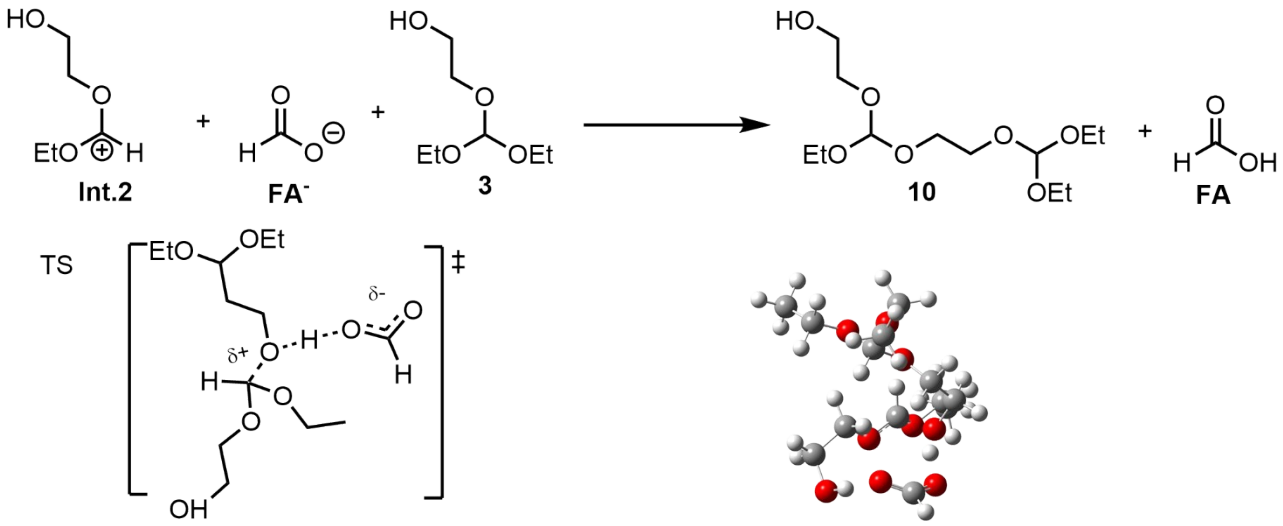
Table S18 Transition state: addition of **1** on int.2 to **5**



Coordinates of the TS (atom, X, Y, Z)	Energies
0 1 C 0.94873400 -0.98430000 -1.08133000 H 0.64952600 -0.97426200 -2.12792000 O 1.91102600 -0.20115600 -0.68324900 O 0.81084200 -2.14654400 -0.50464400 O -0.63290200 -0.09812200 -0.49443500 C 2.16740100 1.01469200 -1.47134000 H 1.43831000 1.75909600 -1.14448800 H 2.00653000 0.77346700 -2.52649100 C 3.58753600 1.44582700 -1.19179200 H 4.30440000 0.68073000 -1.50892200 H 3.79167800 2.36601700 -1.75122000 H 3.73145100 1.65264300 -0.12582200 C 1.32591100 -2.38958200 0.85258700 H 1.27857300 -3.47713100 0.92243600 H 2.36653000 -2.06113000 0.89589900 C 0.49759900 -1.75776400 1.96264200 H -0.56835900 -1.82134700 1.71471500 H 0.67100600 -2.38271000 2.85103900 C -1.79331300 -0.35169700 -1.29591200	H= -842.01323 Hartree G = -842.08294 Hartree

H -1.85389800 0.37123300 -2.11856500 H -1.69020900 -1.35709000 -1.71691700 C -3.03653800 -0.28278900 -0.42101500 H -2.95008600 -1.00937900 0.39795400 H -3.13978600 0.72112400 0.01115100 O 0.89171100 -0.43191800 2.27092500 H 0.17946900 0.22076500 2.07364700 H -0.55145900 0.92549700 -0.28334900 C -0.83880100 2.56741000 1.25036600 H -1.08390600 3.61379000 1.52457200 O -0.84533200 1.70904500 2.16177200 O -0.57755500 2.37451600 0.01657500 O -4.15333400 -0.59005200 -1.26372200 H -4.96658900 -0.49824500 -0.73872600	

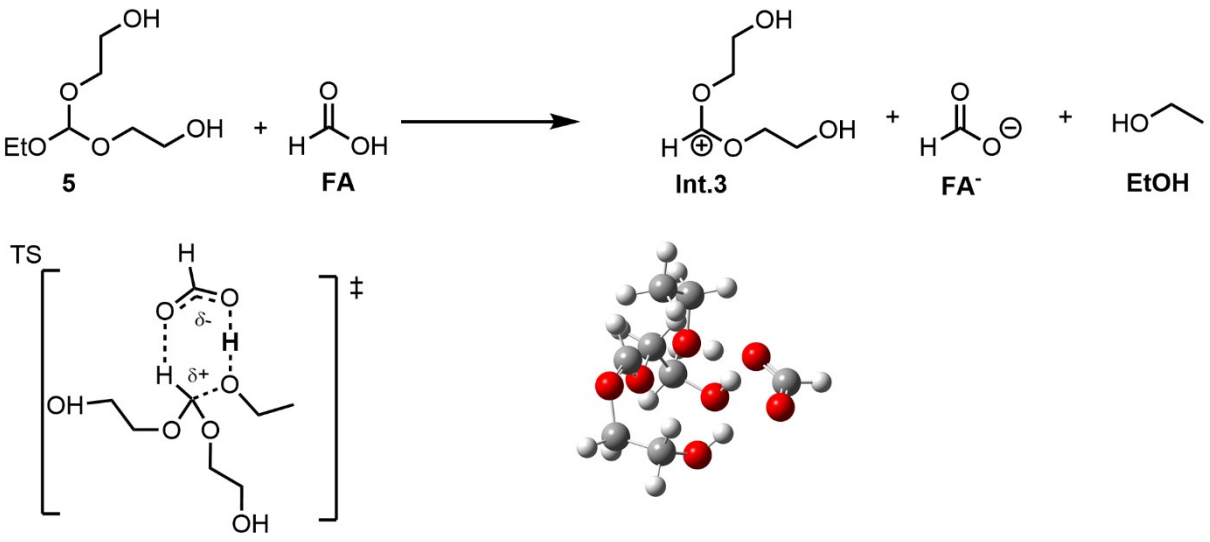
Table S19 Transition state: addition of **3** on int.**2** to **10**



Coordinates of the TS (atom, X, Y, Z)	Energies
0 1 C 2.03041800 -0.87510100 0.17758500 H 1.13860000 -1.44595500 -0.08273700 O 2.00907100 -0.12566100 1.25501900 O 3.21361100 -1.40574300 -0.02674700 C 0.68860100 0.29443900 1.71996200 H 0.08489900 -0.59691400 1.91120500 H 0.23116000 0.89650200 0.93354500 C 0.86323700 1.11083400 2.98037600 H -0.14938000 1.30662300 3.36879000 H 1.40662300 0.53482400 3.73691800 C 3.33298000 -2.33276200 -1.15382500 H 2.41931700 -2.93380200 -1.20367400 H 3.42103900 -1.72772100 -2.05954400 C 4.55931700 -3.18515400 -0.92252400 H 4.67733800 -3.87138900 -1.76898100 H 5.46072600 -2.56646200 -0.85319600 H 4.46146800 -3.77797000 -0.00662500 H 1.89616800 1.33183500 -1.02010500 C 1.28751000 3.62991700 -0.52652700 H 1.31316100 4.65669900 -0.94650100 O 2.02947300 2.78876300 -1.12772400	H= -1188.8997Hartree G = -1188.9905 Hartree

O 0.55006300 3.42951300 0.46697000 C -2.07753400 -0.51538900 -0.20772400 H -2.01259500 0.45848400 0.30461200 O -2.14818600 -1.55876800 0.70626700 O -0.90442000 -0.77458900 -0.92204100 O -3.19371300 -0.51614400 -1.06281900 C -3.17466600 -1.38317500 1.69772000 H -4.15662500 -1.37647500 1.20894300 H -3.03012100 -0.41307400 2.19516600 C -3.07204600 -2.52300900 2.69118600 H -2.09447100 -2.52504400 3.18712100 H -3.84804500 -2.41445800 3.45806200 H -3.21386100 -3.48906200 2.19272400 C -0.54826200 0.25444200 -1.85160200 H -1.19232000 0.20542800 -2.73854700 H -0.66648100 1.24293900 -1.38767000 C 0.88793400 0.03122900 -2.26903700 H 1.04024600 -1.00266000 -2.58996700 H 1.13634800 0.69412400 -3.10381100 C -3.93566900 0.71924500 -1.11419500 H -4.28437900 0.97771400 -0.10562400 H -3.28135000 1.52684000 -1.46760100 C -5.10680200 0.52523200 -2.05526300 H -5.69154000 1.45104300 -2.11219300 H -4.76010600 0.27351800 -3.06437300 H -5.76421100 -0.27728500 -1.70081100 O 1.84092900 0.29569000 -1.21834600 O 1.58161300 2.31802000 2.77387200 H 1.22075200 2.74854300 1.96247200	

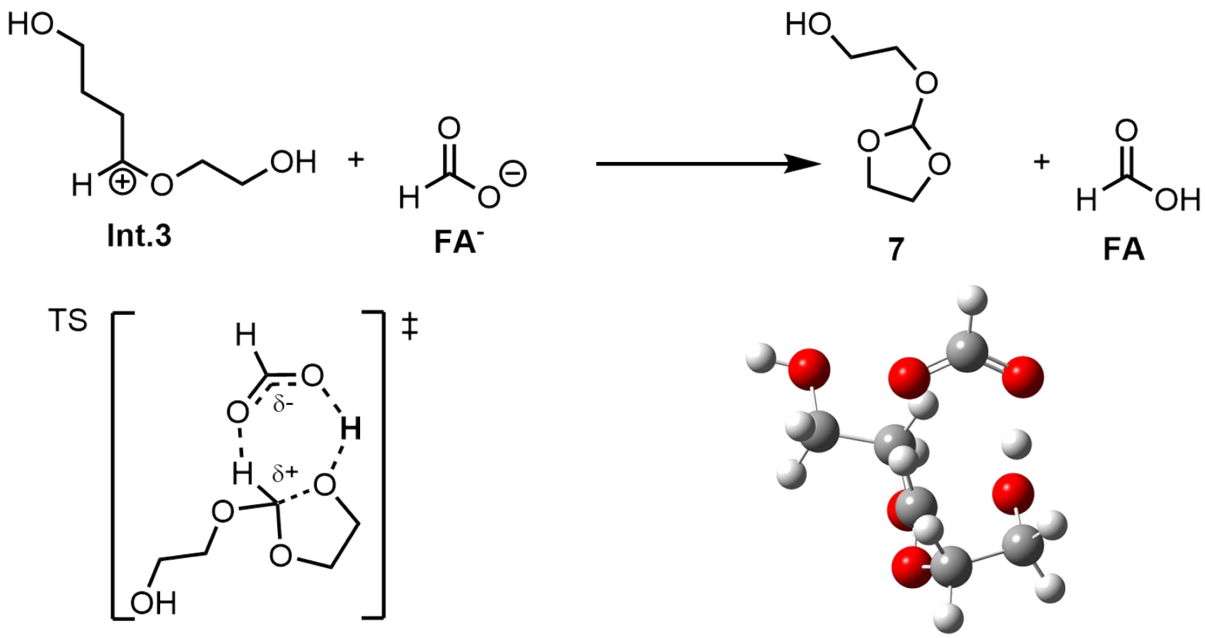
Table S20 Transition state: activation of **5** to carbocation int.**3**



Coordinates of the TS (atom, X, Y, Z)	Energies
0 1 C -0.84405300 -1.35417900 -0.53732300 H -1.13362400 -1.53133000 -1.57100100 O 0.38626100 -1.59495100 -0.16981800 O -1.80666300 -1.53156900 0.31790300 O -0.86075100 0.56413300 -0.78170900 C 1.37987600 -1.62049500 -1.25054400	H= -842.01746 Hartree G = -842.0836 Hartree

H 1.23748500 -0.72788000 -1.86496900 H 1.19853100 -2.51557400 -1.85256500 C 2.76310000 -1.66236700 -0.64461000 H 2.86472300 -2.54494600 -0.00289900 H 3.46045300 -1.78011600 -1.48896000 C -1.57730900 -1.53672500 1.77138700 H -2.46584400 -2.04971900 2.14153200 H -0.68687900 -2.12992500 1.98803400 C -1.47966800 -0.14472600 2.37574400 H -2.17948200 0.53141100 1.87023500 H -1.80962500 -0.24637000 3.41996700 C -1.36995600 1.00868200 -2.06126600 H -1.05989900 2.05173100 -2.18388000 H -0.90485800 0.41759000 -2.86116500 C -2.88054800 0.88049600 -2.08854000 H -3.26060800 1.25144900 -3.04786100 H -3.19854600 -0.16228600 -1.97866000 H -3.33387500 1.46978200 -1.28343600 O -0.15515300 0.35930100 2.36905800 H -0.07571400 1.18384400 1.83743600 H 0.07765100 0.95414400 -0.64116700 C 1.45474100 2.57739500 0.32438700 H 2.31159000 3.27988400 0.29725400 O 0.57086200 2.75820400 1.18783000 O 1.47834100 1.64572300 -0.55438600 O 3.09867000 -0.52559300 0.13790900 H 2.58889300 0.25785100 -0.16758500	

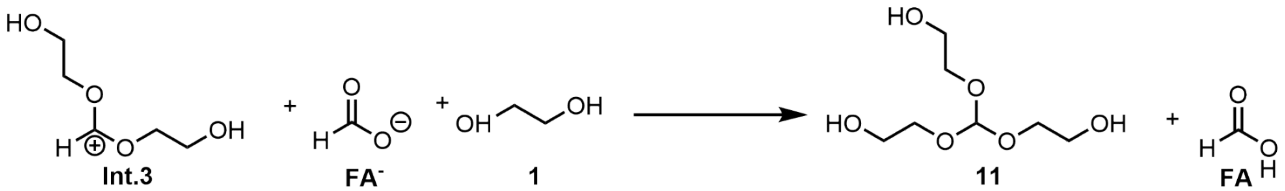
Table S21 Transition state: intramolecular cyclization of int.**3** to **7**

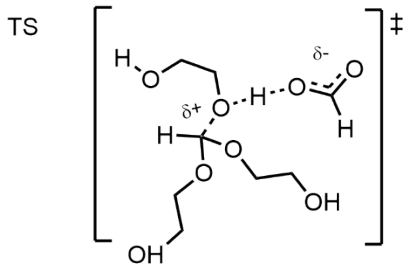


Coordinates of the TS (atom, X, Y, Z)	Energies
0 1 C 0.06522200 -0.91953400 0.20722900 H 0.03733100 0.08133200 0.65220700 O 0.81400700 -1.85979400 0.74717700 O -0.96139900 -1.37710600 -0.44959400	H= -687.02806 Hartree G = -687.08555 Hartree

C -2.00290900 -0.40628100 -0.78552000 H -1.54081100 0.56092100 -0.99984000 H -2.46811000 -0.80054300 -1.68918700 C 2.18275000 -1.39234500 0.90945000 H 2.75405200 -2.23280900 1.30076000 H 2.19468300 -0.55398000 1.61129700 C -2.99220200 -0.32065000 0.36496900 H -3.40927100 -1.31515300 0.57224700 H -2.48620300 0.04465400 1.26913100 C 2.58451100 -0.96642900 -0.50536200 H 3.43032500 -0.27305800 -0.47995100 H 2.83288000 -1.83493700 -1.11995800 O 1.42933400 -0.33531900 -1.06772500 H 1.49044600 0.72247400 -0.94884200 C 1.08634000 2.63543000 0.25142200 H 1.17313200 3.73744000 0.35028100 O 1.58328700 2.15475600 -0.82513800 O 0.53032200 2.00195700 1.17328800 O -4.00886800 0.58868800 -0.05818700 H -4.64417900 0.69705300 0.67016200	

Table S22 Transition state: addition of **1** on int.**3** to **11**





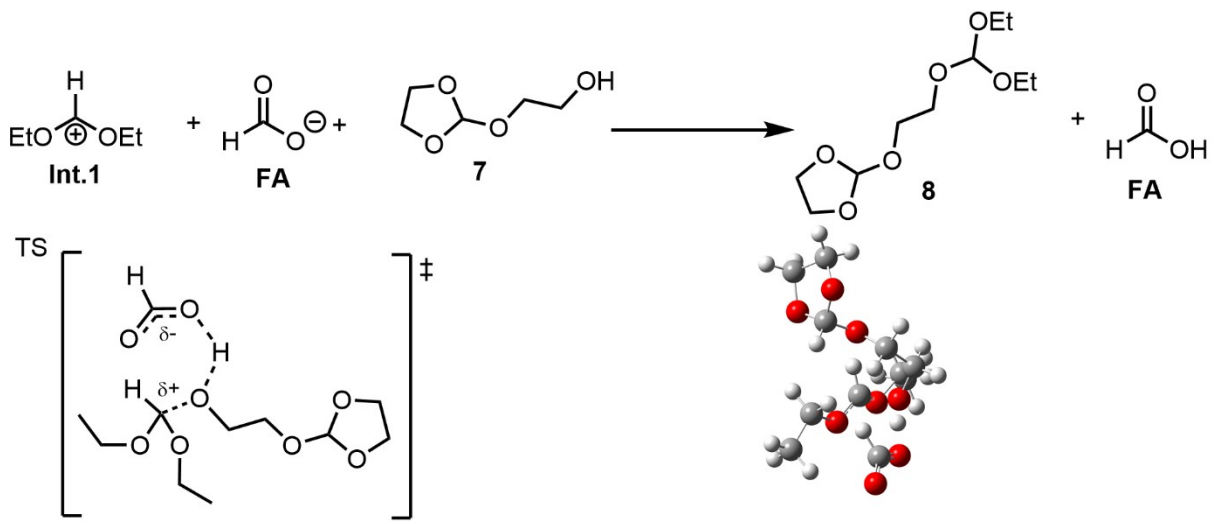


Coordinates of the TS (atom, X, Y, Z)	Energies
0 1 C -0.80614000 -1.08259700 0.63092600 H -1.42926600 -1.75776900 0.05003500 O 0.46336900 -1.37685900 0.82266700 O -1.45591200 -0.51081600 1.61169700 O -0.74952400 0.23148300 -0.66462900 C 1.06641000 -2.25715900 -0.17837000 H 0.82719800 -1.86834900 -1.17189300 H 0.63109600 -3.25462900 -0.06309500 C 2.56018900 -2.30768700 0.05055000 H 2.77085500 -2.67918900 1.05990100 H 2.95512600 -3.04390400 -0.66692900 C -0.77606700 0.27380600 2.64716300 H -1.47902900 0.21888900 3.48022700 H 0.15872200 -0.21889900 2.92132000 C -0.54398900 1.72729500 2.25871400 H -1.38416000 2.09177000 1.65515900	H= -917.23056 Hartree G = -917.29952 Hartree

H -0.53867500 2.29565600 3.19917800 C -1.54253100 0.04825500 -1.86157300 H -1.27727100 0.86501000 -2.54024900 H -1.28400700 -0.90622300 -2.33653600 C -3.01881100 0.10921300 -1.55633200 H -3.56062500 0.21778300 -2.50606000 H -3.23484500 0.98114700 -0.92620000 O 0.70335100 1.94339400 1.61707600 H 0.60150400 2.18630000 0.67116600 H 0.23455800 0.41709700 -0.95778000 C 1.83696900 1.93884600 -1.55306800 H 2.74221500 2.24502800 -2.11257500 O 1.15499400 2.81846700 -0.99113100 O 1.59257600 0.67886900 -1.55295200 O 3.22321700 -1.05765700 -0.08899900 H 2.71015400 -0.46886300 -0.68651400 O -3.40614500 -1.10501700 -0.89729200 H -4.30714900 -0.99559300 -0.54870400	

10.2.2 DCE mechanism for the formation of 8,9 and 12

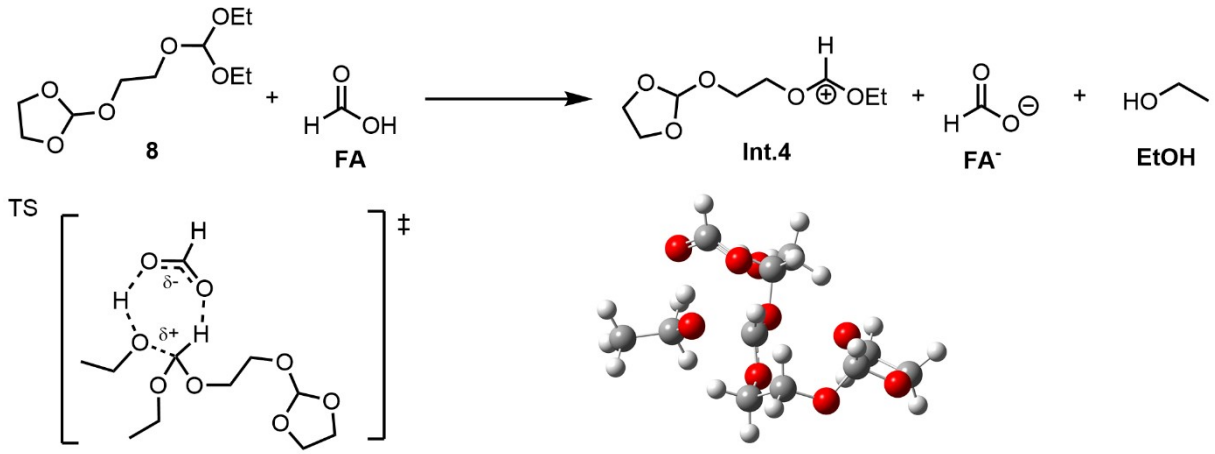
Table S23 Transition state: addition of **7** on int.**1** to **8**



Coordinates of the TS (atom, X, Y, Z)	Energies
0 1 C -1.04378200 1.24441200 0.58570400 H 0.03192800 1.24232600 0.41349700 O -1.55814600 0.43420500 1.47241400 O -1.72444900 2.35143100 0.45922300 C -0.73440600 -0.71911200 1.86191900 H 0.15769700 -0.33122600 2.36031000 H -0.44577300 -1.24489600 0.95126200 C -1.57027600 -1.58693900 2.77090800 H -2.46682600 -1.94646100 2.25527900 H -0.97421400 -2.45547700 3.07347500 H -1.86958600 -1.04200700 3.67284100 C -1.19425600 3.35028700 -0.47464000 H -0.10153100 3.32185200 -0.42224000 H -1.51997600 3.05088600 -1.47340400 C -1.74881200 4.69748600 -0.07404100	H= -1033.9133 Hartree G = -1033.9916 Hartree

H -1.38344500 5.45284100 -0.77918100 H -2.84379900 4.69775500 -0.10685200 H -1.42119200 4.97629400 0.93336600 H -2.00176400 -0.51485700 -1.00725600 C -2.47586800 -2.74747800 -0.65558200 H -1.38193100 -2.80756400 -0.46382400 O -3.14415100 -3.78840200 -0.53248300 O -2.91596600 -1.59118400 -0.99293200 O 1.51439100 -0.02592000 -0.60088800 C 0.79229600 -0.67885600 -1.65550000 H 1.45045000 -0.84169700 -2.51860100 H 0.42460300 -1.65413000 -1.30811900 C -0.35734800 0.21392700 -2.07203700 H 0.01251700 1.21557100 -2.31248600 H -0.82489200 -0.20349800 -2.97169600 O -1.37935200 0.35822400 -1.07586200 C 2.41893100 -0.86549500 0.08014200 H 1.92202900 -1.79556100 0.37568000 C 4.46334800 -0.10320500 -0.51973200 C 4.23629000 0.27062300 0.94243700 H 5.46675700 -0.47603500 -0.72953800 H 4.21806100 0.71904200 -1.20101400 H 4.89945600 -0.27623500 1.62052500 H 4.31416300 1.34403900 1.13028300 O 2.87474700 -0.15558700 1.19357000 O 3.53549700 -1.19337500 -0.70176300	

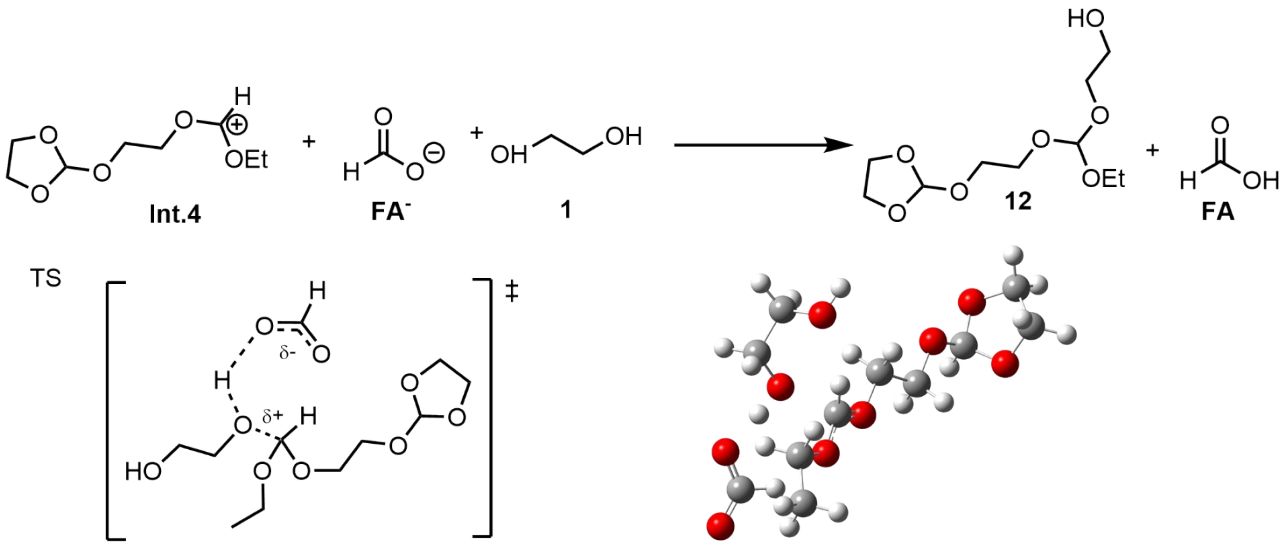
Table S24 Transition state: activation of **8** to int.**4**



Coordinates of the TS (atom, X, Y, Z)	Energies
0 1 C -0.39311200 -0.20262600 -0.33428500 H -0.33139400 -0.62847000 0.66825400 O 0.26315900 -0.71420000 -1.34383600 O -0.60489900 1.07901600 -0.48288400 O -2.12301400 -1.02955900 -0.53435200 C 0.70061700 -2.10185200 -1.23302200 H 1.07379400 -2.32797500 -2.23212400 H -0.16847700 -2.72846900 -1.01503600 C 1.78146100 -2.31062100 -0.19050700 H 1.40873900 -2.11885400 0.82065000 H 2.07385200 -3.36678800 -0.24133500	H= -1109.1258 Hartree G = -1109.2068 Hartree

C -1.11666100 1.79070900 0.68763700 H -2.09774900 1.38149000 0.94044000 H -0.42141600 1.63538800 1.51589700 C -1.20267300 3.25348500 0.34509600 H -1.42154900 3.79505900 1.27598300 H -0.23812100 3.60646900 -0.04307700 C -2.96502400 -0.38150300 -1.50953000 H -3.33083200 0.56775400 -1.10193200 H -2.32719000 -0.16318400 -2.37122100 C -4.11550300 -1.29207600 -1.90537800 H -4.73087700 -0.79586600 -2.66630000 H -3.74082700 -2.23391000 -2.32246500 H -4.75481400 -1.51951300 -1.04447300 C -2.30258700 -1.04621400 2.70874400 H -2.69962300 -1.00781600 3.74622800 O -1.06826300 -1.18313700 2.55905600 O -3.18228500 -0.94090400 1.78968600 H -2.57036100 -1.01236200 0.40546100 O 2.93249600 -1.50593600 -0.46957300 C 3.25414600 -0.57694500 0.54491100 H 3.32184900 -1.08136800 1.51392900 C 4.21712500 1.35669300 -0.27188900 C 2.69389100 1.44082100 -0.32192700 H 4.65041000 2.05564900 0.45065400 H 4.68739200 1.49111100 -1.24882700 H 2.29470200 2.40418600 -0.00328000 H 2.29442900 1.17504100 -1.30552600 O 4.46942900 0.00801300 0.19380500 O 2.30422100 0.45292100 0.65419100 O -2.24316900 3.44680900 -0.61664100 H -2.26342600 4.38902500 -0.85661400	

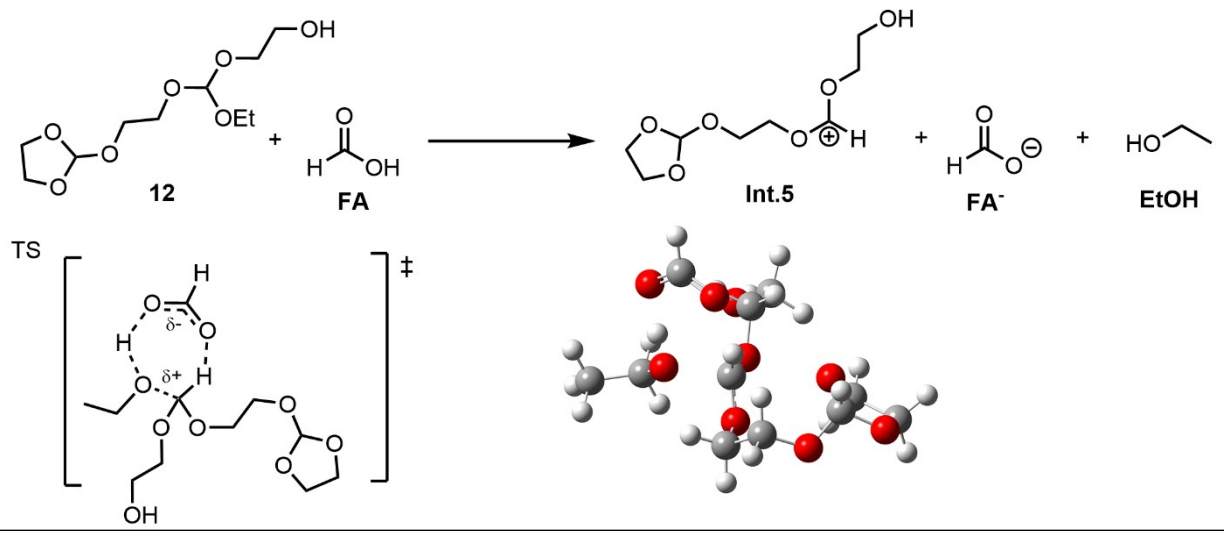
Table S25 Transition state: addition of **1** on int.**4** to **12**



Coordinates of the TS (atom, X, Y, Z)	Energies
0 1 C -1.38271100 0.02732500 0.84215100 H -1.26229800 1.01365900 1.28954300 O -0.34548400 -0.62048800 0.39705700	H= -1109.12 Hartree G = -1109.2037 Hartree

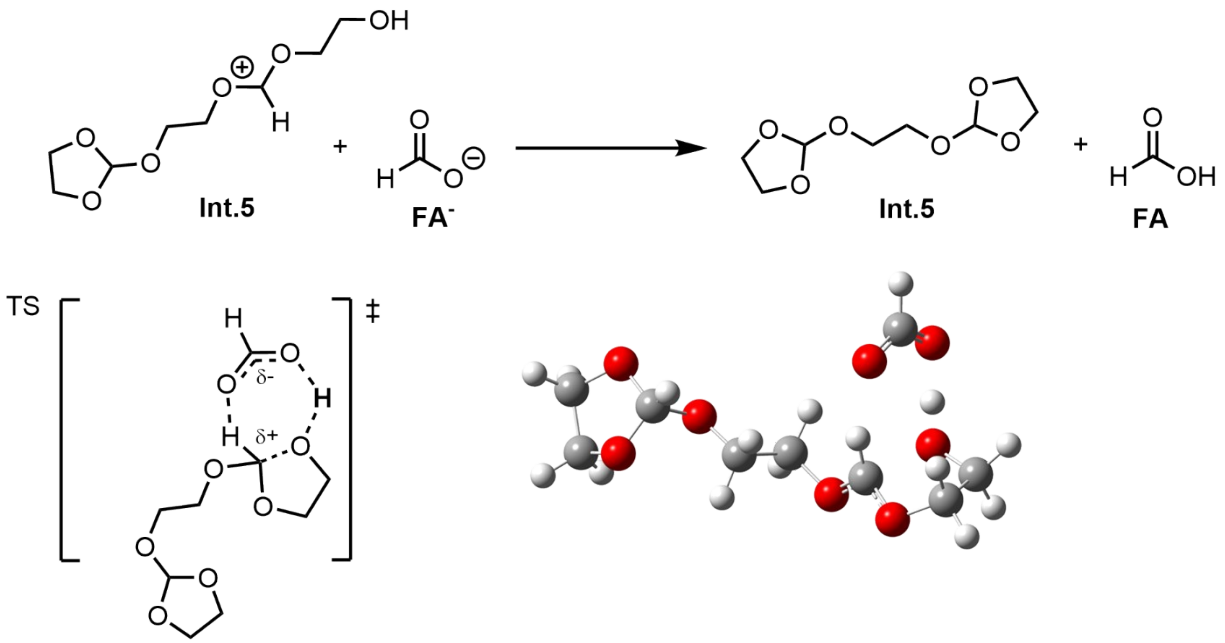
O -2.00253300 0.91478100 -0.85926800 O -2.36685500 -0.74748100 1.17439600 C 0.83893200 0.16871200 0.07782800 H 1.00942300 0.89551200 0.87479600 H 0.65287700 0.68123600 -0.86741400 C 1.98744300 -0.81555200 -0.03189500 H 1.78731300 -1.55282600 -0.82155600 H 2.13459000 -1.34368700 0.91771700 C -2.45440400 2.27985000 -0.80165500 H -2.92570700 2.52178700 -1.76161800 H -3.20272000 2.39978700 -0.00727300 C -1.29811600 3.22278900 -0.57400600 H -0.49502500 3.01520400 -1.29281800 H -1.65106000 4.25169600 -0.72572100 C -3.56100000 -0.11166200 1.75999700 H -3.22266100 0.67864400 2.43533900 H -4.12053000 0.31908500 0.92812600 C -4.34291600 -1.19060700 2.46905600 H -5.25099600 -0.74473100 2.89052500 H -4.63952700 -1.98001900 1.77018500 H -3.76166600 -1.63194700 3.28578400 O -0.82381100 3.05396400 0.77292100 H -0.01576600 3.58322100 0.88731800 H -2.79838900 0.32783900 -1.19711200 C -3.96448800 -1.68262000 -1.55422700 H -2.96042800 -2.10346100 -1.31857600 O -4.90227400 -2.48544000 -1.72124900 O -4.02248600 -0.40703200 -1.62987100 O 3.13475700 -0.03270100 -0.35978100 C 4.26923600 -0.80880600 -0.68598200 H 4.00850000 -1.55392400 -1.44531000 C 6.24305700 0.24332100 -0.11558600 C 5.66165100 -0.51868000 1.07337900 H 7.18356000 -0.19015200 -0.47012800 H 6.37446400 1.31008600 0.08043800 H 6.40528600 -1.07193600 1.64849700 H 5.07970500 0.12932000 1.73784600 O 4.79472000 -1.47602000 0.42894400 O 5.24533800 0.07056500 -1.15226600	

Table S26 Transition state: activation of **12** to int.**5**



Coordinates of the TS (atom, X, Y, Z)	Energies
0 1 C -0.39311200 -0.20262600 -0.33428500 H -0.33139400 -0.62847000 0.66825400 O 0.26315900 -0.71420000 -1.34383600 O -0.60489900 1.07901600 -0.48288400 O -2.12301400 -1.02955900 -0.53435200 C 0.70061700 -2.10185200 -1.23302200 H 1.07379400 -2.32797500 -2.23212400 H -0.16847700 -2.72846900 -1.01503600 C 1.78146100 -2.31062100 -0.19050700 H 1.40873900 -2.11885400 0.82065000 H 2.07385200 -3.36678800 -0.24133500 C -1.11666100 1.79070900 0.68763700 H -2.09774900 1.38149000 0.94044000 H -0.42141600 1.63538800 1.51589700 C -1.20267300 3.25348500 0.34509600 H -1.42154900 3.79505900 1.27598300 H -0.23812100 3.60646900 -0.04307700 C -2.96502400 -0.38150300 -1.50953000 H -3.33083200 0.56775400 -1.10193200 H -2.32719000 -0.16318400 -2.37122100 C -4.11550300 -1.29207600 -1.90537800 H -4.73087700 -0.79586600 -2.66630000 H -3.74082700 -2.23391000 -2.32246500 H -4.75481400 -1.51951300 -1.04447300 C -2.30258700 -1.04621400 2.70874400 H -2.69962300 -1.00781600 3.74622800 O -1.06826300 -1.18313700 2.55905600 O -3.18228500 -0.94090400 1.78968600 H -2.57036100 -1.01236200 0.40546100 O 2.93249600 -1.50593600 -0.46957300 C 3.25414600 -0.57694500 0.54491100 H 3.32184900 -1.08136800 1.51392900 C 4.21712500 1.35669300 -0.27188900 C 2.69389100 1.44082100 -0.32192700 H 4.65041000 2.05564900 0.45065400 H 4.68739200 1.49111100 -1.24882700 H 2.29470200 2.40418600 -0.00328000 H 2.29442900 1.17504100 -1.30552600 O 4.46942900 0.00801300 0.19380500 O 2.30422100 0.45292100 0.65419100 O -2.24316900 3.44680900 -0.61664100 H -2.26342600 4.38902500 -0.85661400	H= -1109.1258 Hartree G = -1109.2068 Hartree

Table S27 Transition state: intramolecular cyclization of int.**5** to **9**

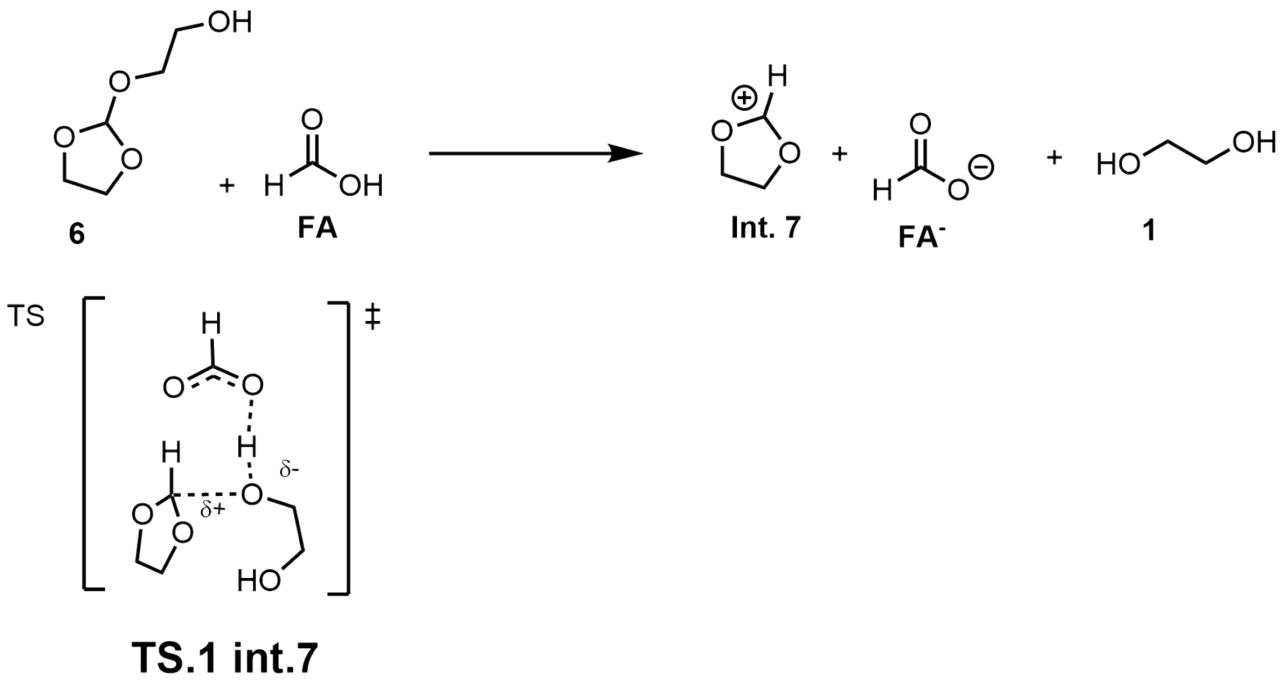


Coordinates of the TS (atom, X, Y, Z)	Energies
0 1 C 1.89698500 -0.95324100 0.13026900 H 1.72343100 0.03304100 0.57521300 O 2.69310700 -1.81599400 0.72893400 O 0.98468200 -1.51085100 -0.61367200 C -0.12362500 -0.65194000 -1.03054900 H 0.25508700 0.35186200 -1.23812600 H -0.49355000 -1.10456900 -1.95054000 C 3.98682500 -1.20982800 1.00715400 H 4.60896700 -1.99055300 1.44244200 H 3.85219300 -0.38286900 1.70990400 C -1.18391800 -0.64835600 0.05800400 H -1.50177400 -1.67365800 0.28200200 H -0.79027400 -0.19132400 0.97737500 C 4.45622900 -0.72871100 -0.36835800 H 5.22339200 0.04515300 -0.27203000 H 4.83837200 -1.56084700 -0.96433500 O 3.29189300 -0.20935200 -1.01957700 H 3.23504000 0.84760300 -0.88844600 C 2.54403100 2.67940900 0.29548700 H 2.51058100 3.78137700 0.42203100 O 3.17290700 2.27903100 -0.74430100 O 1.98167300 1.96862700 1.15510700 O -2.27100400 0.12044400 -0.45340200 C -3.25457900 0.41493600 0.51879100 H -2.78710000 0.86961800 1.39870000 C -5.36925000 0.53650600 -0.39666300 C -5.00098700 -0.90501100 -0.05069600 H -6.18604900 0.91964300 0.22304800 H -5.60553900 0.67721800 -1.45400100 H -5.80962700 -1.46554700 0.42006400 H -4.61745200 -1.45544500 -0.91662300 O -3.95473400 -0.72754900 0.92788900	H= -954.14042 Hartree G = -954.20885 Hartree

O -4.16927000 1.28273100 -0.07439200	

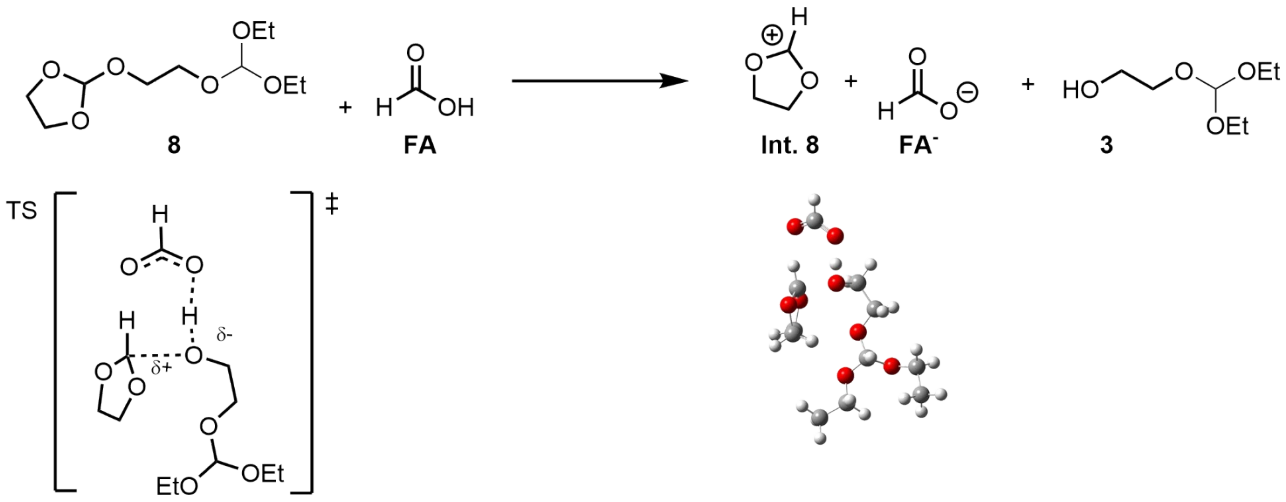
10.2.3 DCE mechanism for the formation of 7, 8, 12 and 9 through the substitution of carbocations

Table S28 Transition state: activation of **7** to int.**7**



Coordinates of the TS (atom, X, Y, Z)	Energies
0 1 C -1.06946300 -0.90483800 0.26247900 H 0.13992200 -1.77458400 0.48062600 O -1.53451400 -0.06048300 1.13669500 O 0.59451700 1.15616100 -0.76263900 C -2.63267700 0.75241000 0.55687700 H -2.30196300 1.78976700 0.58225300 H -3.50657800 0.60260000 1.18990000 C -2.76800800 0.17415200 -0.84504600 H -3.72094100 -0.31795800 -1.03668600 H -2.51856900 0.87258800 -1.64253100 O -1.72570700 -0.88224300 -0.86053700 H 1.18818700 0.37344000 -0.78669900 C 2.11412500 -2.10339400 0.04031000 H 2.94746300 -2.80667000 0.19677400 O 2.26784100 -1.09763900 -0.66059500 O 1.02499300 -2.46158900 0.65622400 C 0.98026700 1.96794700 0.34974400 H 1.02356000 1.35690200 1.26348900 H 0.17640200 2.70063500 0.48157000 C 2.31062800 2.67844800 0.12989600 H 2.54998100 3.31422700 0.99280700 H 3.12633500 1.95526700 0.00463700 H 2.26992400 3.31177300 -0.76487900	H= -611.80236 Hartree G = -611.86099 Hartree

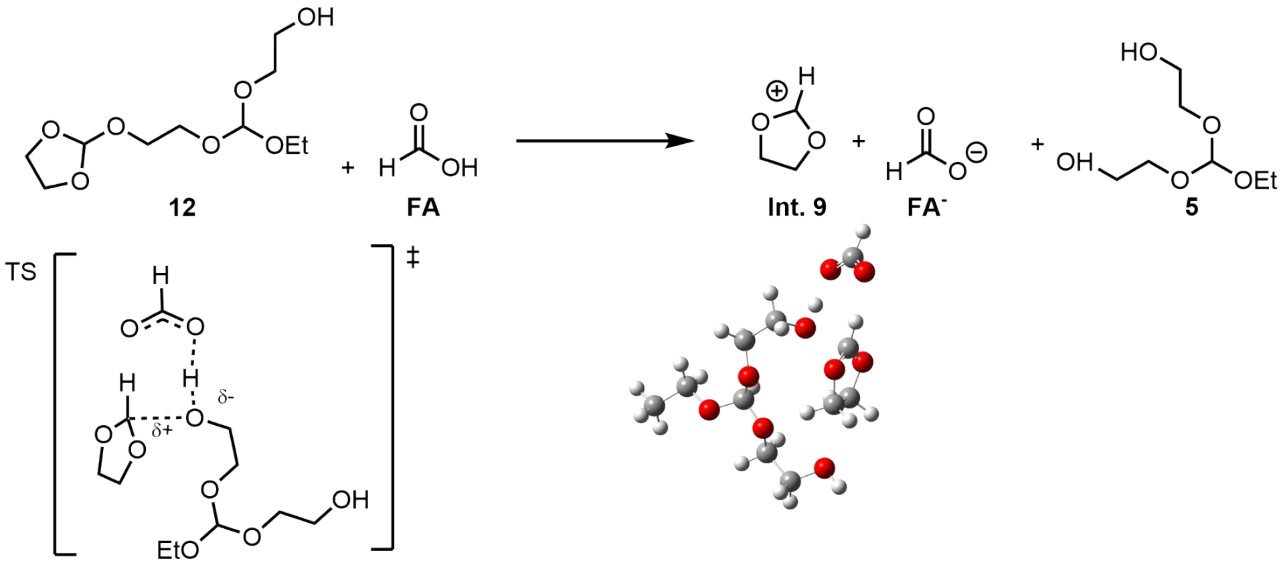
Table S29 Transition state: activation of **8** to int.**8**



Coordinates of the TS (atom, X, Y, Z)	Energies
0 1 C -2.42076600 1.15146400 0.20642700 H -3.46778500 0.84883500 0.29138200 O -1.73244900 1.44408400 1.27913100 O -1.89797200 -0.70479900 -0.20837000 C -0.56813900 2.26294500 0.87555100 H 0.32397900 1.79435300 1.27942600 H -0.73688800 3.25704000 1.29152100 C -0.63777300 2.21038100 -0.64653900 H -0.52948800 3.17650300 -1.13594200 H 0.02965800 1.46556800 -1.07856700 O -2.02108500 1.75579900 -0.88419300 H -2.78837800 -1.12703800 -0.53690100 C -5.13154000 -1.14556100 -0.63529300 H -6.08882300 -1.61313800 -0.95050100 O -4.07989100 -1.76157400 -1.00960600 O -5.19250900 -0.08978600 0.03601900 C -1.34277900 -1.51182300 0.84193500 H -1.86933200 -2.47205400 0.87088000 H -1.48681000 -1.00616300 1.80406200 C 0.12897700 -1.74797800 0.58897500 H 0.27490200 -2.14305100 -0.42514900 O 0.80454700 -0.49711200 0.73179200 C 2.05169500 -0.42212200 0.10730700 H 1.97187600 -0.71618500 -0.95238900 H 0.51865900 -2.47716600 1.31169400 O 2.39184700 0.91844900 0.23887000 O 2.99879700 -1.23816200 0.75230000 C 3.50787000 1.33727200 -0.56196000 H 4.42223000 0.85360500 -0.19879500 H 3.34193200 1.02380800 -1.60227500 C 3.61046800 2.84645100 -0.46166800 H 3.77156600 3.15909400 0.57669400 H 4.45660800 3.20029800 -1.06244900 H 2.69716700 3.32582000 -0.83328800 C 3.45152100 -2.40085400 0.02708200 H 3.71463900 -3.13102100 0.79814900 H 2.62489900 -2.81778200 -0.56082200	H= -1033.9099 Hartree G = -1033.9882 Hartree

C 4.64852400 -2.09997300 -0.86084700 H 4.99737800 -3.02704900 -1.33381700 H 4.38981800 -1.38911400 -1.65351100 H 5.47356100 -1.68157000 -0.27276500	

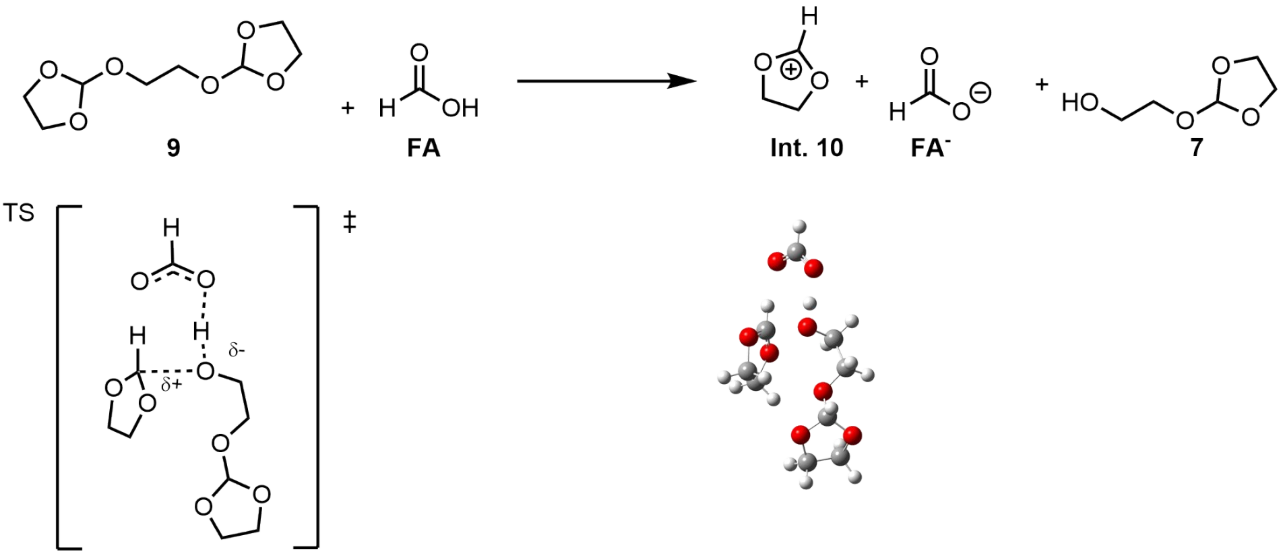
Table S30 Transition state: activation of **12** to int.**9**



Coordinates of the TS (atom, X, Y, Z)	Energies
0 1 C 2.51449900 -1.01675400 0.42650000 H 3.48857200 -0.54266300 0.57749000 O 1.74227700 -1.30249100 1.43035800 O 1.74859000 0.79493100 -0.19304000 C 0.64320900 -2.17307500 0.94065300 H -0.29333300 -1.66694700 1.15346800 H 0.73757100 -3.11302400 1.48324200 C 0.93969300 -2.28165500 -0.55474400 H 1.01213400 -3.29904300 -0.93001600 H 0.27720100 -1.67779100 -1.17160300 O 2.29150700 -1.68838600 -0.66497400 H 2.57195600 1.17647500 -0.67271300 C 4.93387300 1.39697600 -0.76546000 H 5.86183100 1.84983400 -1.17807600 O 3.85377400 1.76272000 -1.33140200 O 5.05876200 0.59401200 0.18986700 C 1.34571900 1.71111800 0.83218100 H 1.96559400 2.61446900 0.78214300 H 1.49560200 1.24348700 1.81314400 C -0.10997600 2.09173000 0.66102500 H -0.28903500 2.41435300 -0.37044600 O -0.94661400 0.97371800 0.99311000 C -1.91757400 0.60168300 0.06117600 H -1.55238600 0.77128900 -0.96528500 H -0.35247100 2.92253800 1.33508100 O -2.13830400 -0.74661400 0.31194900 O -3.14098000 1.27098400 0.23905900 C -2.93064400 -1.41217000 -0.67833100 H -3.94325700 -0.99250500 -0.69671800 H -2.47390300 -1.27605500 -1.66912200	H= -1109.1233 Hartree G = -1109.2046 Hartree

C -3.01195900 -2.87798200 -0.32915300 H -3.37608600 -2.99585400 0.70038400 H -3.73135200 -3.35241600 -1.01052300 C -3.22628400 2.58505400 -0.33695600 H -2.64462500 3.29298500 0.26725900 H -2.79839200 2.56617200 -1.34932600 C -4.68631700 2.99297000 -0.37619600 H -4.77834700 4.00039900 -0.79953400 H -5.26901000 2.30182000 -0.99632500 H -5.11542800 3.00427600 0.63262900 O -1.71542600 -3.47555400 -0.47298800 H -1.78695800 -4.41572400 -0.23483000	

Table S31 Transition state: activation of **9** to int.**10**

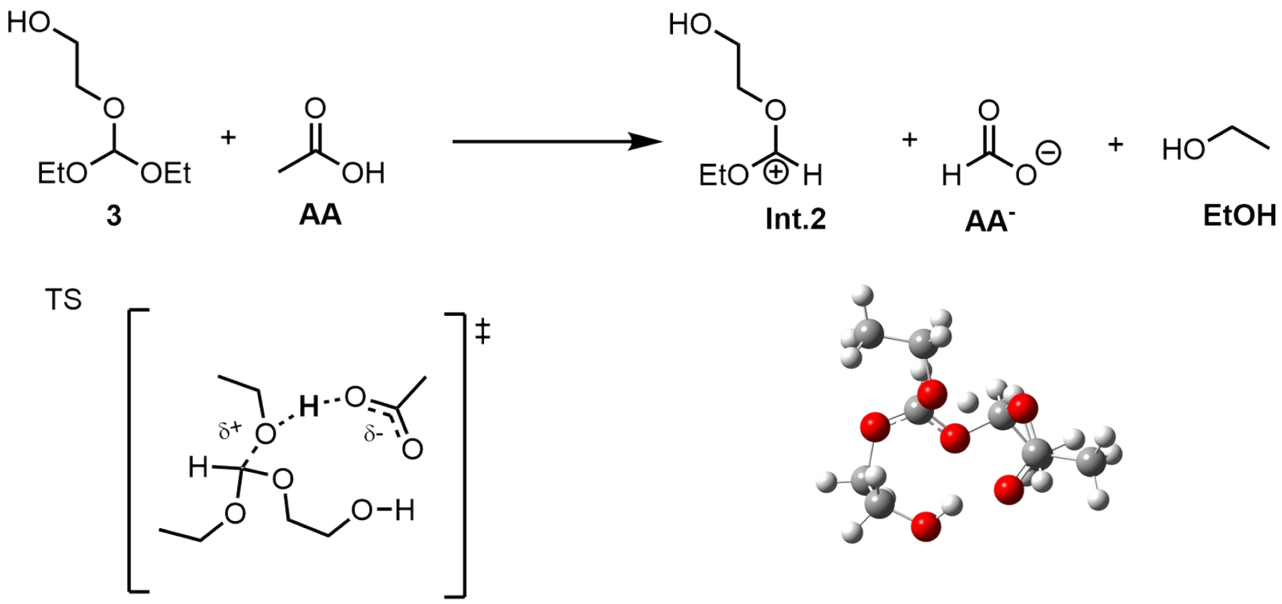


Coordinates of the TS (atom, X, Y, Z)	Energies
0 1 C -1.80662800 1.20511300 0.29566200 H -2.82668000 0.93201700 0.58100100 O -0.89460100 1.40108900 1.20983700 O -1.46823500 -0.66757100 -0.30811200 C 0.21325300 2.17223200 0.60389900 H 1.13265700 1.62304800 0.78495100 H 0.21132200 3.14546200 1.09571600 C -0.18238500 2.22129200 -0.86869600 H -0.12686000 3.21206900 -1.31586900 H 0.33239700 1.47779000 -1.47633500 O -1.60774200 1.84264300 -0.82784600 H -2.42595500 -1.02584200 -0.47121100 C -4.74810400 -0.91875200 -0.09427100 H -5.77747300 -1.31385800 -0.23175400 O -3.83399500 -1.56572400 -0.70208800 O -4.60727200 0.09668100 0.62663200 C -0.77575800 -1.54379700 0.59250300 H -1.34412300 -2.47452400 0.69874500 H -0.70263900 -1.06775600 1.57768200 C 0.60489600 -1.85673500 0.06225500 H 0.53926800 -2.25211100 -0.96063700 O 1.37063400 -0.64694700 0.06739300	H= -954.14259 Hartree G = -954.21109 Hartree

C 2.53486200 -0.69107900 -0.71557000 H 2.31011900 -1.07784900 -1.71540700 C 4.17993800 0.71512500 0.09708600 C 4.21223200 -0.64009700 0.80090000 H 5.06827800 0.88664500 -0.51917700 H 4.03623500 1.55288200 0.78395400 H 5.21801700 -1.03422700 0.95244400 H 3.66758100 -0.62621000 1.75142300 H 1.08147900 -2.61069400 0.70242000 O 3.03092900 0.61664600 -0.77913300 O 3.53684800 -1.49265000 -0.14675100	

10.2.4 Computations for the screening of catalysts

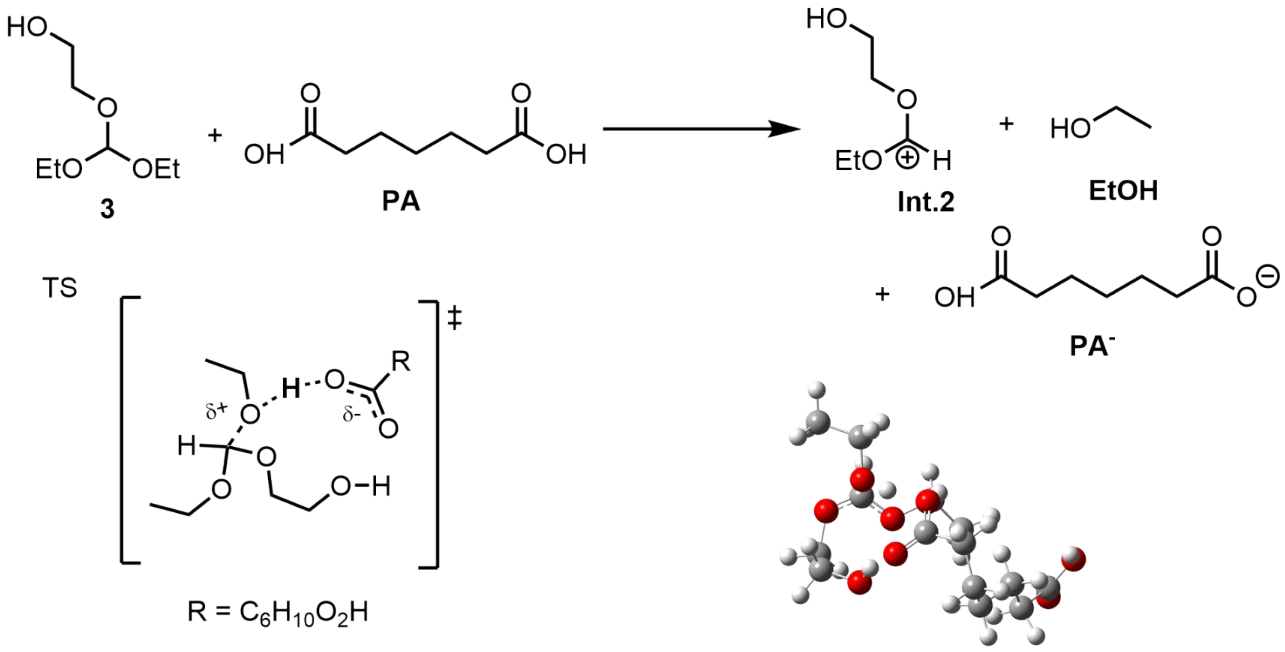
Table S32 Transition state: activation of **3** to int2 with acetic acid (AA)



Coordinates of the TS (atom, X, Y, Z)	Energies
0 1 C 1.38591800 0.24722600 -1.11575600 H 1.61075300 -0.53283000 -1.83772800 O 0.31872900 0.96283400 -1.22707900 O 2.39737600 0.70285200 -0.45831500 O 0.76079600 -1.27051100 0.20959400 C -0.72801100 0.47835600 -2.15750300 H -1.05317000 -0.49460900 -1.78747000 H -0.25983000 0.38194500 -3.14034800 C -1.84300900 1.49421500 -2.14111800 H -1.49554100 2.47210100 -2.49159700 H -2.63680700 1.14809100 -2.81288900 H -2.26035100 1.59878900 -1.13531400 C 2.28194000 1.88021100 0.42751100 H 3.33002900 2.10555700 0.62486500 H 1.82353400 2.69344400 -0.13900500 C 1.53112000 1.61303500 1.73083700 H 1.66009800 0.56341300 2.02265000 H 2.02344900 2.23338100 2.49039600 C 1.24884700 -2.57106400 -0.16035400 H 0.66558500 -3.32227300 0.38629900	H= -806.10096 Hartree G = -806.17237 Hartree

H 1.08091300 -2.73788700 -1.23535100 C 2.72441400 -2.69365000 0.17600100 H 3.07768800 -3.70198600 -0.07211100 H 3.32695300 -1.97420000 -0.38933400 H 2.89296800 -2.52063600 1.24548300 O 0.17041200 1.99804200 1.70944500 H -0.43616700 1.24770700 1.49529800 H -0.26314300 -1.31665900 0.24415000 C -2.46560500 -0.61924800 0.80094400 O -1.95505100 0.34609000 1.42950200 O -1.80571800 -1.53403900 0.20232800 C -3.98429900 -0.70975700 0.70846400 H -4.46971500 -0.04156200 1.42511700 H -4.29549100 -0.42113800 -0.30429300 H -4.32201200 -1.73874200 0.87321500	

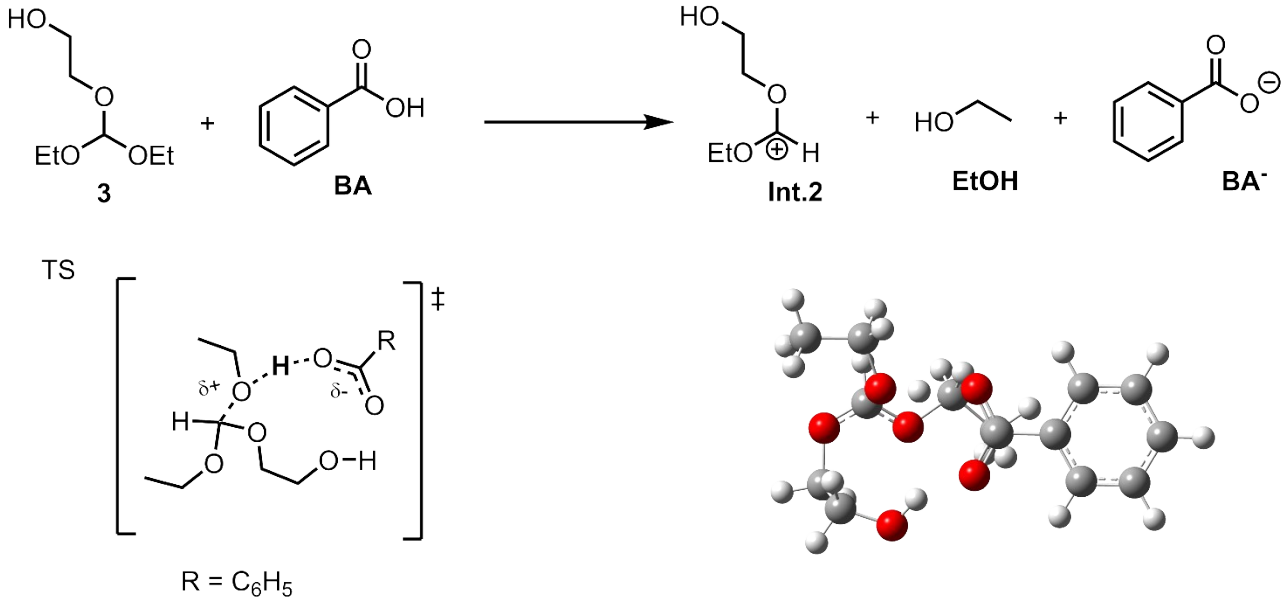
Table S33 Transition state: activation of **3** to int2 with pimelic acid (PA)



Coordinates of the TS (atom, X, Y, Z)	Energies
0 1 C -2.55171000 -1.64242300 -0.12686600 H -2.95948000 -1.98093000 -1.07520400 O -1.28765100 -1.73025800 0.11105600 O -3.39243200 -1.60731000 0.85172700 O -2.75942900 0.32129600 -0.84987300 C -0.37773800 -1.86245900 -1.04711500 H -0.27589200 -0.85932200 -1.46347000 H -0.85293900 -2.53361400 -1.76778500 C 0.93407000 -2.39651600 -0.52730300 H 0.82022100 -3.39918300 -0.10142500 H 1.64254500 -2.45195600 -1.36106500 H 1.34913100 -1.72906200 0.23308700 C -2.97187700 -1.32297800 2.23854500 H -3.84617400 -1.64220800 2.80616200	H= -1151.8352 Hartree G = -1151.924 Hartree

H -2.11653600 -1.95792100 2.47840600 C -2.66940900 0.14531000 2.50089900 H -3.34645100 0.77396500 1.91004100 H -2.90363300 0.31044400 3.56354000 C -3.43944600 0.37785400 -2.11421000 H -3.21373800 1.34361800 -2.58259300 H -3.05436600 -0.41149300 -2.77791700 C -4.93506500 0.21959400 -1.90533800 H -5.45464500 0.27750000 -2.86961900 H -5.17453400 -0.74729400 -1.44786200 H -5.32040900 1.01371800 -1.25497100 O -1.31107300 0.46858500 2.27414500 H -1.20884800 1.19437500 1.60744600 H -1.84102600 0.76277300 -0.95679700 C -0.04469100 2.25106000 -0.43117400 O -0.63599100 2.52059900 0.65149300 O -0.45723400 1.40192800 -1.28964900 C 1.24652600 3.00074100 -0.76424800 H 1.72049700 2.51905700 -1.62521000 H 0.96054400 4.01295300 -1.08450700 C 2.22759900 3.11129000 0.41219200 H 1.77065700 3.71688800 1.20374100 C 2.66165200 1.76699000 1.01328600 H 1.79632700 1.27328600 1.47485600 H 3.37869300 1.96165600 1.82312200 C 3.29897400 0.79998900 0.00688600 H 2.53941000 0.46090800 -0.70775100 H 4.06836600 1.34137100 -0.56465100 C 3.91728400 -0.40992800 0.71917500 H 3.20225200 -0.84868900 1.42238900 H 4.78164500 -0.08789200 1.31790500 C 4.40808500 -1.54680600 -0.15395300 H 3.11840400 3.65572000 0.06838700 O 4.53664700 -2.69174200 0.23745300 O 4.75503300 -1.25887900 -1.43175400 H 4.61148900 -0.31273500 -1.62968800	

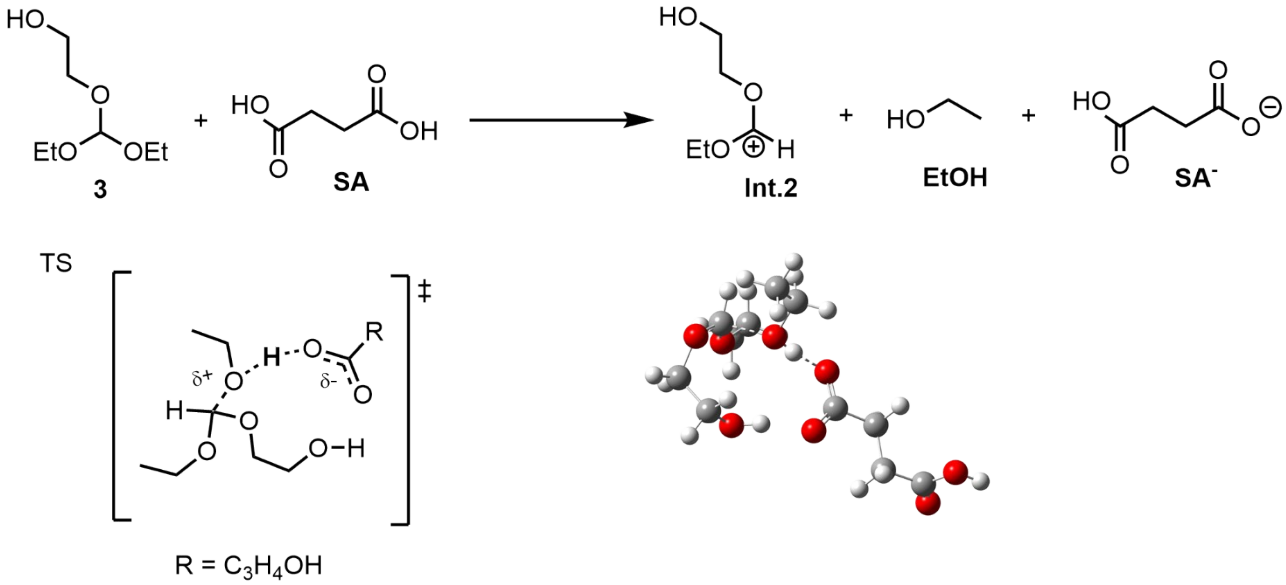
Table S34 Transition state: activation of **3** to int2 with benzoic acid (BA)



Coordinates of the TS (atom, X, Y, Z)	Energies
0 1 C 2.65999500 -0.09633200 -1.04231500 H 2.86234400 -1.00142700 -1.61049100 O 1.69007600 0.69010900 -1.38808600 O 3.68166100 0.39562800 -0.41660600 O 1.82765200 -1.21633300 0.43165500 C 0.69150800 0.14789500 -2.33577400 H 0.24138600 -0.72635100 -1.86381000 H 1.23472900 -0.14063100 -3.23936800 C -0.31977300 1.23788600 -2.59155300 H 0.15062900 2.11709500 -3.04503600 H -1.07677500 0.85394200 -3.28488100 H -0.81862000 1.53483200 -1.66435000 C 3.63593700 1.72698600 0.21624700 H 4.69102400 1.90373800 0.42667100 H 3.27628300 2.44916500 -0.51981300 C 2.81462200 1.78539800 1.50319500 H 2.83435700 0.80706200 1.99925600 H 3.33060900 2.50045000 2.15585100 C 2.21813000 -2.60194700 0.36937900 H 1.50241200 -3.17657100 0.96873200 H 2.14571100 -2.95659400 -0.66940100 C 3.62824600 -2.77569500 0.90301200 H 3.89826900 -3.83861200 0.88908000 H 4.35824900 -2.23096800 0.29462800 H 3.69837500 -2.41336300 1.93530200 O 1.49661300 2.27274100 1.33637100 H 0.83684800 1.55307200 1.19211200 H 0.79953700 -1.17261600 0.37699700 C -1.32814000 -0.20237900 0.61982100 O -0.77170100 0.79956800 1.13950000 O -0.72685900 -1.26223800 0.23975200 C -2.82791100 -0.16326700 0.41955600 C -3.56241500 0.96841600 0.80253100 C -3.50102800 -1.25106800 -0.15563400	H= -997.81688 Hartree G = -997.89401 Hartree

C -4.94566400 1.01317400 0.61438500 H -3.03823400 1.80873400 1.24638000 C -4.88448700 -1.20902400 -0.34474700 H -2.93075000 -2.12535200 -0.45208400 C -5.61033100 -0.07622400 0.03994000 H -5.50501000 1.89582900 0.91435600 H -5.39618000 -2.05777000 -0.79164700 H -6.68687000 -0.04238400 -0.10745100	

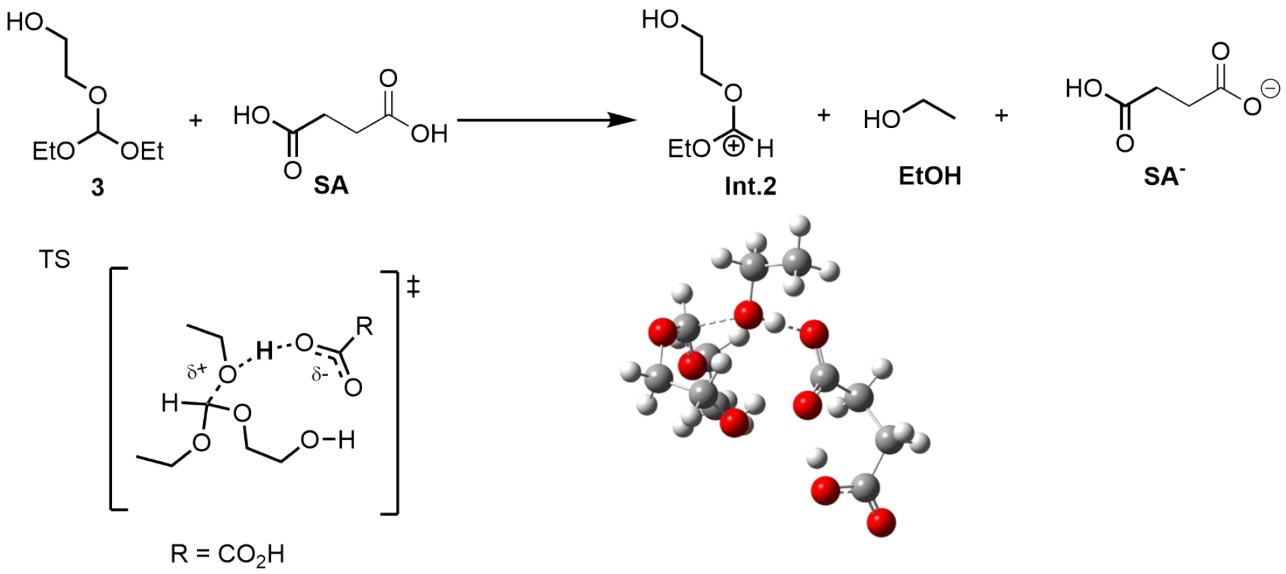
Table S35 Transition state: activation of **3** to int2 with succinic acid (SA)



Coordinates of the TS (atom, X, Y, Z)	Energies
0 1 C 3.15769600 0.14770600 -0.37756900 H 3.57864500 -0.24892800 -1.29849500 O 2.59905500 1.31834800 -0.37755200 O 3.73235000 -0.27942300 0.70550600 O 1.62537800 -1.11498900 -0.52693100 C 2.07396600 1.82234800 -1.65806900 H 1.07156900 1.40235500 -1.76155000 H 2.72159500 1.45132500 -2.45805300 C 2.05896600 3.33055100 -1.58262800 H 3.06998200 3.73312500 -1.45729900 H 1.64263100 3.72350800 -2.51732500 H 1.42986000 3.67535000 -0.75495000 C 3.41452100 0.28680000 2.02787600 H 4.22613000 -0.10353500 2.64284900 H 3.48344500 1.37500600 1.96729000 C 2.06924500 -0.15574800 2.58161900 H 1.88766800 -1.20467900 2.31796500 H 2.16475600 -0.09890400 3.67705300 C 1.79897100 -2.10363000 -1.56120200 H 0.81193600 -2.52264500 -1.78601100 H 2.17292400 -1.61682700 -2.47355200 C 2.75298200 -3.18695100 -1.09258100 H 2.85782200 -3.94938700 -1.87402400 H 3.74808900 -2.78110000 -0.87869000 H 2.37327300 -3.66959700 -0.18456100	H= -1033.9654 Hartree G = -1034.0483 Hartree

O 1.01130400 0.68573800 2.16217600 H 0.28387200 0.17086400 1.73082200 H 0.72522000 -0.63452400 -0.67839800 C -1.51000900 -0.18388700 -0.09750700 O -1.23303500 -0.41831800 1.10720200 O -0.65706700 -0.07440900 -1.04110000 C -2.97329800 -0.02138700 -0.51736600 H -3.06119000 0.91757400 -1.07709000 H -3.20400500 -0.82728800 -1.22485000 C -3.96377400 -0.03906000 0.65855500 H -3.74605200 0.78000000 1.34724000 H -3.87623400 -0.98474600 1.20064000 C -5.37540100 0.12827100 0.16484100 O -5.89126200 -1.02388700 -0.32507300 H -6.79223700 -0.83853300 -0.66328800 O -6.01083500 1.16962700 0.16183100	

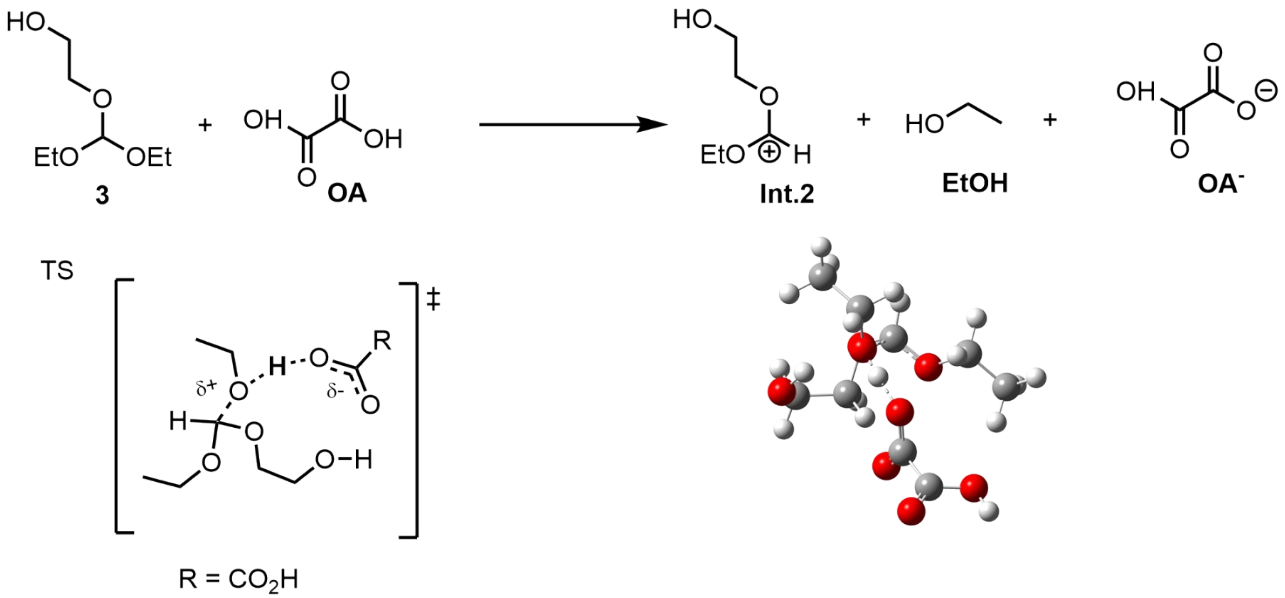
Table S36 Transition state: activation of **3** to int.**2** with SA (intramolecular stabilization)



Coordinates of the TS (atom, X, Y, Z)	Energies
0 1 C -2.57470200 -0.58974500 -0.91491700 H -3.02641200 -0.06227100 -1.75208500 O -1.49728100 -1.29692800 -1.10168600 O -3.42325300 -0.96693700 -0.00147700 O -1.89131400 1.02736600 -0.09437900 C -0.75341800 -1.06101500 -2.35588100 H -0.51406300 0.00256900 -2.40326800 H -1.42047100 -1.33411600 -3.17793700 C 0.48584000 -1.92120600 -2.30984100 H 0.22750700 -2.98415700 -2.25212200 H 1.06170800 -1.75450500 -3.22721400 H 1.11390000 -1.65990100 -1.45317200 C -3.00792100 -1.84898900 1.10258900 H -3.96867000 -2.16921800 1.50745100 H -2.47570000 -2.70632900 0.68538800 C -2.19136300 -1.14931800 2.18351000 H -2.55135300 -0.12076500 2.31204000 H -2.39607900 -1.69365800 3.11291100	H= -1033.9786 Hartree G = -1034.0583 Hartree

C -2.80113900 2.14435000 -0.19651400 H -2.78761900 2.52809800 -1.22446100 H -3.79774000 1.74496000 0.01244900 C -2.43286200 3.22734400 0.80313300 H -3.14884200 4.05502400 0.72637000 H -2.46167000 2.83708800 1.82671300 H -1.43006300 3.62316500 0.60688700 O -0.78608200 -1.20158400 2.00693300 H -0.45651300 -0.51574700 1.38874000 H -0.96505400 1.30080400 -0.45364900 C 1.32010500 1.09074600 -0.36135100 O 1.08437800 0.33976800 0.63892500 O 0.41816000 1.71037400 -0.99759800 C 2.75513600 1.23531700 -0.85811700 H 2.89693600 0.49031300 -1.65396900 C 3.86376700 1.09624000 0.20525000 H 4.78681800 1.53052800 -0.18493000 C 4.19710500 -0.32325800 0.64178400 H 2.84681100 2.21518900 -1.33485800 H 3.58756900 1.66731300 1.10194700 O 5.33795500 -0.76822900 0.62704000 O 3.18329500 -1.07407200 1.07441500 H 2.30884400 -0.55523600 0.98151800	

Table S37 Transition state: activation of **3** to int**2** using oxalic acid (OA)



Coordinates of the TS (atom, X, Y, Z)	Energies
0 1 C -1.60344800 1.17223100 -0.41546300 H -2.14615300 1.91010700 0.17426600 O -0.43777500 1.50728000 -0.92013000 O -2.38179800 0.41366500 -1.14898100 O -1.18648700 0.05758400 0.99265700 C 0.32201400 2.54235900 -0.20503500 H 0.66373700 2.10907700 0.73690800 H -0.35864200 3.37616500 -0.00649200 C 1.48024500 2.93980700 -1.08863400 H 1.12852800 3.34917500 -2.04186300	H= -955.37332 Hartree G = -955.44716 Hartree

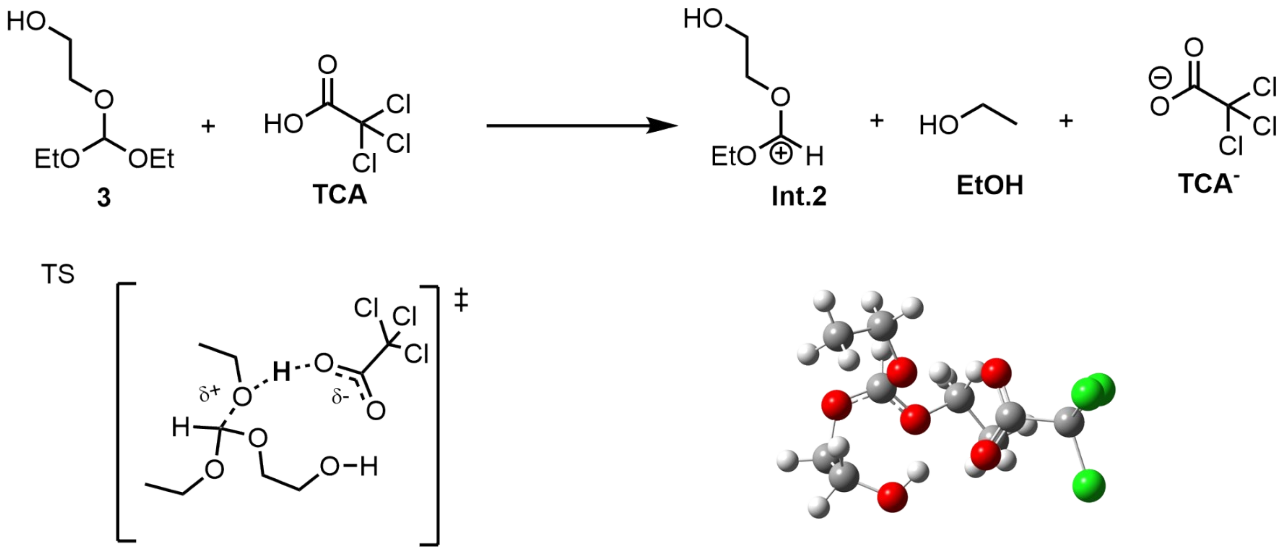
H 2.06685500 3.71045600 -0.57560000 H 2.13375200 2.08360900 -1.28399000 C -1.79082500 -0.67798400 -1.94436700 H -1.95887600 -0.42322800 -2.99321700 H -0.72153000 -0.74760800 -1.73289500 C -2.52315900 -1.94518600 -1.56277200 H -3.60621800 -1.79171100 -1.67612100 H -2.21710300 -2.73647300 -2.25607100 C -1.62110300 0.53483900 2.30026600 H -1.01491900 0.00348600 3.03956300 H -1.39772200 1.60527200 2.37161500 C -3.09805700 0.25588500 2.48893100 H -3.41077800 0.62231900 3.47385700 H -3.70288900 0.76418900 1.72976000 H -3.30429800 -0.81920500 2.44032600 O -2.21834700 -2.39484000 -0.24257500 H -2.02114400 -1.61822100 0.31602800 H -0.13873300 -0.12298000 1.00715200 C 1.89262100 -0.83401800 0.15811100 O 1.42023000 -1.30225000 -0.88743800 O 1.28747200 -0.30845000 1.15068600 C 3.41376500 -0.91643300 0.33179700 O 3.99515200 -1.85665900 0.84131100 O 4.04204500 0.16469500 -0.16731700 H 5.00986500 0.04838700 -0.04593700	

Table S38 Transition state: activation of **3** to int.**2** with oxalic acid (OA) and featuring an intramolecular stabilization

Coordinates of the TS (atom, X, Y, Z)	Energies
0 1 C -1.47976800 0.86240500 -0.93325200 H -1.99503500 1.81455600 -0.81694400 O -0.26230500 0.86978900 -1.43383300 O -2.27435700 -0.11477100 -1.30635900 O -1.24798000 0.52752000 0.83975700 C 0.52274100 2.09737300 -1.24362800 H 0.73003000 2.19865900 -0.17658300	H= -955.37825 Hartree G = -955.44914 Hartree

H -0.08965100 2.93784600 -1.58478600 C 1.79304300 1.95042300 -2.04717700 H 1.57430200 1.82462000 -3.11312900 H 2.39555000 2.85714400 -1.92117300 H 2.38312000 1.09549800 -1.70073700 C -1.72675700 -1.47356600 -1.46277600 H -1.81010500 -1.72135900 -2.52346300 H -0.68090800 -1.48664200 -1.14873300 C -2.57950100 -2.39277700 -0.61692000 H -3.63828700 -2.26118200 -0.88337300 H -2.29672300 -3.42628700 -0.84473500 C -1.73229600 1.58192100 1.72787300 H -1.24296100 1.41696900 2.69166100 H -1.40393200 2.54796000 1.32879500 C -3.24011700 1.50313500 1.84567100 H -3.58967300 2.29911600 2.51355000 H -3.72698700 1.63763800 0.87349400 H -3.55183600 0.53985900 2.26456600 O -2.38882700 -2.20225200 0.78542500 H -2.20161200 -1.25853700 0.94978400 H -0.22379000 0.34135700 1.03274500 C 1.83701800 -0.64044400 0.67787200 O 1.40210200 -1.59979600 0.00626700 O 1.19419800 0.22961600 1.33263300 C 3.39208300 -0.50564200 0.69010600 O 4.02563400 0.34844800 1.27145500 O 3.97873700 -1.46425000 -0.04174000 H 3.23220500 -2.00860800 -0.39638900	

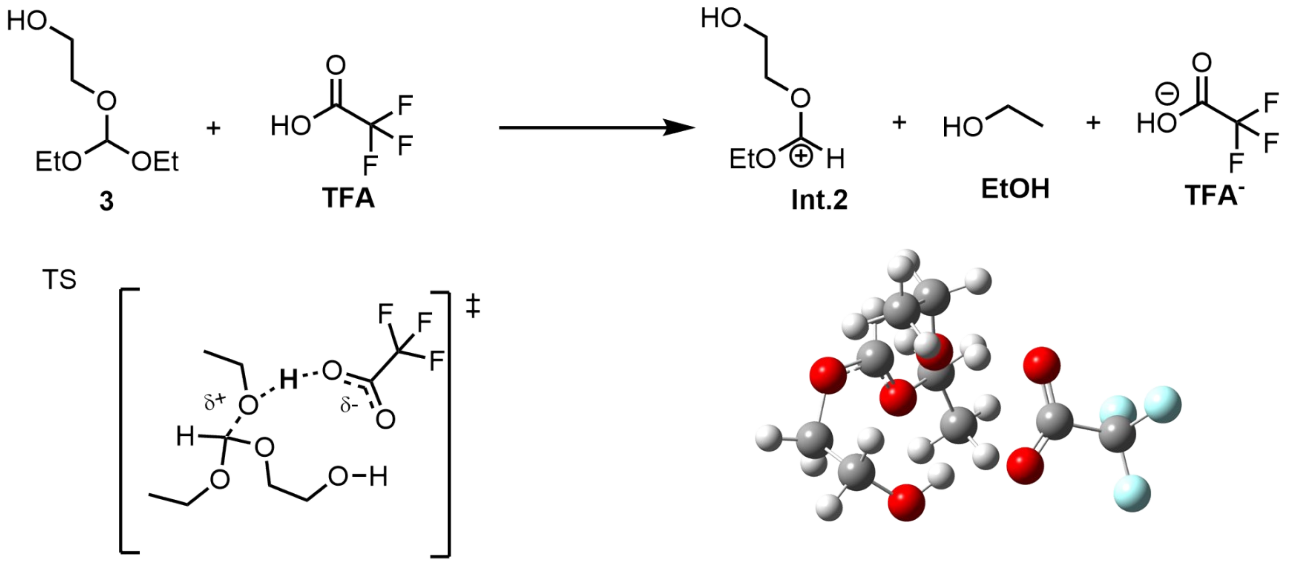
Table S39 Transition state: activation of **3** to int**2** with trichloroacetic acid (TCA)



Coordinates of the TS (atom, X, Y, Z)	Energies
0 1 C 2.69347600 0.58745500 -0.99638200 H 2.81422500 0.37930100 -2.05856700 O 1.82944500 1.49829300 -0.62203400 O 3.80575900 0.47655600 -0.31389600 O 1.84039600 -1.00805600 -0.60253600	H= -2184.9058 Hartree G = -2184.9842 Hartree

C 0.83685800 1.92506300 -1.62658700 H 0.29206800 1.03939500 -1.95815300 H 1.39340200 2.35702700 -2.46286100 C -0.07036900 2.93197300 -0.96207800 H 0.49571900 3.80373300 -0.61622800 H -0.81400400 3.27002400 -1.69219700 H -0.59776900 2.48912800 -0.11176400 C 3.89738600 0.96376900 1.07027000 H 4.97278900 0.92562500 1.24890700 H 3.55506200 2.00061000 1.10072400 C 3.16904700 0.10718000 2.10166500 H 3.21445600 -0.94913200 1.81179900 H 3.73160300 0.22062900 3.03577800 C 2.33149300 -2.17206300 -1.32311800 H 1.45710900 -2.77112500 -1.59487300 H 2.80972700 -1.82881800 -2.24852800 C 3.29700800 -2.95991300 -0.46007700 H 3.64374100 -3.83931100 -1.01669200 H 4.17029400 -2.35764300 -0.19048400 H 2.80750300 -3.30329700 0.45810200 O 1.84408200 0.51940800 2.39924400 H 1.18573200 0.16073700 1.76920200 H 0.81935200 -0.93269900 -0.70949400 C -1.20091800 -0.41989600 0.22453100 O -0.65079100 -0.16523900 1.30290400 O -0.70021600 -0.85833500 -0.84737400 C -2.77244100 -0.21953400 0.14844400 Cl -3.39978200 0.75016500 1.51998200 Cl -3.23478100 0.59572800 -1.38974500 Cl -3.52953400 -1.86527000 0.20181300	

Table S40 Transition state: activation of **3 to** int**2** with trifluoroacetic acid (TFA)

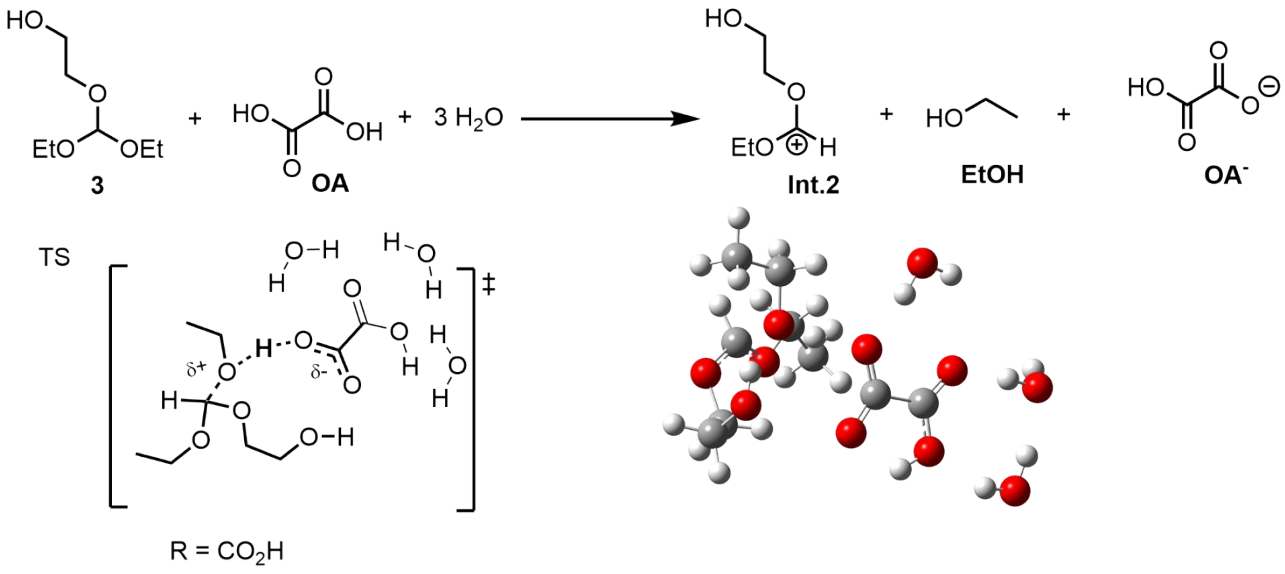


Coordinates of the TS (atom, X, Y, Z)	Energies
0 1 C 2.06009500 0.61456400 -1.03526200 H 2.16857000 0.39571000 -2.09655000 O 1.16627300 1.49627800 -0.65825700 O 3.19173700 0.56617600 -0.37656300	H= -1103.8624 Hartree G = -1103.9386 Hartree

O 1.28844000 -1.00225200 -0.59875500 C 0.13369800 1.85801700 -1.64730300 H -0.38417400 0.94401100 -1.94331500 H 0.65118500 2.28945300 -2.50858200 C -0.79763400 2.84463200 -0.98540900 H -0.26221500 3.75181500 -0.68490200 H -1.57856700 3.12443900 -1.70150000 H -1.27735600 2.40562000 -0.10512500 C 3.29386200 1.08644200 0.99453600 H 4.37379100 1.09790400 1.14787200 H 2.90814400 2.10827800 1.01162100 C 2.62754600 0.22221400 2.06109100 H 2.70883600 -0.83707300 1.79026100 H 3.20860800 0.37686000 2.97777300 C 1.81839500 -2.15862400 -1.30506800 H 0.96462400 -2.78927100 -1.57040400 H 2.28555700 -1.80948100 -2.23369300 C 2.80906800 -2.90338400 -0.43237000 H 3.18297900 -3.77894100 -0.97735000 H 3.66315100 -2.27013700 -0.17239000 H 2.33157900 -3.24950000 0.49109000 O 1.29490800 0.58619400 2.38622500 H 0.63545900 0.19274300 1.77830000 H 0.26252400 -0.97645800 -0.67925400 C -1.75966500 -0.53263400 0.30711500 O -1.19785600 -0.21019200 1.36385800 O -1.26681000 -0.97799000 -0.76904100 C -3.30933800 -0.36976000 0.24134100 F -3.84932400 0.07663300 1.39519500 F -3.66441200 0.51343400 -0.73004400 F -3.92097600 -1.54678900 -0.05355100	

10.2.5 Computations for the catalyst screening with 3 molecules of water

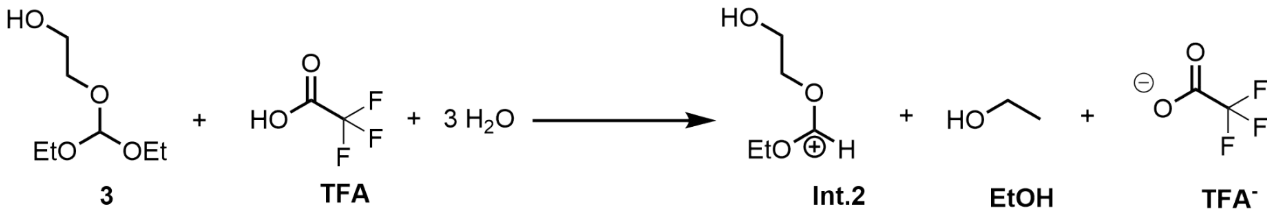
Table S41 Transition state: activation of **3** to int.**2** with OA and explicit water (cluster of 3), featuring an intramolecular stabilization

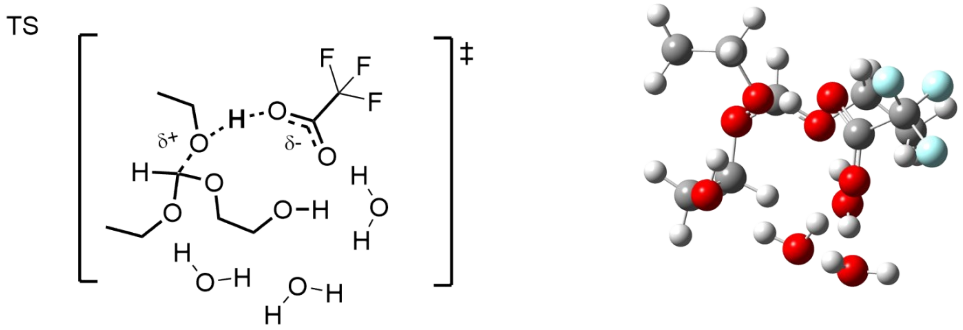


Coordinates of the TS (atom, X, Y, Z)	Energies

0 1 C 2.49310900 0.17023900 1.20706600 H 3.01229800 1.04997400 1.58713300 O 1.29848600 -0.10310600 1.70651300 O 3.30185300 -0.85502700 1.02150900 O 2.18758500 0.75322100 -0.42702400 C 0.52629600 1.03547200 2.21902700 H 0.26314500 1.67430700 1.37337500 H 1.16954400 1.58799300 2.91092700 C -0.70167900 0.48144000 2.90224300 H -0.42703200 -0.17163200 3.73767100 H -1.29282400 1.31671700 3.29450500 H -1.32696300 -0.08159900 2.20134300 C 2.75427000 -2.12539800 0.52150600 H 2.85627600 -2.85075800 1.33239700 H 1.70242000 -1.99765500 0.25860600 C 3.58625200 -2.52388600 -0.67713200 H 4.65082200 -2.53148400 -0.40224800 H 3.30181000 -3.53906300 -0.97245400 C 2.61817200 2.13135500 -0.69726900 H 2.04313100 2.45526900 -1.56807200 H 2.34049700 2.74978800 0.16202200 C 4.10690900 2.15625700 -0.96534100 H 4.41003600 3.18666700 -1.18472600 H 4.68008300 1.81219800 -0.09750600 H 4.36055800 1.53146000 -1.82902700 O 3.36506000 -1.68561100 -1.81246800 H 3.29038500 -0.76373400 -1.50648900 H 1.17463700 0.65134000 -0.64690600 C -0.91687100 -0.43973200 -0.74923500 O -0.46372200 -1.59625000 -0.69487100 O -0.30107700 0.65585300 -0.91293900 C -2.45996200 -0.33783800 -0.57708300 O -3.10002400 0.69626000 -0.60394300 O -3.02637600 -1.53047700 -0.38355600 H -2.28266100 -2.18597800 -0.40892000 O -5.89404400 0.86040100 -0.23875500 H -6.07175500 1.37439400 0.56803500 H -4.91843100 0.87453500 -0.35231900 O -6.02262400 -1.94043900 0.06666200 H -5.06747500 -2.07720000 -0.05190800 H -6.11897500 -0.96484900 -0.01020700 O -1.39129100 3.26012000 -0.93694600 H -2.35220700 3.15889500 -0.84004000 H -1.06690900 2.33340800 -0.93134200	H= -1184.6235 Hartree G = -1184.7175 Hartree

Table S42 Transition state: activation of **3** to int**2** using TFA and explicit water (cluster of 3), featuring an intramolecular stabilization



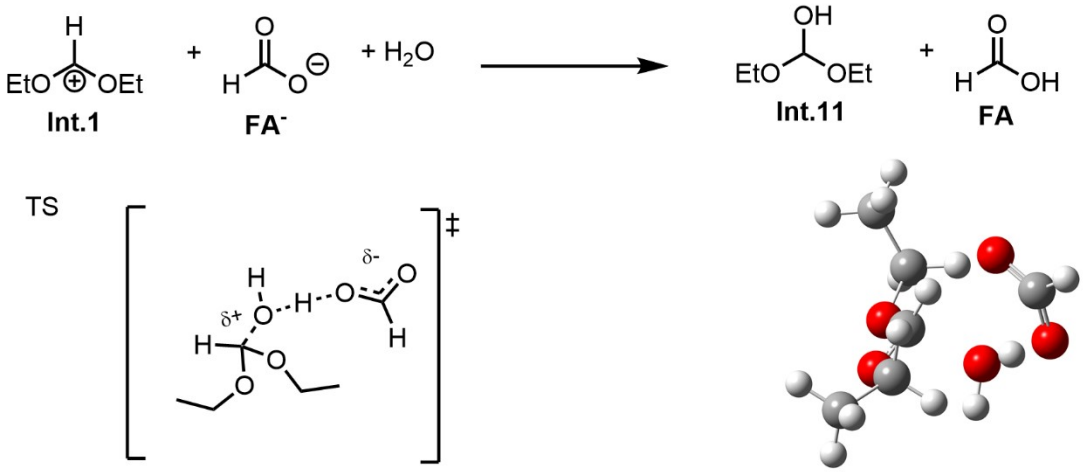


Coordinates of the TS (atom, X, Y, Z)	Energies
0 1 C -1.67190200 0.69828600 -1.28267600 H -1.56308900 1.30693700 -2.17988800 O -1.05705400 -0.47804700 -1.26089300 O -2.90567500 0.73884800 -0.80698900 O -0.73775100 1.68200400 -0.18788400 C 0.02867100 -0.65280800 -2.24634500 H 0.70101300 0.20315600 -2.16778900 H -0.43971500 -0.66566700 -3.23469700 C 0.73582400 -1.94862400 -1.92919400 H 0.06582700 -2.80702900 -2.03893300 H 1.56871700 -2.07055300 -2.63090900 H 1.13864500 -1.94242500 -0.91226100 C -3.32877800 -0.14258000 0.28493000 H -4.32584600 -0.47757000 -0.00696300 H -2.66064700 -1.00005400 0.34924900 C -3.39842100 0.61953400 1.59179400 H -3.95277300 1.55644400 1.45747000 H -3.93702300 -0.00124700 2.31378800 C -0.64305400 3.10791400 -0.55859900 H 0.14629300 3.51180500 0.07902000 H -0.31971100 3.15723000 -1.60299300 C -1.96055600 3.81522000 -0.33145400 H -1.81941400 4.87839100 -0.55857500 H -2.75208500 3.43177800 -0.98132100 H -2.28342100 3.73075800 0.71191400 O -2.11246500 0.88008600 2.16996500 H -1.58882500 1.39526600 1.52467300 H 0.24965200 1.31586500 -0.09797200 C 2.30820600 0.20219000 0.56496600 O 1.91091900 -0.57550200 1.44234100 O 1.68685900 1.07412700 -0.10778100 C 3.81698300 0.12479500 0.17658100 O -1.36893400 -3.58057800 1.03044700 H -1.07001200 -2.77461100 1.53199200	H= -1333.1167 Hartree G = -1333.2101 Hartree

H -0.56309500 -4.10331100 0.87947300 O -0.52965200 -1.40933500 2.45059000 H 0.31891000 -1.08324600 2.07215200 H -1.13478900 -0.63411700 2.41145000 O -2.70758500 -3.21640000 -1.38744600 H -2.39074400 -2.37147800 -1.74436200 H -2.22106500 -3.31872500 -0.53506900 F 3.95936800 -0.25993800 -1.11919400 F 4.51413800 -0.75021600 0.92904200 F 4.42450000 1.33206800 0.30145600	

10.2.6 Computations for the mechanism of hydrolysis

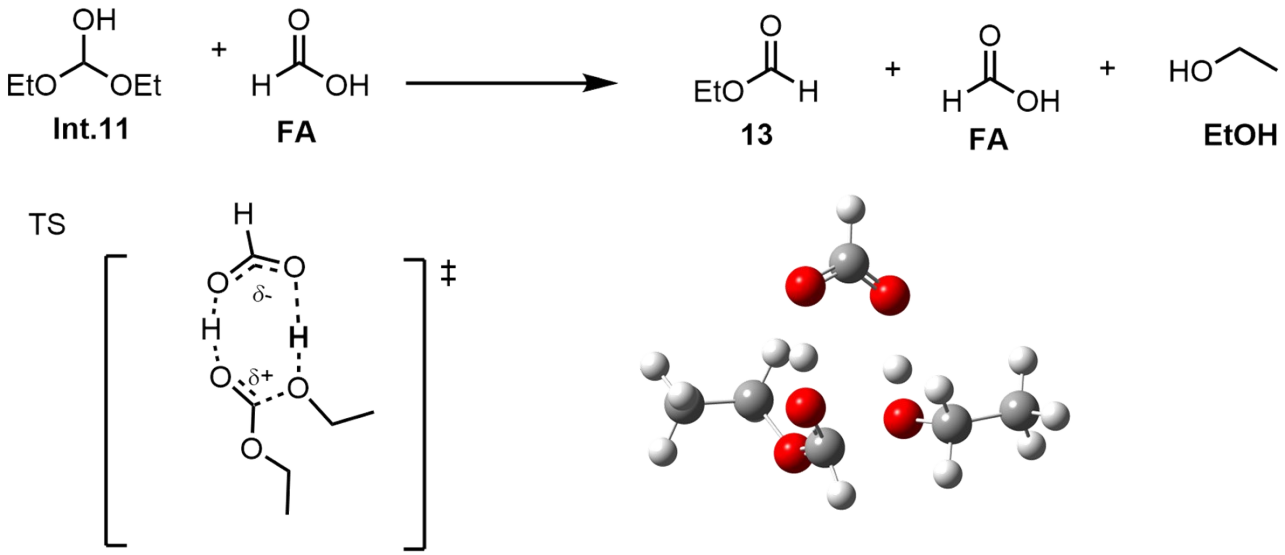
Table S43 Transition state: Addition of H_2O on int.**1** to int**11**



Coordinates of the TS (atom, X, Y, Z)	Energies
0 1 C -0.54300800 0.54554200 0.22038800 H -0.36212000 -0.24474700 -0.51186900 O -1.76694500 0.84757600 0.57736800 O 0.25873800 1.58509500 0.25272800 O 0.03269800 -0.57663800 1.60776000 C -2.77963400 -0.18710600 0.32147400 H -3.57766700 0.05339900 1.02461500 H -2.34926500 -1.15567300 0.58716500 C -3.25204300 -0.13407800 -1.11650600 H -2.43737000 -0.35634200 -1.81512000 H -4.03666800 -0.88689400 -1.25837400 H -3.66908900 0.85004100 -1.35672400 C 1.61156200 1.39314800 -0.28703700 H 2.18528100 0.83878900 0.46023700 H 1.53306500 0.79771500 -1.19986500 C 2.19587300 2.76182800 -0.54622100 H 2.24104500 3.35249600 0.37529200 H 3.21598500 2.64278100 -0.92899600 H 1.60771600 3.30737800 -1.29211300 C 1.65753700 -2.33835900 -0.53323500 H 2.43421200 -3.00133500 -0.96735500 O 0.75370600 -1.91197500 -1.27989400 O 1.80269700 -2.09479400 0.71658700 H 0.80578300 -1.23111500 1.23332300	H= -613.01626 Hartree G = -613.07493 Hartree

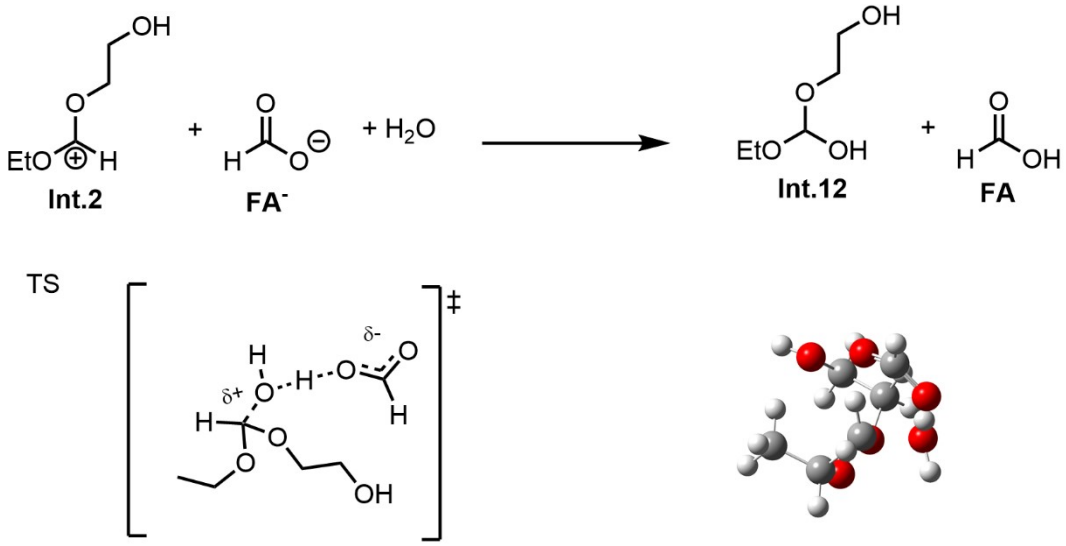
H 0.42021300 -0.00645100 2.30020900	

Table S44 Transition state: Elimination of EtOH from int**11** to **13**



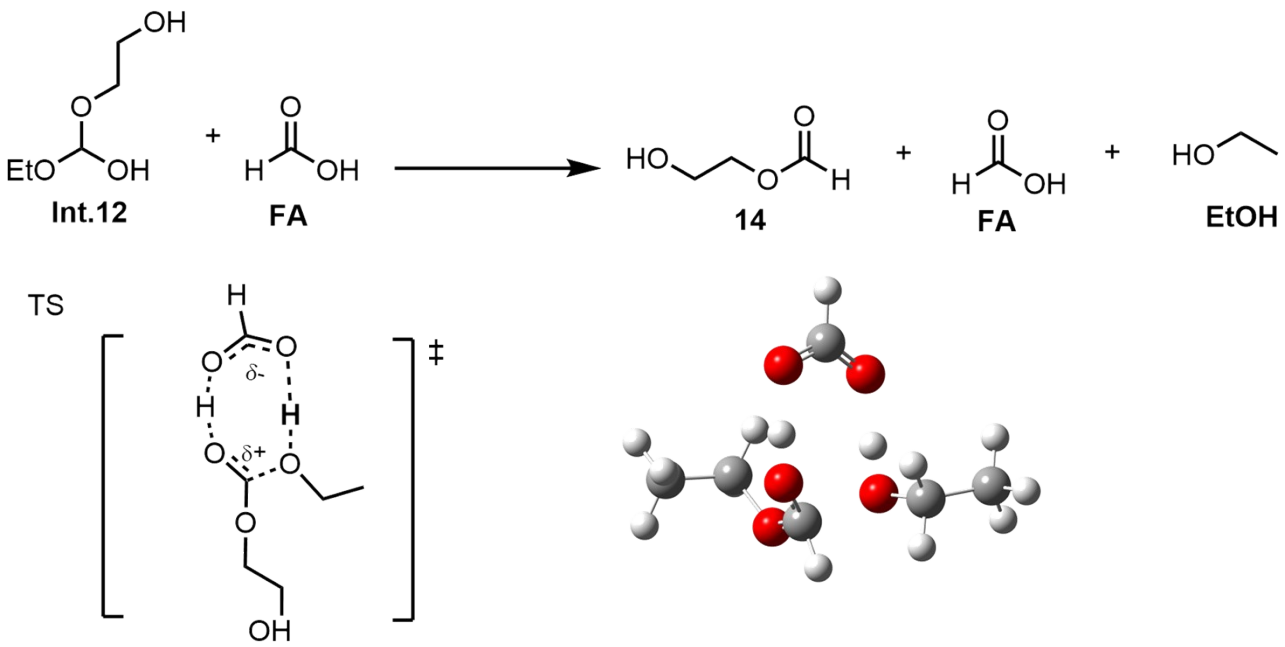
Coordinates of the TS (atom, X, Y, Z)	Energies
0 1 C -0.31468400 -1.29645900 0.47385800 H 0.09798600 -2.25007900 0.79437400 O -1.17616100 -1.46813100 -0.52507300 O 1.15657200 -0.73605000 -0.37682700 O -0.50884300 -0.43250000 1.44187300 C -2.10709100 -0.40943700 -0.92141300 H -2.30027400 -0.62574300 -1.97343400 H -1.61113900 0.55909900 -0.85637000 C -3.38286600 -0.46168400 -0.10373000 H -3.20027500 -0.23981200 0.95202700 H -4.08297100 0.28556300 -0.49665900 H -3.85340100 -1.44805400 -0.18265500 C 2.34853300 -0.79259600 0.46211100 H 2.25087300 -0.05114000 1.26158800 H 2.35447700 -1.79232000 0.90412300 C 3.58407300 -0.55282000 -0.38324000 H 3.56803000 0.44396600 -0.83796700 H 4.47340300 -0.62161700 0.25486300 H 3.66730100 -1.30347700 -1.17685200 C 0.08301300 2.44634600 -0.07684300 H 0.09210300 3.53988600 -0.22835400 O -0.62658600 2.01752900 0.88198600 O 0.76888100 1.75283900 -0.87886900 H 0.98133200 0.25635400 -0.61641400 H -0.61421900 0.57776000 1.15255300	H= -613.02495 Hartree G = -613.08115 Hartree

Table S45 Transition state: Addition of H_2O on int**2** to int**11**



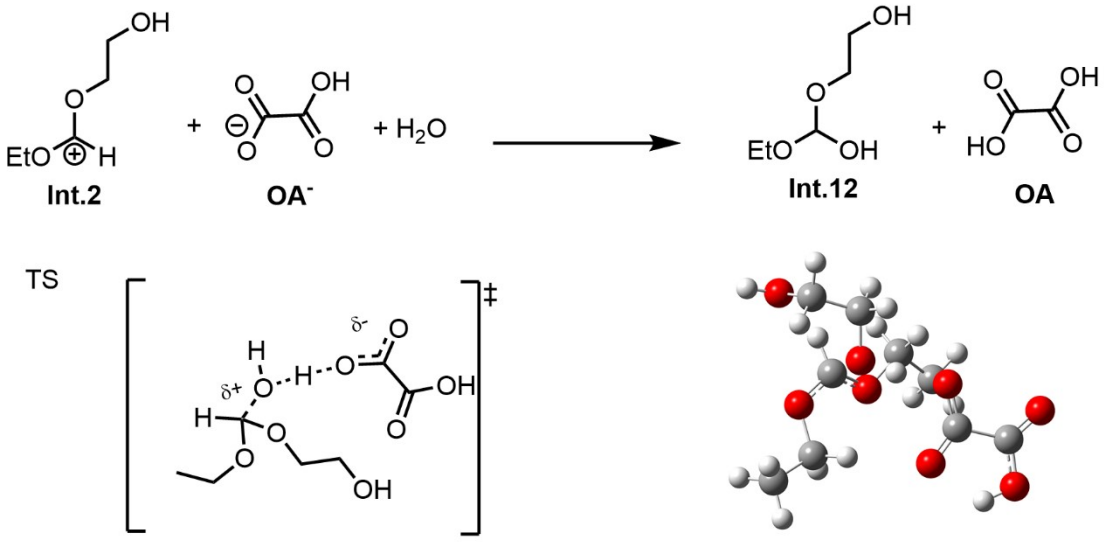
Coordinates of the TS (atom, X, Y, Z)	Energies
0 1 C 0.34910900 0.30290800 -0.68164900 H 0.04750200 -0.09127300 0.28894000 O 1.55731000 0.07363200 -1.14155500 O -0.12255900 1.45988200 -1.08721500 O -0.66965700 -0.98154200 -1.57434500 C 2.28297300 -1.04437200 -0.54679600 H 2.84817500 -1.49324700 -1.36494600 H 1.56766000 -1.77240400 -0.15524400 C 3.21262700 -0.53754300 0.52852300 H 3.82824800 -1.38177500 0.86980400 H 3.87480400 0.23624200 0.11862600 C -1.33472800 1.94712700 -0.41005200 H -1.76437400 2.64645300 -1.12803200 H -2.01792500 1.10563900 -0.27735600 C -0.98398400 2.61843800 0.90056200 H -0.30300300 3.46126900 0.73935200 H -1.90467100 2.99872700 1.35906200 H -0.52188500 1.91339800 1.59928000 C -2.55446000 -1.39671400 0.99688200 H -3.43680400 -1.67598900 1.60890100 O -1.54269300 -0.95378700 1.57335500 O -2.70462700 -1.57238000 -0.26522100 H -1.55863600 -1.23022400 -1.00388600 H -0.95438300 -0.57041100 -2.41371800 O 2.41506900 -0.01342700 1.59441100 H 3.00332500 0.41551600 2.23894800	H= -688.22803 Hartree G = -688.28821 Hartree

Table S46 Transition state: Elimination of EtOH from int**12** to **14**



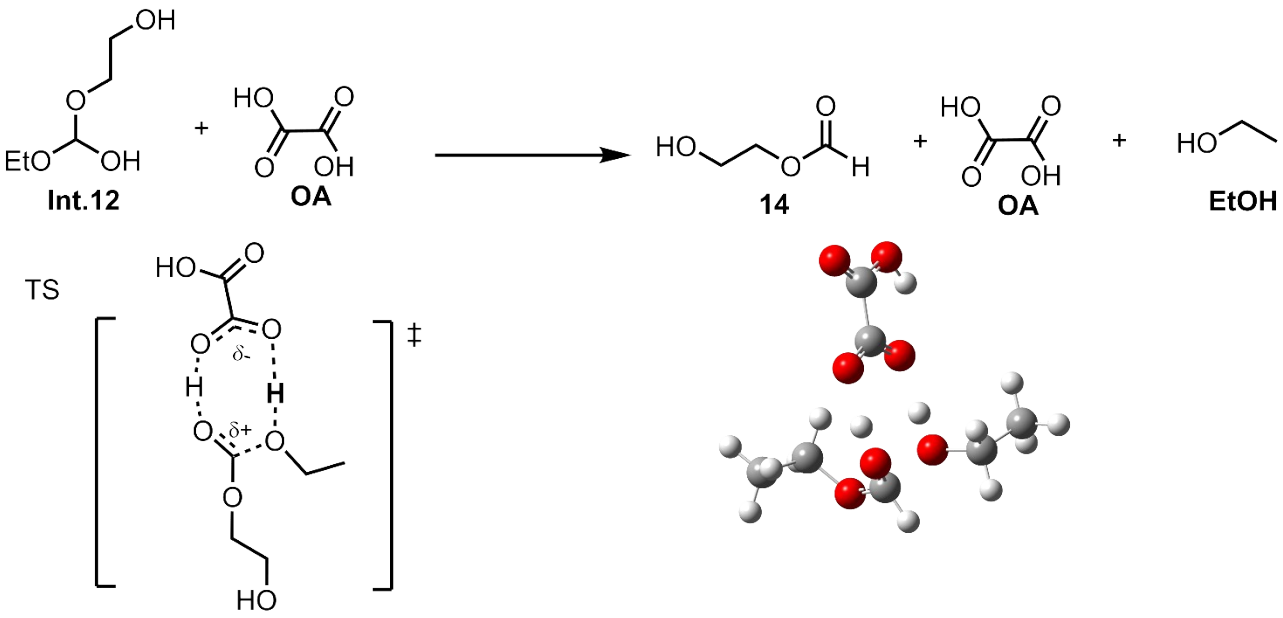
Coordinates of the TS (atom, X, Y, Z)	Energies
0 1 C -0.13154100 -1.14820400 0.55005800 H 0.14642600 -2.14030700 0.89862400 O -1.03570000 -1.23297700 -0.42469600 O 1.38031600 -0.83616300 -0.35846500 O -0.17384800 -0.23128200 1.48436600 C -1.77606200 -0.06205200 -0.87621000 H -2.05470400 -0.30932100 -1.90228300 H -1.12777200 0.81422700 -0.89378100 C -3.01003000 0.20281300 -0.04395300 H -2.75395800 0.31695900 1.01561300 H -3.44244500 1.14947800 -0.39920700 C 2.57683300 -1.05223400 0.44850800 H 2.62154500 -0.27994000 1.22306300 H 2.44166600 -2.02617200 0.92551600 C 3.80528700 -1.03508100 -0.43961800 H 3.93212900 -0.06150100 -0.92612800 H 4.69350900 -1.22756800 0.17423700 H 3.74139000 -1.81113100 -1.21029500 C 0.77791200 2.48300900 -0.11901900 H 0.94127900 3.55981600 -0.29815800 O 0.02869900 2.18453100 0.86032900 O 1.34213600 1.67748400 -0.90984100 H 1.34768200 0.16413600 -0.61728200 H -0.14233000 0.78171600 1.16428500 O -3.92889700 -0.87886700 -0.22857300 H -4.70045100 -0.72169800 0.34223800	H= -688.23606 Hartree G = -688.2961 Hartree

Table S47 Transition state: Addition of H_2O on int**2** to int**11** with OA (explicit water), featuring an intramolecular stabilization.



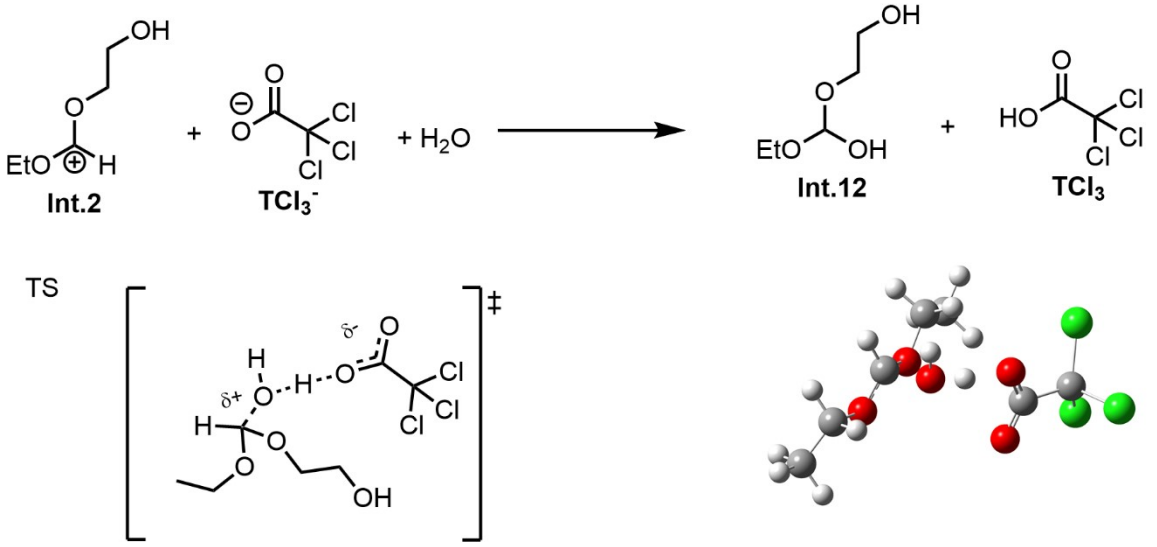
Coordinates of the TS (atom, X, Y, Z)	Energies
0 1 C -1.51954200 0.16774900 0.87169500 H -2.26095200 -0.55890500 1.19624300 O -0.34580000 0.20003500 1.48350000 O -2.04128300 1.33474700 0.56324500 O -1.17558100 -0.57492100 -0.71434500 C 0.12801600 -1.05303200 2.07325000 H 0.29324500 -1.76839500 1.26483600 H -0.65424700 -1.42553100 2.74245800 C 1.41227000 -0.74397300 2.80692600 H 1.24447200 -0.01526000 3.60757100 H 1.79909600 -1.66712800 3.25323100 H 2.16913900 -0.35021300 2.11977100 C -1.12559600 2.44139200 0.25334400 H -0.70324000 2.79555400 1.19761900 H -0.32074500 2.05814800 -0.37819100 C -1.93953000 3.51120900 -0.43784600 H -2.75873200 3.86147500 0.20034200 H -1.28848800 4.36477500 -0.66027600 C -1.81456000 -1.84775100 -1.00094800 H -1.28846000 -2.27324800 -1.86021500 H -1.69603600 -2.51845900 -0.14232600 C -3.27126100 -1.65891400 -1.34353700 H -3.64693300 -2.60383100 -1.76019900 H -3.37845500 -0.87267200 -2.10167400 H -0.13965600 -0.68275400 -0.83947000 C 2.06693400 0.00508900 -0.93058700 O 1.79020900 1.21178000 -1.10955900 O 1.30027000 -0.99781100 -0.95898600 C 3.57185300 -0.27728100 -0.62547600 O 4.06629700 -1.36780700 -0.43822700 O 4.29129100 0.85419900 -0.58811200 H 3.64113700 1.57621100 -0.77677600 H -2.35722400 3.14061500 -1.38054000 O -3.98651500 -1.31676300 -0.14905400 H -4.89654200 -1.07497600 -0.39102800	H= -955.3771 Hartree G = -955.45176 Hartree

Table S48 Transition state: Elimination of EtOH from int**12** to **14** with OA, featuring an intramolecular stabilization



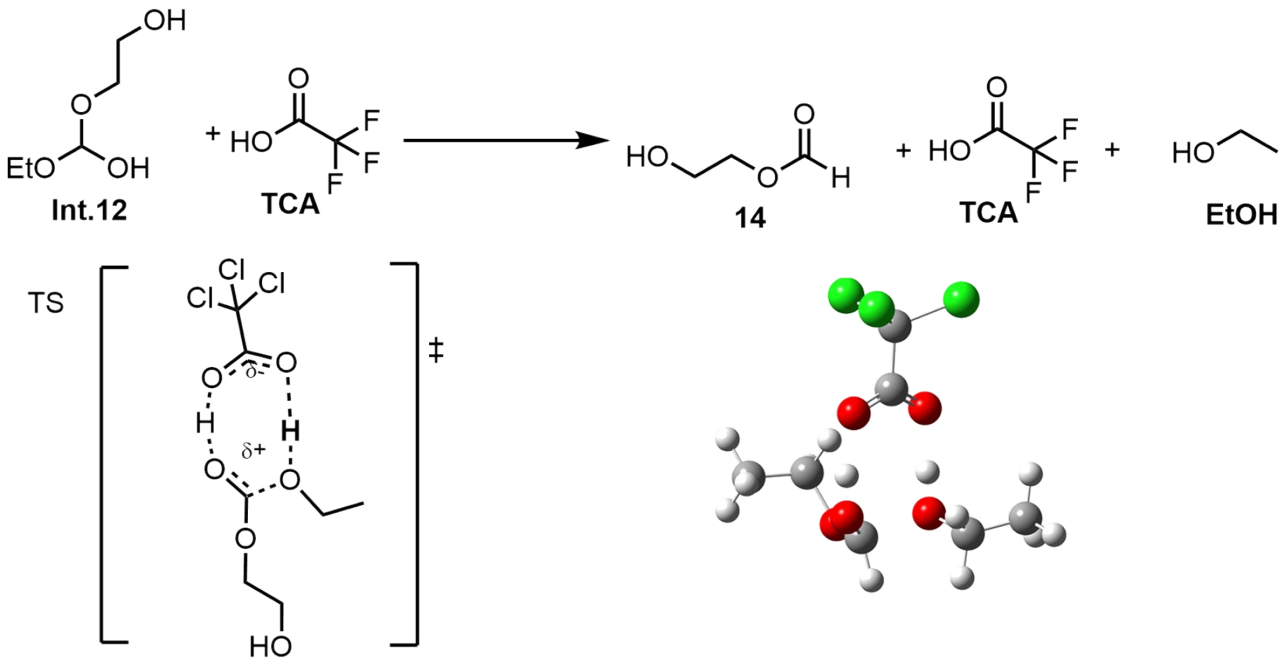
Coordinates of the TS (atom, X, Y, Z)	Energies
0 1 C -0.13154100 -1.14820400 0.55005800 H 0.14642600 -2.14030700 0.89862400 O -1.03570000 -1.23297700 -0.42469600 O 1.38031600 -0.83616300 -0.35846500 O -0.17384800 -0.23128200 1.48436600 C -1.77606200 -0.06205200 -0.87621000 H -2.05470400 -0.30932100 -1.90228300 H -1.12777200 0.81422700 -0.89378100 C -3.01003000 0.20281300 -0.04395300 H -2.75395800 0.31695900 1.01561300 H -3.44244500 1.14947800 -0.39920700 C 2.57683300 -1.05223400 0.44850800 H 2.62154500 -0.27994000 1.22306300 H 2.44166600 -2.02617200 0.92551600 C 3.80528700 -1.03508100 -0.43961800 H 3.93212900 -0.06150100 -0.92612800 H 4.69350900 -1.22756800 0.17423700 H 3.74139000 -1.81113100 -1.21029500 C 0.77791200 2.48300900 -0.11901900 H 0.94127900 3.55981600 -0.29815800 O 0.02869900 2.18453100 0.86032900 O 1.34213600 1.67748400 -0.90984100 H 1.34768200 0.16413600 -0.61728200 H -0.14233000 0.78171600 1.16428500 O -3.92889700 -0.87886700 -0.22857300 H -4.70045100 -0.72169800 0.34223800	H= -688.23606 Hartree G = -688.2961 Hartree

Table S49 Transition state: Addition of H_2O on int**2** to int**11** with TCA



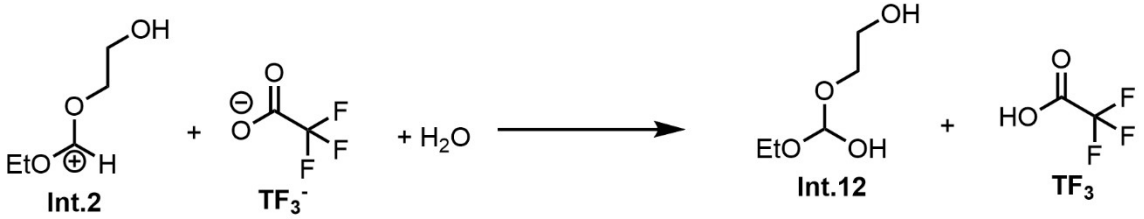
Coordinates of the TS (atom, X, Y, Z)	Energies
0 1 C 2.88525700 0.55874300 -0.34098100 H 3.40813600 1.10479800 -1.12925600 O 1.94735900 1.18727100 0.33417200 O 3.58862400 -0.24411700 0.42785700 O 2.02782100 -0.56618600 -1.44350600 C 1.26613200 2.28813300 -0.35251300 H 0.72285900 1.86931000 -1.20294700 H 2.02968300 2.98704300 -0.70831300 C 0.32881700 2.92407200 0.64693300 H 0.88206000 3.34614700 1.49301500 H -0.22245100 3.73240300 0.15370300 H -0.39441800 2.19352800 1.02304800 H 0.97280200 -0.56278600 -1.25807200 C -0.95682500 -0.73214700 -0.03012300 O -0.46482900 -1.31947100 0.93153200 O -0.44366200 -0.42988400 -1.15040900 C -2.49252700 -0.33373000 0.07333300 C 4.74877400 -0.88577900 -0.19326700 H 4.37274900 -1.66056200 -0.86636700 H 5.28698900 -0.12819000 -0.77247500 C 5.60125700 -1.46266000 0.91315800 H 5.04082100 -2.20088800 1.49714600 H 6.46837600 -1.96311800 0.46722300 H 5.96265400 -0.67598400 1.58445300 H 2.14637800 -0.27241400 -2.36970000 Cl -3.00835500 -0.13017800 1.78066300 Cl -3.43460000 -1.69693400 -0.66763000 Cl -2.86318900 1.18417200 -0.81937700	H= -2031.1167 Hartree G = -2031.1887 Hartree

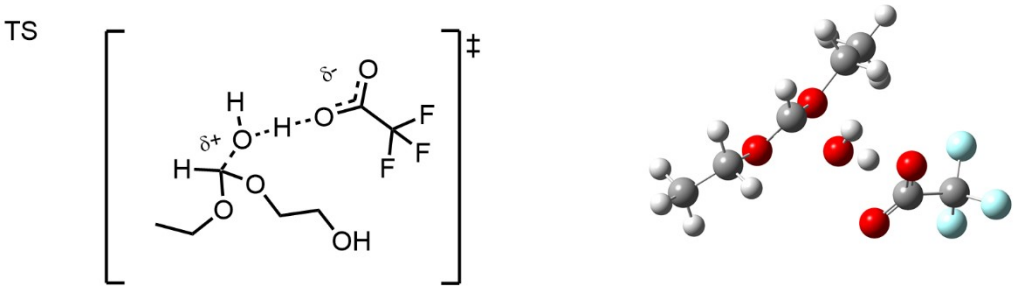
Table S50 Transition state: Elimination of EtOH from int**12** to **14** with TCA



Coordinates of the TS (atom, X, Y, Z)	Energies
0 1 C 3.09798900 -0.34391700 0.38303000 H 4.09140900 0.03674900 0.60453000 O 3.12898400 -1.21133800 -0.61848600 O 2.49653500 1.14179800 -0.40133200 O 2.34047500 -0.50510200 1.45046800 C 2.00032700 -2.10271700 -0.90881300 H 2.11598900 -2.31103600 -1.97328200 H 1.06301100 -1.56493500 -0.76737600 C 2.07136300 -3.37263000 -0.08481100 H 1.95218000 -3.17649800 0.98490800 H 1.26169900 -4.03990500 -0.40379500 H 3.02515200 -3.88640700 -0.24732200 C 2.65275300 2.33519600 0.43238400 H 2.01431800 2.22884800 1.31445100 H 3.69959900 2.33584500 0.74446000 C 2.30728400 3.57020200 -0.37454300 H 1.26075700 3.55535900 -0.69869400 H 2.45624700 4.45692800 0.25315100 H 2.95207300 3.65616500 -1.25581200 C -0.68132800 0.11591100 0.16954200 O -0.21575400 -0.58163600 1.09994200 O -0.07109900 0.79494200 -0.68560900 H 1.49960200 0.99746600 -0.56174900 H 1.33985000 -0.61941000 1.26713100 C -2.24926700 0.05537600 0.00819300 Cl -2.59735700 -1.43255500 -0.96645000 Cl -3.06357000 -0.07435900 1.60141700 Cl -2.88964600 1.48791400 -0.85675300	H= -2031.1234 Hartree G = -2031.1941 Hartree

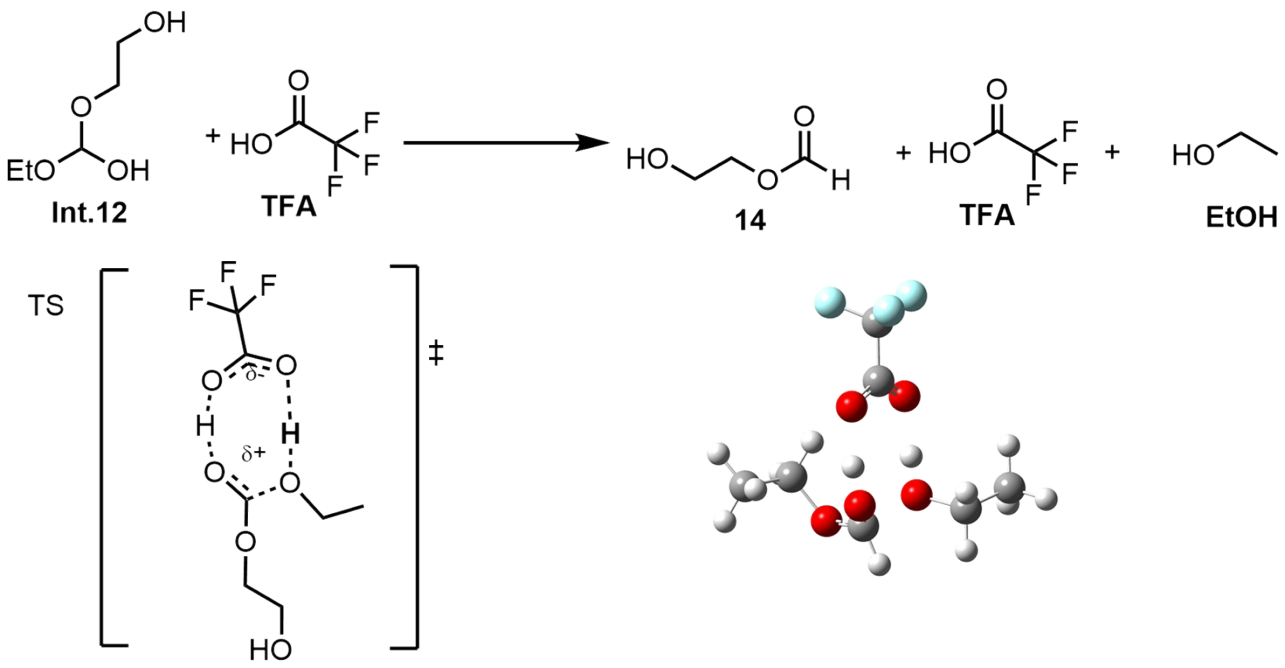
Table S51 Transition state: Addition of H_2O on int**2** to int**11** with TFA





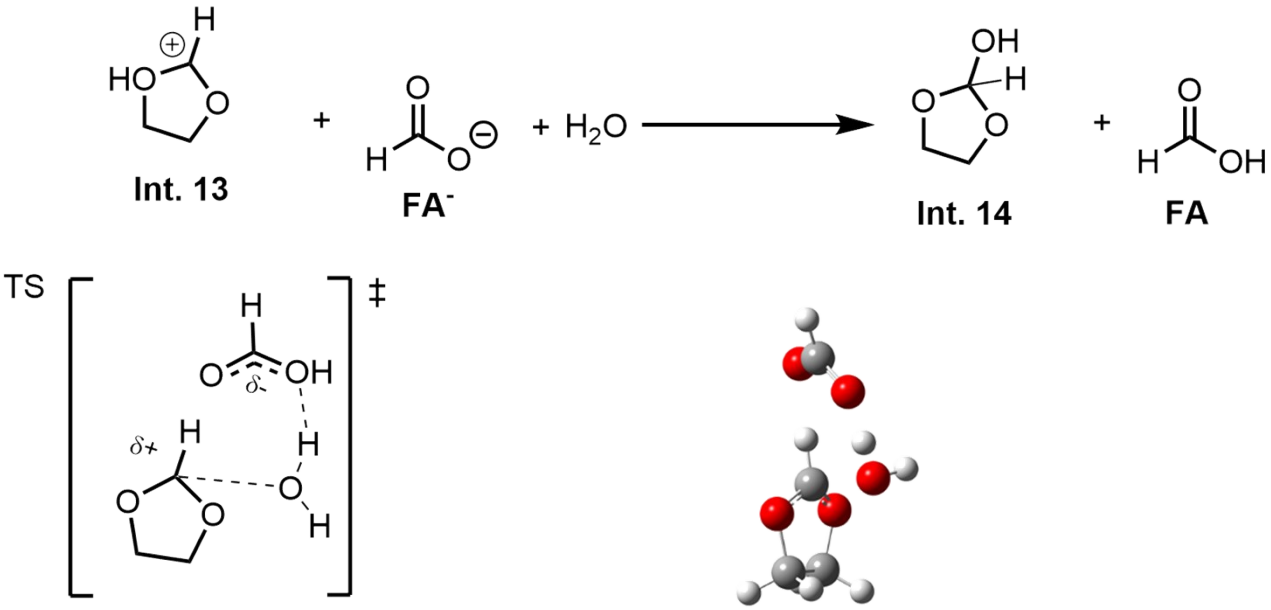
Coordinates of the TS (atom, X, Y, Z)	Energies
0 1 C -2.23631200 0.64076900 0.29571100 H -2.83189000 1.21548400 1.00822600 O -1.30571700 1.26876100 -0.38923400 O -2.84189000 -0.27783600 -0.42228000 O -1.36439100 -0.31968200 1.55048700 C -0.72210300 2.45880900 0.23596300 H -0.18076900 2.13701800 1.12943400 H -1.54200700 3.12519200 0.52155500 C 0.20305500 3.09156600 -0.77654500 H -0.34472600 3.39838400 -1.67422700 H 0.66242500 3.98062400 -0.32982400 H 1.00062900 2.39820100 -1.06317700 H -0.32110300 -0.36144000 1.32427800 C 1.56522600 -0.87603600 0.09967400 O 1.01779800 -1.63807100 -0.69923400 O 1.09951700 -0.28457300 1.12483600 C 3.07483600 -0.54532400 -0.12572300 C -3.99290600 -0.93630100 0.19995500 H -3.60610700 -1.61418400 0.96492700 H -4.61048100 -0.16567700 0.67272100 C -4.74048200 -1.67444000 -0.88617600 H -4.10031000 -2.42417400 -1.36387900 H -5.59788300 -2.18929500 -0.43786700 H -5.11231700 -0.98299900 -1.65019000 H -1.44320900 0.12802100 2.41738600 F 3.82803800 -0.89768500 0.95058800 F 3.26663000 0.78713500 -0.31995400 F 3.60281200 -1.17703000 -1.19653600	H= -950.07353 Hartree G = -950.14236 Hartree

Table S52 Transition state: Elimination of EtOH from int**12** to **14** using TFA



Coordinates of the TS (atom, X, Y, Z)	Energies
0 1 C 2.49370700 -0.35520300 0.42619300 H 3.46729100 0.03778000 0.70600100 O 2.59759200 -1.21999900 -0.57357400 O 1.91132000 1.11486800 -0.37848800 O 1.68509200 -0.53941100 1.45354700 C 1.48694700 -2.09963300 -0.95256400 H 1.66844400 -2.28879500 -2.01149000 H 0.54430500 -1.55955400 -0.85981200 C 1.50056500 -3.38560000 -0.15050500 H 1.32016900 -3.20974800 0.91419100 H 0.70741100 -4.04124300 -0.52947800 H 2.45925100 -3.90286600 -0.26639200 C 2.09827500 2.32684800 0.42357200 H 1.45451900 2.26201900 1.30574600 H 3.14391600 2.30774300 0.73861300 C 1.79068600 3.54695700 -0.42008300 H 0.74494500 3.55455400 -0.74681800 H 1.96543100 4.44679600 0.18173000 H 2.43977400 3.58733900 -1.30147000 C -1.29539900 0.08235000 0.11072900 O -0.85600600 -0.70116500 0.98694300 O -0.66878000 0.83236200 -0.67244800 H 0.91065600 0.99044000 -0.53497800 H 0.70152700 -0.69143200 1.22142300 C -2.84580400 0.07501500 -0.02768700 F -3.26884500 -1.12135400 -0.51338000 F -3.44990400 0.25481000 1.17111400 F -3.30961000 1.02980300 -0.85807200	H= -950.08002 Hartree G = -950.14626 Hartree

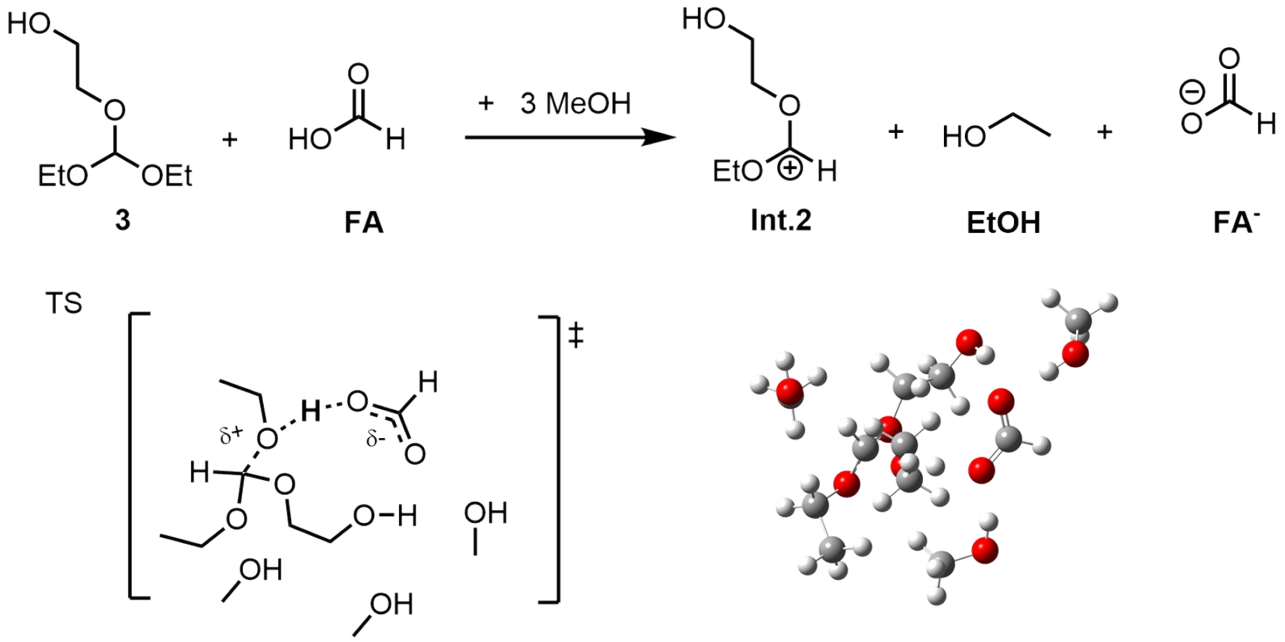
Table S53 Transition state: addition of H_2O on int**13** to int**14**



Coordinates of the TS (atom, X, Y, Z)	Energies
0 1 C -0.57339200 -0.47545700 0.15779600 H 0.37312100 -0.99575500 0.31993400 O -1.53311700 -0.54235300 1.04437600 O 0.24041400 1.27332500 0.57191800 C -2.78353800 -0.07972500 0.40997700 H -3.14564200 0.77628900 0.97767700 H -3.48435500 -0.91280400 0.46353500 C -2.33903400 0.27117700 -1.01299900 H -2.91019400 -0.22770000 -1.79385900 H -2.27387600 1.34395700 -1.19633000 O -0.96952600 -0.26874700 -1.06927500 H 1.23429200 1.16038100 0.25783000 C 3.02700500 -0.26293900 -0.19344800 H 4.07902500 -0.42981600 -0.50840400 O 2.64426200 0.95417300 -0.21370000 O 2.35147600 -1.26394100 0.13750800 H 0.27330300 1.34745800 1.54504600	H= -533.24244 Hartree G = -533.29094 Hartree

10.2.7 Computations for the screening of solvents and reagents

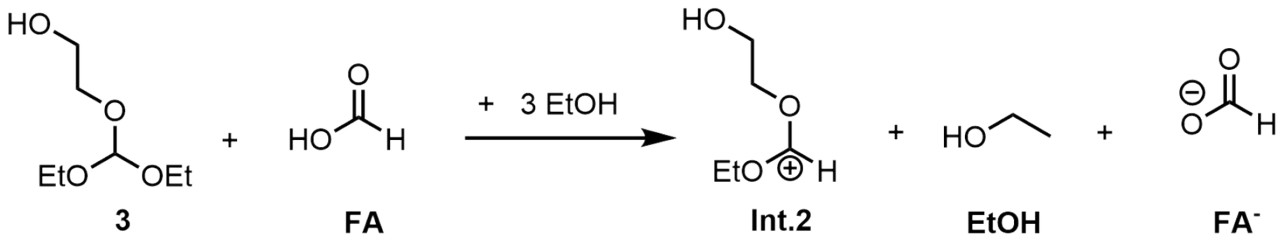
Table S54 Transition state: Activation of **3** to int**2** in acetonitrile (SMD), featuring a cluster of **3** molecules of methanol

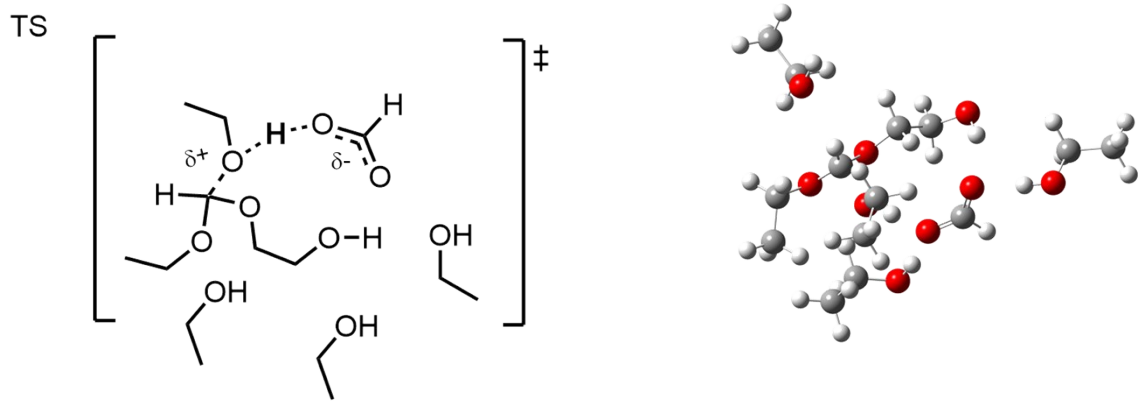


Coordinates of the TS (atom, X, Y, Z)	Energies
0 1 C -1.63839500 0.60389200 0.15820600 H -1.76558000 1.14025100 1.09691000 O -2.70545500 0.09773700 -0.41766200 O -0.80612400 -0.79454400 0.87143500 O -0.79911400 1.09975800 -0.73492400 C -3.79828300 -0.32801900 0.45949200 H -4.67461200 0.21972200 0.10526400 H -3.57387900 -0.01368000 1.48249800 C -3.99084100 -1.82595600 0.35332000 H -3.10901500 -2.36488200 0.70959300 H -4.85109100 -2.11433600 0.96954300 H -4.19564900 -2.12210500 -0.68120100 C -0.39944700 -0.72135000 2.26935300 H 0.66783700 -0.48164300 2.29943400 H -0.95579700 0.10618600 2.71753800 C -0.70872700 -2.03238900 2.96459400 H -0.16746500 -2.86252200 2.49705300 H -0.39719900 -1.96726200 4.01443900 H -1.78224000 -2.24784800 2.93342500 C 0.33162600 1.83107900 -0.18578600 H -0.02430000 2.79753700 0.18178800 H 0.75864900 1.25592600 0.63831500 C 1.36811400 1.97178900 -1.29573900 H 1.40649800 1.03999700 -1.87516300 H 1.10967600 2.78796300 -1.97585400 C 2.34475600 -1.23448300 -0.37018100 H 3.09752800 -1.71520600 -1.02206100 O 2.73031500 -0.35201700 0.43638600 O 1.14881400 -1.64315800 -0.51757200 H 0.00454900 -1.09190700 0.28953600	H= -1113.8615 Hartree G = -1113.9672 Hartree

O 2.64122300 2.28061300 -0.73502500 H 2.92527400 1.47683200 -0.25420900 C -1.38992100 -3.11809200 -1.99995700 H -2.02034200 -3.67652100 -2.69962300 H -1.54146100 -3.52809500 -0.99114800 H -1.70918100 -2.06712400 -2.00311300 C 5.97494500 0.77758200 0.21937100 H 5.58529000 1.71617300 0.64173200 H 7.06391000 0.77591900 0.33234200 H 5.73739800 0.74966400 -0.85450100 C -2.97872200 3.65395800 -0.76334100 H -3.38031400 2.79259000 -1.30166600 H -3.67028500 4.49903400 -0.87822600 H -2.00578900 3.92237300 -1.19499800 O -0.03731200 -3.26167700 -2.43015700 H 0.51319500 -2.73106900 -1.81275200 O 5.46910500 -0.36462900 0.90492800 H 4.49457800 -0.38925400 0.76433700 O -2.85653500 3.26345900 0.61042100 H -2.51013400 4.02089000 1.11213400	

Table S55 Transition state: Activation of **3** to int**2** in acetonitrile (SMD), featuring a cluster of **3** molecules of ethanol

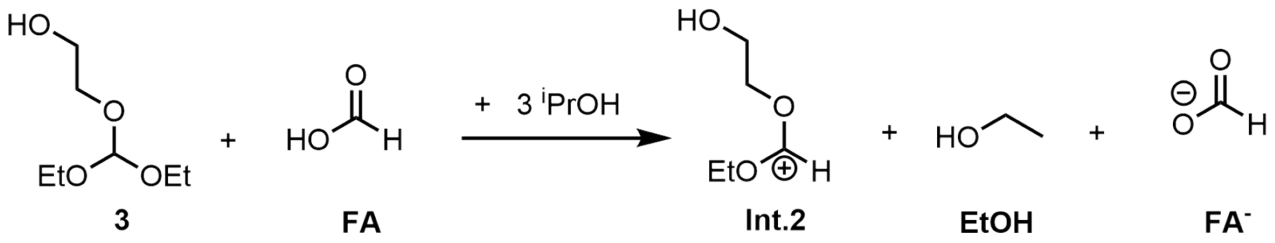


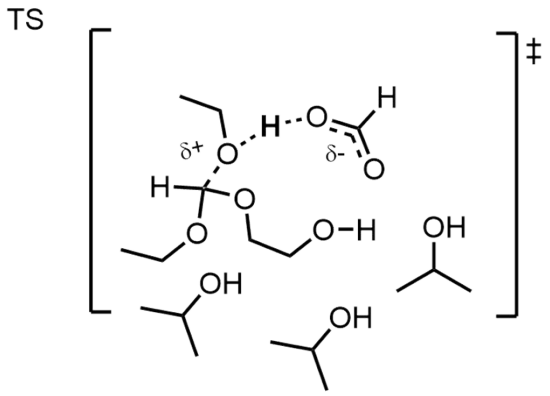


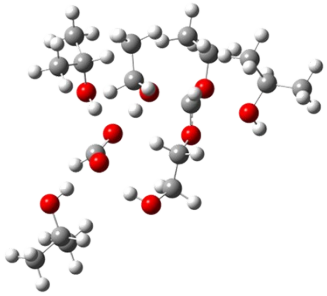
Coordinates of the TS (atom, X, Y, Z)	Energies
0 1 C -1.70078100 0.48396300 0.29393500 H -1.79095900 1.18587100 1.12086800 O -2.77683500 -0.15667600 -0.10014900 O -0.76395200 -0.73076100 1.21372000 O -0.93765900 0.82215700 -0.72999800 C -3.78486900 -0.45449900 0.92063500 H -4.70278800 0.01535500 0.55988200 H -3.48843400 0.02055300 1.85955800 C -3.93742300 -1.95366900 1.06252600	H= -1231.7495Hartree G = -1231.8654 Hartree

H -3.01066900 -2.41405000 1.41549100 H -4.73115400 -2.15964600 1.79077700 H -4.22113000 -2.40940700 0.10794900 C -0.29530200 -0.37864200 2.54722200 H 0.77881100 -0.17949500 2.48460300 H -0.80348100 0.54777200 2.83019000 C -0.61298200 -1.49845600 3.51829900 H -0.11720100 -2.42893700 3.21964400 H -0.25550500 -1.22380600 4.51846200 H -1.69274100 -1.67520400 3.57216500 C 0.20073800 1.66858500 -0.40524200 H -0.16228400 2.68130900 -0.20980900 H 0.69287200 1.27266000 0.48527000 C 1.16495000 1.61166300 -1.58498800 H 1.21317000 0.58279800 -1.96487000 H 0.83147000 2.26188200 -2.39835600 C 2.32872000 -1.29470700 -0.11458700 H 3.06576500 -1.85643600 -0.71816200 O 2.71530000 -0.26472700 0.49173300 O 1.14860200 -1.77037500 -0.10582000 H 0.02614000 -1.10995900 0.65356100 O 2.45173100 2.07121500 -1.18035800 H 2.79936400 1.39275900 -0.56644200 C -1.43216700 -3.43628800 -1.40115500 H -1.54254600 -3.72739600 -0.34545000 H -1.73358500 -2.38253700 -1.48523600 C 5.92045700 0.88223100 -0.14213600 H 5.45708700 1.85707300 0.07712800 H 5.61693200 0.59225600 -1.16009700 C -3.20065900 3.41999200 -0.77124800 H -3.67230700 2.49500500 -1.11490800 H -2.25494900 3.53975200 -1.31786400 O -0.07043900 -3.59454000 -1.81439000 H 0.47223400 -2.99514600 -1.25582000 O 5.47931000 -0.09765200 0.80183600 H 4.50144900 -0.17778700 0.71729100 O -2.93125000 3.20685100 0.62660100 H -2.47955600 3.99755800 0.97046600 C -4.11266500 4.61241500 -1.01592500 H -3.64497600 5.54309600 -0.66863800 H -4.31539200 4.71699500 -2.08961700 H -5.06852600 4.48690400 -0.49333800 C 7.43220000 0.99957900 -0.06421300 H 7.79332700 1.74955800 -0.77877500 H 7.74712600 1.30339300 0.94185600 H 7.90960700 0.04058800 -0.30082000 C -2.31917400 -4.30440900 -2.27520500 H -2.03845400 -5.36141700 -2.18798900 H -3.36871300 -4.20199900 -1.97304300 H -2.23471300 -4.01040200 -3.32884100	

Table S56 Transition state: Activation of **3** to int**2** in acetonitrile (SMD), featuring a cluster of **3** molecules of isopropanol



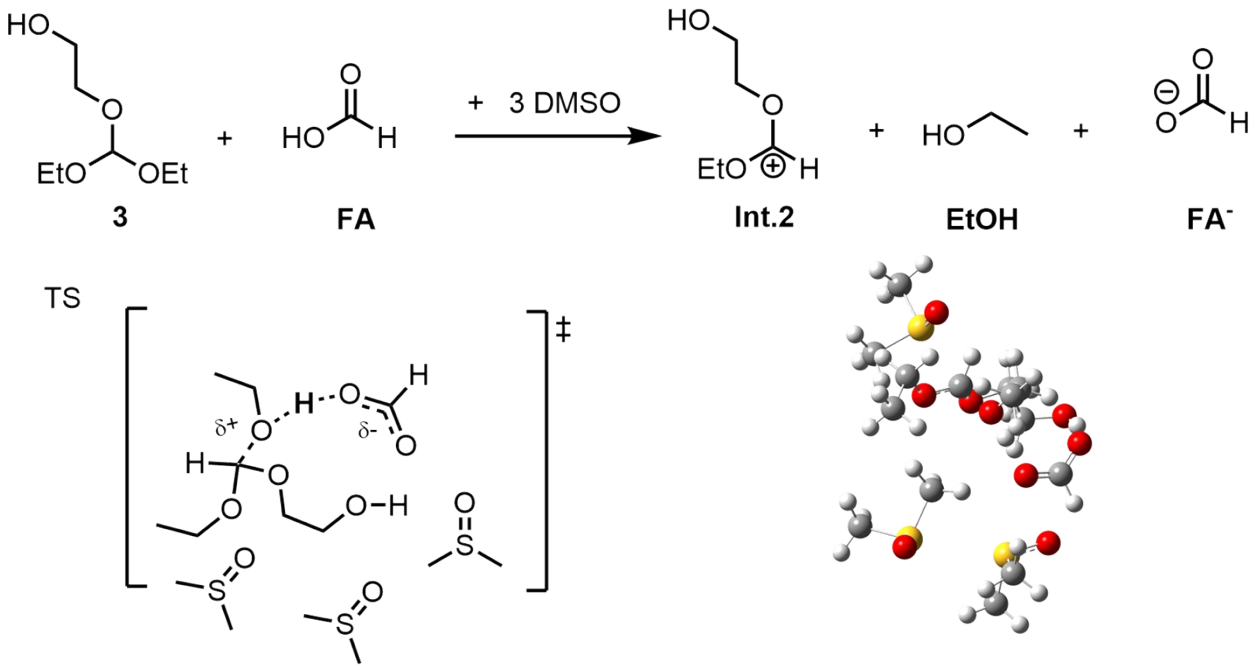




Coordinates of the TS (atom, X, Y, Z)	Energies
0 1 C 1.94290700 -0.36962700 -0.45664900 H 2.35255700 -0.71664700 0.49099200 O 2.71636400 0.31453300 -1.26831600 O 0.86005200 0.85534500 0.27894800 O 1.14204800 -1.17653500 -1.12828600 C 3.74991800 1.15913900 -0.66392800 H 4.68055500 0.85370000 -1.14664400 H 3.81233400 0.92982600 0.40208800 C 3.43611400 2.61747500 -0.92147000 H 2.49199200 2.90925700 -0.45361500 H 4.24119700 3.23186100 -0.50045400 H 3.37768000 2.81888100 -1.99683300 C 0.70625700 0.84670300 1.72941400 H -0.36048200 0.97342600 1.93146200 H 1.00762900 -0.13858600 2.10158200 C 1.53389100 1.94928200 2.35707000 H 1.23083000 2.93128900 1.98135100 H 1.38503000 1.93265200 3.44371000 H 2.60150000 1.80838600 2.15761400 C 0.31646800 -2.06500800 -0.32299300 H 0.95242100 -2.85503700 0.08475400 H -0.13161100 -1.49150600 0.48998800 C -0.78996600 -2.60104400 -1.22521000 H -1.14518300 -1.79364400 -1.87883200 H -0.42764300 -3.41976300 -1.85318600 C -2.48240000 0.46294300 -0.35643500 H -3.43574000 0.87405800 -0.73619100 O -2.52920400 -0.48942200 0.45994200 O -1.43011200 1.02295800 -0.80372300 H -0.07303800 0.83360900 -0.17716800	H= -1349.6396 Hartree G = -1349.759 Hartree

O -1.85194400 -3.11830600 -0.42863000 H -2.26494300 -2.33938200 -0.00238100 C -0.66087700 4.24535300 -0.16681700 H 0.28012200 3.68755100 -0.04921800 C -5.61954000 -2.10874800 0.31752100 H -4.95190800 -2.98245300 0.39354900 C 5.02842400 -2.28563400 0.20104300 H 5.19656500 -1.47070500 -0.51788000 O -1.33914400 3.76030100 -1.33760900 H -1.44807100 2.78919400 -1.23342300 O -5.14981100 -1.08783000 1.21136000 H -4.22372700 -0.86295900 0.96107300 O 3.68133000 -2.77947000 0.02289900 H 3.60850400 -3.14167000 -0.87761400 C -7.00970500 -2.51531900 0.78667300 H -7.40651300 -3.32412100 0.16175200 H -6.98213800 -2.86426200 1.82579800 H -7.69863500 -1.66268000 0.72633400 C -0.33213400 5.71189600 -0.40695200 H -1.25237200 6.29538000 -0.54069700 H 0.21794600 6.12736800 0.44574400 H 0.28530100 5.82894900 -1.30545900 C 5.10202500 -1.72794300 1.61374400 H 6.09031700 -1.29123600 1.79728800 H 4.34919000 -0.94657600 1.76599900 H 4.93216800 -2.52344700 2.35022200 C -5.62137900 -1.62085900 -1.13147700 H -4.61356300 -1.33409900 -1.45385800 H -5.97764600 -2.41163800 -1.80413600 H -6.28016600 -0.74958000 -1.24071600 C -1.51149600 4.04201800 1.08708900 H -1.75077700 2.98239500 1.23356900 H -0.97926700 4.39546000 1.97911700 H -2.45362600 4.59928300 1.00312700 C 6.05025700 -3.38948300 -0.05120800 H 5.95491900 -3.78636400 -1.07025600 H 7.06972800 -3.00109100 0.06401900 H 5.90935400 -4.21453400 0.65827400	

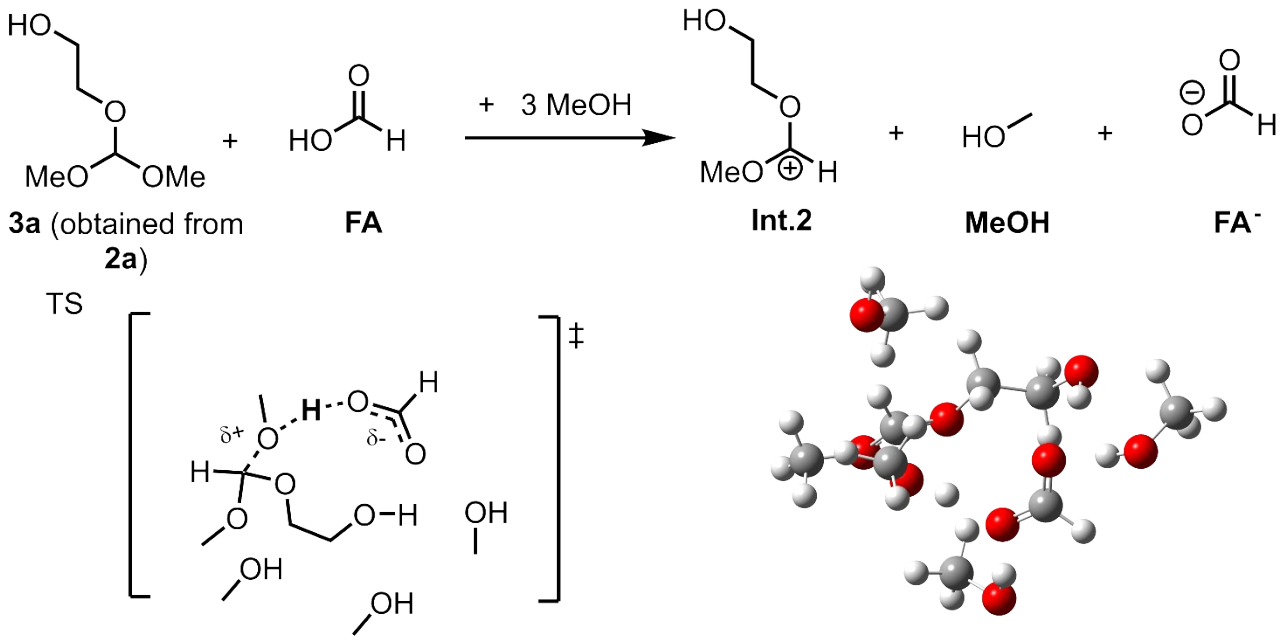
Table S57 Transition state: Activation of **3** to int**2** in acetonitrile (SMD), featuring a cluster of **3** molecules of dimethyl sulfoxide



Coordinates of the TS (atom, X, Y, Z)	Energies
0 1 C 1.94182100 -0.34265200 0.70996500 H 2.77924900 -0.99562500 0.94436500 O 2.00259100 0.91847900 1.05361600 O 0.85240900 -1.09063100 1.98752600 O 1.30591400 -0.51388100 -0.42894900 C 2.81856900 1.25774200 2.22145700 H 3.63691100 1.87071900 1.83635400 H 3.23035700 0.33868000 2.64589300 C 1.96064300 2.00991300 3.21484500 H 1.13078100 1.38949200 3.56649300 H 2.57768800 2.29165200 4.07638800 H 1.55616600 2.92500100 2.76856000 C 1.36629000 -2.22490100 2.72865200 H 0.79494600 -3.11010900 2.43087500 H 2.40764200 -2.37484400 2.42313200 C 1.27280300 -1.96497500 4.22078400 H 0.23199100 -1.80680400 4.52556000 H 1.66514700 -2.83018200 4.76988900 H 1.85862700 -1.08249100 4.50154300 C 1.30998500 -1.87779400 -0.94319800 H 2.29307300 -2.07823300 -1.37708900 H 1.11655900 -2.56242100 -0.11563100 C 0.18236000 -1.98663800 -1.96306700 H -0.69593600 -1.44573900 -1.58778900 H 0.47298200 -1.54684700 -2.92160300 C -1.83930700 -2.71287500 0.79000100 H -2.92284300 -2.87535700 0.63513500 O -1.05152000 -3.61727300 0.42661400 O -1.53205300 -1.60071000 1.33451500 H -0.12091800 -1.30823500 1.64473000 O -0.12058900 -3.35785600 -2.19880400	H= -2426.2413 Hartree G = -2426.3665 Hartree

H -0.52154900 -3.68487000 -1.36317100 C 5.63953500 0.69530000 -2.92909600 H 5.42017300 1.25525100 -3.84388000 H 6.33292900 1.24968700 -2.28904600 H 6.05537800 -0.28323500 -3.18428000 C 3.71171800 2.14975400 -1.64966600 H 2.79281200 2.17062700 -1.06075800 H 4.54173800 2.58045500 -1.08093500 H 3.56437300 2.68854000 -2.59124800 S 4.08586300 0.40675100 -2.02394800 O 4.47938500 -0.25670600 -0.69071600 C -1.14559700 1.58733500 0.06518100 H -0.94215300 1.48742300 -1.00455300 H -0.26271500 1.95113600 0.59533400 H -1.46391500 0.62662700 0.47545300 C -1.63525200 4.23906300 -0.35052100 H -2.30435600 5.09610300 -0.23417400 H -0.71427600 4.39263000 0.22074200 H -1.41321300 4.08320600 -1.41124000 S -2.50413200 2.77305100 0.29564400 O -2.65378400 2.98306200 1.81409400 C -5.48449600 0.63653500 -2.00517400 H -6.37676600 0.05548000 -1.75141400 H -5.55175700 1.65076200 -1.59927900 H -5.35476500 0.67942800 -3.09011500 C -4.58228700 -0.23980100 0.41748900 H -3.76788800 -0.64487700 1.02243400 H -4.82998400 0.77179500 0.75151900 H -5.46486200 -0.88550100 0.46890200 S -4.01059700 -0.18348200 -1.31359400 O -4.03116100 -1.63154500 -1.83447600	

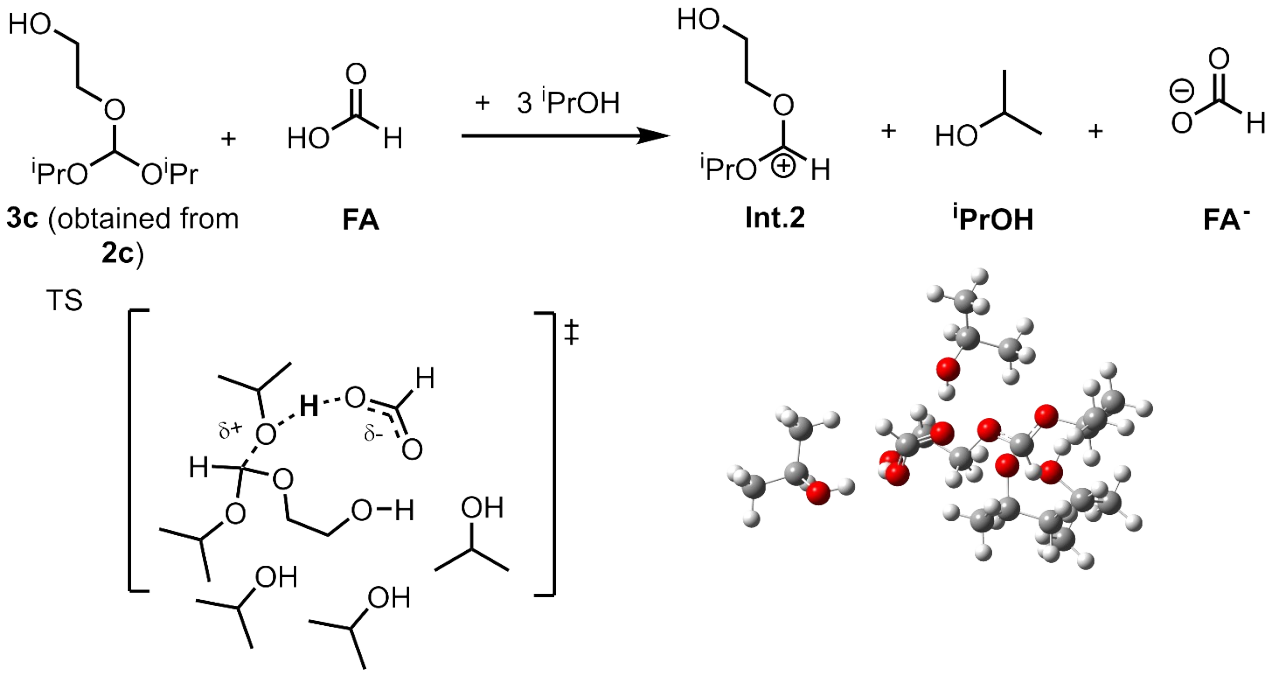
Table S58 Transition state: Activation of **3a** (derived from trimethyl orthoformate, **2a**) to int**2** in acetonitrile (SMD), featuring a cluster of **3** molecules of methanol



Coordinates of the TS (atom, X, Y, Z)	Energies

0 1 C 1.94231800 -0.12996100 0.47684500 H 2.03294800 -0.82250100 1.31262900 O 3.00047500 0.56440200 0.12281600 O 0.92290000 1.06488000 1.37331200 O 1.22040200 -0.48717900 -0.56338700 C 3.90644300 0.92751800 1.19354400 H 4.83887500 1.20846000 0.70480600 H 4.06624900 0.07444300 1.85859200 C 0.59659200 0.70425300 2.73387500 H 0.03384000 -0.23342900 2.76803300 H 1.53273000 0.60356500 3.28586400 C 0.15178300 -1.43842100 -0.28776100 H 0.60109600 -2.41853700 -0.10913500 H -0.39359300 -1.11001900 0.59909400 C -0.78479700 -1.43381300 -1.48981100 H -0.93971400 -0.40073400 -1.82769000 H -0.36268400 -2.00629500 -2.32019300 C -2.28838400 1.22395300 0.10858100 H -3.08370800 1.72356000 -0.47541400 O -2.55794900 0.13529300 0.67370000 O -1.16776300 1.82619200 0.13705300 H 0.05271000 1.29659800 0.85493400 O -2.01975800 -2.05213700 -1.13842700 H -2.44897100 -1.45395400 -0.49361400 C 1.16347500 3.15087300 -1.83919100 H 1.66543900 3.75914600 -2.59867400 H 1.70286500 3.26737800 -0.88810400 H 1.21604300 2.09659500 -2.14476400 C -5.55535200 -1.41127800 0.01238400 H -5.01274000 -2.33937500 0.24782500 H -6.62909100 -1.61968800 0.05928600 H -5.30543200 -1.10836000 -1.01535900 C 3.52279700 -2.79495400 -1.13643900 H 3.81251800 -1.79636200 -1.47083200 H 4.32424500 -3.50123900 -1.39005400 H 2.60218200 -3.09192000 -1.65568200 O -0.18385000 3.60895100 -1.74488600 H -0.63928600 3.03583300 -1.08872600 O -5.27557200 -0.37834400 0.95334100 H -4.31583900 -0.16746900 0.88625900 O 3.32667600 -2.71616500 0.28104300 H 3.10021700 -3.60340700 0.60711300 H 3.49326400 1.77672400 1.74223800 H 0.00210600 1.51483100 3.16288800	H= -1035.2687 Hartree G = -1035.3685 Hartree

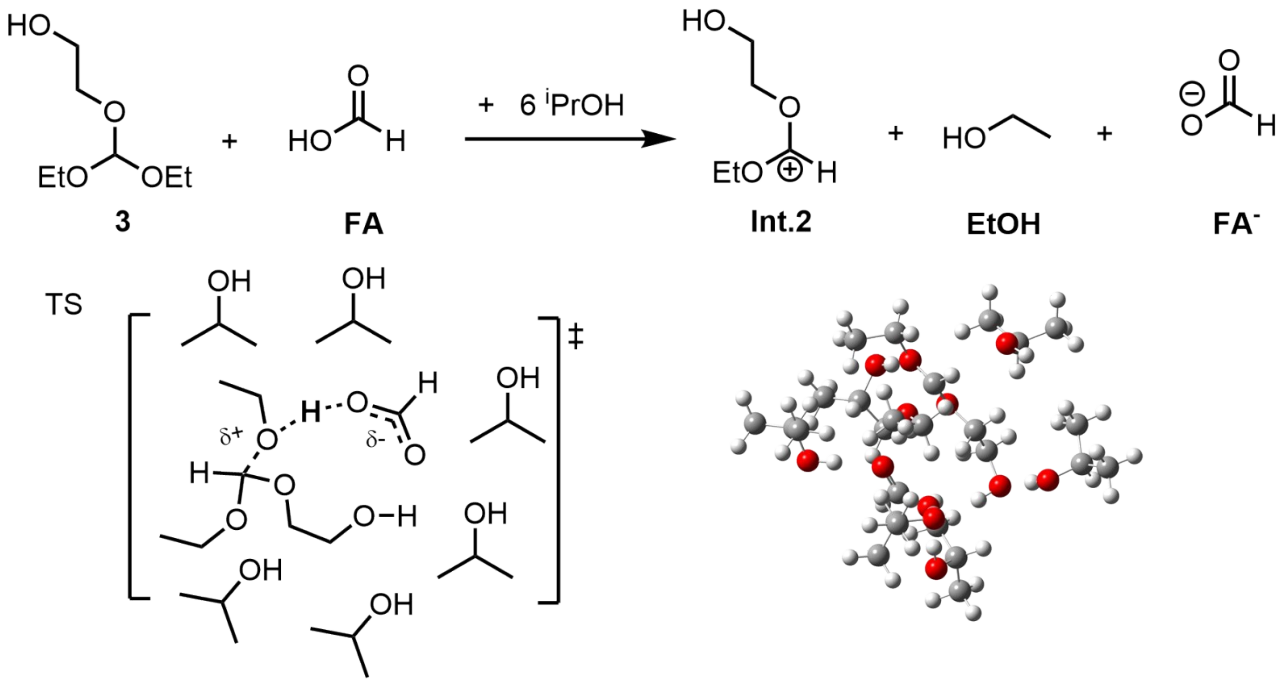
Table S59 Transition state: Activation of **3c** (derived from triisopropyl orthoformate, **2c**) to int**2** in acetonitrile (SMD) with **3** molecules of isopropanol



Coordinates of the TS (atom, X, Y, Z)	Energies
0 1 C 1.70342800 -0.03540600 -0.30389700 H 2.25905600 -0.88636400 0.08310300 O 2.37494100 1.04302600 -0.65627300 O 0.87911700 0.37984700 1.18110400 O 0.73989500 -0.28454900 -1.18493800 C 3.67530800 1.30556100 -0.01203000 H 3.92899000 0.42833500 0.58761400 C 3.52860600 2.53231500 0.87089100 H 2.75005100 2.38539200 1.62396000 H 4.47836400 2.72273900 1.38389100 H 3.27830200 3.41281500 0.26894200 C 0.96971300 -0.57547600 2.30869100 H 0.84946800 -1.57949400 1.88848800 C 2.33940500 -0.43738700 2.94925900 H 2.49270900 0.58132900 3.32127200 H 3.14680200 -0.68782100 2.25609700 C 0.01331400 -1.52733400 -0.99825600 H 0.69927900 -2.36351400 -1.15964700 H -0.38231800 -1.55902400 0.01789300 C -1.15330900 -1.52104000 -1.98040000 H -1.56500700 -0.50483200 -2.04403300 H -0.83341400 -1.82571300 -2.98071900 C -2.56559600 0.45115100 0.57104000 H -3.49455300 1.01546800 0.36692600 O -2.65085700 -0.79162900 0.73416300 O -1.50305100 1.14865100 0.62426300 H -0.10899800 0.60939500 0.95674900 O -2.14841000 -2.44929900 -1.55681300 H -2.52598000 -2.07420600 -0.73536300 C -1.13834200 4.31575200 -0.81531300	H= -1428.2321 Hartree G = -1428.3559 Hartree

H -1.42893200 3.70477700 -1.68573300 C -5.79697000 -1.98527400 -0.21242100 H -5.15669200 -2.78459000 -0.62003900 C 4.45921600 -2.57149200 -0.45710700 H 4.77469800 -1.61217100 -0.02090800 O -1.89952200 3.88798200 0.32426100 H -1.74104400 2.92422600 0.45084200 O -5.29745900 -1.60513100 1.07886900 H -4.36231600 -1.31387800 0.97147800 O 3.42342100 -2.30998400 -1.43146900 H 3.80445800 -1.76308100 -2.14113500 C -7.19961500 -2.54136300 -0.00925300 H -7.61949000 -2.88655100 -0.96145600 H -7.18427400 -3.38763600 0.68782300 H -7.86252300 -1.76796100 0.40022400 C -1.50809100 5.76671400 -1.09021700 H -1.23696200 6.39908200 -0.23465700 H -0.97816400 6.13876400 -1.97512800 H -2.58577300 5.86732700 -1.26603200 C 3.82464500 -3.42889500 0.62719700 H 4.54543000 -3.61732000 1.43088200 H 2.95089600 -2.92997100 1.06127200 H 3.50379700 -4.39383600 0.21513500 C -5.78078000 -0.80418300 -1.18315400 H -4.76461900 -0.41456900 -1.31511900 H -6.15484700 -1.10956900 -2.16882700 H -6.41601200 0.00832000 -0.80720000 C 0.35936600 4.13573500 -0.57065200 H 0.60032800 3.08800700 -0.36441300 H 0.93838800 4.44604300 -1.45023000 H 0.68128800 4.73987300 0.28754200 C 5.66519100 -3.23897700 -1.10893400 H 6.08234900 -2.60480000 -1.90184000 H 6.45410100 -3.41172600 -0.36654000 H 5.38172500 -4.20389900 -1.54755000 C 4.68773500 1.47779600 -1.13030500 H 4.41590700 2.32456800 -1.77114100 H 5.67588100 1.67365400 -0.69899300 H 4.75303900 0.57518500 -1.74719700 H 2.40285300 -1.13103500 3.79515000 C -0.16262900 -0.27650800 3.27876800 H -1.14113400 -0.42886400 2.81652500 H -0.07867500 -0.95705300 4.13336100 H -0.09460300 0.75271400 3.64995900	

Table S60 Transition state: Activation of **3** to int**2** in acetonitrile (SMD), featuring a cluster of **6** molecules of isopropanol

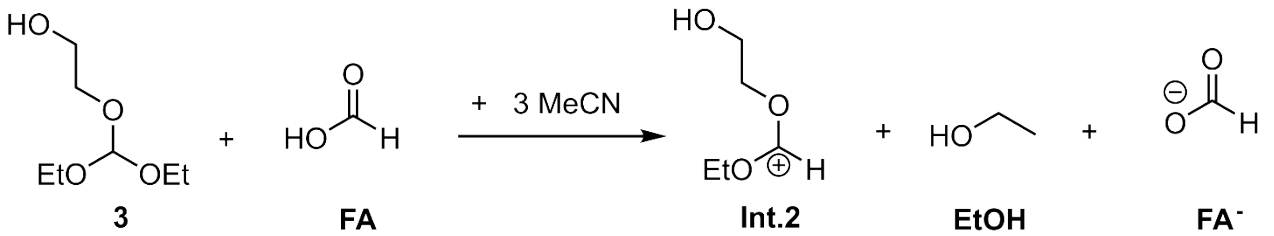


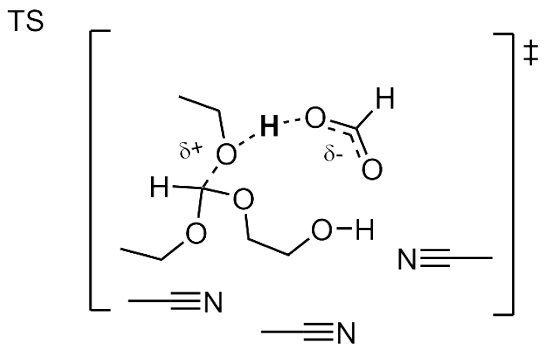
Coordinates of the TS (atom, X, Y, Z)	Energies
0 1 C 0.17405400 2.12996600 0.55718800 H 0.82261000 2.42919300 1.37831300 O -0.70438200 2.98626100 0.09401400 O -0.82507000 1.00501700 1.60631900 O 0.65862600 1.37373900 -0.39994800 C -1.24872200 3.99130500 1.02288100 H -1.05912200 4.94862700 0.53376600 H -0.67903300 3.94359400 1.95413300 C -2.72446500 3.73605700 1.23277700 H -2.89346200 2.76284400 1.69969100 H -3.12299300 4.51640900 1.89219200 H -3.26858300 3.77868100 0.28370900 C -0.27514900 0.60978500 2.89885300 H 0.07569200 -0.42284600 2.82307900 H 0.58808600 1.25706900 3.08199600 C -1.32005200 0.78402100 3.98289400 H -2.18081100 0.12992800 3.81263700 H -0.87850200 0.52628800 4.95308400 H -1.66747100 1.82226500 4.02659600 C 1.68085800 0.41885100 -0.00075600 H 2.50073500 0.95896400 0.47402500 H 1.23577300 -0.27711300 0.71213900 C 2.10576300 -0.33320300 -1.25711800 H 1.25128300 -0.42421900 -1.93583300 H 2.91290500 0.18302300 -1.78072100 C -1.15447500 -1.87462200 -0.47857900 H -1.71267300 -2.30704500 -1.32641200 O -0.03573400 -2.39288500 -0.19548500 O -1.71464000 -0.91958900 0.13041700 H -1.11273100 0.19375200 1.05844800	H= -1932.4835 Hartree G = -1932.6532Hartree

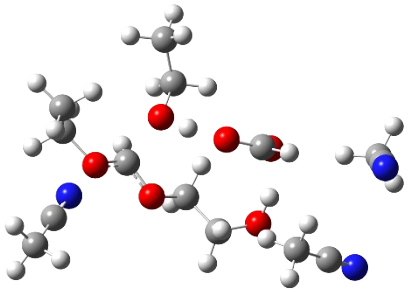
O 2.59639000 -1.62826900 -0.90036300 H 1.81060000 -2.13192900 -0.60202500 C -4.96813100 0.50196800 0.27208100 H -4.38693800 1.36021700 -0.09827700 C 0.98203400 -4.24360500 -3.02166200 H 1.98725100 -3.91543000 -2.71311900 C 3.25163900 3.61731300 -0.90116500 H 3.22838400 2.58553000 -1.28052500 O -4.47420200 -0.69535600 -0.34686300 H -3.50787500 -0.75559000 -0.17739400 O 0.24973300 -4.65227600 -1.85401200 H 0.16506700 -3.87919800 -1.25291900 O 2.85173000 3.60007900 0.48957100 H 3.56023100 3.16743400 0.99858100 C 1.11983100 -5.46844400 -3.91480000 H 1.71384100 -5.23052100 -4.80509700 H 1.61549300 -6.28618000 -3.37826700 H 0.13169300 -5.81760900 -4.24168900 C -6.41702600 0.67124800 -0.16228900 H -7.02326100 -0.17515500 0.18597200 H -6.83922600 1.59253500 0.25626600 H -6.49093500 0.72341700 -1.25468900 C 2.21582800 4.44579300 -1.64474700 H 2.43859200 4.45224800 -2.71785300 H 1.21103300 4.03439100 -1.50699600 H 2.22094500 5.48181200 -1.28341100 C 0.28907200 -3.08361800 -3.73662700 H 0.20891700 -2.20712300 -3.08502600 H 0.85706100 -2.78725100 -4.62772000 H -0.72178000 -3.37432800 -4.05030600 C -4.82283900 0.43428600 1.79181000 H -3.77467900 0.29812500 2.07922800 H -5.18320700 1.35947000 2.25910600 H -5.40301900 -0.40647400 2.19376900 C 4.66495000 4.16916800 -1.05257200 H 5.38598400 3.56666300 -0.48595900 H 4.96898700 4.15264900 -2.10631600 H 4.71545700 5.20424800 -0.69200200 C -1.87615400 -4.16358200 2.40290600 H -1.34665300 -5.08123100 2.68972900 H -1.88161700 -4.09683800 1.30848100 H -2.91738200 -4.24352500 2.74049600 C -1.20399800 -2.94175500 3.02769500 H -1.75877000 -2.04229500 2.72252900 C -1.17713300 -3.01192800 4.54743000 H -0.63034100 -3.90362700 4.88036600 H -0.68548100 -2.12771900 4.96839700 H -2.19651200 -3.06293200 4.94761700 C 5.61174600 -0.81873700 0.90938300 H 6.02357700 -1.39460000 0.06551800 C 6.55812100 -0.93957500 2.09586800 H 6.68466600 -1.98879600 2.38729300 H 7.54353000 -0.52894900 1.84633800 H 6.16225000 -0.38654500 2.95768300 C 5.43068500 0.63458200 0.46852200 H 6.39336900 1.06611000 0.16689000 H 4.74752200 0.70918400 -0.38435800 H 5.02541000 1.23657400 1.29217800 C -2.57503700 1.49593800 -2.61320200 H -2.79949100 1.18262700 -1.58682800	

C -1.62963600 0.47565700 -3.24211600 H -1.39339000 0.75716000 -4.27650700 H -0.69458100 0.41590200 -2.67658400 H -2.08683100 -0.52103700 -3.24964100 C -3.87749900 1.63481600 -3.38746100 H -4.38700500 0.66751900 -3.45968900 H -4.55058600 2.34502900 -2.89374300 H -3.67986100 1.99534300 -4.40550800 O -1.96095800 2.80268500 -2.56785600 H -1.39327800 2.83517800 -1.77904000 O 4.36157600 -1.40774500 1.30447700 H 3.78621900 -1.49445000 0.51409500 O 0.15923700 -2.81346400 2.58609100 H 0.15087500 -2.66513600 1.61607500	

Table S61 Transition state: Activation of **3** to int.**2** in acetonitrile (SMD), featuring a cluster with **3** molecules of acetonitrile





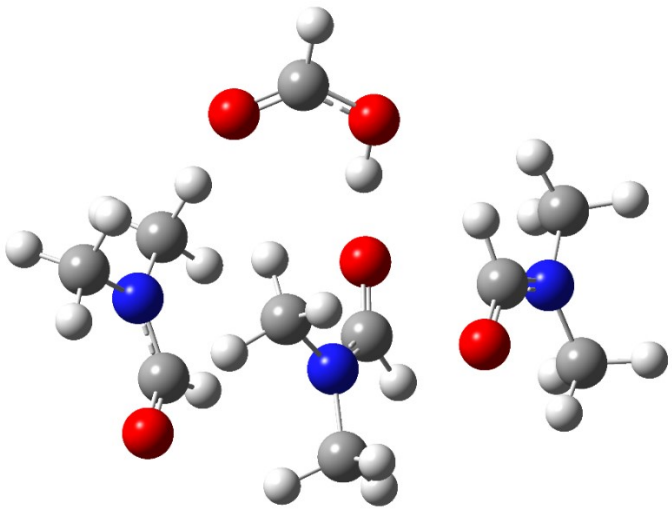


Coordinates of the TS (atom, X, Y, Z)	Energies
0 1 C -2.40555700 -0.02227400 -0.04456800 H -2.80422800 0.18746100 -1.03631800 O -3.17265000 0.11508500 0.99961300 O -1.40905600 1.59448100 -0.06432500 O -1.51486200 -0.96988800 0.10045300 C -4.29468100 1.05987800 0.89302000 H -5.18766900 0.45798300 1.07369000 H -4.32473300 1.45105400 -0.12667300 C -4.12650500 2.15224800 1.92495700 H -3.21709100 2.73101600 1.74037300 H -4.99002100 2.82567600 1.86807100 H -4.08572500 1.73180400 2.93578000 C -1.35256300 2.33747500 -1.30441300 H -0.35810800 2.20148100 -1.74324300 H -2.08755500 1.89561600 -1.98660500 C -1.66257600 3.80303600 -1.05703900	H= -1164.9909 Hartree G = -1165.1029 Hartree

H -0.93295500 4.24649700 -0.36972800 H -1.62164100 4.35409800 -2.00509600 H -2.66467300 3.92278300 -0.62995700 C -0.68766300 -1.24266700 -1.07485400 H -1.30403700 -1.76416000 -1.81187500 H -0.33927900 -0.28983600 -1.47558900 C 0.50966800 -2.06629700 -0.61328300 H 0.84091000 -1.69790500 0.36653000 H 0.24857600 -3.12362300 -0.51318700 C 1.94340500 1.12894500 0.19335300 H 2.92096800 1.22576300 0.70491100 O 1.94287300 0.72036100 -0.99465000 O 0.93660600 1.46238500 0.89387700 H -0.44077100 1.47300400 0.31010000 O 1.55260100 -1.97326200 -1.57595300 H 1.88155500 -1.04890600 -1.51449000 C -4.99094600 -2.82191600 0.77199300 H -5.56766900 -3.75043700 0.71119600 H -4.03742500 -3.02337000 1.27055200 H -5.55418000 -2.08737800 1.35633800 C -4.74611500 -2.30334900 -0.56598000 N -4.53789100 -1.87690800 -1.62686000 C 3.65109000 -1.41983800 2.12512500 H 3.67803800 -2.09688800 2.98527000 H 4.04685700 -0.44399300 2.42233500 H 2.61488200 -1.30182600 1.79476100 C 4.45783700 -1.96708100 1.04374500 N 5.10676400 -2.40087600 0.18294100 C 5.32066300 0.80277500 -1.32427800 H 5.61155200 1.63252700 -1.97719000 H 4.22908000 0.69324500 -1.34376700 H 5.78424100 -0.11998400 -1.68670100 C 5.76191500 1.07187000 0.03656700 N 6.10386700 1.28466700 1.12710700	

10.2.8 Computations for the calculation of the dissociation energies of complex catalysts-solvents

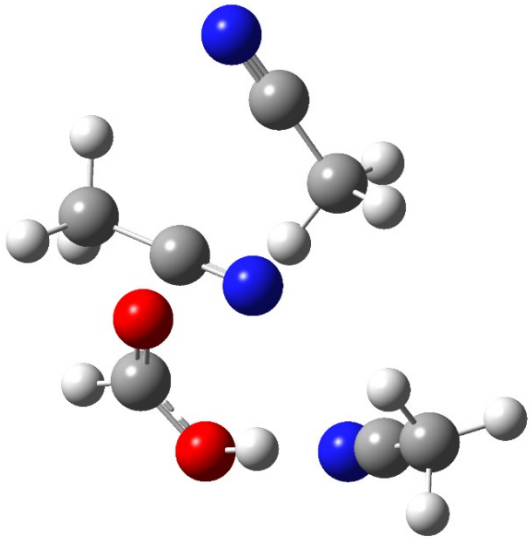
Table S62 Explicit solvation of FA in DMF, featuring a cluster with 3 molecules of DMF (computed in the gas phase)



Coordinates of the TS (atom, X, Y, Z)	Energies
0 1 C -0.33459800 3.21758500 0.73477600 O -1.45397700 2.75078100 0.82580500 O 0.68713600 2.67641800 0.08291500 H 0.42142400 1.81033500 -0.36358800 H -0.03842800 4.16819800 1.20298800 C 3.01910000 0.00850400 0.98049100 H 2.74123800 1.01716500 1.33084500 C 3.89353100 -1.21971900 -0.93984500 H 3.27782800 -1.40106400 -1.83080700 H 4.94370500 -1.16277900 -1.25252200 H 3.76860600 -2.04077300 -0.23269600 C 3.55265800 1.23697700 -1.07812000 H 2.89610800 1.16006700 -1.95292900 H 3.21337900 2.08063800 -0.47357500 H 4.58051400 1.42366000 -1.41409600 N 3.49066500 0.01560600 -0.29208100 O 2.89060600 -0.98657000 1.69055200 C -2.93713800 -1.45466300 -0.67938100 H -2.52106100 -1.62148100 -1.68978800 C -3.93149600 0.25200700 0.76371300 H -3.35808700 1.07949900 1.19288200 H -4.96157000 0.58868500 0.58756100 H -3.94355600 -0.59639100 1.44879000 C -3.16960200 0.83713500 -1.52612500 H -2.56877500 1.66816200 -1.14588100 H -2.65946800 0.40186300 -2.38891200 H -4.15064800 1.21541900 -1.84315600 N -3.32539400 -0.17266000 -0.49037100	H= -935.06127 Hartree G = -935.14854 Hartree

O -3.00765000 -2.36338700 0.14752400 C 0.35557400 -0.77963200 -0.91861700 H 0.70576400 -1.50444900 -1.66914000 C -0.45241000 -0.56679100 1.38177100 H -1.29176200 -1.11666800 1.81610000 H 0.33412600 -0.44118900 2.13343400 H -0.80635800 0.40276500 1.03593500 C 0.29668700 -2.75698400 0.50229200 H -0.64899300 -3.23384800 0.77698300 H 0.68447100 -3.22798400 -0.40469600 H 1.03454700 -2.86713800 1.30325000 N 0.06412100 -1.33780800 0.25616200 O 0.25731100 0.42461100 -1.22288200	

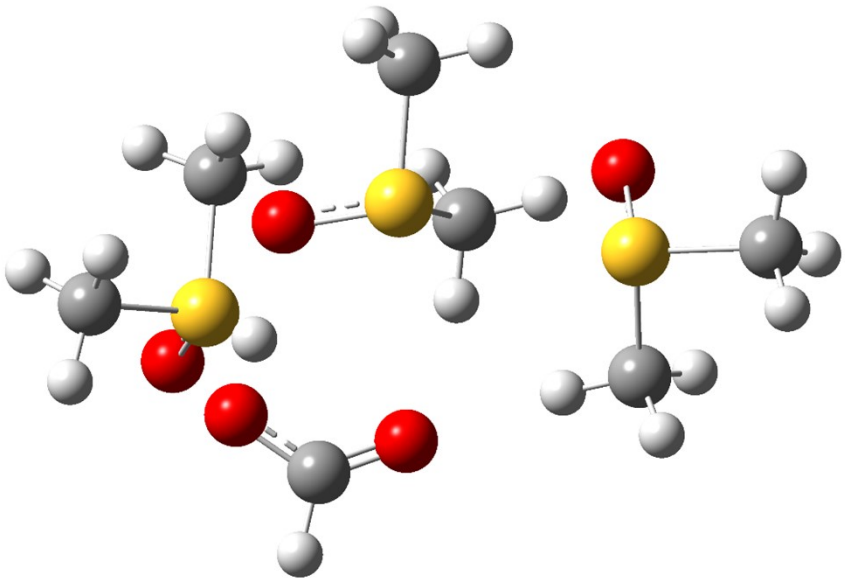
Table S63 Explicit solvation of FA in MeCN, featuring a cluster with 3 molecules of MeCN (computed in the gas phase)



Coordinates of the TS (atom, X, Y, Z)	Energies
0 1 C 1.09710400 2.78125100 -0.31812300 O 0.11456500 2.06830600 -0.40534800 O 2.31609600 2.39253000 0.03210100 H 2.33900000 1.41017700 0.19463800 H 1.07964200 3.86105600 -0.52410900 C -2.33203700 -0.02694700 1.54383700 C -1.39249800 -0.99310400 -1.48763300 C 2.29964700 -1.52834600 0.24128800 N 2.44925300 -0.39116400 0.40501800 N -3.44907700 0.08568400 1.24666200 N -0.78609200 -1.91983200 -1.13868900 C 2.09799800 -2.95638800 0.03232600 H 2.17031400 -3.48953100 0.98559300 H 1.10402700 -3.10534100 -0.40210000	H= -587.91529 Hartree G = -587.98739 Hartree

H 2.85984100 -3.34464300 -0.65096200 C -0.91997700 -0.16625000 1.88709900 H -0.31725000 0.43752800 1.20200500 H -0.74498200 0.16651800 2.91516900 H -0.61820500 -1.21284800 1.78883100 C -2.15009500 0.17928300 -1.91179800 H -3.12873100 0.17906900 -1.42298700 H -1.60835000 1.08262300 -1.61438700 H -2.28001900 0.16888800 -2.99862800	

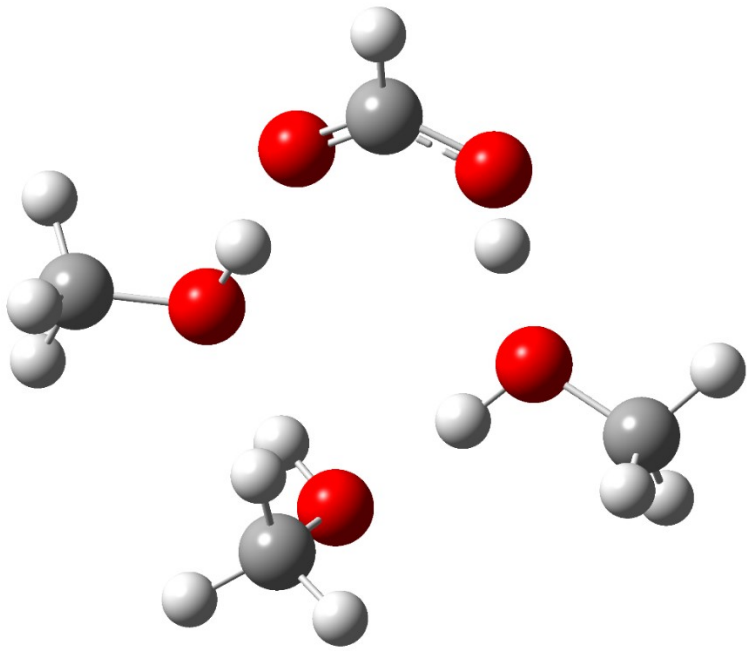
Table S64 Explicit solvation of FA in DMSO, featuring a cluster with 3 molecules of DMSO (computed in the gas phase)



Coordinates of the TS (atom, X, Y, Z)	Energies
0 1 C -0.73694100 -2.68065400 0.48833600 O 0.14567400 -2.19420000 -0.20283800 O -1.47979100 -2.03539900 1.36556000 H -1.25020500 -1.03914300 1.35832100 H -1.00457500 -3.74658400 0.44371200 C -3.42684400 1.81801800 -0.61931200 H -2.70443500 2.10126700 0.14976300 C -4.16253400 -0.21551400 1.02216500 H -4.29158600 -1.28583900 1.19361600 H -3.43587500 0.19190200 1.72886800 H -5.12629800 0.29804500 1.09125200 C 5.64578900 -0.05794500 -0.47593800 H 6.14326700 0.78680000 0.00599600 C 3.34029500 -1.47605100 -0.89808400 H 2.28498600 -1.64590900 -0.67294800 H 3.46947200 -1.20424700 -1.95025300 H 3.91630400 -2.37435500 -0.65365000	H= -1849.1657 Hartree G = -1849.2501 Hartree

O -0.95753200 0.52806800 1.24596100 C 0.81448200 2.51241700 1.08313500 H 1.77054100 2.77515100 0.62562900 H -0.00364600 3.14041200 0.72004900 H 0.87936200 2.57564500 2.17178400 S 0.46864300 0.77672400 0.67097300 C 0.24178100 0.97279400 -1.12386300 H 1.20742500 1.25107900 -1.55030700 H -0.08748100 0.00182500 -1.49680700 H -0.52069600 1.73361000 -1.30648700 S -3.52800800 -0.01307700 -0.68490700 H -3.10037500 2.15948500 -1.60512700 O -4.68028400 -0.34964500 -1.62386600 S 3.92486900 -0.09325500 0.14104200 O 3.26564300 1.17671200 -0.40622100 H 6.15040100 -0.99152700 -0.20868700 H 5.63265000 0.08638700 -1.56015600 H -4.42314300 2.21703900 -0.40569800	

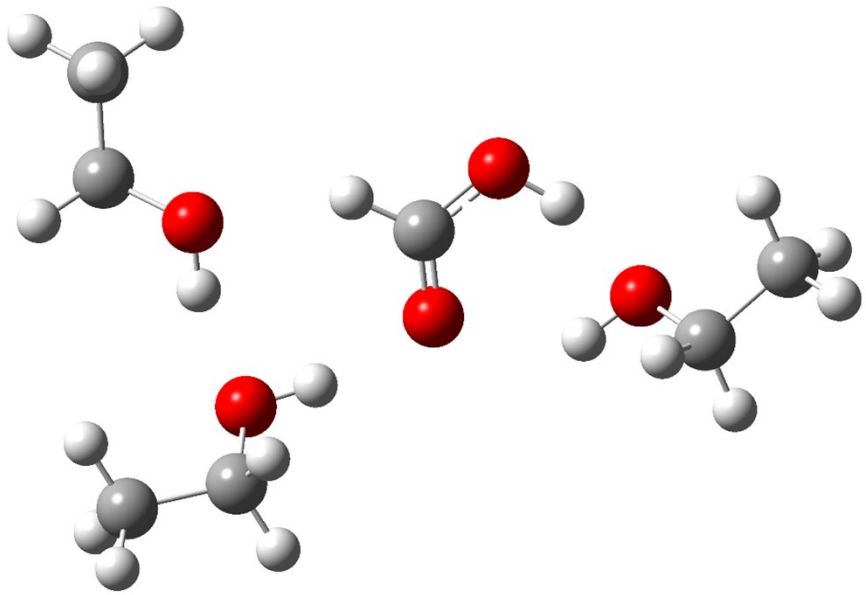
Table S65 Explicit solvation of FA in MeOH, featuring a cluster with 3 molecules of MeOH (computed in the gas phase)



Coordinates of the TS (atom, X, Y, Z)	Energies
0 1 C 0.60306400 2.50150900 0.48977700 C 2.96275000 -1.23232600 -0.55485900 H 2.95661600 -2.09327000 -1.23370900 H 3.77111600 -0.55655100 -0.84544800 H 3.13958500 -1.57975500 0.47210000 C -0.57750400 -2.14781500 1.37232700 H 0.24109900 -2.76665600 1.74951800 H -0.55605300 -1.17519600 1.88352200 H -1.52801900 -2.64969000 1.59491500 C -3.36841500 0.21179500 -0.40995300 H -3.77569100 1.11166400 -0.88768400	H= -536.80763 Hartree G = -536.87201 Hartree

H -3.95547500 -0.65357500 -0.72811100 H -3.44525500 0.31763600 0.68072300 O -2.02300300 -0.01855400 -0.82137700 H -1.46257300 0.73235600 -0.52988000 O 1.73931300 -0.50620800 -0.65867100 H 0.97058900 -1.10261800 -0.44193200 O -0.39272000 -2.00422200 -0.03436900 H -1.09628300 -1.39540400 -0.37925900 O -0.50584100 2.04491400 0.24758500 O 1.75934700 1.90168600 0.32216400 H 1.66966900 0.95751800 -0.05944100 H 0.73453100 3.51362800 0.89826800	

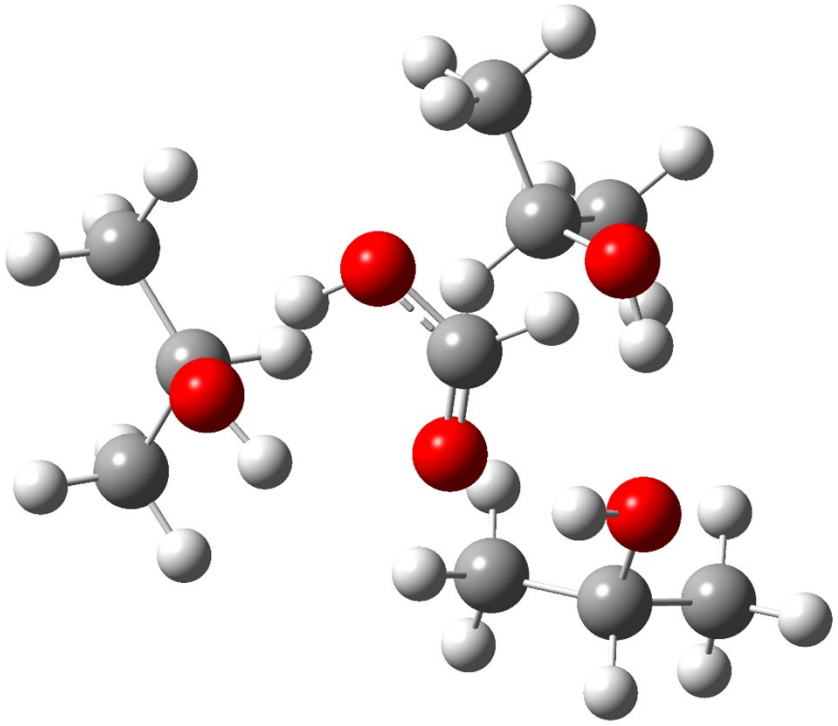
Table S66 Explicit solvation of FA in EtOH, featuring a cluster with 3 molecules of EtOH (computed in the gas phase)



Coordinates of the TS (atom, X, Y, Z)	Energies
0 1 C 0.68020000 0.82862700 -0.15049000 C 4.46946100 -0.64574800 0.28890600 H 4.87247700 -1.58709500 -0.10653200 H 3.89454600 -0.87242100 1.19806500 C -3.64026300 1.53702800 -0.21919600 H -3.65813300 1.54464700 -1.32027500 H -4.51271300 0.95788200 0.12274500 C -1.84628400 -2.58397400 0.28050700 H -1.42393300 -2.24919600 1.23954500 H -1.28392200 -3.47001100 -0.04770600 O -1.72011200 -1.54591300 -0.69761400 H -0.78260500 -1.25672900 -0.74022800 O 3.60388700 -0.05409200 -0.69721900 H 2.83419200 -0.63636400 -0.85462200	H= -654.67908 Hartree G = -654.75507 Hartree

O -2.43689600 0.93661000 0.25148500 H -2.35581100 0.02606900 -0.11559400 O 0.80677900 -0.33471200 -0.53832200 O 1.68807200 1.66506600 0.02018700 H 2.54393600 1.19297100 -0.21541300 H -0.29682800 1.26895000 0.08694700 C -3.31979000 -2.91830500 0.43790300 H -3.74498900 -3.23685500 -0.52017200 H -3.45305800 -3.72806100 1.16479600 H -3.87879400 -2.04411900 0.79078700 C 5.58834200 0.33500600 0.58782500 H 5.18902700 1.26956100 0.99776500 H 6.28072400 -0.09337600 1.32139700 H 6.14800000 0.56873400 -0.32401200 C -3.71585100 2.95737300 0.31695600 H -2.86130500 3.54725700 -0.03398700 H -4.63718900 3.44833500 -0.01881200 H -3.70235900 2.95410800 1.41270400	

Table S67 Explicit solvation of FA in iPrOH, featuring a cluster with 3 molecules of iPrOH (computed in the gas phase)



Coordinates of the TS (atom, X, Y, Z)	Energies
0 1 C -0.55673800 0.60477000 2.31795900 C -2.49669100 -0.93046200 -0.75342100 H -1.52439200 -0.46539800 -0.96987900 C 0.62220400 1.89666600 -0.79657900 H 0.11551800 0.92326200 -0.91673600 C 2.70849300 -1.68782200 0.20079800 H 2.86376000 -2.56782200 0.84419000 O 2.40335300 -0.56444000 1.03982500	H= -772.56725 Hartree G = -772.64872 Hartree

H 1.57290300 -0.73907100 1.53005400 O -2.64356700 -1.01365300 0.68540900 H -1.84897100 -1.44553500 1.05581100 O 1.26648700 1.92812000 0.47652100 H 1.85514300 1.14524200 0.54743800 O -0.20685200 -0.54749800 2.06796600 O -1.74543300 1.10292700 2.03345500 H -2.26952200 0.40762900 1.52871600 H 0.08824500 1.33285200 2.81595800 C 4.01264200 -1.36472800 -0.51509400 H 4.80202500 -1.14449100 0.21059900 H 4.33227000 -2.20956500 -1.13554100 H 3.88762600 -0.48845900 -1.16218900 C -3.61113200 -0.02451400 -1.25393400 H -3.53641600 0.97172400 -0.80506600 H -3.55097900 0.08542600 -2.34214300 H -4.58939800 -0.44840400 -1.00008700 C -0.43057300 2.99828100 -0.79695500 H 0.04948700 3.97581800 -0.67021700 H -0.98597400 3.00436300 -1.74234600 H -1.13730500 2.85407000 0.02598600 C -2.53803000 -2.32662100 -1.36502300 H -2.41044800 -2.27279800 -2.45261200 H -1.73454000 -2.95652600 -0.96499100 H -3.49700100 -2.81020100 -1.14770800 C 1.56176300 -1.98093600 -0.76849800 H 1.78703100 -2.86241400 -1.38101500 H 0.63142900 -2.17577600 -0.22286100 H 1.39525100 -1.12847900 -1.43724600 C 1.63402200 2.05949100 -1.93248300 H 2.38917400 1.26528000 -1.90206300 H 1.13743500 2.01849100 -2.91039500 H 2.14998100 3.02238600 -1.84169000	

11 Mechanistic study of dynamic covalent exchanges toward orthoesters (DCE)

11.1 Mechanism of DCE sequence toward the formation of 3, 4, 5, 6, 7, 10 and 11

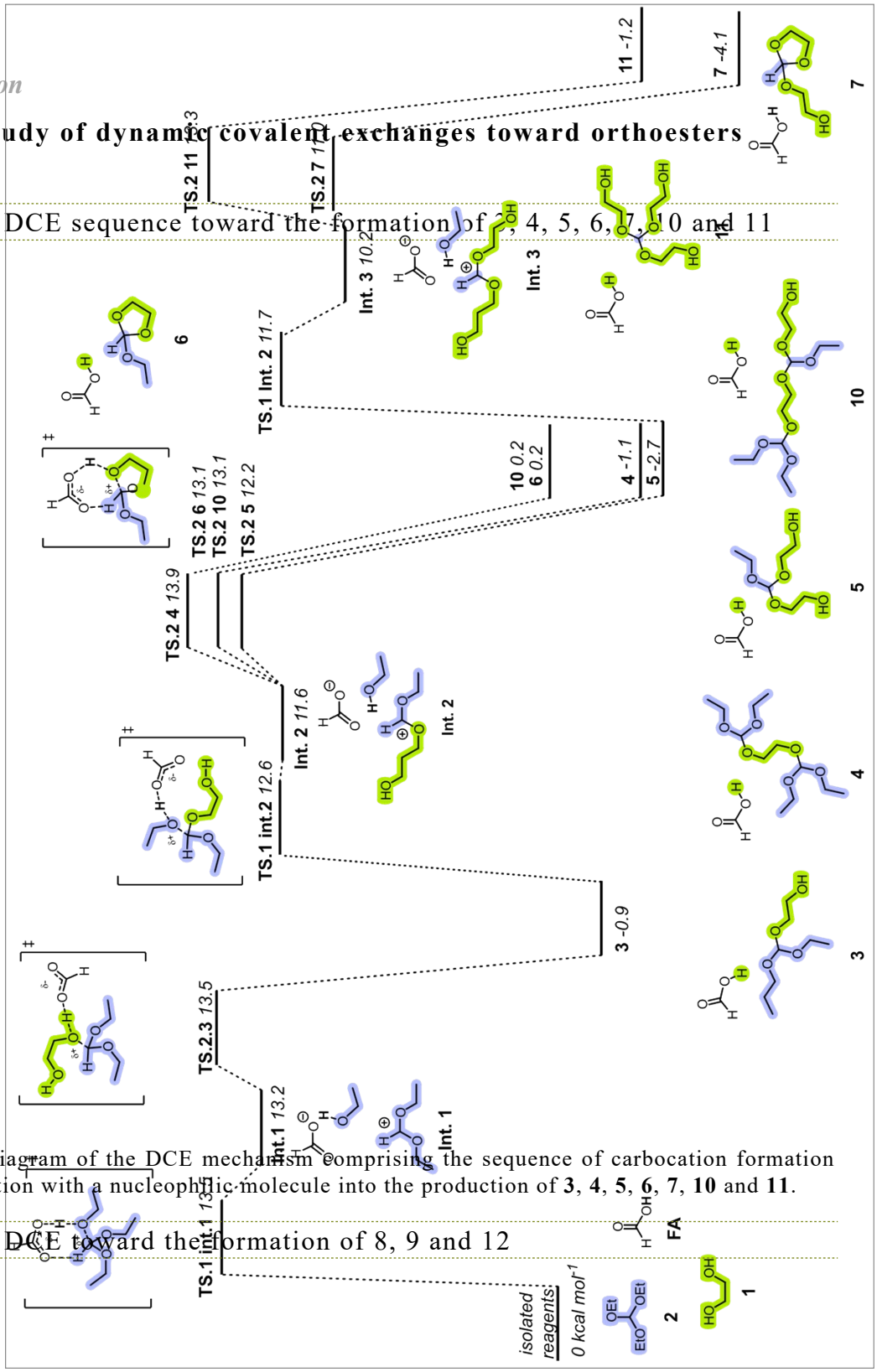


Figure S53 Energetic diagram of the DCE mechanism comprising the sequence of carbocation formation and subsequent substitution with a nucleophilic molecule into the production of **3**, **4**, **5**, **6**, **7**, **10** and **11**.

11.2 Mechanism of DCE toward the formation of 8, 9 and 12

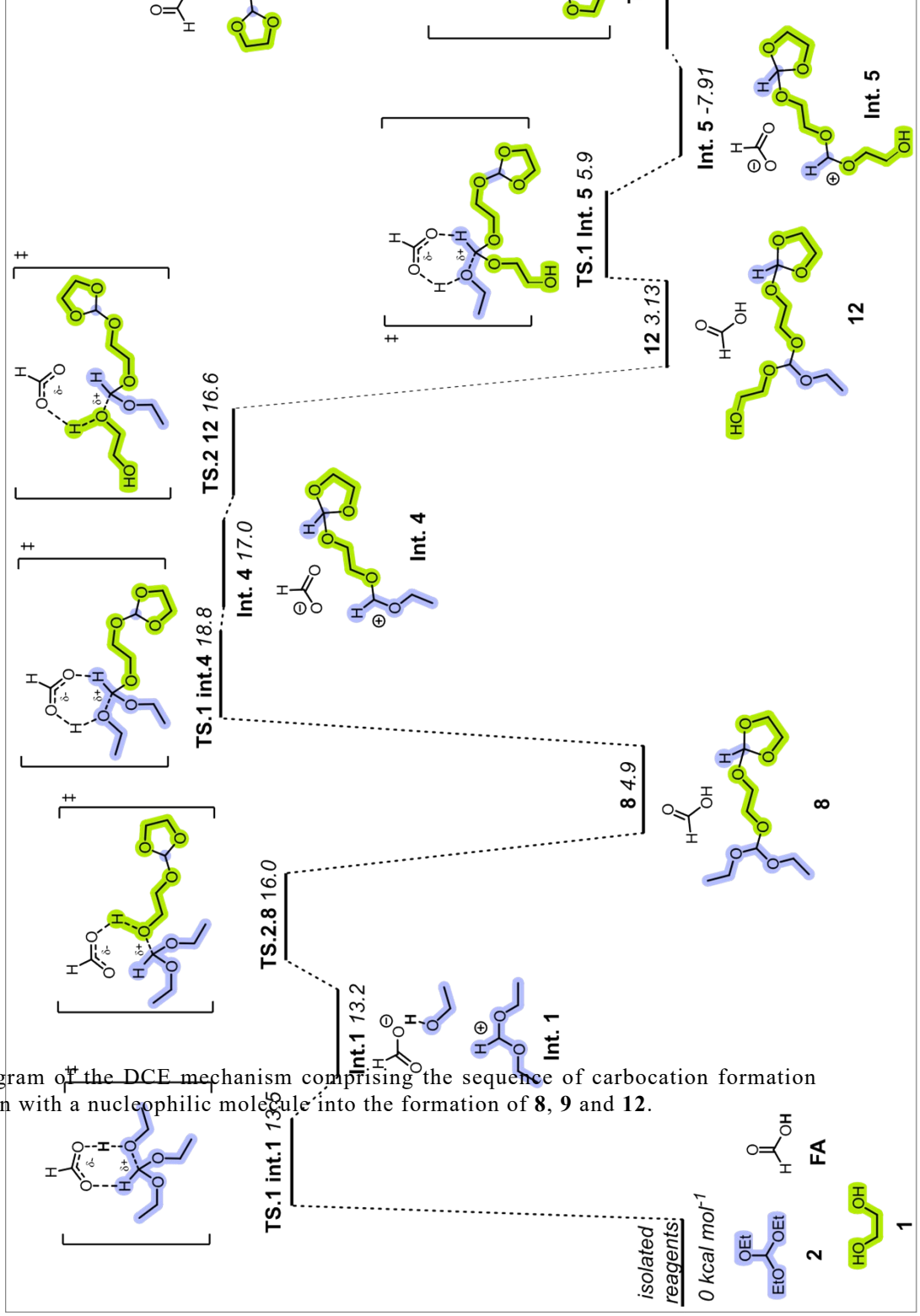


Figure S54 Energetic diagram of the DCE mechanism comprising the sequence of carbocation formation and subsequent substitution with a nucleophilic molecule into the formation of **8**, **9** and **12**.

11.3 DFT computations on the screening of catalysts

Computational analysis identified the acid-mediated formation of carbocation intermediates as the rate demining step (RDS). Therefore, variations of the acid catalyst offered a straightforward way to modulate this step. The effect was evaluated first using DFT to compute the transition state for key compound **3** in presence of a selection organic acids (see below, Figure S58). The activation barriers ($\Delta G^{\ddagger}$) and Gibbs energies (ΔG°) for the formation of **int. 2** decreased linearly with decreasing pK_a of the acid as a result of the greater proton exchange ability between the acid and substrate. Experimental data was collected using various organic acids including acetic acid (AA), pimelic acid (PA), benzoic acid (Bz), succinic acid (SA), oxalic acid (OA), trichloro- and trifluoro- acetic acid (TCA and TFA). Analysis of the data obtained focused on the conversion of **2b** and formation of **3** and **6** after 45 min.

Use of AA (pK_a = 4.76) or PA (pK_a = 4.71) resulted in similar $\Delta G^{\ddagger}$ (17.7 vs 17.4 kcal mol^{-1}) and product distributions, with ca. 41% conversion of **2b** after 45 min, mostly due to the formation of **3** (ca. 30%) and modest amounts of **6** (>5%). Using more acidic catalyst Bz (pK_a = 4.20), a significantly increased the conversion of **2b** (69%) and formation of **6** (21%) was observed.

Succinic acid (SA, pK_a = 4.16) led to a higher reagent conversion and production of **6** compared to Bz, despite having a similar pK_a. A catalyst loading of 5 mol% instead of 10 mol% was used for this dicarboxylic acid to maintain the active acid loading as the monocarboxylic acids (e.g. AA, PA, Bz, and FA). To explain the increase in reactivity, the TS was recalculated considering a possible intramolecular H bonding between the catalytically involved COOH and the second COOH (**TS.SA.H**, Figure S58), which decreased the $\Delta G^{\ddagger}$ from 16.5 to 11.6 kcal mol^{-1}. A significant decrease of enthalpy variation (ΔH) was also observed for **TS.SA.H** (-4.6 kcal mol^{-1}), suggesting an important stabilizing effect of the hydrogen bond.

FA (pKa of 3.75) led to 83% conversion of **2b** and formation of 67% of **6** over 45 min. All acids tested with lower pKa than FA resulted in varying degrees of hydrolysis of **2b** and **3**, to afford ethyl formate (**13**) and 3-hydroxypropyl formate (**14**). Use of 5 mol% of dicarboxylate OA (pKa of 1.20) led to complete consumption of **2b** in less than 30 seconds, yielding 85% of **6**. A stabilization effect comparable to that of SA was observed with dicarboxylate OA (**TS.OA.H**, Figure S58), resulting in a similar $\Delta G^{\ddagger}$ value to the one obtained when using TFA, despite the greater acidity of the latter. Experiments using TCA (pK_a = 0.77) and TFA (pK_a = 0.33) led to a substantial product degradation, with more than 65% of combined **13** and **14**. The significant differences in the amount of degradation products obtained with OA compared to TCA and TFA prompted us to calculate the TS involved in the hydrolysis of **3** in presence of OA, TCA and TFA, which revealed very little differences between the three acids. An alternative explanation was investigated, relying on the availability of water. Computation of **TS.OA.H** in presence of three molecules of water showed that the conjugated base was highly solvated, limiting water availability to attack **int.2**. On the other hand, TCA and TFA resulted in more stable carboxylates that were less available to interact with water. The transition state for TFA catalysis shows a dispersed arrangement of the water molecules, more likely to promote hydrolysis. These findings strongly suggest that orthoester hydrolysis is influenced by both catalyst acidity and its water solvation ability. Hydrolysis products **13** and **14** were always produced in a 1:1 ratio, indicating that **2b** and **3** underwent hydrolysis to the same extent, which agreed with $\Delta G^{\neq}$ values obtained by DFT for these reactions.

11.4 DFT computations on the screening of solvents

Thus far, the DCE system has been studied using acetonitrile as solvent in both experiments and DFT calculations (implicit solvation). As the reaction progresses, ethanol is released, with the final solvent composition reaching a 1:13 ratio between acetonitrile and ethanol. We were interested in understanding better how differences in solvent properties impact the reaction system. A selection of metrics were selected to quantify the impact of the solvent: Hansen parameters measuring dispersion (δ_d), polarity (δ_p) and hydrogen bonding ability (δ_H) of a solvent; and donor (DN) and acceptor numbers (AN), developed by Guttman to quantify the Lewis basicity or acidity of a solvent. Aside from acetonitrile, three additional solvents were screened: dimethyl sulfoxide (DMSO), dimethylformamide (DMF) and propylene carbonate (PC). Notably, the use of ethanol as solvent cannot be pursued because the involvement of ethanol in the DCE equilibria leads to convoluted results.

Reactions using each of these four solvents were monitored for 45 min and analyzed using **model VIII** to obtain the corresponding rate constants. In parallel, DFT computations of **TS.2** solvated by three molecules of solvent were performed for DMSO, DMF, MeCN, MeOH, EtOH and ^{i}PrOH.

In aprotic solvents (DN: DMF 26.6, DMSO 29.8, ACN 14.1), hydrogen-bond acceptor interaction with the acidic proton of the carbocation and the non-hydroxylated proton of formic acid were found to stabilize the transition state, reducing the activation barriers to 12.8, 9.3 and 11.6 kcal mol^{-1} versus to 13.5 kcal mol^{-1} calculated for the unsolved system.

In contrast, alcohols solvents exhibit dual hydrogen bond donor/acceptor behavior (high values of AN and moderate values of DN). While similar carbocation occurred, stabilization of formic acid proceeded via two simultaneous H-bonds involving catalyst oxygen atoms. This resulted in lower activation barriers of 6.8, 7.2, and 8.6 kcal mol^{-1} for systems involving MeOH, EtOH and ^{i}PrOH.

Dissociation energies (ΔE) were also calculated for the solvation of the catalysts with the various solvents. Methanol and dimethyl sulfoxide gave negative values of -6.8 and -2.3 kcal mol^{-1}, highlighting the favorable formation of FA-solvent complexes. In contrast, EtOH, ^{i}PrOH, DMF and MeCN exhibited positive dissociation energies of 0.6, 2.4, 4.2 and 6.0 kcal mol^{-1}, respectively, indicating that complex formation with formic acid is energetically unfavored to different extents.

Considering both the DFT and experimental results, although DMSO provided the highest stabilization of the **TS.2** compared to DMF and ACN, its complexation with FA was also favored, reducing catalyst availability for the DCE reactions. This likely resulted in a lowered formation of alcohol by-products and thus, negatively affecting the overall reaction kinetics as experimentally observed. DMF depicted a $\Delta\Delta G^{\ddagger}$ of 3.5 kcal mol^{-1} indicating a lower stabilization of the **TS2**, but exhibited a positive value ΔE, which was experimentally translated by similar reaction kinetic than this of DMSO.

Solvent with lower δ_H and DN values such as MeCN, exhibited lower affinity for the catalyst (ΔE = 6.0 kcal mol^{-1}), thereby promoting the reaction, which is further accelerated by the consequent release of EtOH. Other solvent parameters such as London dispersion forces (δ_d) or polarity (δ_p) appear to have little influence on reaction kinetics (Figure S59).

The reaction was also performed using different orthoester reagents, including trimethyl orthoformate (**2a**) and triisopropyl orthoformate (**2c**), following the same protocol described for triethyl orthoformate (**2b**) (Figure S59). The rate constants varied depending on the reagent used and the by-product formed during the reaction, i.e. methanol (MeOH), ethanol and isopropanol (^{i}PrOH).

Triisopropyl orthoformate **2c** exhibited the highest rate constants, attributed to its by-product ^{i}PrOH, which depicted lower affinity for FA (ΔE = 2.4 kcal mol^{-1}), due to its low hydrogen bond donor ability (δ_H = 8 cal mol$^{-1/2}$) and moderate DN of 21.1. Triethyl orthoformate **2b** showed intermediate rate constants due to **EtOH** as its by-product (δ_H = 9.5 cal mol$^{-1/2}$; DN = 19.2). Trimethyl orthoformate **2a** resulted in the slowest rate due to the release of MeOH (δ_H = 10.9 cal mol$^{-1/2}$; DN = 19.0), which exhibited a high affinity for FA (ΔE = -6.7 kcal mol^{-1}). Overall, by-products and solvents that strongly stabilization **TS2.** (e.g DMSO and MeOH) were those that led to the most stable solvent-FA complexes, hence negatively affection the reaction kinetics.

11.5 Mechanism of hydrolysis for species 2b, 3 and cyclic carbocation (from cyclic species)

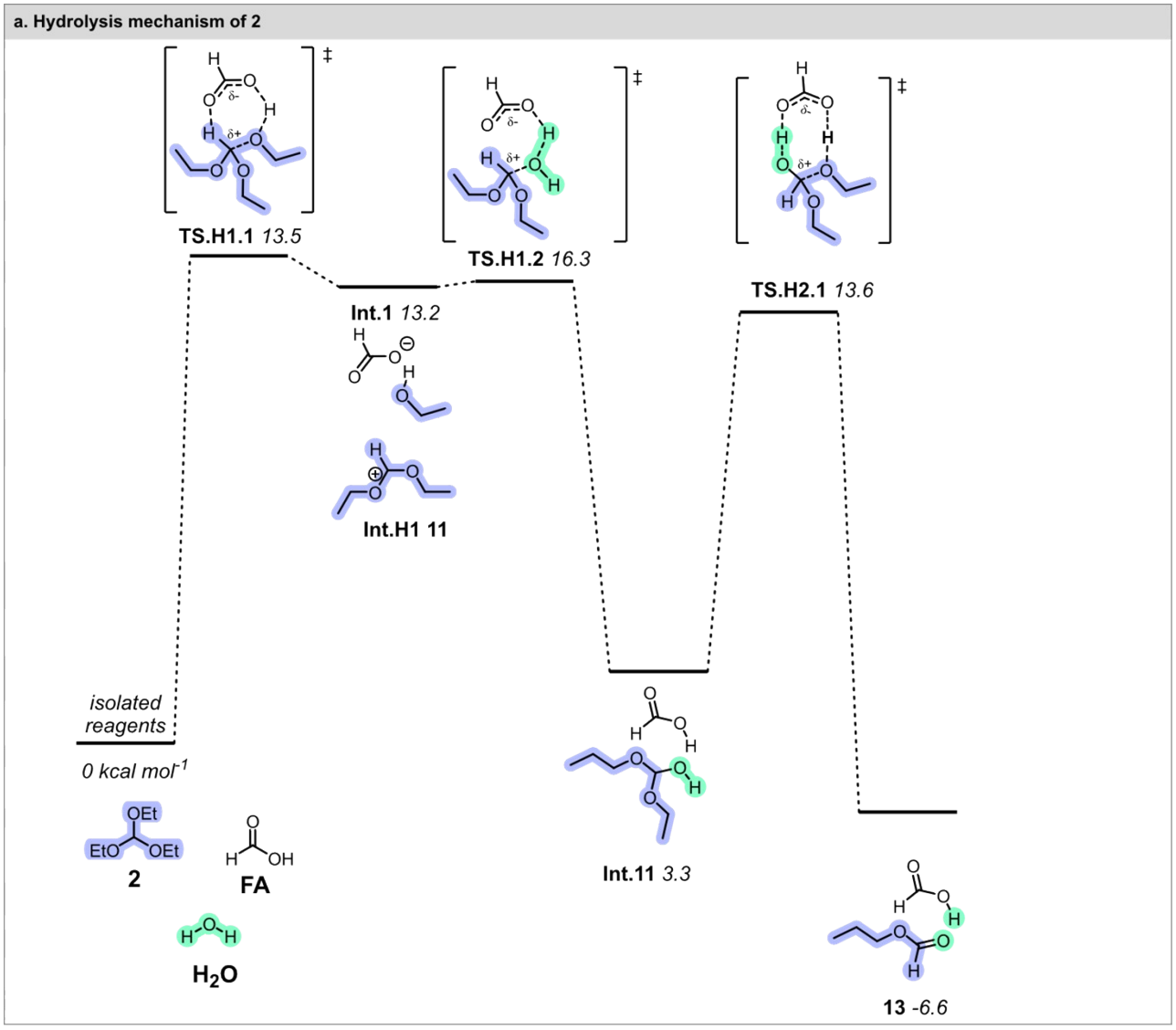


Figure S55 Elucidated mechanism for the hydrolysis of **2b**.

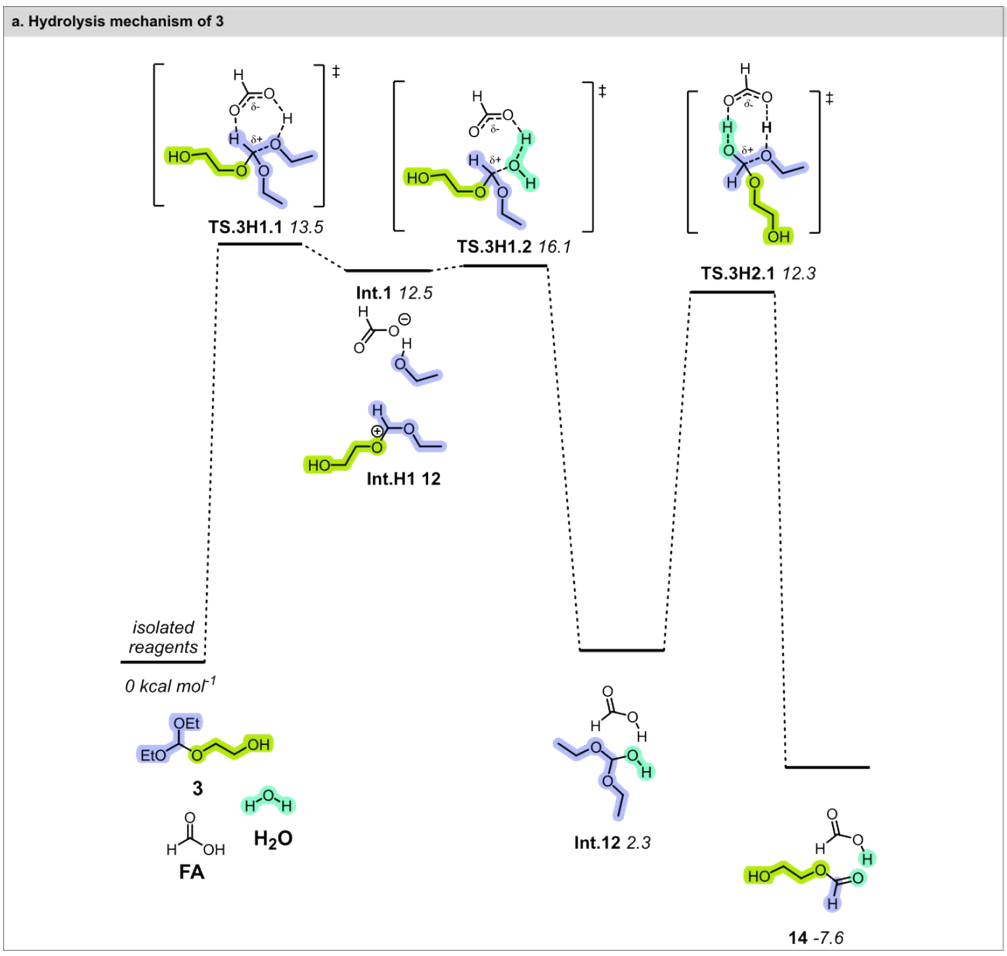


Figure S56 Elucidated mechanism for the hydrolysis of **3**.

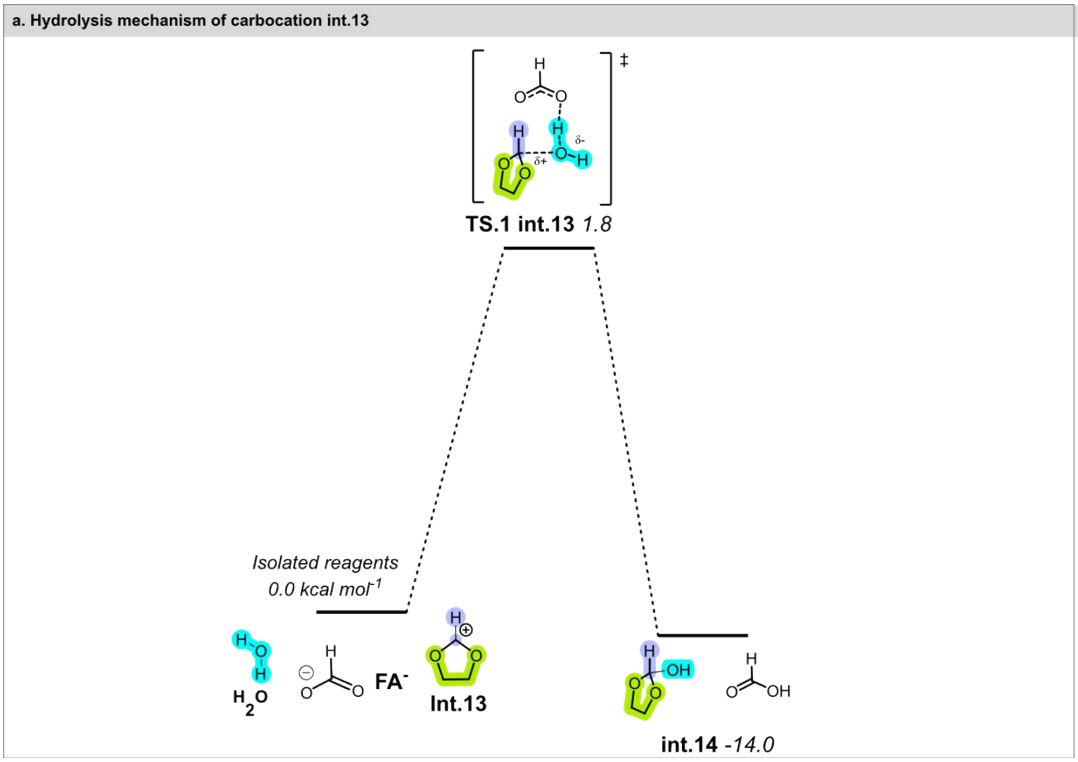


Figure S57 Mechanism of hydrolysis of carbocation intermediate **int.13**.

11.6 Mechanistic interpretation of the computational results

To complement the kinetic and mechanistic mapping of the DCE system, the influence of Brønsted acid catalysts, solvent effects and the nature of the parent orthoesters on reactivity was systematically investigated through a combination of experimental screening and DFT computations (Figures 6, 7). These parameters were found to exert distinct yet intertwined effects on both the rate and selectivity of the dynamic covalent exchange, enabling precise modulation of the reaction network. They further confirmed that the rate-determining steps (RDS) involves orthoester activation via protonation and C–O bond cleavage, consistent with the formation of a stabilized carbocation intermediate.

The catalytic performance of a panel of mono- and dicarboxylic acids was evaluated by monitoring the conversion of compound **2b** and the formation of the most abundant products (**3** and **6**) over a 45-minute period. Experimental data was collected using various organic acids (Figure S58a) including acetic acid (AA), pimelic acid (PA), benzoic acid (BA), succinic acid (SA), oxalic acid (OA), trichloro- and trifluoro- acetic acid (TCA and TFA).

The activation ($\Delta G^{\neq}$) and reaction (ΔG^{rea}) parameters for the forward step connecting primary hybrid orthoester **3** to cationic **int.2** decreased linearly with decreasing pK_a of the acid (Figure S58b) as a result of the greater proton exchange ability between the acid and substrate. However, the screening of catalysts revealed that acid strength alone was insufficient to predict reactivity trends. Carboxylic acids of comparable strength, such as AA (pK_a = 4.76) and PA (pK_a = 4.71), led to similar activation parameters ($\Delta G^{\neq}$ (AA) = 17.7 kcal mol^{-1}, $\Delta G^{\neq}$ (PA) = 17.4 kcal mol^{-1}, respectively). A modest conversion of parent orthoester **2b** (~41%), mostly to form primary hybrid orthoester **3** (~30%) and **6** as minor component (~5%), was experimentally observed (Figure S58c). Slightly increasing the acidic strength with BA (pK_a = 4.20) substantially improved the conversion (69%), with the formation of **6** in 21%. Interestingly, dicarboxylic acids featuring a short carbon backbone (C ≤ 4) such as SA (pK_a = 4.16) and OA (pK_a = 1.20), exhibited superior catalytic activity. OA led to complete conversion of parent orthoester **2b** in less than 30 s and yielded over 85% of **6**. These effects were rationalized by DFT calculations, which showed that intramolecular hydrogen bonding (HBD) between the two carboxyl groups in dicarboxylic acids significantly stabilized the transition state. When the second carboxylic acid moiety became involved in an HBD interaction with the catalytically active one, $\Delta G^{\neq}$ decreased from 16.5 kcal mol^{-1} to 11.6 kcal mol^{-1} (see **TS.OA.H** in Figure 58b). This stabilization highlights the critical role of non-covalent interactions in promoting DCE.

In contrast, stronger acids such as TCA or TFA (p*K*a = 0.77 and 0.33, respectively) led to extensive degradation of orthoesters, forming hydrolysis products, such as ethyl formate (**13**) and 3-hydroxypropyl formate (**14**), in 65% overall yield (section S11.4 in the Supporting Information). These observations underscore the need for catalytic activation that is both potent and selective, avoiding overactivation that diverts the reaction into non-productive or destructive pathways.

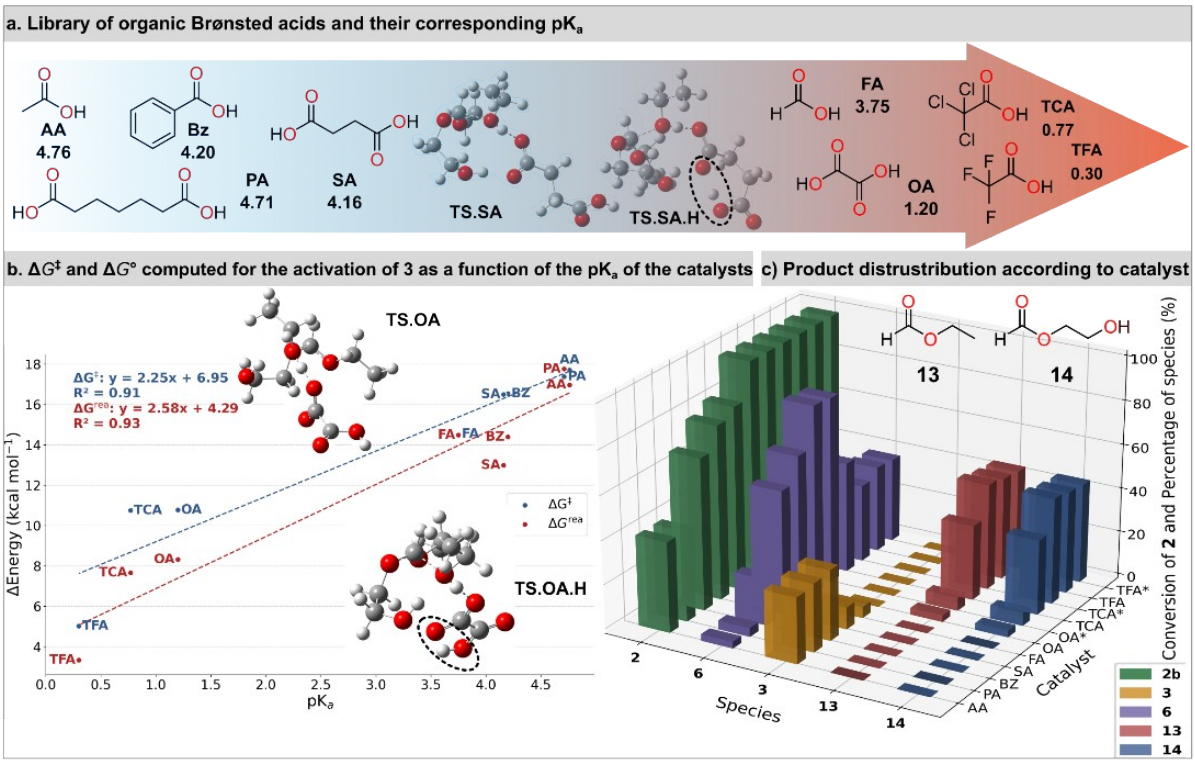


Figure S58 (a) Library of various homogeneous Brønsted acids with their pK$_a$,[33] (b) Correlation of the activation barriers and reaction Gibbs free energies with the pK$_a$ of a range of acid catalysts. Free Gibbs energies (ΔG^{rea}, in red) and activation barriers ($\Delta G^{\neq}$, in blue) plotted as a function of pK$_a$ of the catalysts for the activation of **3** into **int.2**. (c) Experimental conversion of **2b** and resulting product distribution obtained for each catalyst with a loading at 5 or 10 mol% (marked with *).

We were also interested in understanding better how differences in solvent properties impact the reaction system. One strong incentive was the natural propensity of the reaction to self-modify solvent composition. Indeed, as the DCE network expands, ethanol is increasingly released, with the final solvent composition reaching a 13:1 ratio between acetonitrile and ethanol. Several metrics were selected to quantify the impact of the solvent: Hansen parameters for dispersion (δ_d), polarity (δ_p) and hydrogen bonding ability (δ_H), Guttman's donor (DN) and acceptor numbers (AN) (Figure S59). Aside from acetonitrile, two additional solvents were screened: dimethyl sulfoxide (DMSO) and dimethylformamide (DMF). Both experimental and computational data sets using FA as a catalyst (Section S11.4 in the Supporting Information) were used to clarify the effect of solvents. Experimental kinetics (over 45 min) were analyzed using **Model VIII** to obtain the corresponding rate constants. The results indicated that solvent modulation clearly introduced an additional layer of complexity by modulating both TS stabilization and catalyst availability. This phenomenon was also accounted for in the DFT computations, where both implicit and explicit solvation (trimeric solvent clusters) were considered (Section S11.5 in the Supporting Information).

Among the aprotic solvents tested, DMSO (DN = 29.8), DMF (DN = 26.6), and MeCN (DN = 14.1) differed substantially in their influence. DFT calculations showed that DMSO provided the most effective stabilization of the carbocationic transition state ($\Delta G^{\neq}$ = 9.3 kcal mol^{-1}), followed by MeCN ($\Delta G^{\neq}$ = 11.6 kcal mol^{-1}) and DMF ($\Delta G^{\neq}$ = 12.8 kcal mol^{-1}). However, this benefit came at a cost: DMSO also formed highly stable solvation complexes with formic acid (ΔE_{diss} = -2.3 kcal mol^{-1}), which effectively reduced the free concentration of catalyst in solution. In contrast, MeCN, with a positive dissociation energy (ΔE_{diss} = +6.0 kcal mol^{-1}), preserved the catalyst availability, while still offering sufficient transition state stabilization in contrast to DMF (ΔE_{diss} = 4.2 kcal mol^{-1}). These computational results matched experimental observations (Figure S59a): reactions carried out in

MeCN, which is associated with both lower DN and δ_H, were consistently associated with higher rates and yields than those in DMSO or DMF. It is also expected that the reaction is further accelerated by the consequent release of EtOH. These effects translate through the highest yields of compound **6** under otherwise identical conditions. Other solvent parameters such as London dispersion forces (δ_d) or polarity (δ_p) appear to have little influence on reaction kinetics based on the data in Figure S59a. Optimal solvent choice must therefore balance polarity, hydrogen bonding ability, and catalyst coordination to favor productive exchange over sequestration or deactivation, hence modulating the entire DCE network.

In addition to catalyst and solvent effects, the structure of the parent orthoester itself was shown to play a pivotal role in shaping the reaction kinetics (Figure S59b). Specifically, the identity of the alcohol released during exchange, *i.e.*, methanol (MeOH, from **2a**), ethanol (EtOH, from **2b**), or isopropanol (*i*PrOH, from **2c**) had a dual impact on the system. On one hand, DFT demonstrated that smaller, more polar alcohols provided better TS stabilization: $\Delta G^{\neq}$ of 6.8 kcal mol^{-1}, 7.2 kcal mol^{-1} and 8.6 kcal mol^{-1} were computed for MeOH, EtOH and *i*PrOH (explicit solvation with a solvent trimeric cluster). On the other hand, these same alcohols had distinct inhibition behavior through catalyst complexation. MeOH, with its high hydrogen-bond donor ability (δ_H = 10.9 cal mol$^{-1/2}$, DN = 19.0), formed the most stable FA–alcohol complex (ΔE_{diss} = -6.7 kcal mol^{-1}), significantly reducing the effective catalytic activity and reducing the rate. In contrast, *i*PrOH (δ_H = 8.0 cal mol$^{-1/2}$, DN = 21.1) exhibited weaker interactions with FA (ΔE_{diss} = +2.4 kcal mol^{-1}), allowing for faster turnover despite a lower TS stabilization. Experimental results corroborated these insights: triisopropyl orthoformate **2c** yielded the highest rate constants among the three orthoester derivatives tested, followed by triethyl (**2b**) and trimethyl orthoformates (**2a**).

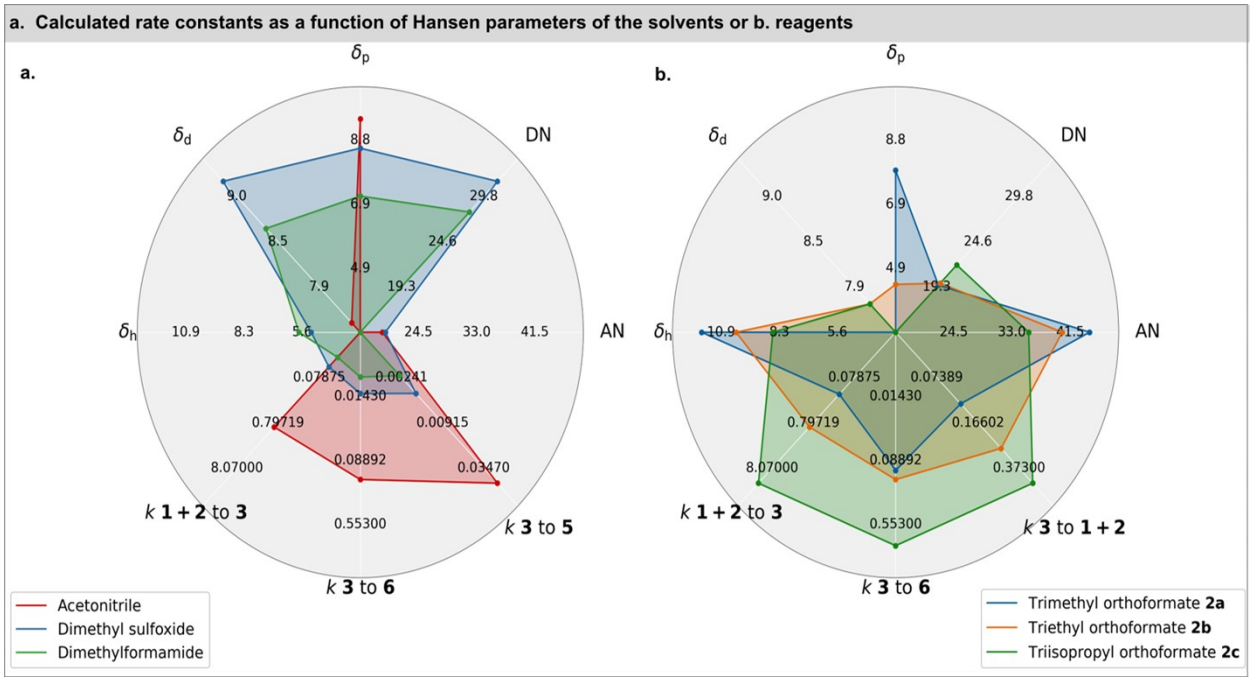


Figure S59. (a) Chart representing the calculated rate constants for the reaction of **1** with **2b** (1:1 ratio) using various solvents including acetonitrile (MeCN), dimethyl sulfoxide (DMSO) and dimethylformamide (DMF) as a function of their Hansen parameters and Guttman numbers (logarithmic scale). (b) Calculated rate constants for the reaction of **1** with **2** (1:1 ratio) using trimethyl orthoformate (**2a**), triethyl orthoformate **2b** and triisopropyl orthoformate **2c** in acetonitrile.

Figures S58 and S59 illustrate that optimal performance in DCE networks does not stem from maximizing any single parameter, such as acidity, solvent polarity, or leaving group ability, but rather from achieving a finely tuned balance among them. Catalysts featuring cooperative hydrogen-bonding motifs (e.g., OA), solvents with low catalyst-binding affinity (e.g., MeCN), and parent

orthoesters that release weakly coordinating alcohols (e.g., **2c**) consistently led to the most favorable reactivity profiles. These components collectively influence not only the rates of individual elementary steps, but also the topology and directionality of the overall reaction network. Taken together, these results establish a coherent framework for modulating DCE reactivity through rational design of medium composition. The combined effects of catalyst structure, solvent environment, and substrate identity define the accessible kinetic landscape and enable the emergence of fast, selective, and robust exchange processes. These general principles potentially extend beyond the present model system and could offer general guidelines for controlling dynamic behavior in complex molecular assemblies, supramolecular systems, and adaptive materials.

This section summarizes the mechanistic trends emerging from the computational dataset provided above.

12 Copies of ^{1}H, ^{13}C NMR spectra and fragmentation of the products observed by GC-MS

12.1 Compound 1

12.1.1 ^{1}H-NMR spectrum

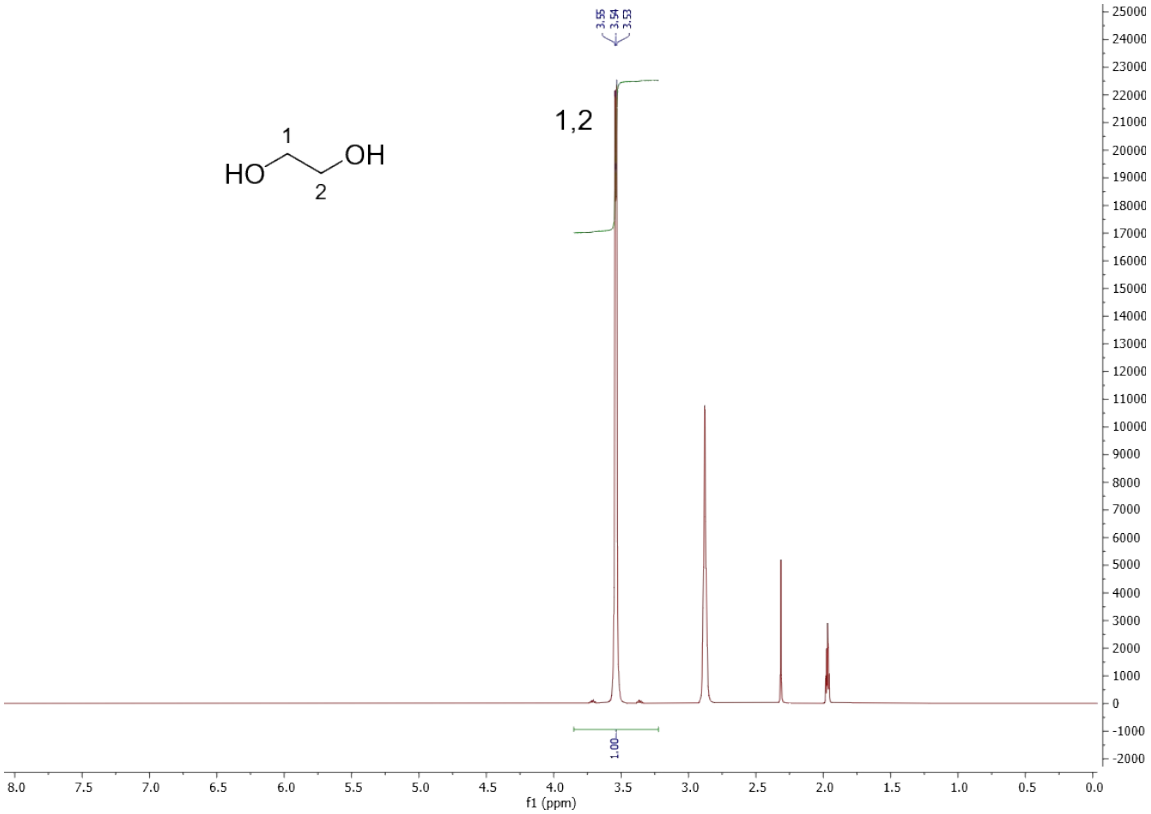


Figure S60 ^{1}H-NMR spectrum (700 MHz – CD_3CN) of **1** (éthane-1,2-diol – CAS 107-21-1).

12.1.2 ^{13}C-NMR spectrum

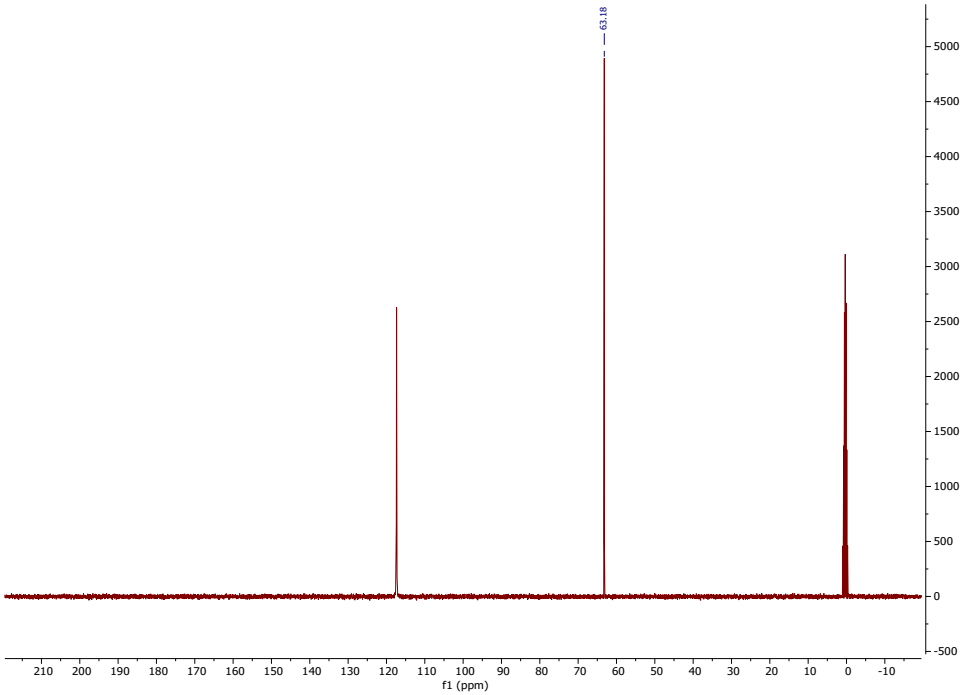


Figure S61 ^{13}C APT NMR spectrum (101 MHz – CD_3CN) of **1**.

12.1.3 Mass spectrum and fragmentation

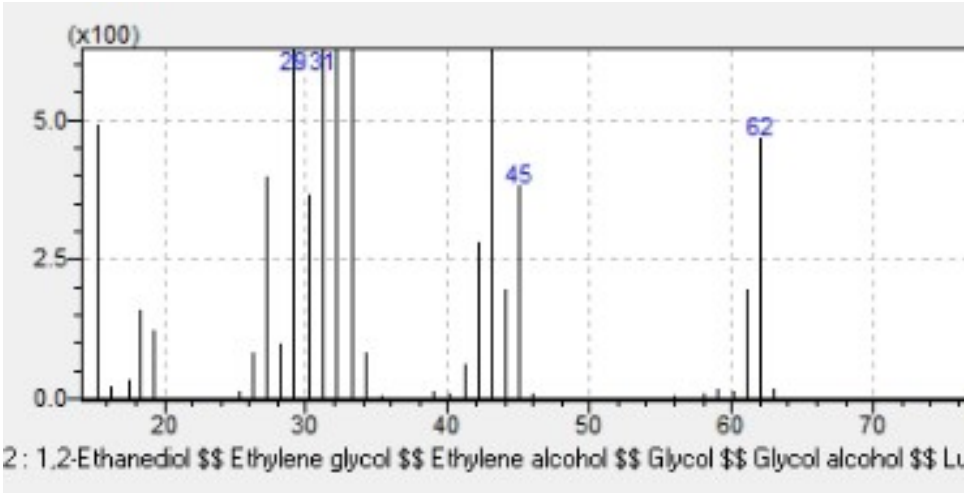


Figure S62 Mass spectrum obtained for **1.**

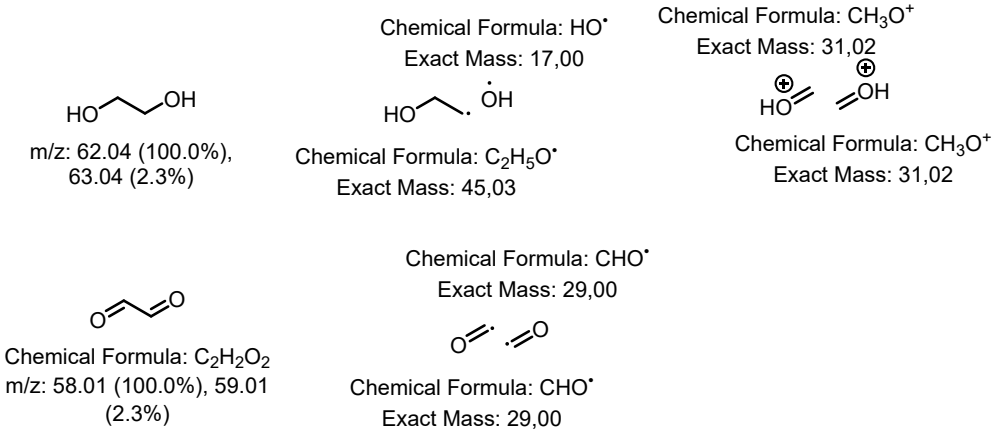


Figure S63 Fragmentation of **1**.

12.2 Compound 2b

12.2.1 ^{1}H-NMR spectrum

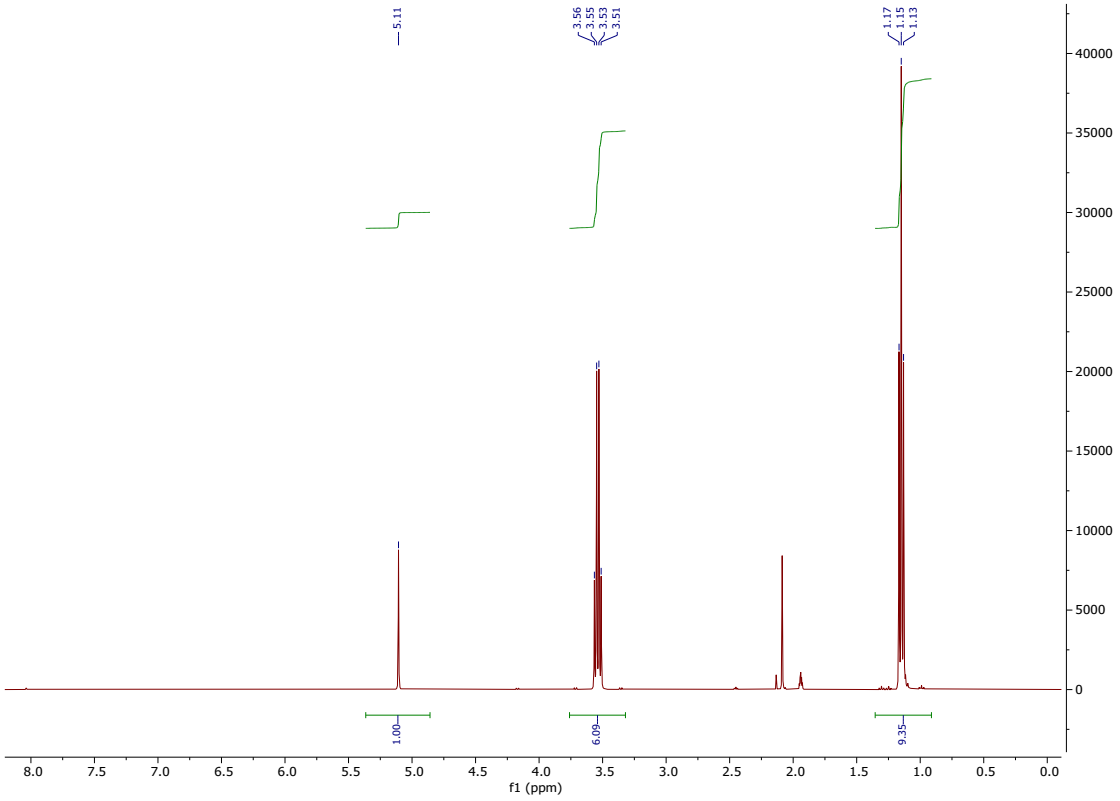


Figure S64 ^{1}H-NMR spectrum (700 MHz – CD_3CN) of **2b**.

12.2.2 ^{13}C-NMR spectrum

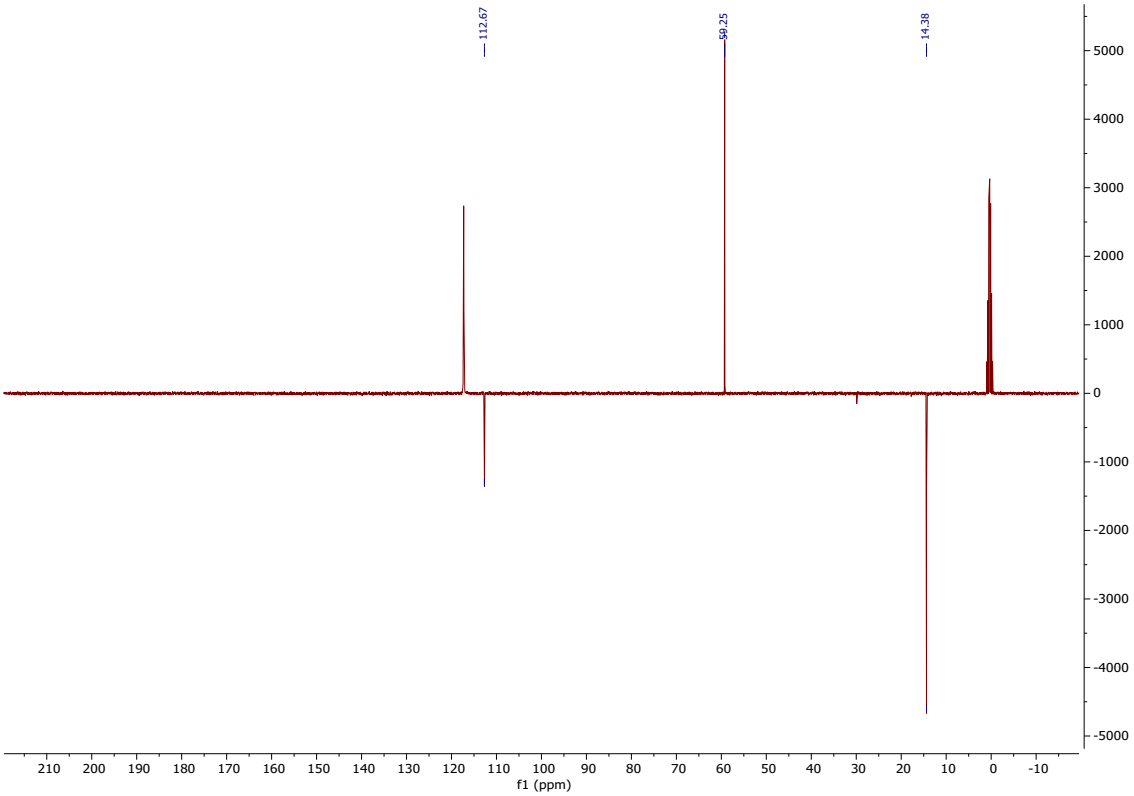


Figure S65 ^{13}C APT NMR spectrum (101 MHz – CD_3CN) of **2b**.

12.2.3 Mass spectrum and fragmentation

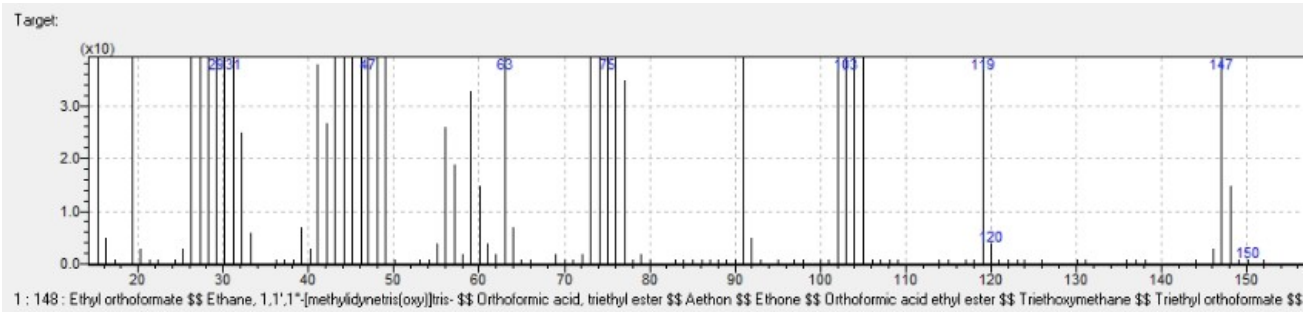
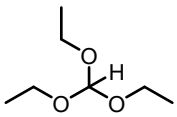
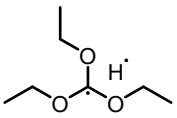


Figure S66 Mass spectrum obtained for **2b**.



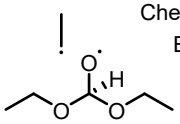
Chemical Formula: $C_7H_{16}O_3$
m/z: 148.11 (100.0%), 149.11 (7.7%)

Chemical Formula: $H^{\bullet}$
Exact Mass: 1,01



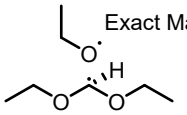
Chemical Formula: $C_7H_{15}O_3^{\bullet}$
Exact Mass: 147,10

Chemical Formula: $C_2H_5^{\bullet}$
Exact Mass: 29,04



Chemical Formula: $C_5H_{11}O_3^{\bullet}$
Exact Mass: 119,07

Chemical Formula: $C_2H_5O^{\bullet}$
Exact Mass: 45,03



Chemical Formula: $C_5H_{11}O_2^{\bullet}$
Exact Mass: 103,08

Figure S67 Fragmentation of **2b**.

12.3 Compound 3

Total purification of **3** was not succeeded, but the species remains in majority in the sample. Remaining content of **1** in the methyl group integration increased the value of 8 to 10 protons. Some minor amount of **4** was also observed, therefore contributing to the methyl group integration.

12.3.1 ^{1}H-NMR spectrum

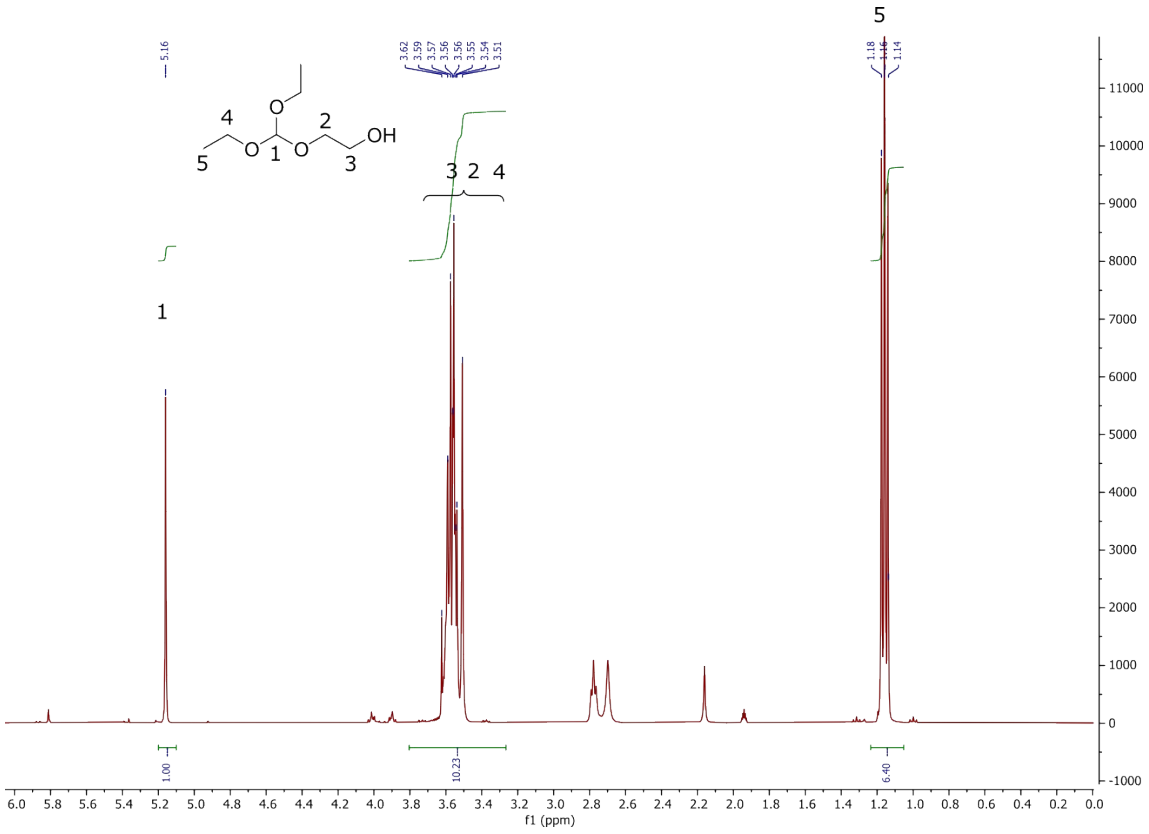


Figure S68 ^{1}H-NMR spectrum (700 MHz – CD_3CN) of **3**.

12.3.2 ^{13}C-NMR spectrum

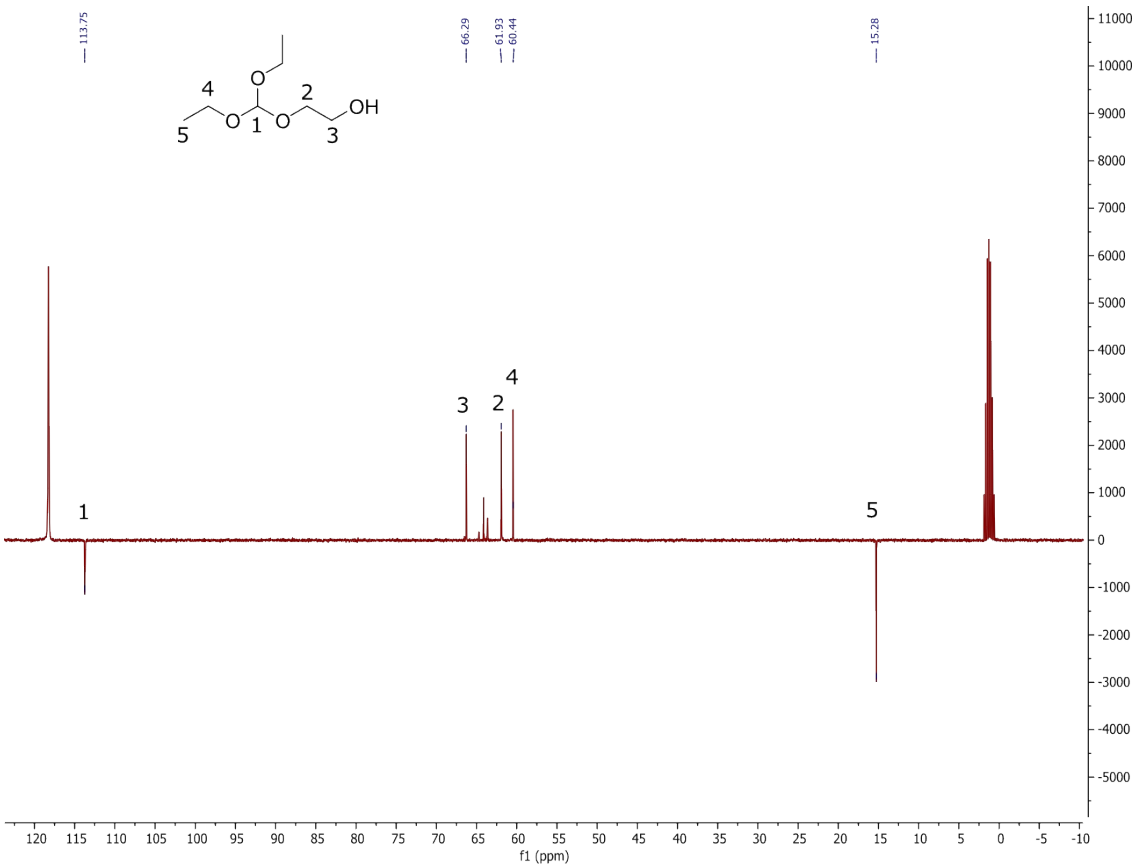


Figure S69 ^{13}C APT NMR spectrum (101 MHz – CD_3CN) of **3**.

12.3.3 Mass spectrum and fragmentation



Figure S70 Mass spectrum obtained for **3**.

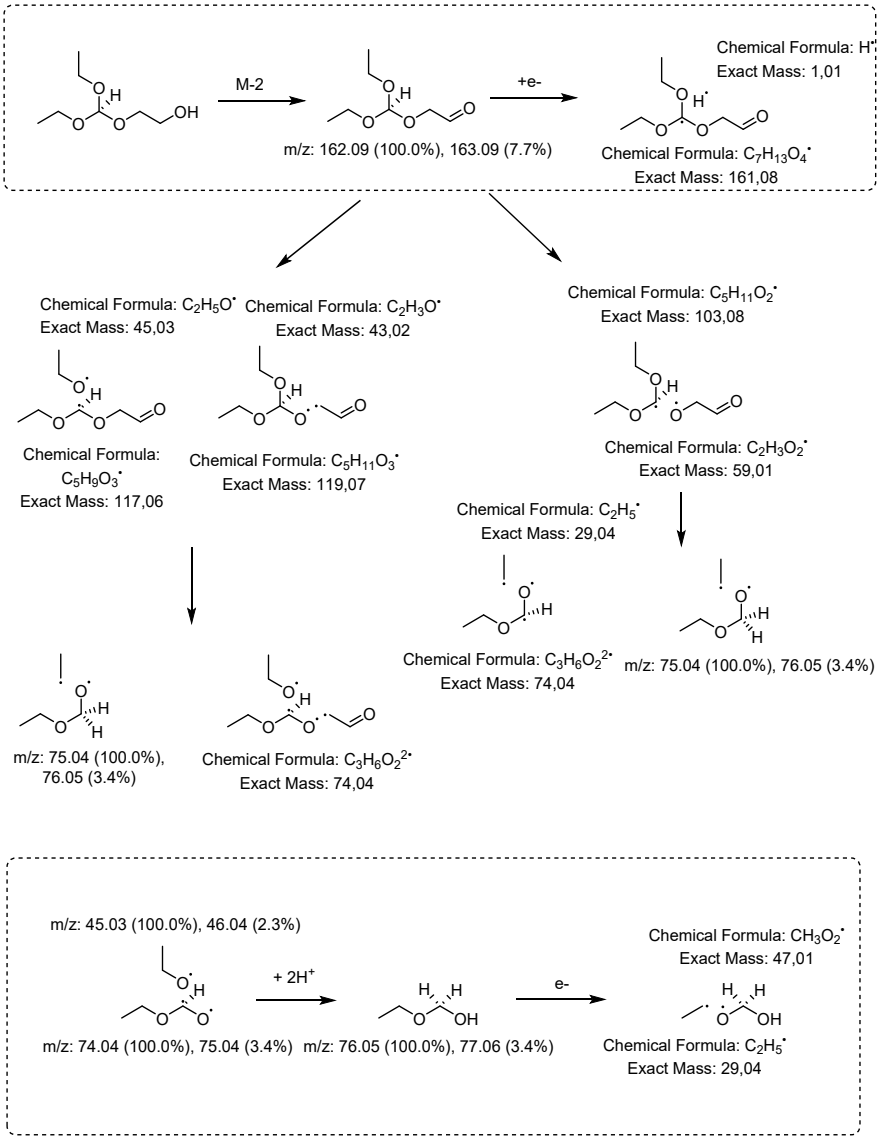


Figure S71 Fragmentation of **3**.

12.4 Compound 4

12.4.1 ^{1}H-NMR spectrum

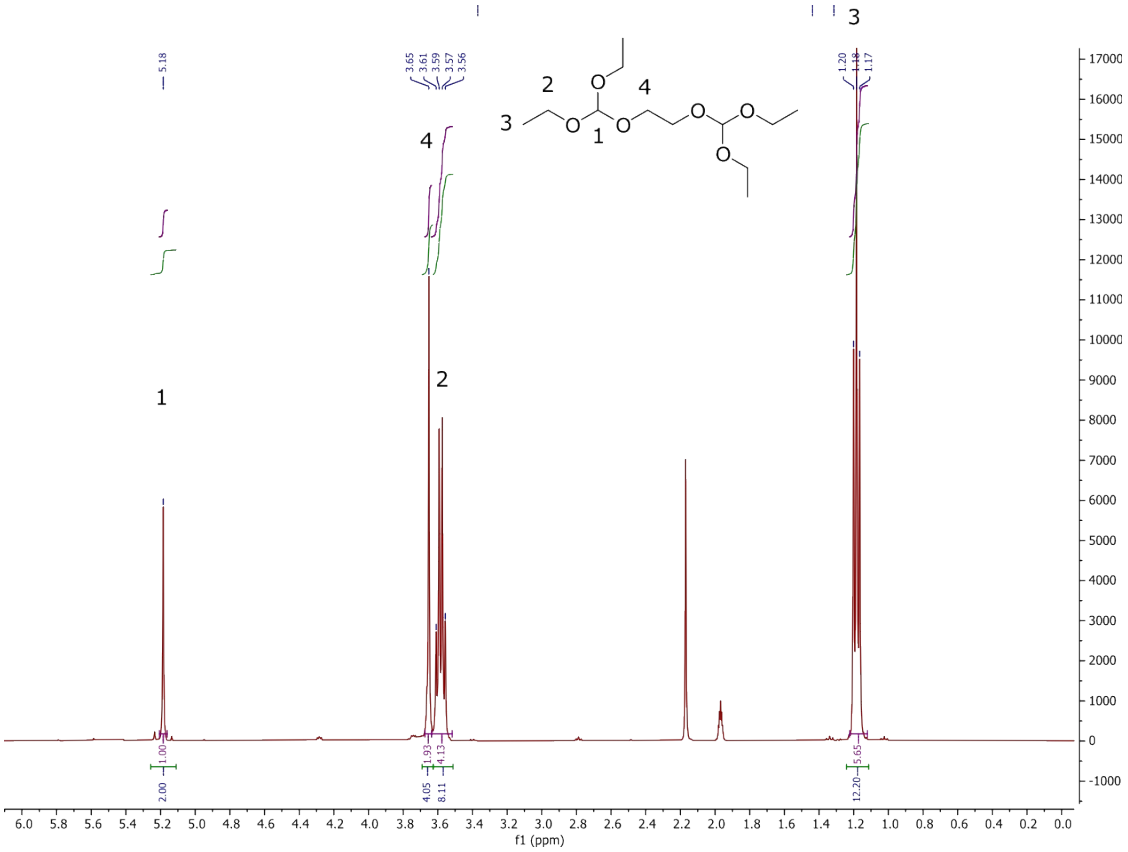


Figure S72 ^{1}H-NMR spectrum (700 MHz – CD_3CN) of **4**.

12.4.2 ^{13}C-NMR spectrum

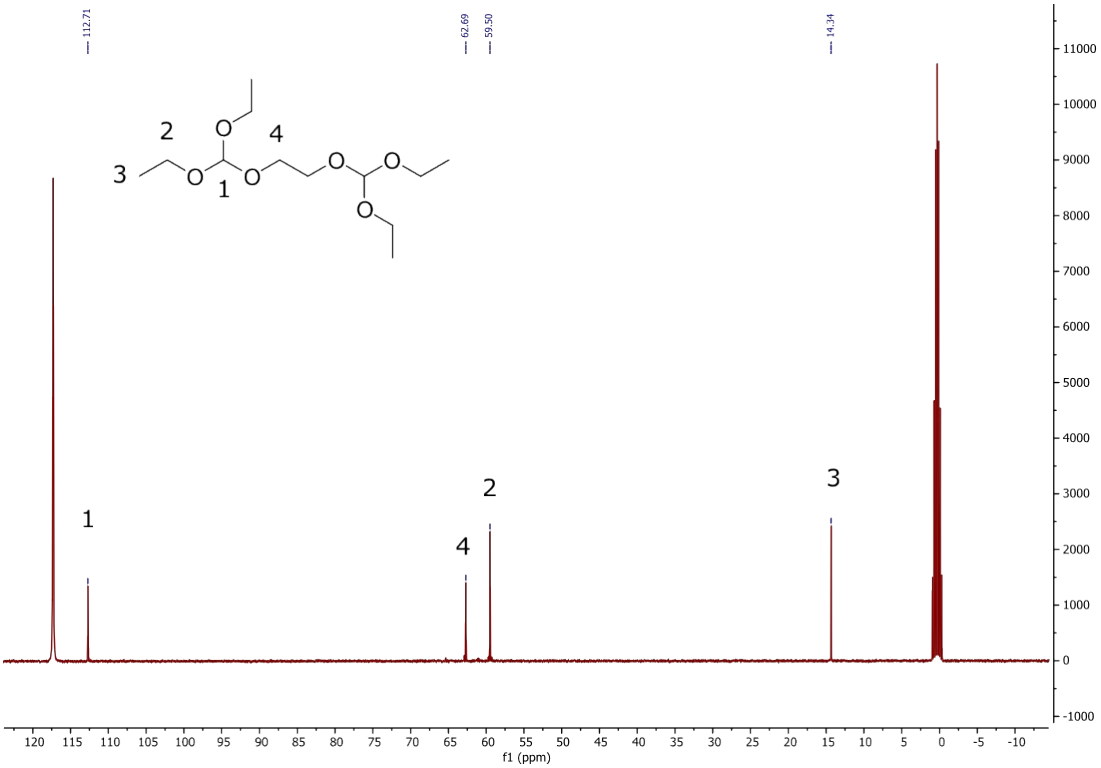


Figure S73 ^{13}C APT NMR spectrum (101 MHz – CD_3CN) of **4**.

12.4.3 Mass spectrum and fragmentation

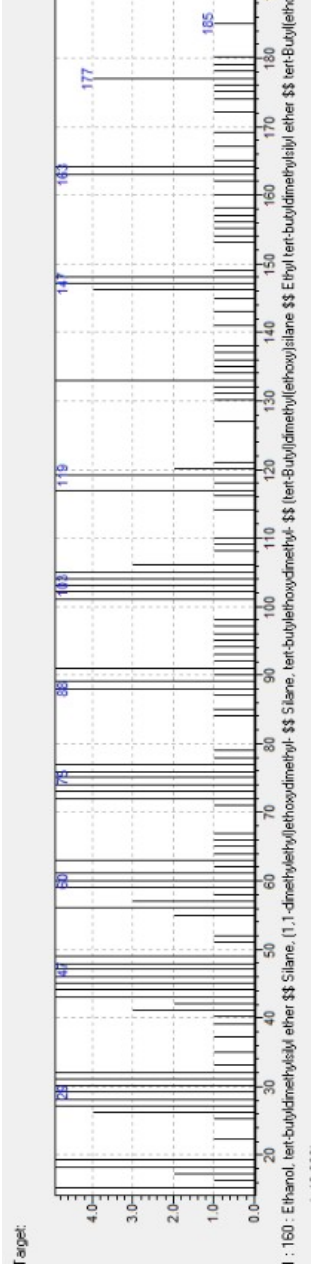


Figure S74 Mass spectrum obtained for **4**

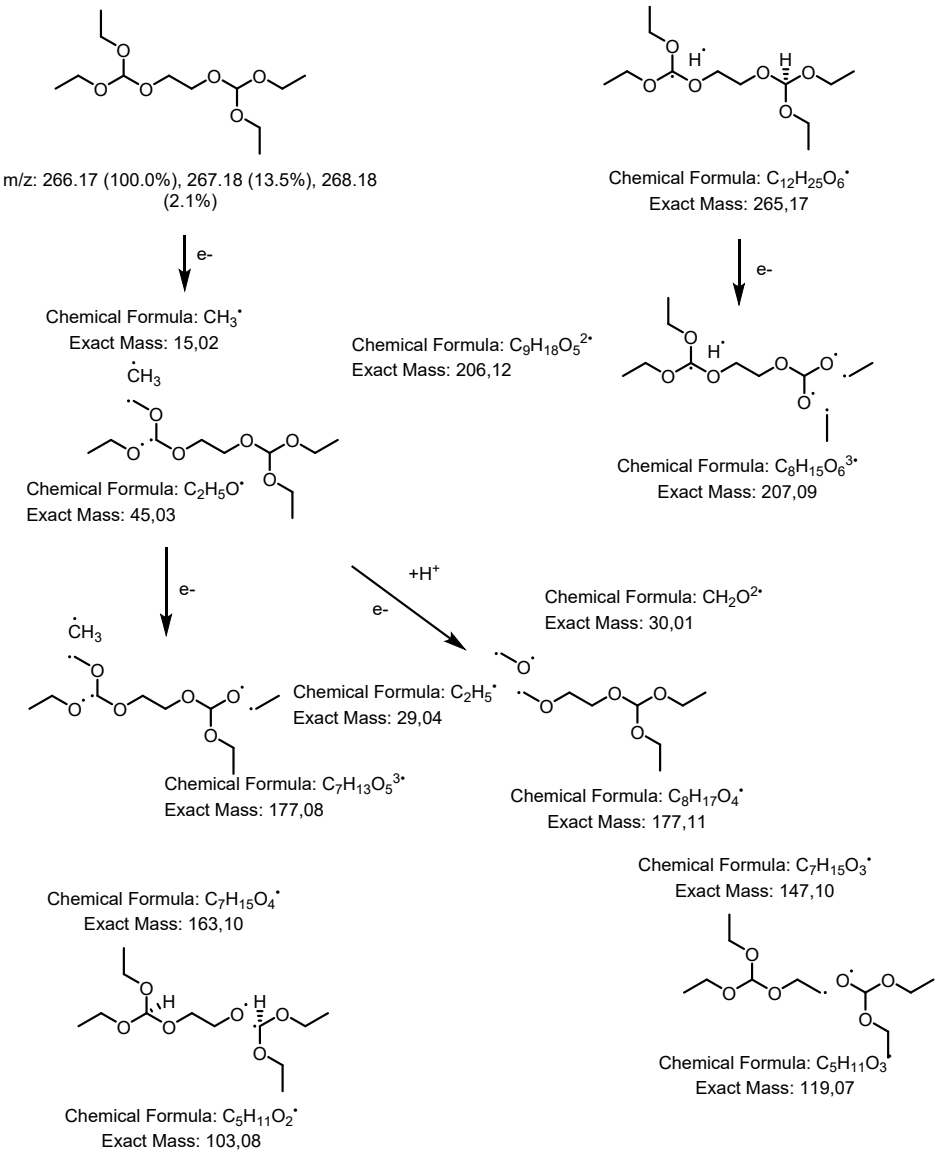


Figure S75 Fragmentation of **4**.

12.5 Compound 5

12.5.1 ^{1}H-NMR spectrum

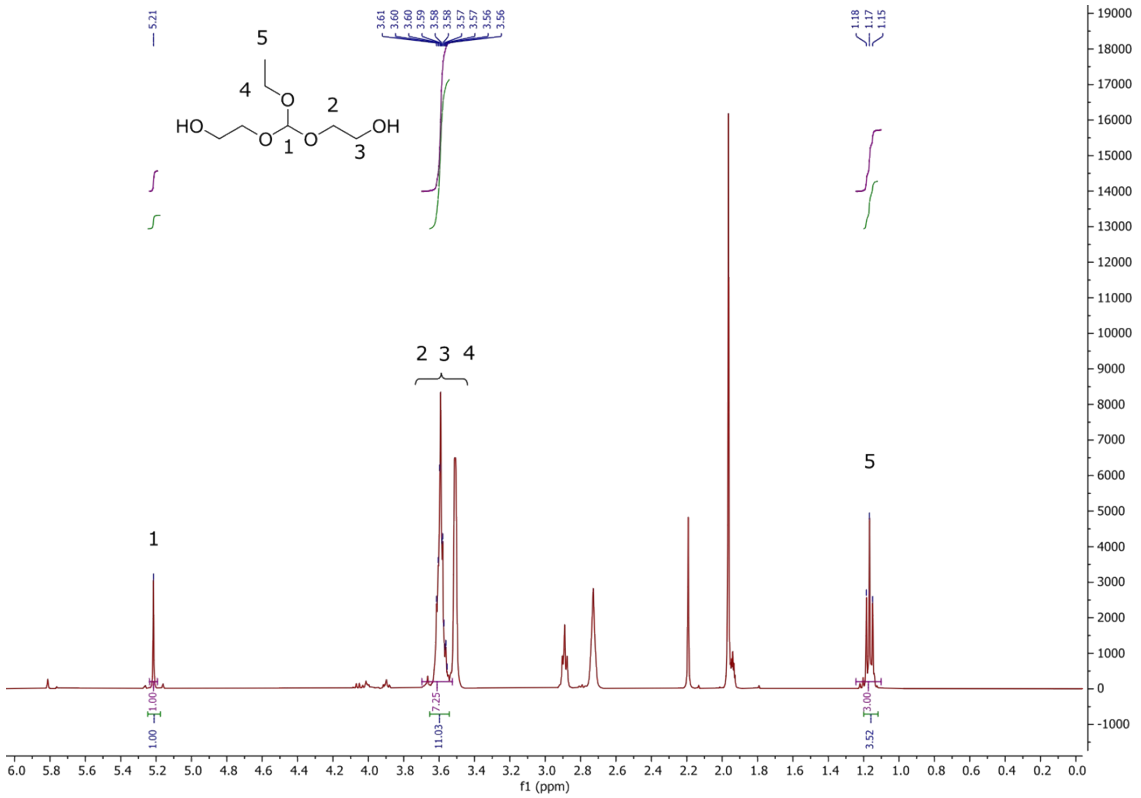


Figure S76 ^{1}H-NMR spectrum (700 MHz – CD_3CN) of **5**.

12.5.2 ^{13}C-NMR spectrum

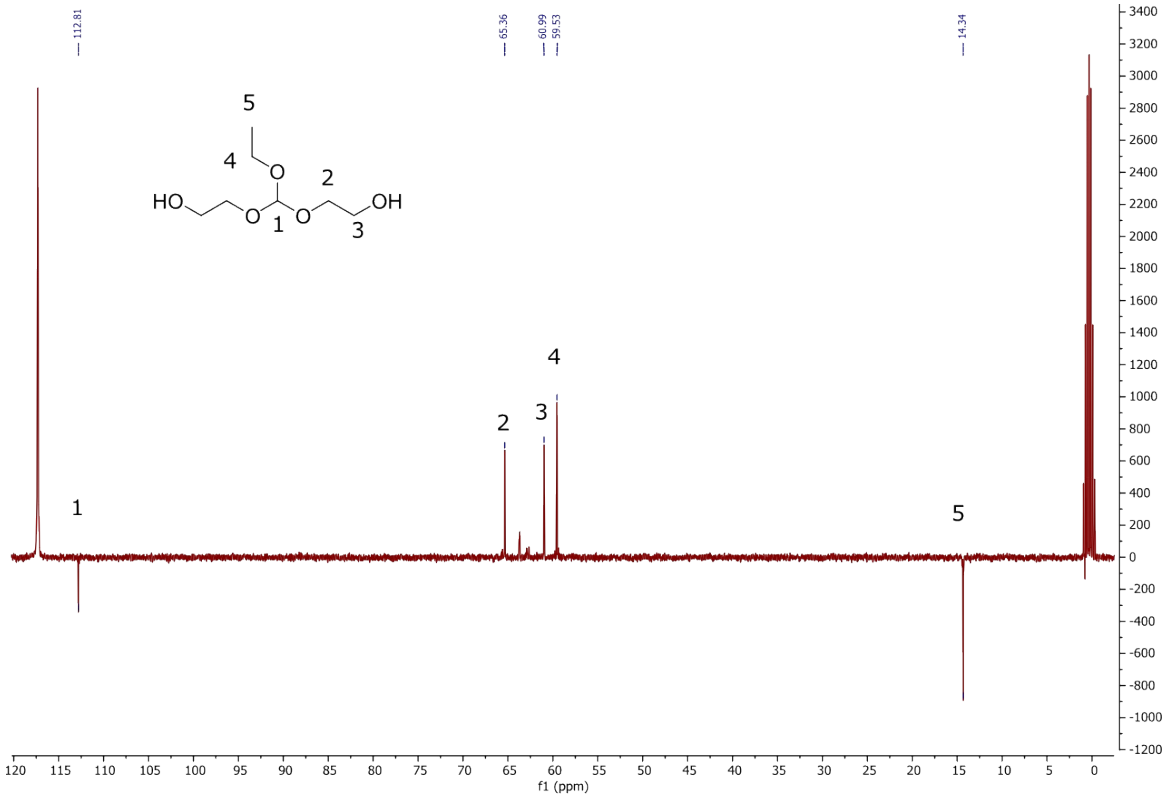


Figure S77 ^{13}C APT NMR spectrum (101 MHz – CD_3CN) of **5**.

12.5.3 Mass spectrum and fragmentation

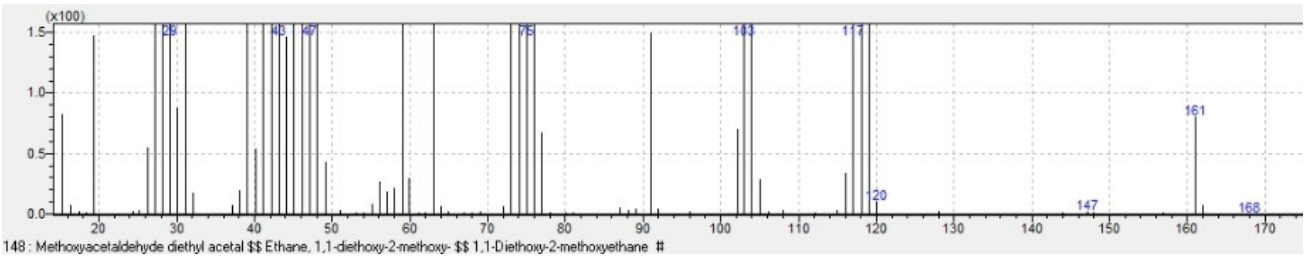


Figure S78 Mass spectrum obtained for **5**.

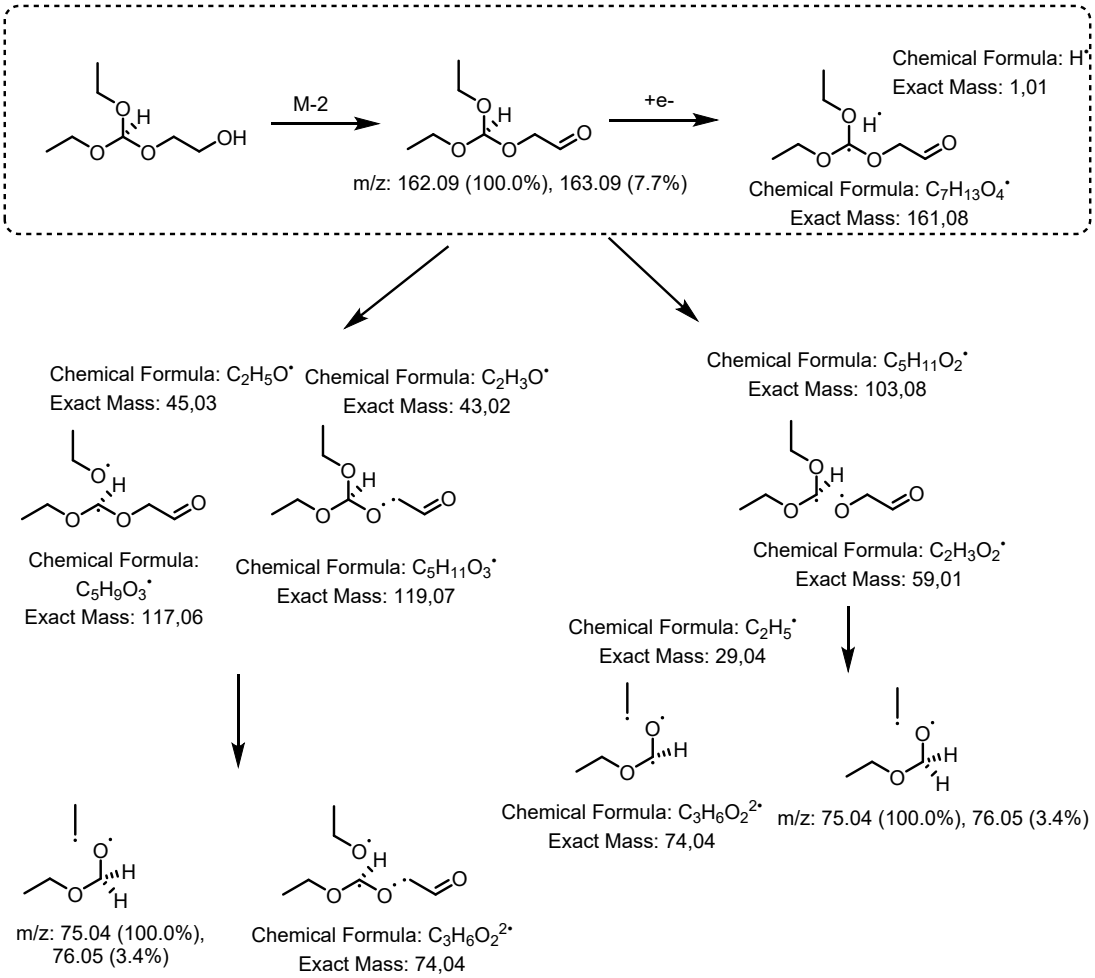


Figure S79 Fragmentation of **5**.

12.6 Compound 6

12.6.1 ^{1}H-NMR spectrum

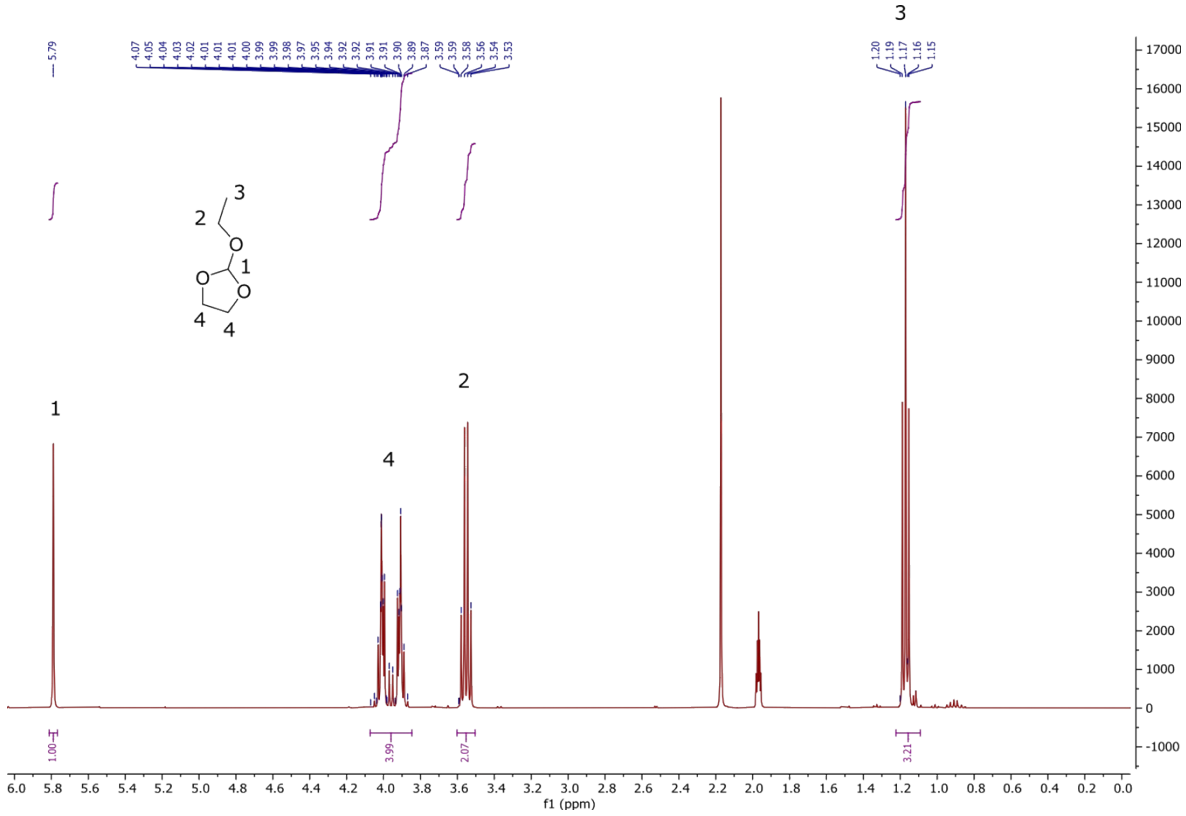


Figure S80 ^{1}H-NMR spectrum (700 MHz – CD_3CN) of 6**.**

12.6.2 ^{13}C-NMR spectrum

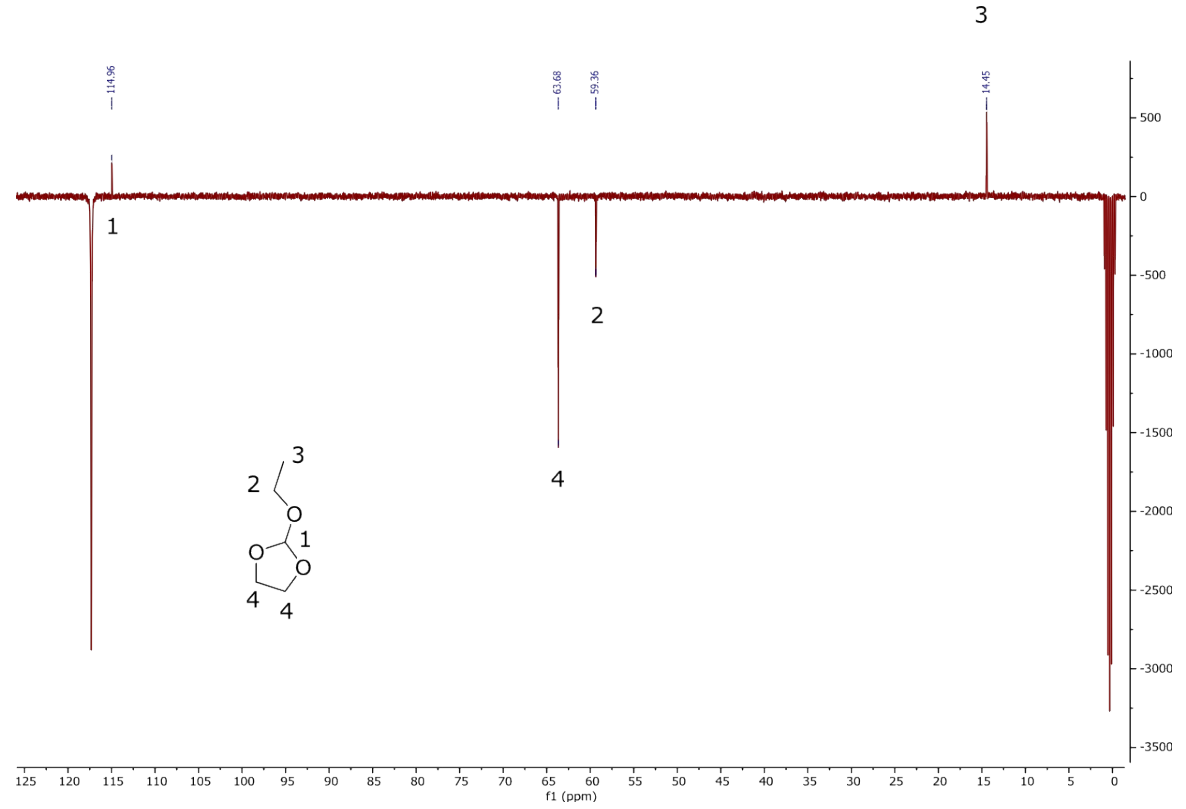


Figure S81 ^{13}C APT NMR spectrum **(101 MHz – CD_3CN)** of **6.**

12.6.3 Mass spectrum and fragmentation



Figure S82 Mass spectrum obtained for **6**.

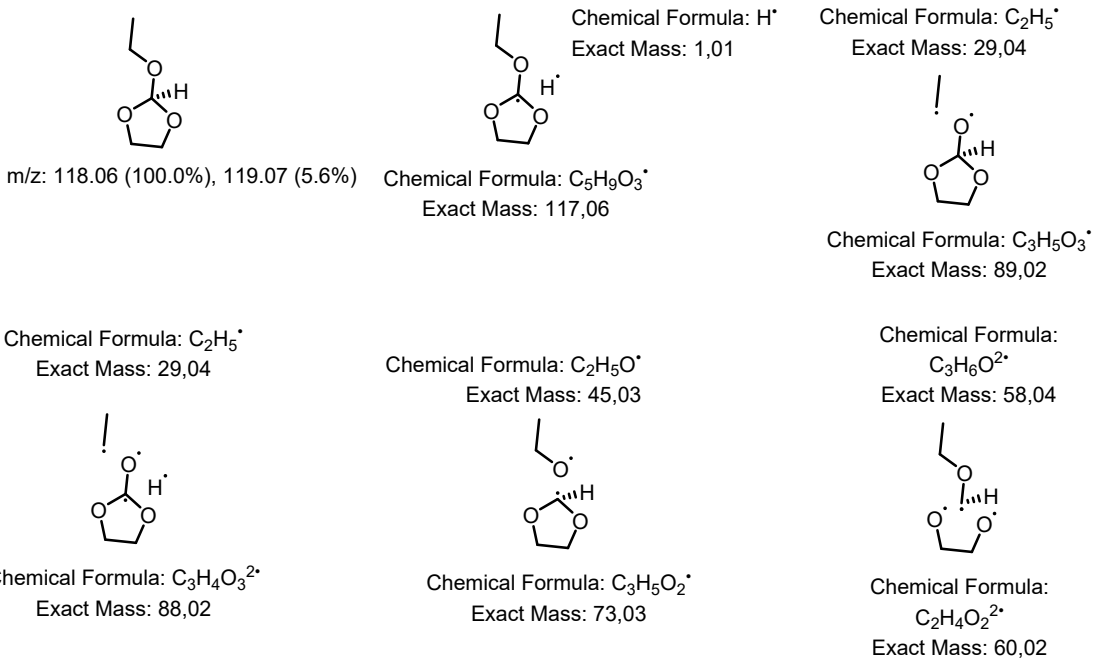


Figure S83 Fragmentation of **6**.

12.7 Compound 7

12.7.1 ^{1}H-NMR spectrum

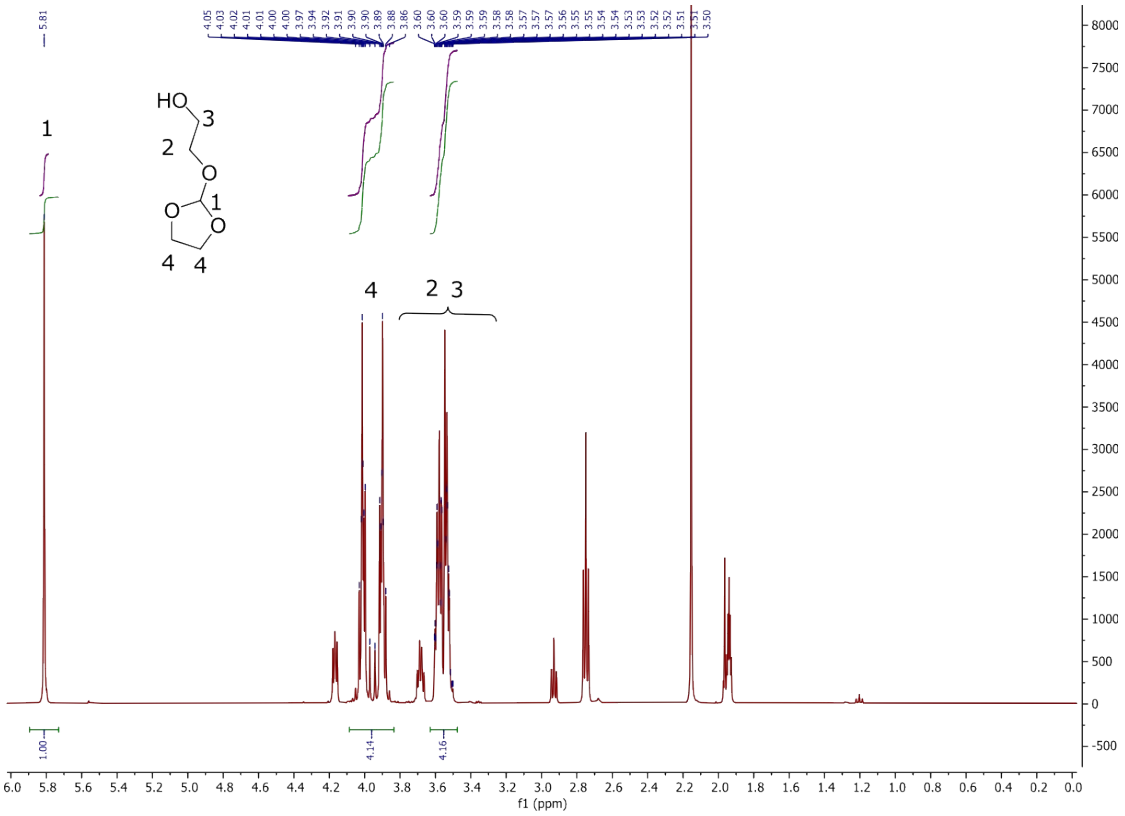


Figure S84 ^{1}H-NMR spectrum **(700 MHz – CD_3CN)** of **7**.

12.7.2 ^{13}C-NMR spectrum

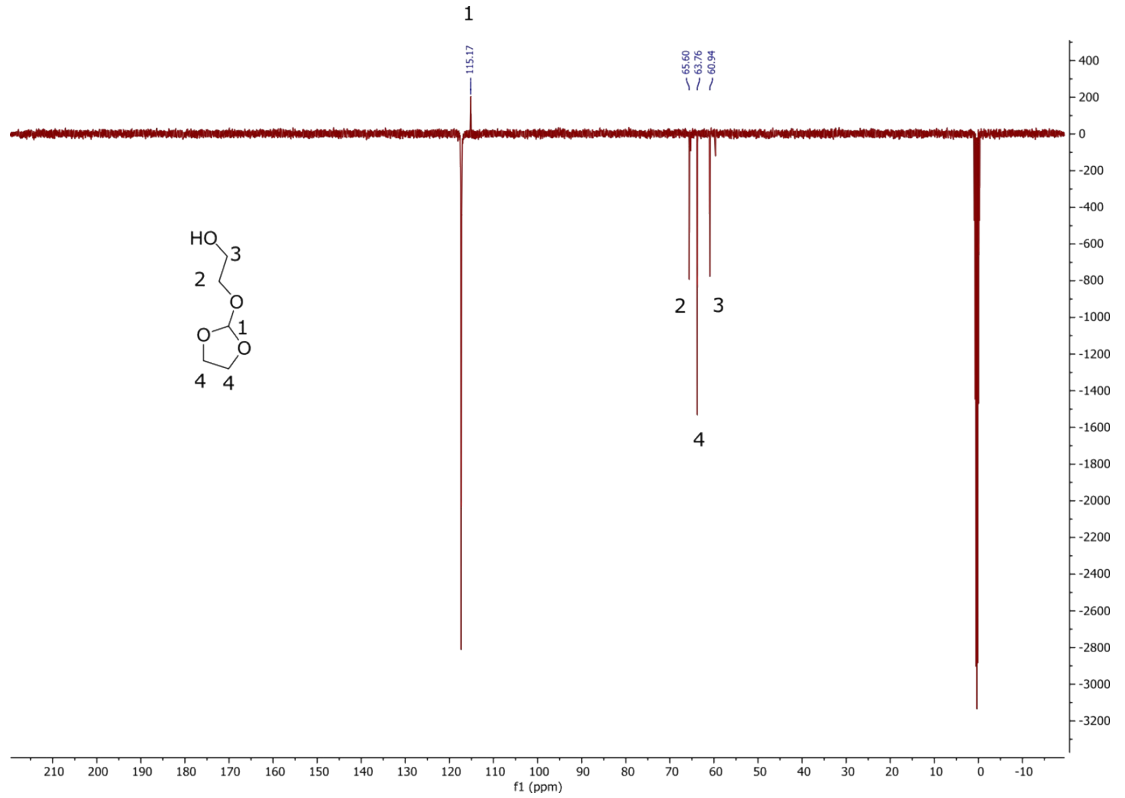


Figure S84 ^{13}C APT NMR spectrum (101 MHz – CD_3CN) of **7**.

12.7.3 Mass spectrum and fragmentation

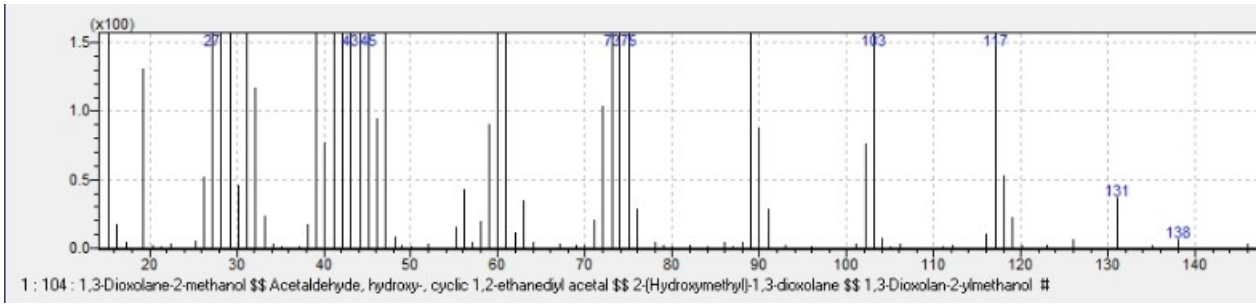


Figure S86 Mass spectrum obtained for **7**.

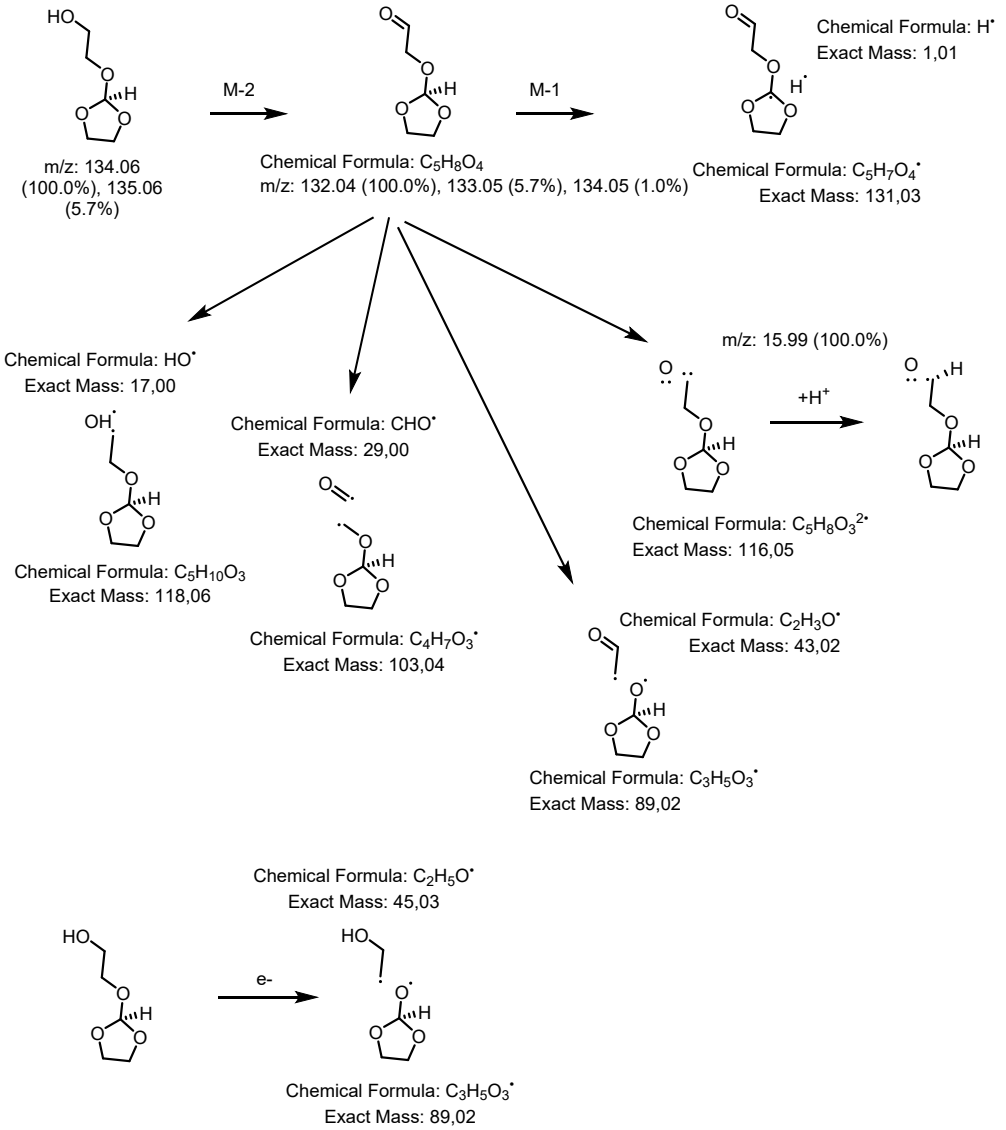


Figure S87 Fragmentation of **7**.

12.8 Compound 8

12.8.1 2 2D-HSQC and HMBC NMR spectra

The Figure S87 shows the correlations between the cyclic and acyclic acidic protons of **8**. Their proton chemical shifts are at 5.183 and 5.836 ppm respectively. Due to the very low content of **8**, it prevented to identify the carbon signals assigned to this species.

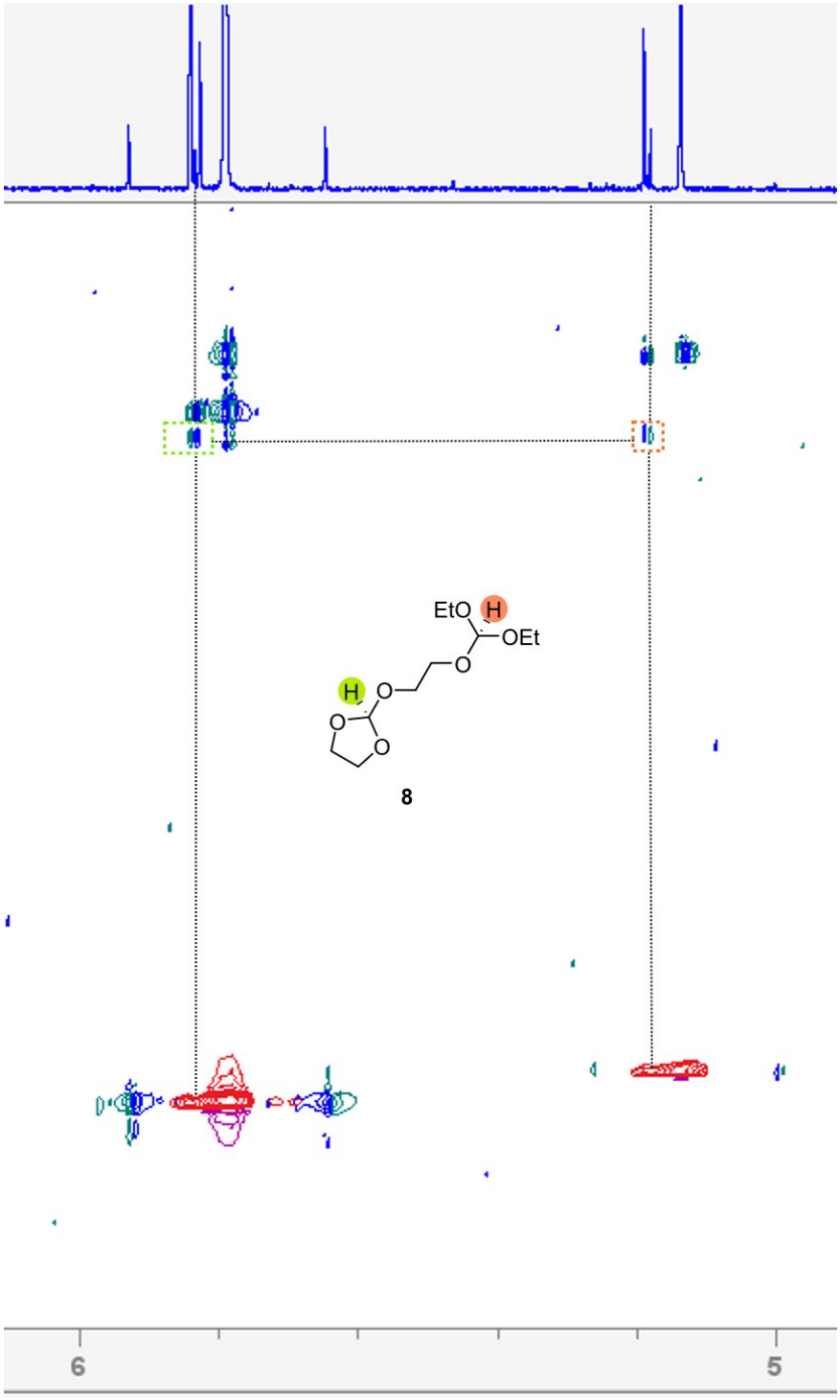


Figure S88 Superimposition of the 2D-HSQC (blue-green signals) and HMBC (red) spectra and corresponding assignments of the structural scaffold of products **8**.

12.8.2 Mass spectrum and fragmentation

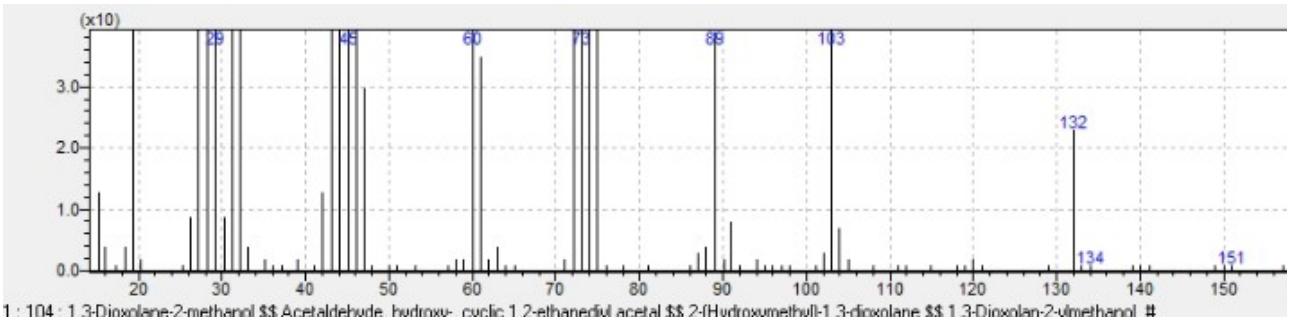


Figure S89 Mass spectrum obtained for **8**.

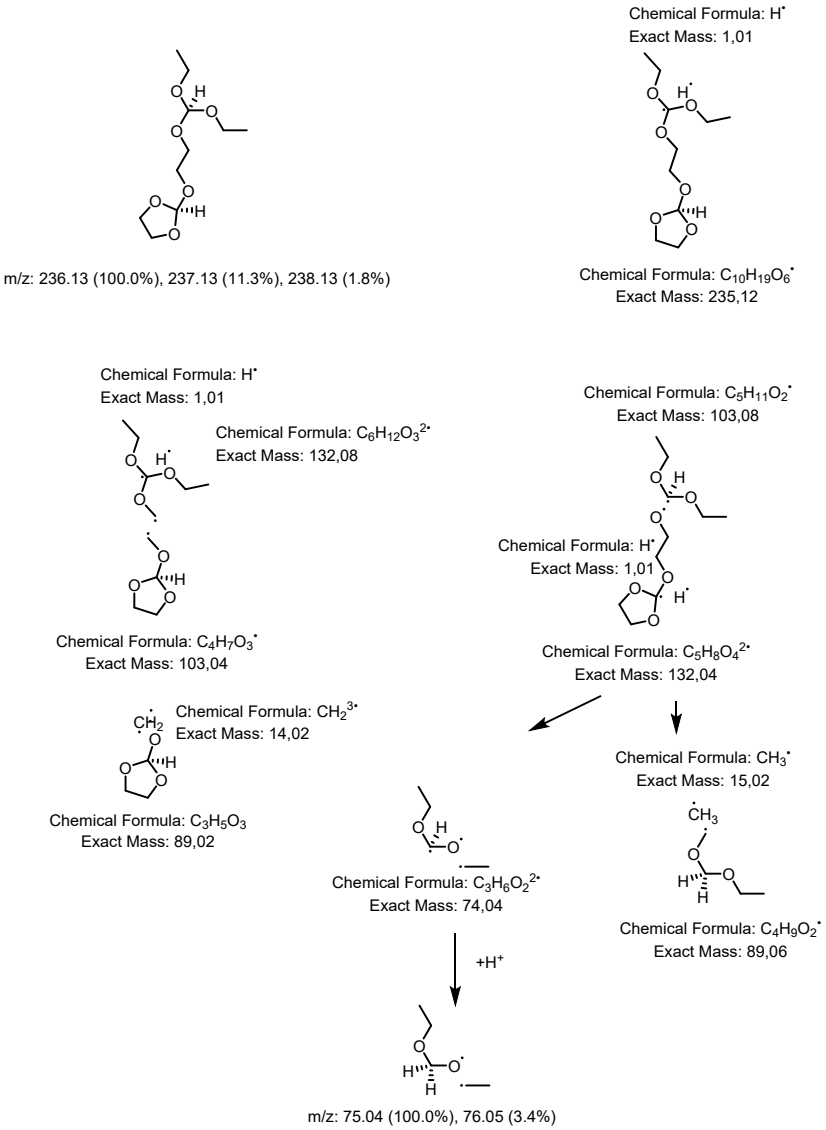


Figure S90 Fragmentation of **8**.

12.9 Compound 9

12.9.1 ^{1}H-NMR spectrum

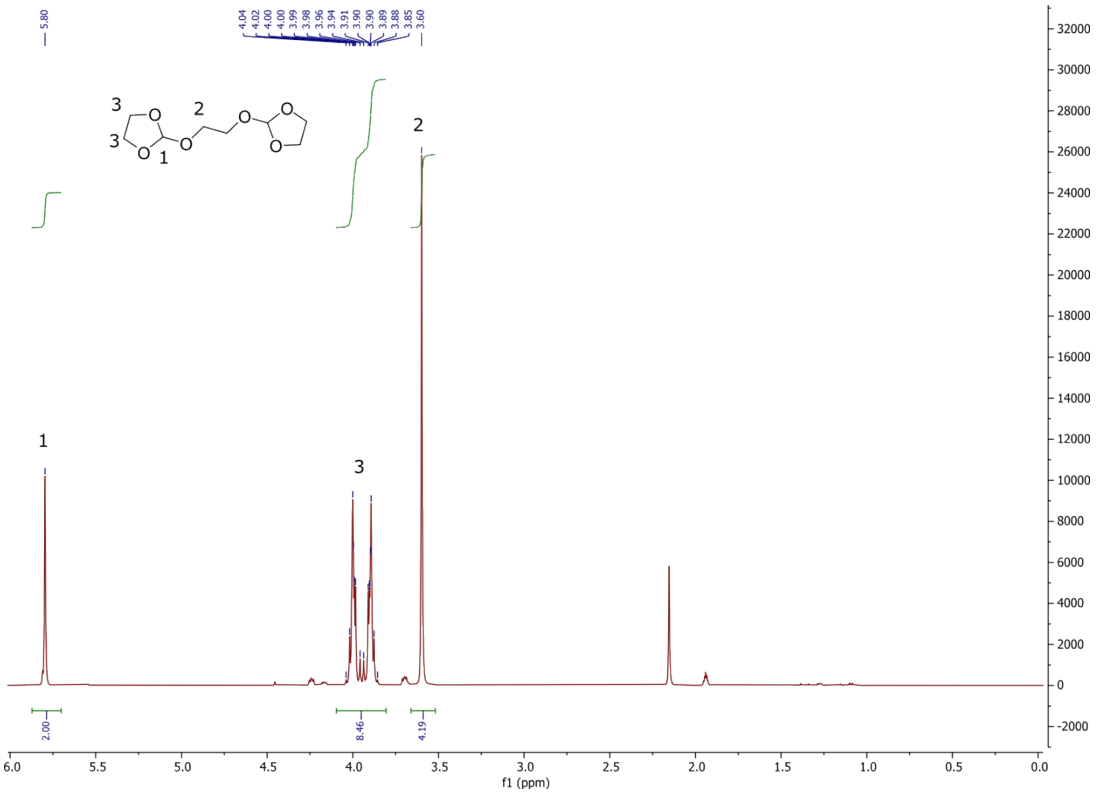


Figure S91 ^{1}H-NMR spectrum (700 MHz – CD_3CN) of **9**.

12.9.2 ^{13}C-NMR spectrum

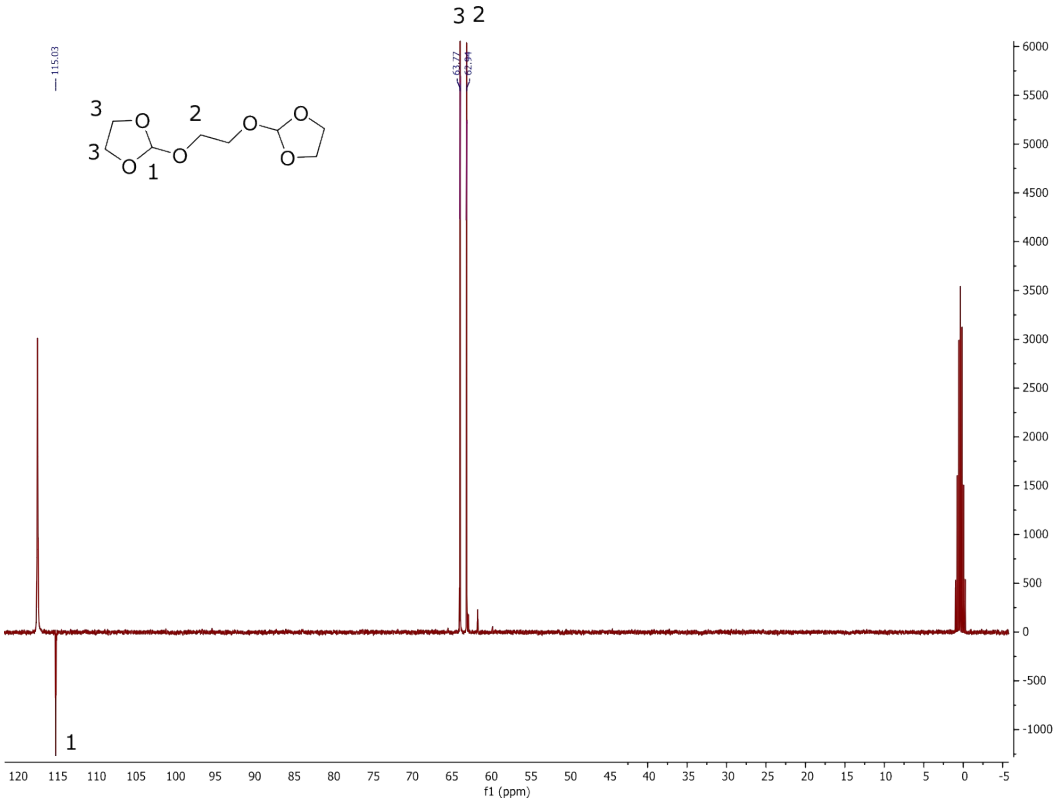


Figure S92 ^{13}C APT NMR spectrum (101 MHz – CD_3CN) of **9**.

12.9.3 Mass spectrum and fragmentation

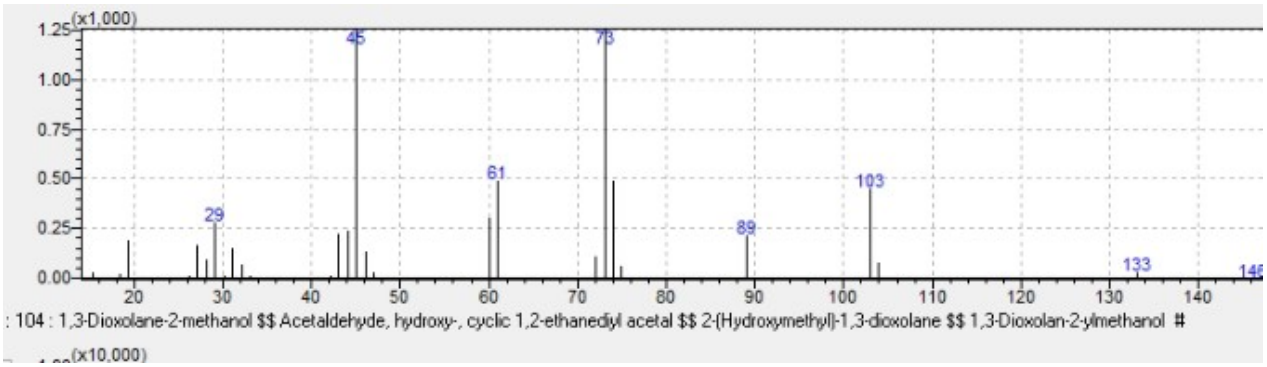


Figure S93 Mass spectrum obtained for **9**.

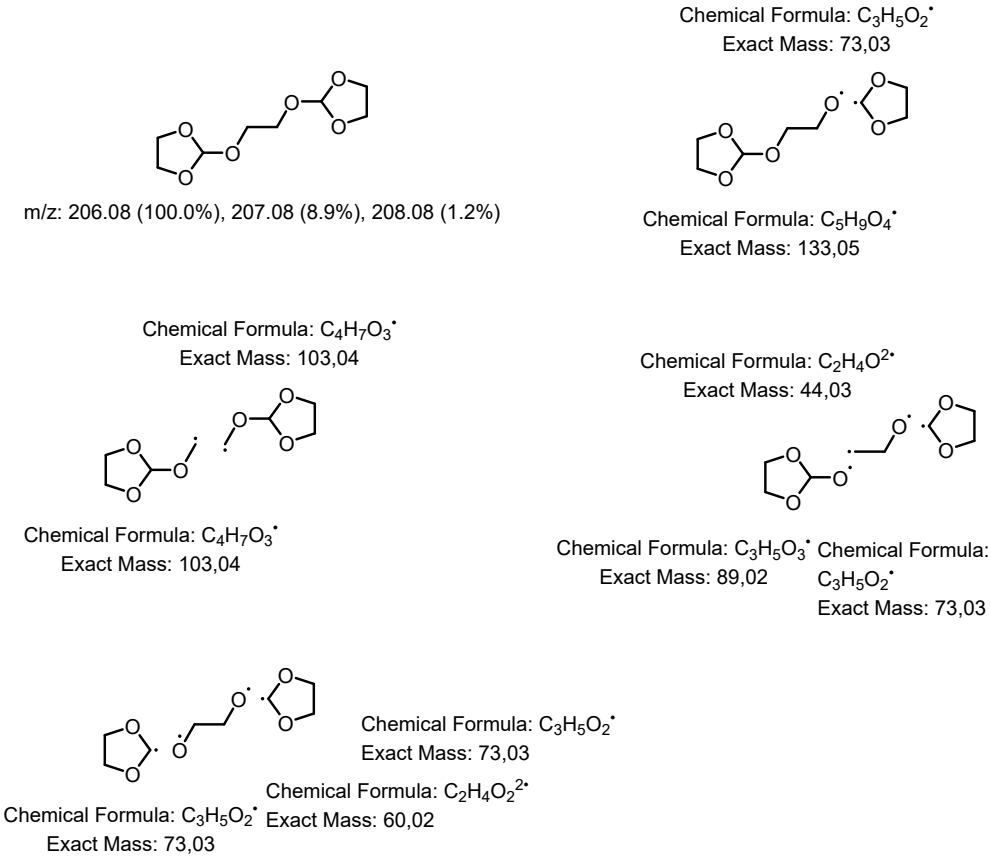


Figure S94 Fragmentation of **9**.

12.10 Compound 10

Compound **10** has never been observed or isolated but the hypothesis of its formation is strongly supported by the positive impact of its addition of the kinetic **model VIII**. This species was also included in the kinetic study starting from **4** (isolated and assigned), resulting in an improved model as well. Figure S94 shows the superimposition of a spectrum from a kinetic with an excess of **1**, promoting the formation of **3** and **5** (both isolated and assigned) versus the kinetic study using **3** as starting reagent. Due to the substitution of ethylene glycol moiety by **2**, it is expected that the acidic proton of **10** will be slightly more shielded compared to species **5**, explaining the difference of chemical shifts. Besides, **4** follows the same logic, with an acidic proton slightly more shielded than **3**. Due to its very low amount, no correlation with 2D HMBC or HSQC could be observed, similarly for the carbon spectrum.

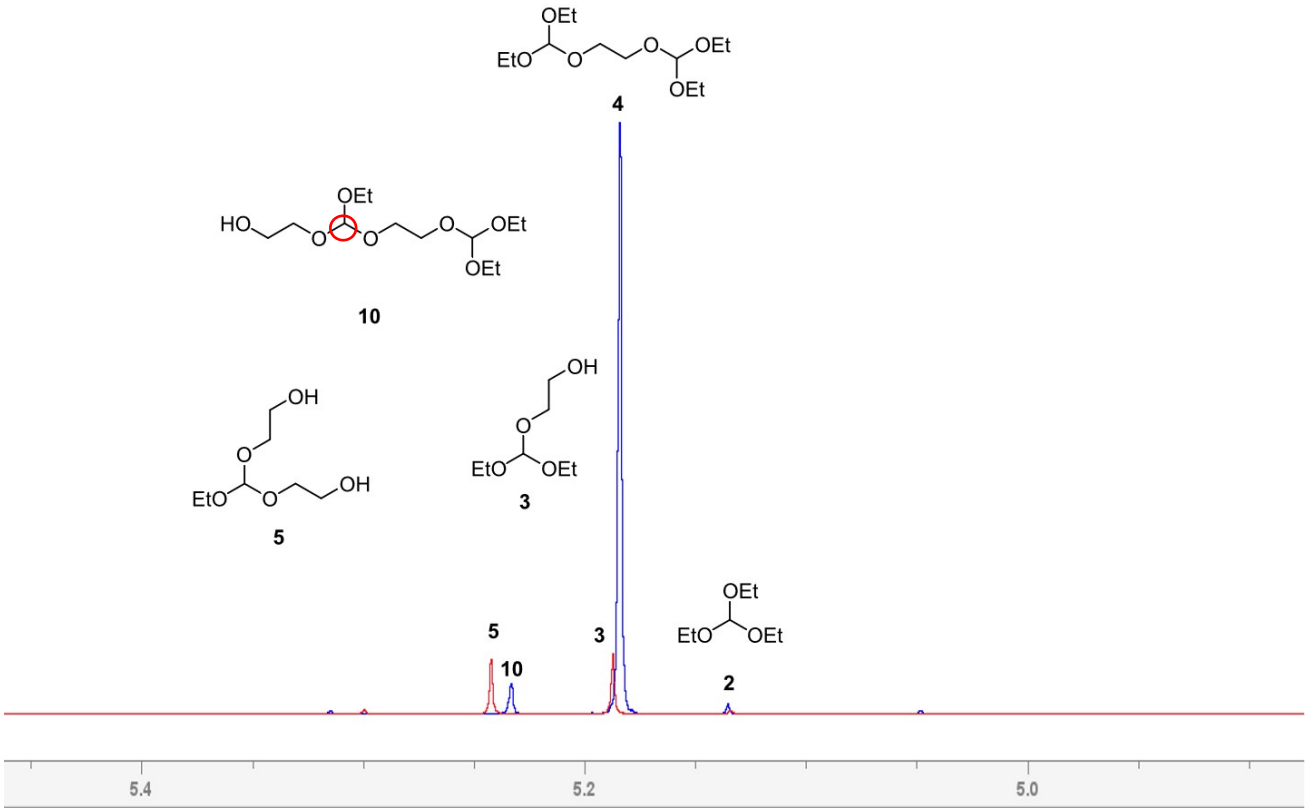


Figure S95 Superimposition of ^{1}H-NMR spectra of products **2**, **3**, **10** (blue spectrum) and **5** (red spectrum).

12.11 Compound 11

12.11.1 ^{1}H-NMR spectrum

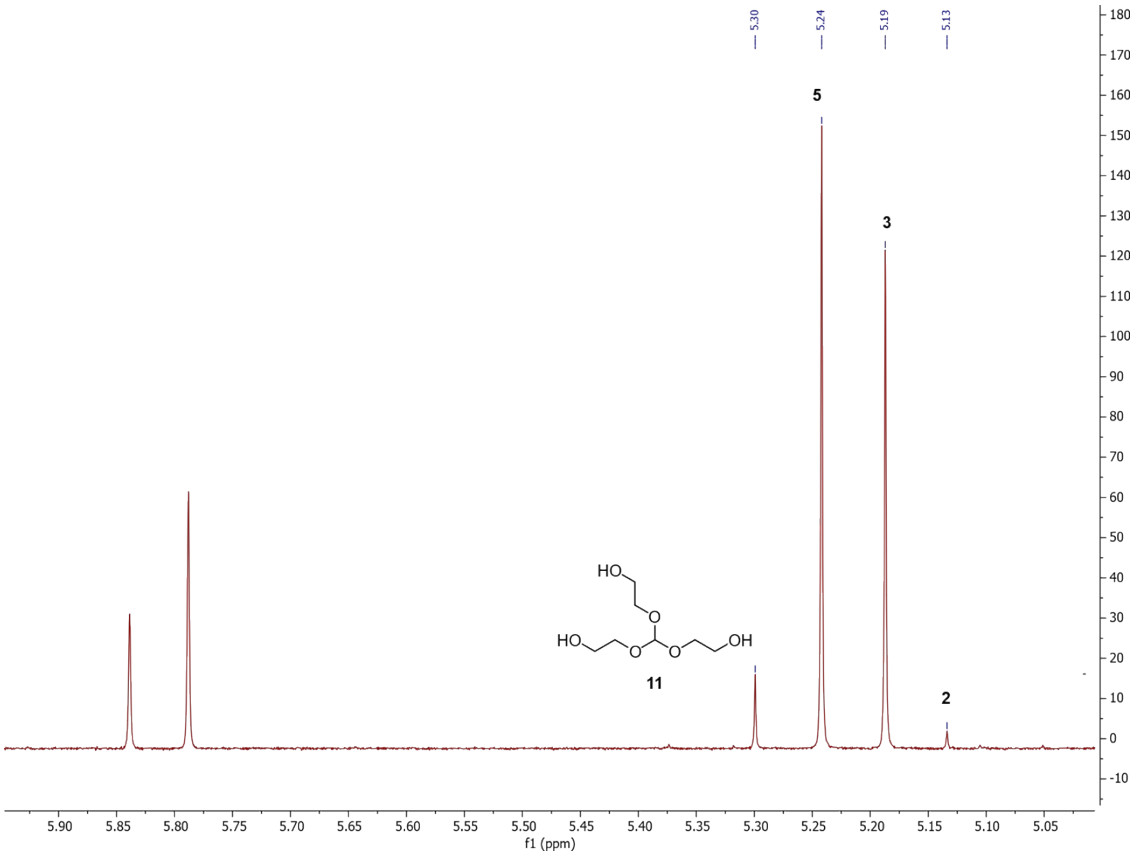


Figure S96 ^{1}H-NMR spectrum (700 MHz – CD_3CN) of **11** (spectral window between 5 and 5.9 ppm).

12.11.2 2D-HSQC and HMBC NMR spectra

The superimposition of the 2D-HSQC and HMBC spectra (Figure S96) reveals the proton-carbon correlation of the acidic proton of compound **11** at a chemical shift of 113.2 ppm (black box 1). The second box shows the two correlations of the "acidic carbon" with the two methylene groups (black box 2).

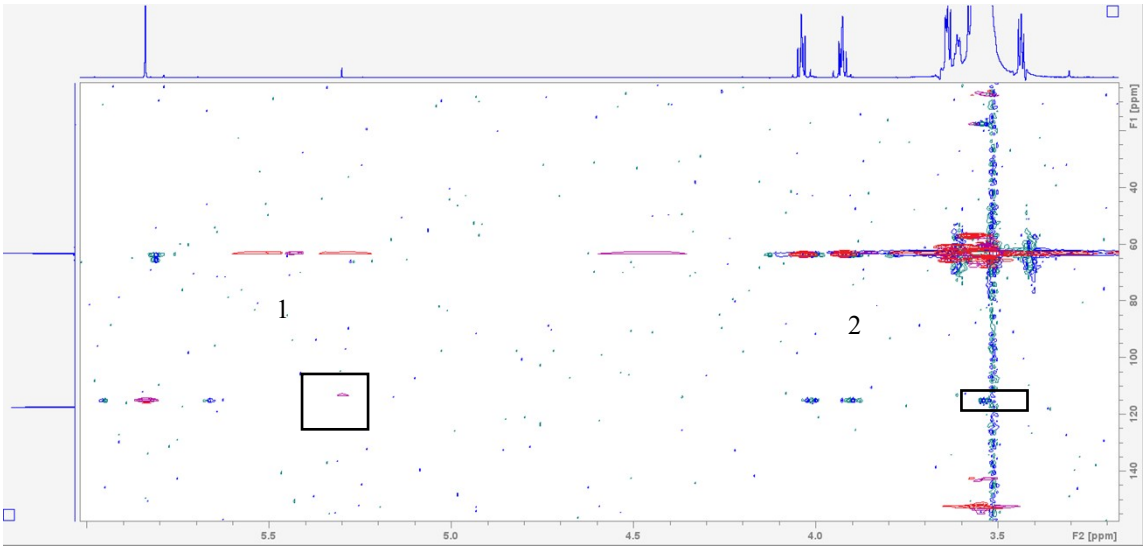


Figure S97 Superimposition of the 2D-HSQC (red signals) and HMBC (blue/green) spectra obtained from a typical crude of DCE and corresponding assignments of the structural scaffold of acyclic orthoester **11**.

12.12 Compound 13 (commercial reference)

12.12.1 ^{1}H-NMR spectrum

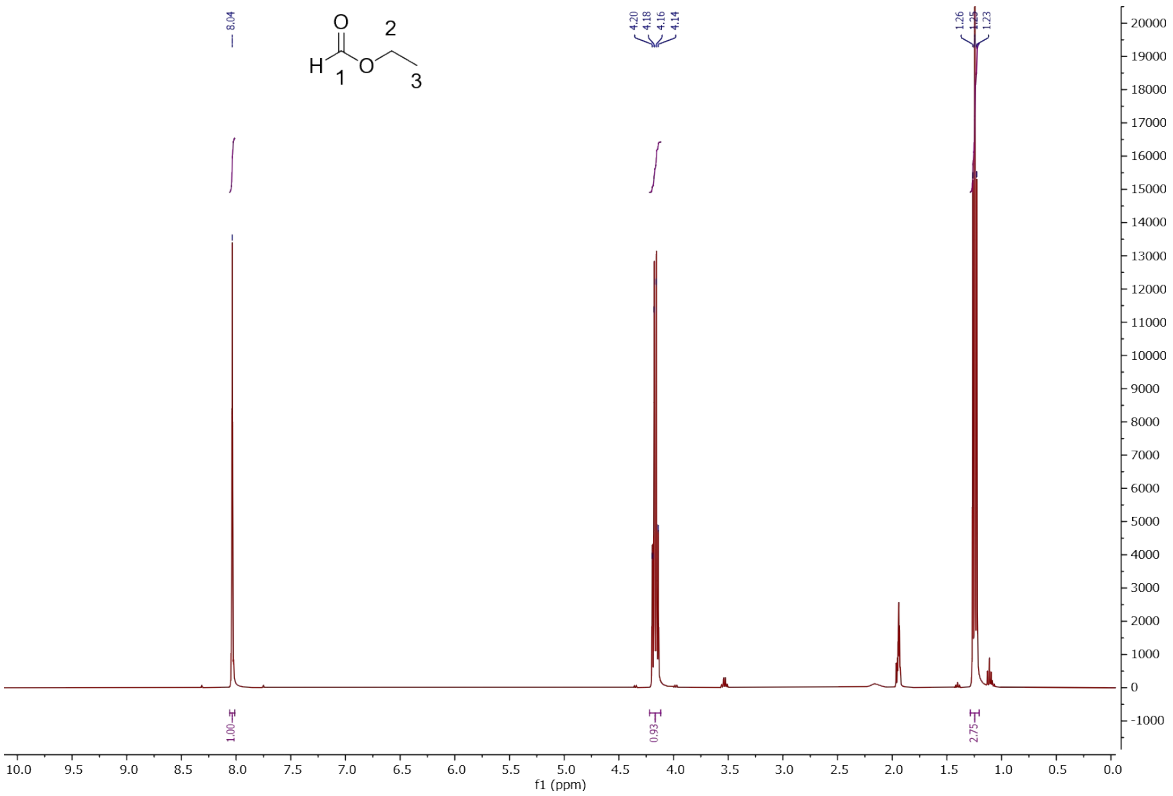


Figure S98 ^{1}H-NMR spectrum (700 MHz – CD_3CN) of **13**.

12.12.2 ^{13}C-NMR spectrum

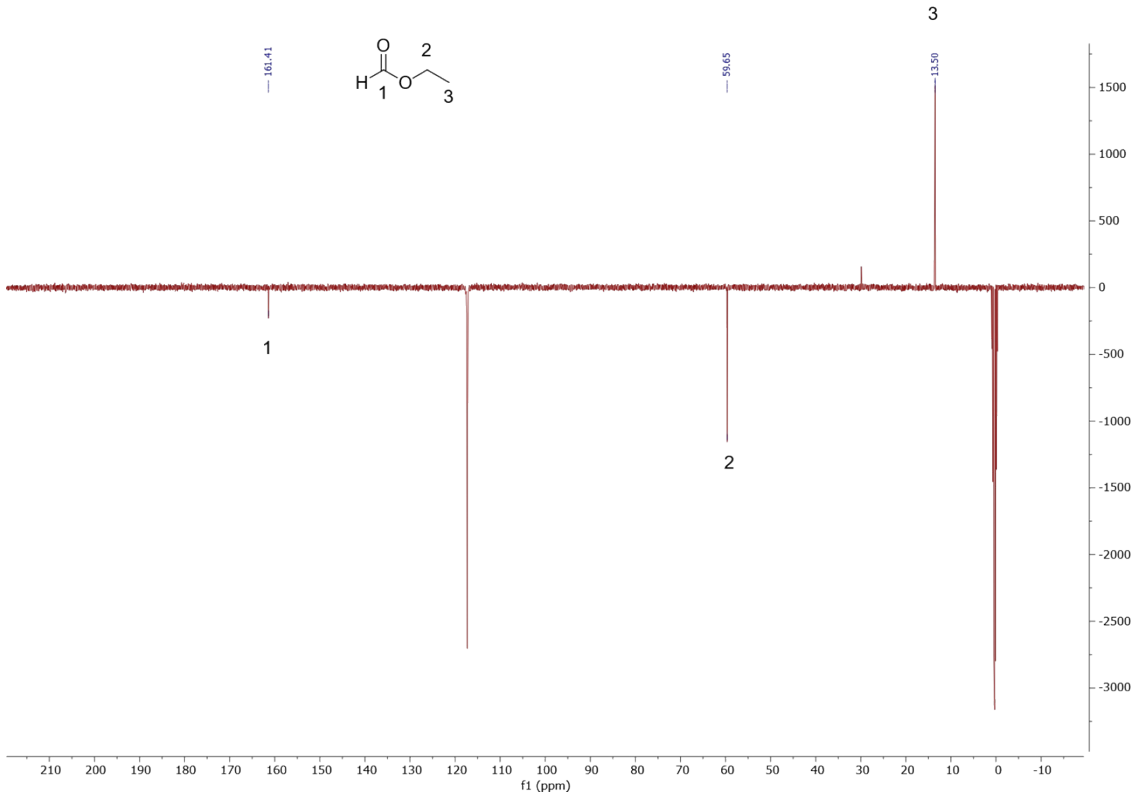


Figure S99 ^{13}C APT NMR spectrum (101 MHz – CD_3CN) of **13**.

12.13 Compound 14

12.13.1 ^{1}H-NMR spectrum

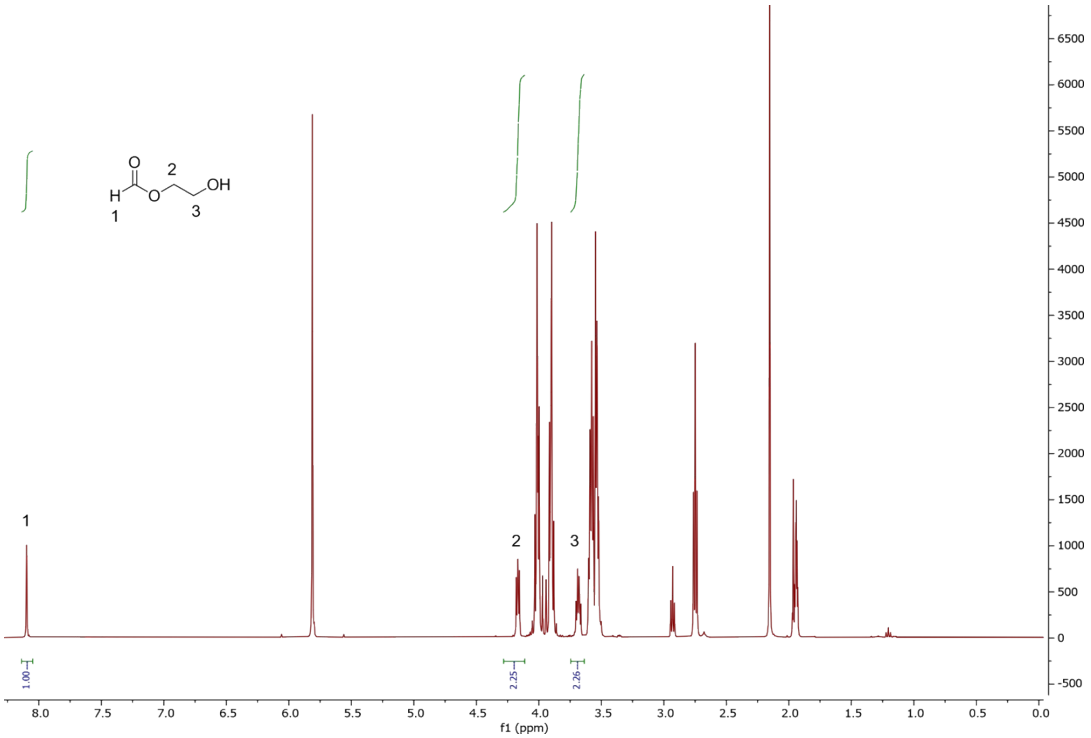


Figure S100 ^{1}H-NMR spectrum (700 MHz – CD_3CN) of **14**.

12.13.2 ^{13}C-NMR spectrum

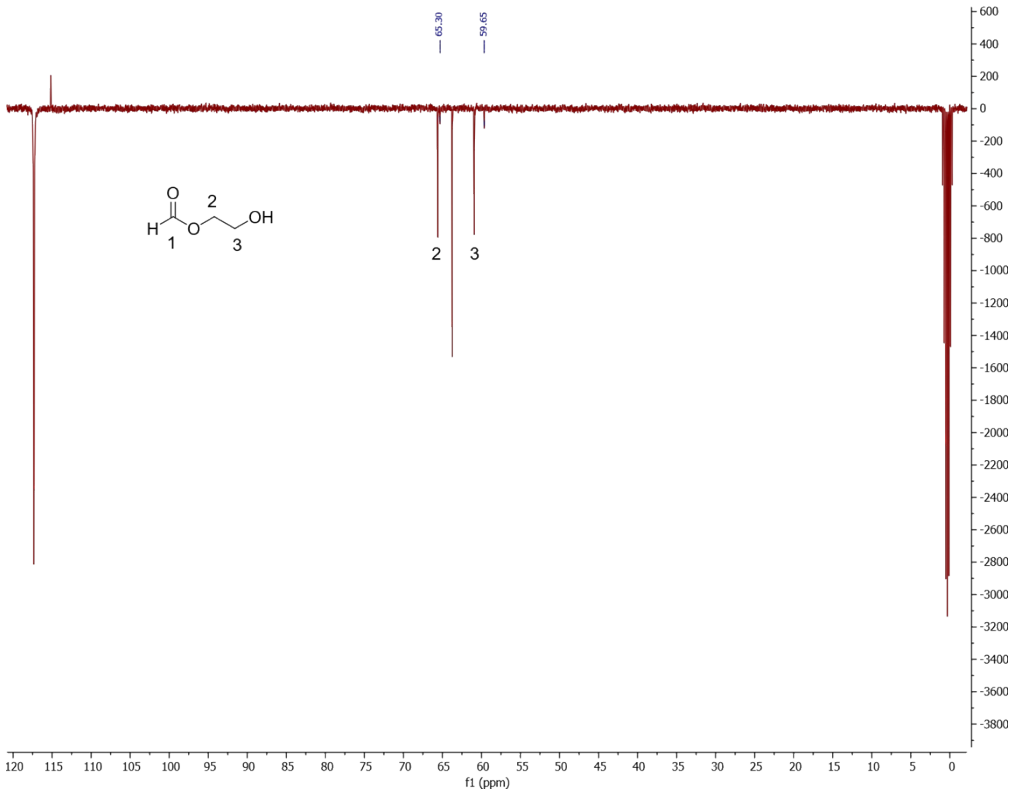


Figure S101 ^{13}C APT NMR spectrum (101 MHz – CD_3CN) of **14**.

The chemical shift of the quaternary carbon (1) was determined by 2D HMBC, at 161.33 ppm.

13 References

(1) M. Newville, T. Stensitzki, D.B. Allen, M. Rawlik, A. Ingargiola, A. Nelson, A. Lmfit: Non-Linear Least-Square Minimization and Curve-Fitting for Python. *Astrophys. Source Code Lib.* **2016**, ascl:1606.014.

(2) Y. Liu, F. Le Formal, F. Boudoire, N. Guijarro, Hematite Photoanodes for Solar Water Splitting: A Detailed Spectroelectrochemical Analysis on the PH-Dependent Performance. *ACS Appl. Energy Mater.* **2019**, *2*, 6825–6833.

(3) Gaussian 16, Revision C.01, M. J. Frisch, G. W. Trucks, H. B. Schlegel, G. E. Scuseria, M. A. Robb, J. R. Cheeseman, G. Scalmani, V. Barone, G. A., Petersson, H. Nakatsuji, X. Li, M. Caricato, A. V. Marenich, J. Bloino, B. G. Janesko, R. Gomperts, B. Mennucci, H. P. Hratchian, J. V. Ortiz, A. F. Izmaylov, J. L. Sonnenberg, D. Williams-Young, F. Ding, F. Lipparini, F. Egidi, J. Goings, B. Peng, A. Petrone, T. Henderson, D. Ranasinghe, V. G. Zakrzewski, J. Gao, N. Rega, G. Zheng, W. Liang, M. Hada, M. Ehara, K. Toyota, R. Fukuda, J. Hasegawa, M. Ishida, T. Nakajima, Y. Honda, O. Kitao, H. Nakai, T. Vreven, K. Throssell, J. A. J. Montgomery, J. E. Peralta, F. Ogliaro, M. J. Bearpark, J. J. Heyd, E. N. Brothers, K. N. Kudin, V. N. Staroverov, T. A. Keith, R. Kobayashi, J. Normand, K. Raghavachari, A. P. Rendell, J. C. Burant, S. S. Iyengar, J. Tomasi, M. Cossi, J. M. Millam, M. Klene, C. Adamo, R. Cammi, J. W. Ochterski, R. L. Martin, K. Morokuma, O. Farkas, J. B. Foresman, D. J. Fox, Gaussian Inc., Wallingford CT, **2016**.